



Université du Québec
à Rimouski

**ÉTUDE DE LA DYNAMIQUE DE PRODUCTION DES
PARTICULES EXOPOLYMÉRIQUES TRANSPARENTES
(TEP) PAR LES ASSEMBLAGES MICROBIENS ET
IMPACTS DES FACTEURS ENVIRONNEMENTAUX**

Thèse présentée

dans le cadre du programme de doctorat en océanographie

en vue de l'obtention du grade de philosophiae doctor

PAR

© **SOUAD ANNANE**

Mai 2024

Composition du jury :

Christian Nozais, président du jury, Université du Québec à Rimouski

Gustavo A. Ferreyra, directeur de recherche, Université du Québec à Rimouski

Émilien Pelletier, codirecteur de recherche, Université du Québec à Rimouski

Michel Starr, codirecteur de recherche, Institut Maurice Lamontagne

Michel Denis, examinateur externe, Institut Méditerranéen d'Océanologie

Dépôt initial le [24 mars 2017]

Dépôt final le [19 avril 2024]

UNIVERSITÉ DU QUÉBEC À RIMOUSKI
Service de la bibliothèque

Avertissement

La diffusion de ce mémoire ou de cette thèse se fait dans le respect des droits de son auteur, qui a signé le formulaire « *Autorisation de reproduire et de diffuser un rapport, un mémoire ou une thèse* ». En signant ce formulaire, l'auteur concède à l'Université du Québec à Rimouski une licence non exclusive d'utilisation et de publication de la totalité ou d'une partie importante de son travail de recherche pour des fins pédagogiques et non commerciales. Plus précisément, l'auteur autorise l'Université du Québec à Rimouski à reproduire, diffuser, prêter, distribuer ou vendre des copies de son travail de recherche à des fins non commerciales sur quelque support que ce soit, y compris l'Internet. Cette licence et cette autorisation n'entraînent pas une renonciation de la part de l'auteur à ses droits moraux ni à ses droits de propriété intellectuelle. Sauf entente contraire, l'auteur conserve la liberté de diffuser et de commercialiser ou non ce travail dont il possède un exemplaire.

Cette thèse de doctorat est
dédiée à ma chère défunte mère
puisse-t-elle reposer en paix

REMERCIEMENTS

Cette thèse a été pour moi une aventure parsemée d'embûches, mais aussi de merveilleux moments - une aventure que je n'aurais pas pu finaliser sans le soutien de tant de personnes, que je tiens à remercier.

Je tiens tout d'abord à remercier mon directeur de thèse, Gustavo Ferreyra, qui m'a accueilli à Rimouski et dans son équipe comme un membre de la famille. Merci pour ton support inconditionnel, ta grande disponibilité et toutes les opportunités scientifiques et humaines que j'ai eues durant mon programme. Je suis reconnaissant pour tous tes précieux conseils, le temps que tu m'as consacré et de ta patience dans les moments difficiles. Je te remercie surtout pour la grande liberté que tu m'as laissée tout au long de ce doctorat. Ces opportunités m'ont permis d'être plus autonome et apprendre à gérer tous les aspects liés au projet; de la prévision à la logistique, en passant par le travail de terrain et de laboratoire à celui de l'analyse et la rédaction scientifique. J'ai beaucoup appris sous ta direction et je me sens maintenant capable de m'aventurer dans de nouvelles aventures.

Mes sincères remerciements à mes deux codirecteurs de recherche, Émilien Pelletier et Michel Starr. Merci énormément pour vos conseils avisés, votre grande disponibilité, votre soutien tout au long de ce processus et tout particulièrement au cours de la rédaction de ce manuscrit. Merci, Émilien, pour toutes nos discussions toujours très enrichissantes pour moi surtout sur la chimie des choses. Michel, merci infiniment pour ton aide précieuse et de m'avoir accueillie dans ton laboratoire durant mes travaux de terrain et lors de mes expériences en microcosmes. Vos points de vue scientifiques m'ont toujours grandement inspiré et aidé à avancer.

Je tiens également à remercier tout spécialement Christian Nozais et Michel Denis pour avoir accepté d'évaluer mon travail de thèse et d'être intervenus en tant que président du jury et examinateur externes lors de ma soutenance et pour leurs précieux conseils et

suggestions. Merci infiniment Michel d'avoir également pris le temps de suivre mon travail à distance et pour tes conseils et encouragements.

Mes remerciements s'adressent aussi à Serge Demers, membre de mon comité de thèse, qui a eu la gentillesse de suivre l'évolution de mon projet et sa contribution au présent travail.

Ce projet de recherche a été rendu possible grâce au soutien financier du Conseil de Recherche en Sciences Naturelles et en Génie du Canada (CRSNG), du Fonds de recherche du Québec nature et technologie (FQRNT), du ministère de Pêches et Océans Canada (MPO), de Québec Océan et du réseau MESOAQUA (septième programme-cadre de l'Union européenne).

Je tiens à remercier l'équipe de l'Institut Maurice-Lamontagne, qui a contribué à la mise en place et au fonctionnement des microcosmes, de même qu'au travail de terrain et du laboratoire. Tout particulièrement merci à Lilianne Saint-Amand, Pierre Joly, Marie-Lyne Dubé, Sylvie Lessard, Jean-François St-Pierre, Caroline Lafleur et Laure Devine. Ce fut un plaisir d'avoir travaillé à vos côtés.

Merci également à toutes les personnes de l'ISMER qui ont contribué à ce projet dans leurs domaines respectifs. Toujours très serviable et travaillant dans la bonne humeur, merci à Mélanie Simard, Dominique Lavallée, Pascal Rioux, Claude Belzile, Richard Saint-Louis, Mathieu Babin, Sylvain Leblanc, Gilles Desmeules, Bruno Cayouette, Wahiba Ait Youcef, Alexandre Boudreau, Nathalie Morin, Rachel Picard, Sylvie Fillion, Martine Belzile, Marielle Lepage, Brigitte Dubé. Tous mes remerciements aussi à Karine Lemarchand pour m'avoir laissé utiliser son laboratoire et tous ses conseils avisés.

Je remercie tout particulièrement Francesca Vidussi et Behzad Mostajir de l'équipe MESOAQUA qui nous ont invités à participer au projet. Ce fut une expérience humaine et scientifique très enrichissante pour moi, merci de votre confiance. Merci également à Romain Pete, Émilie Le Floc'h et David Parin de leur aide sur le terrain.

Je n'y serais également pas arrivée sans le soutien de mes amis de bureau qui au quotidien était là que ce soit pour des échanges amicaux ou scientifiques, grâce à qui la vie à l'ISMER était encore plus sympathique. Merci à vous, Wahiba, Nassim, Marion, Adriano et Amin. Merci également à mes amis, qui ont toujours été là pour moi de près ou de loin, qui m'ont accompagné dans cette aventure de doctorat dans les bons et mauvais moments, et qui m'ont soutenue et encouragée à continuer. Je pense aussi aux membres des lundis dessert, merci. Je ne serai pas ici sans vous tous à mes côtés. Merci d'être là, Wahiba, Nassim, Hanieh, Marion, Manuela, Anouck, Aicha, Amin, Eileen, Anja, Irene, Tarik, Anne-Sophie, Joanna, Ziad, Claire, Guillaume, Annie, Guylaine et Gustavo.

J'aimerais enfin exprimer toute ma gratitude à ma famille. Je n'y serai pas arrivé sans votre soutien et foi en moi. Je remercie spécialement ma mère Kheira, pour son soutien inconditionnel et ses encouragements perpétuels dans les moments de doute et de crise de larmes. Merci à mes sœurs Fatima, Fouzia, Farida ainsi que mon beau-frère Salim.

RÉSUMÉ

Les particules exopolymériques transparentes (en anglais TEP, Transparent Exopolymeric Particles) sont des particules de gel ubiquiste formées abiotiquement par coagulation et agrégation de précurseurs dissous et colloïdaux composés de polysaccharides acides. Il est suggéré que, par ce processus, la transition du carbone du réservoir dissout au particulaire (DOC vers POC) via l'agrégation des TEP, peut faciliter le flux vertical de carbone dans la colonne d'eau. En ce sens, les TEP jouent un rôle central dans la pompe biologique ainsi que dans la dynamique des réseaux trophiques dans les écosystèmes aquatiques. Malgré l'abondance de l'information disponible, il existe encore une grande incertitude quant au budget de carbone des milieux marins en raison de leur grande variabilité et de notre manque de compréhension des aspects importants de la dynamique des TEP. En particulier, la contribution des TEP au réservoir de carbone est mal comprise et a été largement ignorée dans la construction des budgets de carbone. L'objectif principal de cette thèse était de caractériser la dynamique des TEP dans le cycle du carbone organique, en particulier dans l'estuaire maritime du Saint-Laurent (EMSL) et en Méditerranée, et de comprendre les impacts de certains facteurs environnementaux (présents et futurs) susceptibles de contrôler leur variabilité. Notre question a été abordée en trois étapes.

Dans le chapitre 1, nous avons étudié pour la première fois la distribution saisonnière et verticale des TEP et leur contribution au réservoir de carbone organique à une station fixe dans l'EMSL. Nous avons observé que les concentrations des TEP dans l'EMSL étaient positivement corrélées avec la biomasse phytoplanctonique en surface, avec les diatomées étant le groupe principal. Aucune relation significative entre les TEP et d'autres facteurs biologiques et physico-chimiques n'a été trouvée. La teneur en carbone des TEP (TEP-C) représentait dans la couche de surface le second contributeur le plus important au réservoir de carbone organique particulaire après le carbone de phytoplancton (41 et 54 % par rapport au POC, respectivement). La contribution des TEP-C a diminué dans les couches intermédiaires froides et de fond au cours de l'été et de l'automne (entre 24 et 35 % par rapport au POC). Ces résultats suggèrent que le TEP-C combiné au phytoplancton-C contribue largement au réservoir de carbone et pourrait contribuer de manière significative à l'exportation ultérieure de macro-agrégats et possiblement à l'hypoxie et l'acidification des eaux de fond de l'EMSL.

Motivée par les résultats de cette étude de terrain, une expérience suivant un modèle cinétique en microcosme a été réalisée pour étudier les effets présents et futurs de l'acidification croissante attendue vers la fin du siècle sur la communauté planctonique naturelle, les TEP et l'allocation du carbone organique dans l'EMSL. Les résultats de cette étude en microcosme présentés au chapitre 2 ont révélés une accumulation de la biomasse, des taux de croissance et une prise de silice réduites de la communauté phytoplanctonique

sous des conditions de faible pH. Nos résultats suggèrent que le nanophytoplancton, et plus précisément les diatomées du genre *Thalassiosira spp.*, étaient moins vulnérables aux faibles pH que le pico- et le microphytoplancton. L'accumulation des TEP a été positivement corrélée à la biomasse des cellules dans la fraction du nanophytoplancton et aux conditions environnementales (pH, alcalinité et silice) pendant les phases de floraison et post-floraison. D'autre part, les flagellés hétérotrophes étaient favorisés par les faibles pH. La densité des bactéries a diminué sous un faible pH probablement en raison d'une augmentation de la lyse virale et du broutage. À faible pH, le rapport POC: PON était plus faible, bien que nous avons noté un changement dans la partition du carbone dans le réservoir dissous vers celui du POC via l'agrégation des TEP. Nos résultats suggèrent que les changements anticipés de l'alcalinité et des faibles pH pourraient affecter l'agrégation des TEP et leur structure, ce qui pourrait avoir un impact sur l'exportation de la matière organique.

Enfin, les résultats d'une expérience en mésocosme réalisée dans une lagune marine de la mer Méditerranée sont présentés au chapitre 3. Cette expérience a été conçue pour étudier les effets séparés et combinés de l'acidification et du réchauffement futurs sur la formation des TEP et l'allocation de la matière organique dans les écosystèmes chauds de moyenne latitude. Nos résultats ont montré une augmentation de l'accumulation des TEP-C et de la prise du carbone inorganique dissous (DIC) sous une $p\text{CO}_2$ élevée, ce qui était associé à une accumulation de carbone organique colloïdal (3 fois) par rapport aux niveaux actuels. Ces résultats suggèrent une augmentation de l'agrégation des particules et du réservoir de POC sous une $p\text{CO}_2$ élevée. En revanche, le réchauffement a diminué le retrait de DIC et l'accumulation de carbone particulaire (TEP-C et POC), ce qui suggère une réduction de la formation de particules et de l'exportation de carbone en faveur de la dégradation microbienne. De façon inattendue, nos résultats ont révélé que l'effet combiné de l'acidification et du réchauffement ne présentait aucun effet sur les TEP-C, POC et la prise du DIC, jouant ainsi un rôle antagoniste en particulier sur la production de TEP-C. Cependant, le traitement combiné d'acidification-réchauffement a présenté un effet positif sur le carbone phytoplanctonique et bactérien. En conclusion, nos résultats suggèrent que les scénarios océaniques futurs pourraient avoir le potentiel de réduire la séquestration du carbone particulaire en faveur de l'accélération de la respiration de la boucle microbienne avec des conséquences de rétroaction de l'océan sur le changement global.

En conclusion, cette thèse de doctorat a révélé l'importance de la contribution des TEP au réservoir de carbone organique qui devrait être pris en considération dans les modèles biogéochimiques. Notre travail suggère par ailleurs la présence d'une réponse espèces-spécifique de la communauté phytoplanctonique aux changements de CO_2/pH , pour lesquels la croissance du phytoplancton est optimale jusqu'à un $\text{pH} \sim 7,7$ et qu'une diminution supplémentaire du pH ($\text{pH} \leq 7,55$) pourrait avoir des effets très significatifs sur la croissance cellulaire et leur physiologie. Dans le contexte des changements globaux, l'acidification et le réchauffement peuvent jouer de façon antagoniste sur l'accumulation et l'exportation potentielle du carbone organique. Cela pourrait avoir un impact sur les flux

verticaux de matière organique futurs avec des conséquences possibles sur la productivité des écosystèmes marins et le pompage biologique du CO₂ atmosphérique.

ABSTRACT

Transparent exopolymeric particles (TEP) are ubiquitous gel particles formed abiotically by coagulation and aggregation of dissolved and colloidal precursors composed of acid polysaccharides. It is suggested that by this process, the transition of carbon from dissolved to particulate (DOC to POC) pool via TEP aggregation, can facilitate vertical carbon flux in the water column. In this sense, TEP plays a central role in the biological pump and the dynamics of food webs in aquatic ecosystems. Despite the significant amount of information available, great uncertainty regarding the carbon budget of marine environments still exists due to their high variability, as well as our lack of understanding of significant aspects of TEP dynamics. In particular, the contribution of the TEP fraction to the carbon pool is poorly understood and has largely been ignored in the construction of carbon budgets. The main objective of this doctoral thesis was to characterize the dynamics of TEP in the organic carbon cycle, especially in the Lower St. Lawrence Estuary (LSLE) and in a temperate marine coastal environment (Mediterranean) and to understand the impacts of some environmental factors (present and future) that could control its variability. Our question was addressed in three steps.

In chapter 1, we studied, for the first time, the seasonal and vertical distribution of TEP and their contribution to the organic carbon pool at a fixed station in the LSLE. We observed that TEP concentrations in the LSLE were positively correlated with the phytoplankton biomass in surface waters, particularly dominated by diatoms. No significant relationships between TEP and other biological and physico-chemical factors were found. TEP carbon (TEP-C) content represented in the surface layer the second most important contributor to the particulate organic carbon pool after phytoplankton carbon (41 and 54 % compared to POC, respectively). The TEP-C contribution decreased in the cold intermediate and bottom layers over the summer and fall (ranging between 24 and 35 % compared to POC). This result suggests that TEP-C combined with phytoplankton carbon are major contributors to the carbon pool and could significantly contribute to the subsequent export of macro-aggregates, and probably fuel the hypoxia and the acidification of the bottom layer of the LSLE.

Motivated by the results of this field study, a microcosm kinetic experiment was performed to investigate the present and future effects of the growing acidification, expected by the end of the century, on the natural plankton community, TEP and organic carbon matter allocation in the LSLE. The results of this microcosm study presented in chapter 2 revealed a reduced biomass accumulation and growth rates, and silica uptake of phytoplankton community under low pH. Our results suggest that nanophytoplankton, and more precisely diatoms of the genus *Thalassiosira spp.*, were less sensitive to low pH than the pico- and microphytoplankton. TEP accumulation was positively correlated to nanophytoplankton cell fraction biomass and the environmental conditions (pH, alkalinity et silica) during the bloom and post-bloom phases. On the other hand, heterotroph

flagellates were favored by low pH. Bacteria density decreased under low pH probably due to an increase of viral lysis and grazing. At low pH, POC:PON ratios were lower, though we noted a shift of carbon partition from dissolved into the POC pool via TEP aggregation. Our results suggests that the anticipated changes in alkalinity and low pH could affect TEP aggregation and TEP particle structure, which in turn could have an impact on the organic matter export.

Finally, results from a mesocosms experiment carried in a Mediterranean Sea lagoon are presented in chapter 3. This experiment was designed to investigate the separate and combined effects of future acidification and warming on TEP formation and on the organic carbon matter allocation in warm mid-latitude ecosystems. Our results showed an increase in TEP-C accumulation and inorganic carbon drawdown (DIC) at high $p\text{CO}_2$, which was associated with colloidal organic carbon accumulation (3 fold) compared to present levels. These results suggest an increase of particle aggregation and partitioning into the POC pool under high $p\text{CO}_2$. In contrast, warming decreased the DIC drawdown and particle carbon accumulation (TEP-C and POC), suggesting a reduction of particle formation and carbon export in favor of microbial degradation. Unexpectedly, our results revealed that the combined effect of acidification and warming present no effect on TEP-C, POC and DIC drawdown, playing an antagonistic role especially on TEP-C production. However, the warming-acidification combined treatment presented a positive effect on phytoplankton and bacterial carbon accumulation. All together, our results suggest that future oceanic scenarios would have the potential to reduce the particle carbon sequestration in favor of accelerating the microbial loop respiration and driving consequences of ocean feedbacks to global change.

In conclusion, this doctoral thesis revealed the importance of the contribution of TEP to the organic carbon pool, which should be taken into consideration in biogeochemical models. Moreover, our work suggests the presence of a species-specific response of phytoplankton community to changes in CO_2/pH , for which the phytoplankton growth is optimal up to $\text{pH} \sim 7.7$, and that a further decrease in pH (e.g. $\text{pH} \leq 7.55$) could have adverse effects on cell growth and physiology. In the context of global changes, acidification and warming may play antagonistically on the accumulation and potential export of organic carbon. This could have an impact on the future vertical flows of organic matter with possible consequences for marine ecosystems productivity and the biological pumping of atmospheric CO_2 .

Keywords: Transparent exopolymeric particles (TEP), Ocean acidification, Warming, Global change, Estuary, Phytoplankton, particulate and dissolved organic carbon (POC, DOC), Heterotrophic bacteria, pH, mesocosm.

TABLE DES MATIÈRES

| | |
|--|--------------|
| REMERCIEMENTS..... | ix |
| RÉSUMÉ..... | xii |
| ABSTRACT..... | xv |
| TABLE DES MATIÈRES | xviii |
| LISTE DES TABLEAUX..... | xx |
| LISTE DES FIGURES..... | xxii |
| INTRODUCTION GÉNÉRALE | 1 |
| 1.1 LES PARTICULES EXOPOLYMÉRIQUES TRANSPARENTES (TEP) ET LEUR RÔLE DANS LE CYCLE DU CARBONE MARIN | 1 |
| 1.2 ORIGINE ET FORMATION DES TEP..... | 5 |
| 1.3 PROBLEMATIQUE ET PLAN DE LA THÈSE | 10 |
| CHAPITRE 1 CONTRIBUTION DES PARTICULES EXOPOLYMÉRIQUES TRANSPARENTES (TEP) AU RÉSERVOIR DE CARBONE ORGANIQUE PARTICULAIRE ESTUARIEN..... | 19 |
| 1.1 RÉSUMÉ..... | 20 |
| 1.2 CONTRIBUTION OF TRANSPARENT EXOPOLYMERIC PARTICLES (TEP) TO ESTUARINE PARTICULATE ORGANIC CARBON POOL..... | 21 |
| CHAPITRE 2 IMPACT DE L'ACIDIFICATION DES OCÉANS SUR LES PARTICULES EXOPOLYMÉRIQUES TRANSPARENTES (TEP) ET L'ALLOCATION DU CARBONE ORGANIQUE DANS L'ESTUAIRE DU SAINT- LAURENT: UNE EXPÉRIENCE DE MICROSOCOSMES..... | 55 |
| 1.1 RÉSUMÉ..... | 56 |

| | | |
|---|---|------------|
| 1.2 | IMPACT OF OCEAN ACIDIFICATION ON TRANSPARENT EXOPOLYMERIC PARTICLES (TEP) AND ORGANIC CARBON ALLOCATION IN THE ST. LAWRENCE ESTUARY: A MICROSOCOSM EXPERIMENT | 58 |
| CHAPITRE 3 LES EFFETS DE L'ACIDIFICATION ET DU RÉCHAUFFEMENT SUR LES PARTICULES EXOPOLYMÉRIQUES TRANSPARENTE (TEP) DANS UN ENVIRONNEMENT CÔTIER DE LA MÉDITERRANÉE (LAGUNE DE THAU)..... | | |
| 1.1 | RÉSUMÉ | 109 |
| 1.2 | EFFECTS OF ACIDIFICATION AND WARMING ON TRANSPARENT EXOPOLYMERIC PARTICLES (TEP) IN A MEDITERRANEAN COASTAL ENVIRONMENT (THAU LAGOON) | 110 |
| CONCLUSION GÉNÉRALE..... | | 144 |
| ANNEXES | | 157 |
| RÉFÉRENCES BIBLIOGRAPHIQUES | | 160 |

LISTE DES TABLEAUX

CHAPITRE 1

| | |
|--|----|
| Tableau 1 : Seasonal depth intervals (m) for each of the water layers identified at the IML-4 station..... | 33 |
| Tableau 2 : Carbon standing stock (mg C m^{-2}) in the surface layer (SL), the cold intermediate layer (CIL) and the bottom layer (BL) for the three seasons studied (average \pm Std. Dev.). TEP (TEP-C), phytoplankton (Chl <i>a</i> -C), bacteria (Bac-C) and POC | 42 |
| Tableau 3 : Models of POC fitted to the main potential sources of particulate carbon. AIC: Akaike Information Criterion; AICc: corrected AIC; p: probability; Δ : differences between models in relation to the minimum AIC value. Models are ranked from the minimum AIC (minimum loss of information) to maximum (maximum loss of information). POC: particulate organic carbon; TEP-C: transparent exopolymeric particle carbon; Chl <i>a</i> -C: phytoplankton carbon; Bac-C: bacterial carbon (data are log transformed averages for each water layer) | 44 |
| Tableau 4 : Values reported on transparent exopolymer particles (TEP $\mu\text{g GX eq L}^{-1}$) and TEP contribution to the carbon pool for estuarine, marine and freshwater environments (minimum, maximum values are shown, with averages in parentheses) | 48 |

CHAPITRE 2

| | |
|---|----|
| Tableau 1 : Measured and calculated values (mean \pm SD, n=5) of carbonate system parameters for the microcosms pH treatments and the not controlled microcosm during the experiment..... | 68 |
| Tableau 2 : Estimated FWS length (Avg. \pm Std) obtained from the Cytosense flow cytometer for the identified clusters..... | 71 |

CHAPITRE 3

Tableau 1 : Results of the linear correlation analyses between POC ($\mu\text{g C L}^{-1}$) as the dependent variable and the sum of TEP-C, Phyto-C and Bac-C (TPB-C sum, $\mu\text{g C L}^{-1}$) for each treatment (independent variable).....126

LISTE DES FIGURES

INTRODUCTION GÉNÉRALE

Figure 1 : Changements dans les concepts concernant les flux de carbone entre les organismes et particules non vivantes, illustrant la chaîne alimentaire linéaire de broutage, la boucle microbienne et le réseau basé sur les processus d'agrégation. Schéma modifié à partir de Passow (2002b)..... 3

Figure 2 : Modèle conceptuel représentant les voies possibles de la matière organique produite par les cellules autotrophes. Sous l'hypothèse de surconsommation du carbone inorganique dissous (CID) par rapport à l'absorption de l'azote (NID) ou le phosphore inorganique dissous (PID), une fraction du carbone organique intracellulaire accumulée est libérée de la cellule par des processus de diffusion et/ou d'exsudation. En fonction de sa qualité, le carbone organique extracellulaire peut entrer dans la chaîne alimentaire microbienne ou bien être agrégé pour former des particules, telles que les TEP (modifié d'après Engel et al. 2004)..... 7

Figure 3 : Concept de la formation abiotique des particules exopolymériques transparentes (TEP) à partir de leurs précurseurs. Les TEP et leurs précurseurs existent dans un continuum de taille, de la fraction colloïdale à la fraction particulaire. Schéma modifié de Beauvais (2003) 8

CHAPITRE 1

Figure 1 : Map showing the location of the Rimouski fixed sampling station (IML-4) in the Lower St. Lawrence Estuary 28

Figure 2 : Vertical and seasonal distributions of: (a) temperature ($^{\circ}\text{C}$), (b) salinity (PSU), (c) density ($\sigma\text{-t}$) and (d) nitrates (μM) in the water column at the IML-4 station from May to October 2011. Black line: pycnocline depth; white line: euphotic zone depth (Z_{eu}); White dashed line: CIL limit ($T \leq 3^{\circ}\text{C}$) 34

| | |
|--|----|
| Figure 3 : Vertical and seasonal distributions of: (a) chlorophyll a ($\mu\text{g L}^{-1}$), (b) TEP ($\mu\text{g XG eq L}^{-1}$), (c) POC ($\mu\text{g L}^{-1}$) and (d) bacteria (Cell mL^{-1}) in the water column at the IML-4 station. Black line: pycnocline depth; white line: euphotic zone depth (Zeu)..... | 36 |
| Figure 4 : Seasonal averages ($\pm\text{SE}$) of log transformed data: (a) Chl <i>a</i> concentration ($\mu\text{g L}^{-1}$) and (b) TEP concentrations ($\mu\text{g XG eq L}^{-1}$) corresponding to each water layer identified at the IML-4 station. Tukey HSD test results: Different letters above each bar indicate a significant difference between seasons and layers ($\alpha=0.05$)..... | 38 |
| Figure 5 : Relative contributions of TEP (TEP-C), phytoplankton (Chl <i>a</i> -C), bacteria (Bac-C) and other organic matter (Residual-C) to POC in the three water layers identified: (a) Surface layer, (b) Cold intermediate layer, and (c) Bottom layer..... | 41 |
| Figure 6 : Relationship between POC ($\mu\text{g L}^{-1}$) and the sum of TEP-C, Chl <i>a</i> -C ($\mu\text{g L}^{-1}$) (a) the surface layer (SL) and (b) the cold intermediate layer (CIL). Dashed lines represent the 0.95 confidence level..... | 45 |

CHAPITRE 2

| | |
|--|----|
| Figure 1 : Experimental setup of CO ₂ manipulation system and computer control of pH for each microcosm (a) and profile view of microcosm (b). A mixture of air and CO ₂ was bubbled directly in the bottom of each microcosm thus achieving a gradient of 6 pH levels and a pH reference microcosm. The air/CO ₂ mixing was adjusted for each microcosm by instant pH probe monitoring and adjustment..... | 65 |
| Figure 2 : Temporal variation in pH _T <i>In situ</i> (total hydrogen ion scale) during the microcosm experiment..... | 75 |
| Figure 3 : Regression between pH _T <i>in situ</i> values spectrometrically measured (total hydrogen ion scale) and those coming from continuous pH probes (NBS). Dashed lines represent the 0.95 confidence level. | 75 |
| Figure 4 : Nutrient time change for: (a) nitrate (b) SRP and (c) silicic acid in the pH perturbed and reference microcosms. | 76 |
| Figure 5 : Relationship between the proton concentration values ([H ⁺]) and (a) the rate of silicic acid change, (b) the ratio $\Delta\text{Si(OH)}_4 : \Delta\text{NO}_3$ and (c) the ratio $\Delta\text{Si(OH)}_4$ | |

- : Δ Diatoms during the bloom development (day 1 to day 4). Significant regression (solid line) with (95%) confidence intervals (dashed lines) are shown 77
- Figure 6 : Temporal evolution of phytoplankton carbon ($\mu\text{gC L}^{-1}$) during the experiment: (a) Picoplankton-C, (b) Nanophytplankton-C and (c) Microphytoplankton-C. Each curve represents a microcosm with a specific pH treatment..... 79
- Figure 7 : Relationship between the proton concentration values ($[\text{H}^+]$) and phytoplankton growth rate ($\mu \text{ d}^{-1}$) during the bloom development for (a) Nanophytplankton-C (day 2 to day 7), (b) Nanophytplankton-C (day 7 to day 15), (c) Microphytoplankton-C (day 2 to day 9) and (d) Microphytoplankton-C (day 9 to day 15). Linear regressions are shown with solid lines are shown. A negative growth rate indicates a cell loss 81
- Figure 8 : Microscopic relative contributions of (a) autotrophic group to total phytoplankton and (b) diatom species at the beginning (T0), around the bloom (day 4) and at the end of the experiment (day 15) in each pH treatment. Relationship between heterotrophs flagellates (% of the total protists abundance) and the proton concentration values ($[\text{H}^+]$) during (c) the bloom and (d) at the end of the experiment. Linear regressions are shown with solid lines are shown 83
- Figure 9 : Temporal evolution during the experiment ($\mu\text{g C L}^{-1}$) of: (a) transparent exopolymeric particles carbon (TEP-C), (b) particulate organic carbon (POC), (c) particulate organic carbon to particulate organic nitrogen ratio (POC:PON) and (d) dissolved organic carbon (DOC). Each curve represents a microcosm with a specific pH treatment..... 84
- Figure 10 : Relationship between the proton concentration values ($[\text{H}^+]$) and particulate and dissolved organic carbon accumulation rate during the experiment for TEP-C from day 2 to day 7 (a), from day 9 to day 15 (b); POC from day 2 to day 9 (c), from day 9 to day 15 (d); DOC from day 4 to day 15 (e) and DOC:POC ratio for each experimental day (f). Linear regression relationships are shown with solid lines are shown..... 86
- Figure 11 : Temporal evolution of (a) bacteria abundance and (b) viruses. Each curve represents a microcosm with a specific pH treatment..... 88

Figure 12 : Temporal evolution of (a) percentage of bacteria with high nucleic acids (HNA) and (b) virus to bacteria ratio during the experiment. Each curve represents a microcosm with a specific pH treatment89

Figure 13 : Relationship between the proton concentration values ([H+]) and the rate of abundance change during the experiment (a) Bacteria (day 2 to day 7), (b) Bacteria (day 7 to day 15), and (c) viruses (day 2 to day 15). Linear regressions are shown with solid lines are shown.....90

CHAPITRE 3

Figure 1 : Temporal variation of inorganic nutrients (a) nitrate (μM), (b) orthophosphate (μM) and (c) silicates (μM) (averages $\pm\text{SD}$) of the mesocosms experiment with the following treatments: Control, actual temperature and $p\text{CO}_2$ (black); high $p\text{CO}_2$, A (green); high temperature, T (red) and high $p\text{CO}_2$ and high temperature, AT (blue)119

Figure 2 : Temporal variation of (a) temperature ($^{\circ}\text{C}$), (b) $\text{pH}_{\text{T in situ}}$ and (c) DIC ($\mu\text{mol kg}_{\text{sw}}^{-1}$) (averages $\pm\text{SD}$) during the mesocosms experiment with the following treatments: Control, actual temperature and $p\text{CO}_2$ (black); high $p\text{CO}_2$, A (green); high temperature, T (red) and high $p\text{CO}_2$ and temperature, AT (blue).....120

Figure 3 : Temporal variation of (a) Chl a-C, (b) TEP-C, (c) POC and (d) Bac-C (averages $\pm\text{SD}$) during the mesocosms experiment with the following treatments: Control, actual temperature and $p\text{CO}_2$ (black); high $p\text{CO}_2$, A (green); high temperature, T (red) and high $p\text{CO}_2$ and temperature, AT (blue).....122

Figure 4 : Dissolved inorganic carbon changes (ΔDIC) during the bloom phase in the Control (C), Acidified (A), high Temperature (T) and Acidified and high Temperature (AT) treatments during the exponential phytoplankton growth. t-test significant difference (** $P<0.01$)124

Figure 5 : Temporal contribution of the sum of TEP-C, Phyto-C and Bac-C (TPB-C sum) and POC compartments studied for the a) Control and b) Acid, c) Temperature and d) Acid Temperature treatments. Bars represent phytoplankton-C (black);

HBacteria-C (light grey); TEP-C (dark grey) and the black line with points is POC. Units for all variables are $\mu\text{g C L}^{-1}$ 126

Figure 6 : Conceptual model of the carbon pathway implicated for each scenario a) High acidification, b) High temperature and c) High acidification and temperature. Boxes represent the different carbon compartments (DIC, phytoplankton, Bacteria, TEP, colloids, POC and DOC) for each partition. Arrows represent processes of uptake, exudation, assimilation, aggregation, remineralization and sinking. The positive effect in each treatment is in bold black and those negative or presenting no effect to change in CO_2 and/or temperature are grey. The uptake of DIC by phytoplankton is modulated by CO_2 and temperature change. The excess of fixed carbon is exudate as DOC, with a portion of the DOC rapidly transformed into colloids and TEP by abiotic aggregation process, which contributes to a large fraction of the POC. This partitioning into particulate fraction is elevated under the acidification scenario. On the other hand, the warming scenario results in an increase of bacterial carbon leading to an enhanced respiration of the organic carbon, thereby, replenishing the DIC compartment, and reducing the accumulation of particulate organic matter (like TEP and POC) for export. The combined effect of warming and acidification scenario results in enhanced bacterial carbon, which could counteract the phytoplankton carbon increase by enhancing the microbial respiration of the organic carbon, associated with the lack of change in TEP, POC and DIC compartments. Together, these responses to the combined effect may present positive feedback to rising atmospheric CO_2 . The dotted red square represents the surface layer ecosystem ... 137

CONCLUSION GÉNÉRALE

Figure 1 : Diagramme conceptuel illustrant la réponse de l'écosystème de la Méditerranée (à gauche) et du Saint-Laurent (à droite) et la voie du carbone sous des conditions d'acidification. Les flèches représentent des processus d'absorption, exsudation, assimilation, agrégation, reminéralisation et sédimentation. L'effet positif dans chaque traitement est en noir gras et ceux négatifs où ne présentant aucun effet au changement de CO_2 sont en gris. Les compartiments non échantillonnés sont en ligne pointillée. Le carré rouge représente l'écosystème de la couche de surface. CO_2 atmosphérique (CO_2 ATM), carbone inorganique dissous (DIC), phytoplankton (Phyto), hétérotrophes (Heterotroph), carbone organique dissous (COD), bactéries

(BAC), carbone organique colloïdal (Colloids), particules exopolymériques transparentes (TEP) et carbone organique particulaire (POC). 144

Figure 2 : Diagramme conceptuel illustrant la réponse de l'écosystème de Méditerranée et la voie du carbone sous des conditions de réchauffement et d'acidification. Le réchauffement a pour effet d'augmenter la biomasse bactérienne et stimule la respiration microbienne du carbone organique réapprovisionnant ainsi le compartiment du CID, ce qui pourrait contrecarrer l'effet de l'acidification sur l'augmentation de la biomasse phytoplanctonique par surconsommation de CID. Associé à l'absence de changements dans les compartiments des TEP, COP et CID. Ensemble, ces réponses à l'effet combiné de réchauffement et d'acidification peuvent présenter une rétroaction positive à la hausse du CO₂ atmosphérique. Les flèches représentent des processus d'absorption, d'exsudation, d'assimilation, d'agrégation, de reminéralisation et de sédimentation. L'effet positif dans chaque traitement est en noir gras et ceux négatifs où ne présentant aucun effet de changement combiné de CO₂ et température sont en gris. Le carré rouge représente l'écosystème de la couche de surface. CO₂ atmosphérique (CO₂ ATM), carbone inorganique dissous (DIC), phytoplancton (Phyto), hétérotrophes (Heterotroph), carbone organique dissous (COD), bactéries (BAC), carbone organique colloïdal (Colloids), particules exopolymériques transparentes (TEP) et carbone organique particulaire (POC).

..... 146

INTRODUCTION GÉNÉRALE

1.1 LES PARTICULES EXOPOLYMÉRIQUES TRANSPARENTES (TEP) ET LEUR RÔLE DANS LE CYCLE DU CARBONE MARIN

La compréhension de la production et du devenir du carbone organique dans l'océan est un enjeu majeur dans le cycle global du carbone. En fait, la structure et la dynamique du réseau trophique planctonique jouent un rôle fondamental dans la régulation des flux de carbone (Rivkin et al. 1996).

Notre connaissance sur ce type de réseau trophique n'a cessé d'évoluer depuis plus de 30 ans. En effet, il semble que le réseau trophique pélagique soit beaucoup plus complexe que l'on avait considéré. Jusqu'au tout début des années 80, on pensait que la majorité du carbone inorganique dissous (CID) fixé photosynthétiquement par les producteurs primaires transitait à travers une chaîne trophique simple et linéaire jusqu'aux niveaux trophiques supérieurs via le zooplancton herbivore (Williams 1981). C'est ce que l'on appelle « la chaîne trophique basée sur le broutage » (« Grazing food chain ») et les autres microorganismes étaient alors largement ignorés.

Azam et al. (1983) ont élargi notre compréhension à travers le concept de « boucle microbienne », en mettant en évidence l'importance des organismes autotrophes et hétérotrophes de petite taille ($<5 \mu\text{m}$) dans le fonctionnement des processus biogéochimiques en milieu marin. Ainsi, le carbone organique dissous (COD) exsudé par le phytoplancton est recyclé par les bactéries et les archaea hétérotrophes (Azam & Malfatti 2007). Il a été estimé qu'approximativement 50 % de la production primaire océanique est canalisée via le COD et la respiration bactérienne (Azam 1998, Azam & Malfatti 2007, Hansell et al. 2009). Les bactéries dégradent non seulement la matière organique dissoute, mais aussi les organismes et les détritiques particulaires, ce qui contribue significativement au recyclage du carbone dans l'océan. Plus tard, Legendre & Rassoulzadegan (1995) ont

ajouté une plus grande complexité à ce modèle, en y intégrant d'autres types de communautés (continuum du réseau trophique multivore qui relie les bactéries hétérotrophes et les zooflagellés).

De nombreux auteurs ont suggéré qu'une partie significative du carbone organique particulaire (COP) pouvait être formée de façon abiotique dans la colonne d'eau à partir de substances dissoutes, et que ce type de particules aurait un rôle potentiellement important dans les écosystèmes marins (Wiebe & Pomeroy 1972, Jensen & Søndergaard 1982, Johnson et al. 1986, Kepkay & Johnson 1988). Cependant, cette voie de transformation a été largement ignorée du fait que les techniques de visualisation et de quantification de ces particules n'étaient pas encore développées. Cette idée n'a été renforcée qu'à partir de la découverte et de l'étude des particules exopolymériques transparentes (TEP, de l'anglais « Transparent exopolymer particles ») en 1993, après la mise au point de la méthode d'analyse développée par Alice Alldredge (1993) et son équipe.

La dichotomie traditionnelle entre COP versus COD a été remplacée par le concept de continuum du carbone organique (Azam et al. 1994, Verdugo et al. 2004), et cela par la mise en évidence de plusieurs classes de substances polymériques extracellulaires (EPS, de l'anglais « exopolymeric substances »), telles que les colloïdes, les particules submicrométriques, et les TEP (Wells & Goldberg 1992, Kepkay 1994, Kepkay et al. 1997, Kumar et al. 1998, Wells 1998, Stoderegger & Herndl 1999, Passow 2000, Ramaiah et al. 2001, Passow 2002a, Bhaskar & Bhosle 2005, Underwood 2006). En fait, il a été suggéré que la quantité des TEP dans les océans, composés en majorité de polysaccharides, est entre 35 à 70 fois supérieures à celle estimée pour le COP (Verdugo et al. 2004).

Les TEP sont définies comme des particules gélatineuses transparentes. Elles sont formées de précurseurs dissous composés majoritairement de polysaccharides acides (APS, de l'anglais « Acid polysaccharides ») (Passow 2001). Ces précurseurs sont exsudés par le phytoplancton (Grossart et al. 1997, Passow 2001, 2002a b) et dans une moindre mesure par les bactéries via le détachement des enveloppes exopolymère ou des biofilms (Decho 1990, Schuster & Herndl 1995). Il s'agit alors d'une conversion directe de COD en COP.

Les TEP représentent donc un important réservoir de COP (de Vicente et al. 2009b) qui peut contribuer significativement à l'exportation du carbone organique de la surface vers le fond des océans. Leur formation abiotique et leur introduction dans la chaîne trophique représenteraient une dérivation de la boucle microbienne, rendant encore plus complexe la vision du réseau trophique pélagique. Cette nouvelle voie de transfert du carbone est nommée « réseau basé sur l'agrégation » (« aggregation web ») (Passow 2002b; Fig. 1).

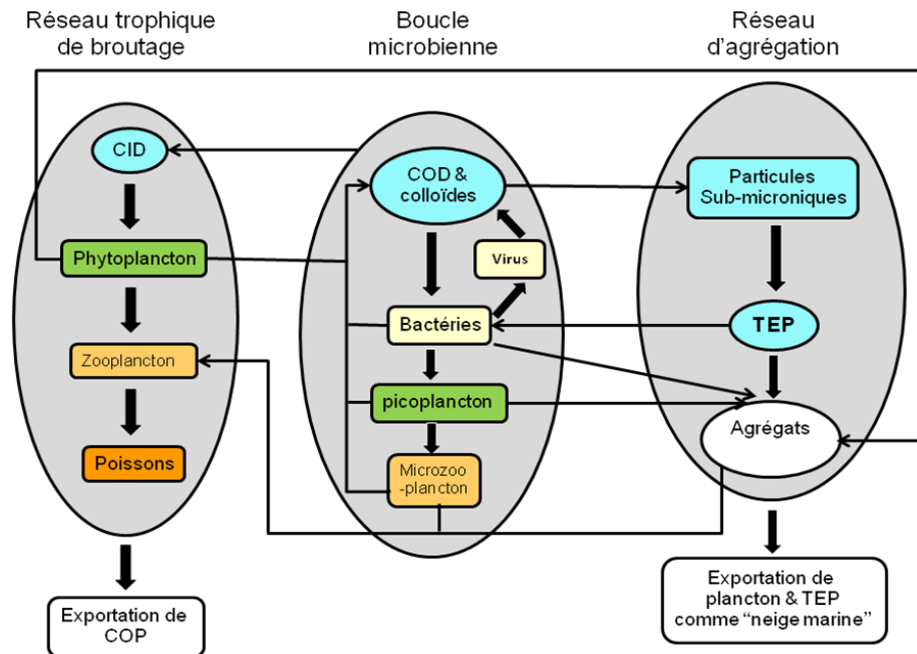


Figure 1 : Changements dans les concepts concernant les flux de carbone entre les organismes et particules non vivantes, illustrant la chaîne alimentaire linéaire de broutage, la boucle microbienne et le réseau basé sur les processus d'agrégation. Schéma modifié à partir de Passow (2002b)

Dans ce réseau d'agrégation, les TEP agissent comme une matrice interstitielle grâce à leur grande propriété adhésive¹ (de l'anglais « stickness ») pour former des agrégats macroscopiques (neige marine) (Engel 2000, de Vicente et al. 2009 b, Mari et al. 2017).

¹ Adhésion : Le degré pour lequel des particules marines adhèrent ensemble est caractérisé par le coefficient d'adhérence (α), qui est défini comme la probabilité que deux particules adhèrent lors de la collision. L'adhésion intraspécifique se rapporte à l'interaction entre des particules similaires (ex. : deux particules de TEP ou deux cellules de la même espèce de phytoplancton) et l'adhérence interspécifique réfère à l'interaction entre différents types de particules (ex. : une particule TEP et une cellule de phytoplancton).

Elles contribuent à la liaison entre les particules organiques vivantes et non vivantes, en incluant les microorganismes de la boucle microbienne et d'autres petites cellules telles que le pico- (0,2-2 μm) et le nanophytoplancton (2-20 μm), rendant leur densité suffisamment élevée pour sédimenter (effet ballaste). Ce processus facilite la perte de particules formées dans les eaux de surface, ainsi les TEP contribuent à la sédimentation rapide du phytoplancton et d'autres petites particules facilitant les flux verticaux de carbone (Passow 2002b). Il faut noter que $\sim 10\%$ du COD de l'océan de surface peut être assemblé pour former des TEP, ce qui donne $\sim 70 \times 10^{15}$ g de carbone organique (Verdugo et al. 2004a). D'autre part, elles rendent disponibles (« bypass », dans la littérature) au mésozooplancton des proies qui ne l'étaient pas sous forme libre, du fait de leur petite taille. Une telle composition représente une source potentielle de nourriture riche pour les organismes de plus grandes tailles (Grossart et al. 1997). Par conséquent, la production du COD par le phytoplancton représente aussi une connexion entre la boucle microbienne et les niveaux supérieurs du réseau trophique marin.

Durant les dernières décennies, plusieurs recherches ont montré que les TEP sont souvent composées à plus de 50 % par de la biomasse bactérienne (Riemann et al. 2000), ainsi que d'autres microorganismes. De plus, elles sont également le siège de divers processus microbiens souvent intenses, tels que la production primaire photosynthétique et microbienne et la reminéralisation qui résulte principalement des propriétés propres aux agrégats (Alldredge & Gotschalk 1990). De ce fait, elles jouent un rôle très important dans le cycle du carbone et des nutriments (Grossart et al. 1997), ainsi que dans la dynamique des réseaux trophiques. Il est donc essentiel de les quantifier et d'étudier leur contribution aux flux de carbone dans l'océan.

La formation des TEP dépend de la quantité de polysaccharides extracellulaires présents dans le milieu. Il a été proposé par certains auteurs que l'exsudation résulte d'un déséquilibre temporaire du carbone cellulaire par un débordement métabolique. Bratbak & Thingstad (1985) considèrent la libération des produits de la photosynthèse en condition de limitation en nutriments comme une situation paradoxale. En effet, le phytoplancton libère

sous condition de faibles teneurs en nutriments de la matière organique (MO) susceptible de favoriser les bactéries, qui sont en potentielle compétition pour les éléments nutritifs dans le milieu marin. Wood & Van Valen (1990) considèrent quant à eux que le gain physiologique d'excrétion sous des conditions de lumière intense et faible en nutriments ne favorise pas la sélection naturelle, sauf si les avantages globaux de la cellule l'emportent sur les coûts. Ils se concentrent sur la nécessité de la cellule d'utiliser l'excédent d'énergie qui est produite, en raison de l'incapacité du phytoplancton d'arrêter la photosynthèse aux fortes intensités lumineuses. Wood & Van Valen (1990) suggèrent que la limitation des nutriments empêche l'accumulation de biomasse, mais pas la photosynthèse de sorte que le carbone est libéré sous forme de COD. Ces auteurs ont donc émis l'hypothèse que cette production de carbone est un mécanisme de protection de l'appareil photosynthétique en condition d'abondance d'énergie lumineuse par rapport à la disponibilité des nutriments. Il semble que c'est une adaptation du phytoplancton qui n'est donc pas en compétition directe avec les bactéries pour les éléments nutritifs au moment de la libération des carbohydrates (Wood & Van Valen 1990). D'autre part, le coût nutritionnel de la libération des carbohydrates doit être également négligeable, puisque le carbone est rarement limitant pour la croissance phytoplanctonique dans les eaux douces et marines (Harris 1980) et la réaction photochimique de la photosynthèse produite de l'ATP et du NADH, typiquement deux sources d'énergie biochimique (Govindjee & Braun 1974).

1.2 ORIGINE ET FORMATION DES TEP

De nombreux organismes marins, incluant le phytoplancton (Alldredge et al. 1993), les bactéries (Simon et al. 2002), le zooplancton et les organismes benthiques génèrent des polysaccharides extracellulaires dissouts, via l'exsudation ou le broutage (Myklestad 1995, Stoderegger & Herndl 1999, Passow 2002b, Heinonen et al. 2007). Pour ce qui est du phytoplancton, les diatomées sont particulièrement bien connues pour exsuder de grandes quantités d'EPS durant toutes les phases de leur cycle de vie (Passow 2002b, Fukao et al. 2010). Le phytoplancton peut aussi produire des particules polysaccharidiques condensées,

sous forme de microgels dans l'eau de mer (Chin et al. 2004). D'autre part, les bactéries libres produisent également des EPS, et peuvent donc être une importante source de microagrégats en dehors des périodes de floraison phytoplanctonique (Stoderegger & Herndl 1999).

À l'échelle cellulaire, l'absorption du carbone se poursuit même lorsque l'acquisition des éléments nutritifs limite la production de biomasse, mais pas la photosynthèse (Fig. 2). Une des conséquences de cet excès d'assimilation de carbone est l'exsudation extracellulaire de la MOD avec un rapport C/N élevé (Engel et al. 2004a). La coagulation de cet excès de MOD riche en carbone produit ainsi un réservoir des TEP naturellement riche en carbone, mais pauvre en azote (rapport C/N élevé > 20 à 40) (Engel & Passow 2001, Mari et al. 2001). Ce processus d'exsudation est considéré comme un « débordement » de carbone cellulaire par lequel les cellules phytoplanctoniques disposent des produits de la photosynthèse en excès dans des conditions de limitation en nutriments (Jensen & Søndergaard 1982, Toggweiler 1993, Obernosterer & Herndl 1995). Ceci, résulterait en la formation d'un grand réservoir de matière organique circulant dans l'océan dont le rapport C/N est très élevé.

La production d'EPS représente une fraction considérable du carbone fixé lors de la photosynthèse. En effet, les EPS peuvent représenter jusqu'à 58 % de la production primaire (Nagata 2000) qui vient enrichir le réservoir océanique du COD. Ces EPS, composés essentiellement d'APS, sont capables de s'agréger spontanément par coagulation² et/ou agrégation³ pour former des TEP (Fig. 2). Chin et al. (1998) ont démontré que le COD pouvait s'assembler spontanément pour former des microgels atteignant des tailles de l'ordre du micromètre. Ce réservoir de carbone organique est constitué par les colloïdes et les TEP. En effet, une fois libérés dans les eaux environnantes,

2 Coagulation : processus physico-chimique qui colle les particules entre elles par adhésion.

3 Agrégation : processus physique dans lequel les microparticules entrent en collision et restent collées les unes aux autres pour former des amas de particules appelées agrégats.

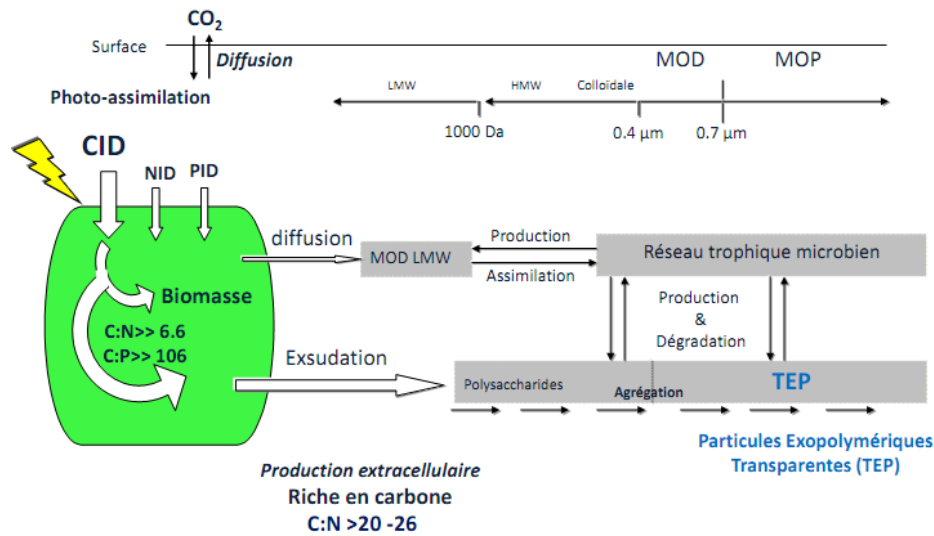


Figure 2 : Modèle conceptuel représentant les voies possibles de la matière organique produite par les cellules autotrophes. Sous l'hypothèse de surconsommation du carbone inorganique dissous (CID) par rapport à l'absorption de l'azote (NID) ou le phosphore inorganique dissous (PID), une fraction du carbone organique intracellulaire accumulée est libérée de la cellule par des processus de diffusion et/ou d'exsudation. En fonction de sa qualité, le carbone organique extracellulaire peut entrer dans le réseau trophique microbien ou bien être agrégé pour former des particules, telles que les TEP (modifié d'après Engel et al. 2004).

par voie active (exsudation) ou passive (diffusion ou lyse cellulaire), ces précurseurs dissous peuvent prendre de nombreuses formes (Kepkay 2000). Fréquemment, ils se présentent sous forme de microfibrilles riches en polysaccharides de poids moléculaire élevé (100-300 kDa; Decho 1990, Mykkestad 1995). Cependant, Bhaskar & Bhosle (2005) ont rapporté que ces précurseurs dissous pouvaient aussi avoir un poids moléculaire plus faible compris entre 10 à 30 kDa. Ces exopolymères dissous vont ensuite s'aligner et se lier par l'intermédiaire des ponts cationiques (Ca^{2+} et Mg^{2+}), et coaguler spontanément en microfibrilles de taille variant de 1 à 100 nm (Alldredge et al. 1993, Chin et al. 1998). La coagulation se poursuit par la formation de colloïdes de taille submicrométrique sous forme de réseaux de polymères enchevêtrés tridimensionnels (Chin et al. 1998), et se terminent par la formation des TEP, de taille supérieure (Fig. 3).

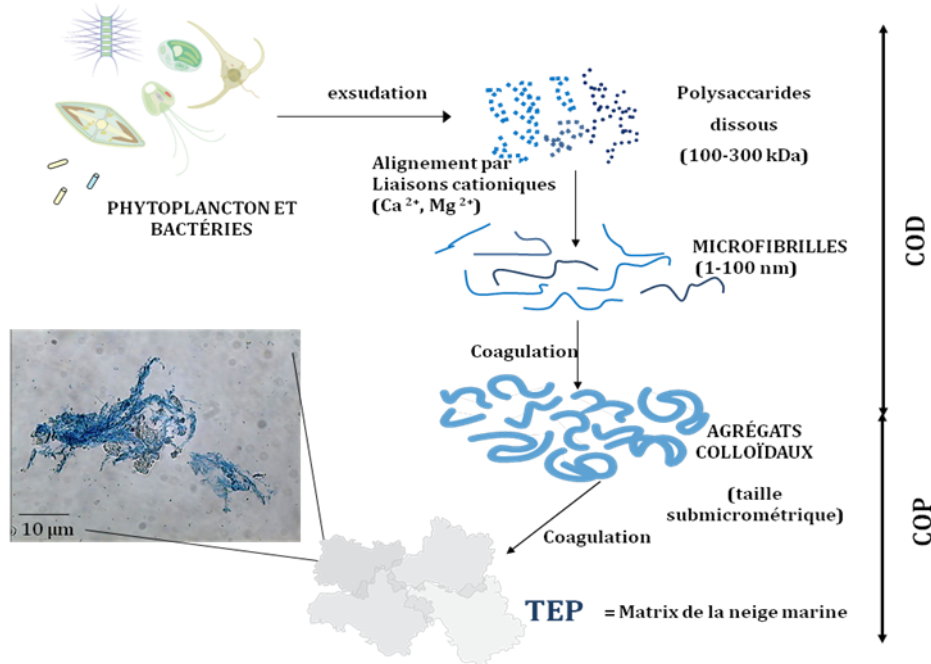


Figure 3 : Concept de la formation abiotique des particules exopolymériques transparentes (TEP) à partir de leurs précurseurs. Les TEP et leurs précurseurs existent dans un continuum de taille, de la fraction colloïdale à la fraction particulaire. Schéma modifié de Beauvais (2003)

Par ce processus, il y a donc une transformation spontanée du COD en COP (Kepkay 1994), tel que décrit précédemment. La définition de la taille des TEP varie dans la littérature selon la méthodologie utilisée. Certains auteurs considèrent la taille des TEP varie entre 0,7 et 200 μm (Mari & Burd 1998), alors que dans d'autres études les TEP sont considérées entre 1 μm et 1 mm de long (Passow 2002b, Fatibello et al. 2004). Cependant, les méthodes colorimétriques usuelles d'analyse de ce type de particules impliquent de travailler sur de la matière retenue sur des filtres de 0,2 ou 0,4 μm (Passow & Alldredge 1995a, Passow 2002a, Bhaskar & Bhosle 2008, Wetz et al. 2009, Sun et al. 2012).

De nombreuses études ont montré que le processus de formation des TEP dépendait de différents paramètres abiotiques et biotiques, incluant des facteurs chimiques (la densité des ions, le pH, le type et la concentration des précurseurs présents et les propriétés adhésives des précurseurs) (Passow et al. 2001), des facteurs physiques (la turbulence : la

fréquence de collision, la vitesse de sédimentation, la densité des particules dans le milieu) (Beauvais et al. 2003), ainsi que des facteurs biologiques, qui dépendent de la composition de la communauté et de l'état physiologique des organismes (Grossart et al. 1997, Passow 2002b).

Certaines études ont montré que la présence des ions divalents dans l'eau de mer était très importante pour la formation des microgels. En effet, il a été mis en évidence que la concentration de cations divalents (Ca^{2+} et Mg^{2+}) pouvait favoriser la stabilisation de la matrice des TEP en créant des liens macromoléculaires (Passow 2002b, Li et al. 2013, Meng & Liu 2016), notamment par la formation de ponts cationiques et des liaisons hydrogène (Chin et al. 1998). En revanche, la présence d'EDTA (éthylènediamine -tétracétique acide; 0,1-1 M), un agent chélateur de Ca^{2+} et Mg^{2+} peut désagréger rapidement la structure des TEP (Alldredge et al. 1993, Chin et al. 1998, Li et al. 2013). D'autre part, il a été montré que la diminution du pH peut réduire le nombre de liaisons hydrogène inter et intrachaine par la protonation des groupes carboxyliques et ainsi empêcher la formation des ponts cationiques entre les groupes carboxyliques et les ions Ca^{2+} et Mg^{2+} (Li et al. 2013). Ceci résulte en une réversibilité d'état de phase des TEP, entre les phases hydratées et désagrégées (Li & Tanaka 1992) et une phase condensée influencent leur volume et densité (Chin et al. 1998)

Il semble également que l'intensité de la turbulence favorise grandement la production des TEP (Beauvais et al. 2006). En effet, l'énergie cinétique turbulente permet d'augmenter la fréquence des collisions entre les particules de taille supérieure à quelques μm , ce qu'on appelle « l'agrégation » (Verdugo et al. 2004). Les collisions répétitives dues aux mouvements browniens et/ou de cisaillement (à la fois laminaire et turbulent) génèrent des agrégats de plus en plus grands ce qui peut alors induire la coagulation par adhésion des particules (Kepkay 1994).

En ce qui concerne la formation biotique des TEP, plusieurs travaux en mésocosmes et en milieu naturel ont montré une forte production des TEP et de leurs précurseurs durant et après les efflorescences phytoplanctoniques de communauté dominées par les diatomées

(Passow & Alldredge 1995b, Mari & Kiørboe 1996, Grossart et al. 1997, Mari & Burd 1998, Passow et al. 2001, Engel 2002), et en conditions oligotrophes (Mari et al. 2005).

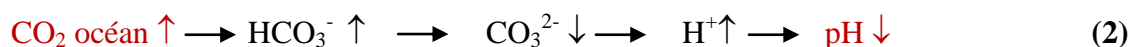
1.3 PROBLÉMATIQUE ET PLAN DE LA THÈSE

La distribution des TEP est encore très mal connue notamment dans le écosystème marin Saint-Laurent. En fait à l'heure actuelle il n'existe aucun résultat publié sur la production en TEP ou en EPS dans l'EMSL. Toutefois, on pense que les TEP pourraient être un important réservoir de carbone dans cet écosystème hautement dynamique et productif. En effet, l'EMSL possède une production primaire élevée (Le Fouest et al. 2005). Cette production primaire est dominée surtout par du phytoplancton de grande taille, en particulier des diatomées telles que *Skeletonema costatum*, *Thalassiosira* spp. et *Chaetoceros* spp., (Levasseur et al. 1984, Roy et al. 1997). Cette forte productivité primaire est supportée par les remontées des eaux à la tête du chenal Laurentien aux environs de Tadoussac (Ingram 1975, Therriault & Lacroix 1976, Savenkoff et al. 1997a). Ceci résulte en un mélange important d'eaux proches de la surface riche en nutriments qui coulent en continu le long de l'EMSL (Saucier & Chassé 2000, Dufour & Ouellet 2007) et qui soutient des floraisons phytoplanctoniques successives (Levasseur et al. 1984, Savenkoff et al. 1997a, Starr et al. 2004). Ces floraisons massives de diatomées sont généralement connues pour produire une grande quantité d'EPS, qui peut s'agréger et être exportée vers les eaux profondes. D'ailleurs, dans des travaux antérieurs menés dans le golfe du Saint-Laurent, il a été estimé que la contribution de la neige marine au flux de C total serait plus de 60 % dans les pièges à sédiments déployés à 150 m (Romero et al. 2000, Romero-Ibarra & Silverberg 2011, Genin et al. 2021). Ce type de processus pourrait donc contribuer significativement au phénomène d'hypoxie observé dans les eaux de fond de l'estuaire et le golfe du Saint-Laurent depuis quelques décennies (Gilbert et al. 2007).

Enfin, les TEP peuvent être un élément important du cycle du carbone estuarien, car leur concentration tend à augmenter le long des gradients de productivité de l'océan vers les régions côtières. Il y a donc fort à parier que la concentration des TEP serait encore plus élevée dans les estuaires (Nixon 1995). Thibodeau et al. (2006) ont d'ailleurs montré à partir de carottes de sédiment prélevées dans deux sites dans l'EMSL, que les flux de carbone organique semblent s'être accélérés au cours des dernières décennies. Les TEP représenteraient une fraction significative du réservoir du COP dans l'EMSL.

Les activités anthropiques telles que l'utilisation des combustibles fossiles et les changements dans l'utilisation des sols ont augmenté le taux de $p\text{CO}_2$ atmosphérique à un rythme sans précédent. Environ, la moitié des émissions anthropiques de CO_2 entre 1750 et 2011 ont eu lieu au cours des 40 dernières années (IPCC, 2014). Les modèles d'émissions de CO_2 prévoient une augmentation du $p\text{CO}_2$ atmosphérique de 400 à 750 μatm (scénario IP92) ou même $>1300 \mu\text{atm}$ (IPCC, 2014) à la fin de ce siècle. L'océan a absorbé environ 30 % du CO_2 anthropogène émis depuis le début de l'ère industrielle par différents processus, servant de tampon aux changements climatiques mondiaux (Sabine et al. 2004). Ce carbone atmosphérique est transféré et immobilisé dans l'océan par des processus chimiques (pompe des carbonates), physiques (mélange vertical en surface) et biologiques (pompe biologique). Ce dernier joue un rôle fondamental dans le cycle du carbone de l'océan, car il aide à transformer le dioxyde de carbone (CO_2) atmosphérique en COP par la « photosynthèse », et à sa séquestration dans le fond de l'océan après sédimentation de façon temporaire ou permanente. Le phytoplancton, principal consommateur du CID par le processus de « photosynthèse », est responsable d'environ 50 % de la production primaire globale (Field et al. 1998). Il utilise donc le CO_2 , l'énergie solaire, l'eau et les sels nutritifs pour produire de l'oxygène et de la matière organique, indispensable au fonctionnement des écosystèmes marins. Cette utilisation du CO_2 par le phytoplancton réduit la concentration de ce composé dans la couche de surface et crée donc un gradient négatif par rapport à l'atmosphère, contribuant aux processus physiques et chimiques qui modulent les flux du CO_2 entre l'atmosphère et l'océan.

En raison des échanges océan-atmosphère, l'augmentation des niveaux de CO₂ atmosphérique s'accompagne d'une augmentation concomitante du CO₂ dans les eaux de surface océaniques, ce qui conduit à une redistribution dans le réservoir du CID océanique (Schulz et al. 2008). Ces processus produisent des altérations du système carbonaté de l'océan (Équation 1), entraînant une diminution du pH de l'eau de mer et une baisse de l'état de saturation des carbonates (Wolf-Gladrow et al. 1999, Zeebe & Wolf-Gladrow 2001, Rost et al. 2008). En fait, ces processus ont déjà modifié chimiquement l'océan, entraînant des concentrations plus élevées de CO₂ (aq) et de HCO₃⁻, de faibles concentrations de CO₃²⁻ et une chute du pH associée (Équation 2), appelée globalement « acidification des océans » (Doney et al. 2009). Le pH de la surface océanique a déjà diminué de 0,12 unités par rapport aux valeurs préindustrielles, ce qui correspond à une augmentation de l'acidité de 30 %, mesurées par la concentration en ions hydrogène [H⁺] (Sabine et al. 2004, Raven et al. 2005, Richardson & Gibbons 2008). Une intensification est prévue à l'avenir pour atteindre une réduction supplémentaire d'environ 0,4 unités d'ici à la fin du 21^e siècle dans le cadre du scénario « business as usual » (Caldeira & Wickett 2003, Orr, 2011). Selon Caldeira & Wickett (2003), les valeurs de pH pourraient même diminuer de 0,7 unités au cours des deux prochains siècles, ce qui serait plus que ce que la vie marine a connu durant les derniers 300 millions d'années.



L'acidification des océans pourrait engendrer des effets importants sur les processus biologiques ainsi que sur les cycles du carbone et des nutriments (Gattuso et al. 2011). Les organismes planctoniques marins pourraient être affectés par les changements de pH et pCO₂, au niveau de la physiologie, de la composition des espèces et des conséquences sur le cycle du carbone (Boyd & Doney 2002, Tortell et al. 2002, Beardall & Raven 2004, Engel et al. 2008). En effet, la plupart des espèces phytoplanctoniques dans l'océan actuel possèdent des mécanismes de concentration de CO₂ (CCM) pour compenser la faible affinité de la RUBISCO pour le CO₂ et saturent la photosynthèse (Giordano et al. 2005).

Dans un environnement à teneur élevée en CO₂, ce mécanisme peut abaisser le coût métabolique du phytoplancton pour l'acquisition du CID, ce qui augmente le taux de croissance et la production primaire (Engel et al. 2008, Rost et al. 2008). Cependant, cette efficacité des CCM varie selon les groupes de phytoplancton rendant les prévisions de l'impact d'une augmentation de CO₂ sur la régulation de la CCM plutôt difficiles (Rost et al. 2008, Raven et al. 2014). D'autre part, la chute prévue de 0,4 unité pH se traduirait par une augmentation de 150 % de la concentration d'ions H⁺ (Orr et al. 2005), ce qui pourrait affecter le pH intracellulaire (pH_i) ainsi que les processus physiologiques des organismes tels que le potentiel membranaire, le transport d'ions, le partitionnement énergétique, l'activité enzymatique, les fonctions protéiques et l'absorption de nutriments (Nimer et al. 1994, Riebesell 2004, Giordano et al. 2005, Gattuso & Hansson 2011). En conséquence, les taux de croissance et la productivité du phytoplancton peuvent être affectés directement par une variation du pH (Berge et al. 2010). Par conséquent, les prédictions des réponses des communautés phytoplanctoniques à l'acidification sont difficiles à prévoir surtout dans un écosystème estuarien.

D'autre part, l'augmentation de CO₂, associée à d'autres gaz à effets de serre, entraîne également une augmentation des températures moyennes mondiales (Meehl et al. 2007, Schulz et al. 2008). Par conséquent, on prévoit une augmentation globale de la température de l'eau de surface (SST de l'anglais : Sea surface temperature) entre 2 et 6 °C d'ici à la fin du siècle selon le scénario d'émissions hypothétiques (IPCC, 2014). En outre, on a estimé que la hausse de température pourrait favoriser la stratification et diminuer la couche de mélange de surface qui, à son tour, pourrait indirectement affecter la production du phytoplancton et la structure des communautés algales en limitant l'apport en nutriments à partir des couches plus profondes (Sarmiento et al. 2004, Doney 2006).

Le réchauffement des océans affectera les niveaux d'organisation biologique, de l'individu à l'écosystème, puisque la température est un facteur clé de régulation des processus métaboliques (Falkowski et al. 1998, Boyd & Doney 2002). Cependant, l'effet du réchauffement sur le cycle du carbone représente l'un des impacts les plus importants

sur les écosystèmes marins. En raison des différences de sensibilité à la température des organismes autotrophes et hétérotrophes, on peut s'attendre à des changements dans l'équilibre entre la production primaire et la reminéralisation de la matière organique, ce qui pourrait changer les cycles biogéochimiques dans les océans (Wohlers et al. 2009, Riebesell et al. 2009, Yvon-Durocher et al. 2010). Ces réponses aux effets du réchauffement sont contrastantes, mais une certaine tendance se dégage néanmoins. En général, les processus autotrophes comme la croissance du phytoplancton ont une sensibilité plus faible aux changements de température que les processus hétérotrophes (Biermann et al. 2014, Taucher et al. 2015). Par exemple, la respiration bactérienne, qui se fait à des taux plus rapides que la production primaire, peut donner comme résultat des modifications dans les flux de carbone et une réduction de la séquestration du carbone (Yvon-Durocher et al. 2010). En outre, Wohlers et al. (2009) ont montré qu'en plus de l'augmentation de la respiration bactérienne, on verra une augmentation concomitante du COD en réponse au réchauffement. Par conséquent, ces auteurs ont suggéré que, dans des conditions de réchauffement, le carbone produit en excès sera stocké dans la masse dissoute au lieu d'être sédimenté à travers le compartiment particulaire, ce qui affaiblirait la pompe de carbone biologique de l'océan et donc constitue une rétroaction positive à la hausse CO₂ atmosphérique.

Le réchauffement et l'acidification affecteront inévitablement la production des TEP. Cependant, l'effet du réchauffement sur la production des TEP reste incertain et sujet à débat. Certaines études *in vitro* ont montré une stimulation de l'accumulation des TEP et d'agrégation de matière organique pour certaines espèces de diatomées et prymnésiophyces (Thornton & Thake 1998, Claquin et al. 2008). Cependant, Taucher et al. (2015) ont montré qu'un réchauffement de 15 °C à 20 °C a eu des effets stimulant sur l'accumulation des TEP pour *Thalassiosira weissflogii* alors qu'il a agi comme un stresser pour *Dactyliosolen fragilissimus*. Ceci montre l'importance d'optimum physiologique d'intervalle de température de l'espèce et/ou de la communauté concernée en réponse au réchauffement. Dans des expériences en mésocosmes Wohlers et al (2009) et Biermann et al (2014) ont montré une augmentation des concentrations des TEP, tandis que la matière

organique particulaire (MOP) et la perte de carbone par sédimentation étaient réduites à des températures élevées. Ce qui montre une limitation du potentiel d'exportation de particules via les TEP. La mesure dans laquelle une formation accrue de TEP pourrait affecter la sédimentation des particules dans des conditions de réchauffement dépend du moment critique de la formation des TEP et de l'interaction avec d'autres processus biologiques (comme la dégradation microbienne et le broutage).

D'autre part, les précédentes expériences portant sur l'effet de l'acidification sur la formation des TEP ont adopté une gamme d'approches différentes selon qu'ils ont utilisé une seule espèce de phytoplancton ou un assemblage naturel et selon qu'ils ont stimulé ou non la croissance par l'ajout d'éléments nutritifs (MacGilchrist et al. 2014). Cependant ces expériences ont montré des résultats plus cohérents. Des expériences d'incubation de Engel (2002) ont permis d'observer une augmentation de la production de TEP à une concentration plus élevée de $p\text{CO}_2$ dans un assemblage phytoplanctonique naturel dans des eaux limitées en nitrates. Des expériences en mésocosme ont suggéré qu'une assimilation plus élevée du carbone dans la matière organique à un taux élevé de CO_2 pourrait augmenter la libération de matière organique extracellulaire des cellules phytoplanctoniques (Engel 2002, Kim et al. 2011, Engel et al. 2014). Cette « surconsommation de carbone » s'est traduite par la formation de grandes quantités de TEP qui peuvent accroître l'exportation verticale du COP par agrégation (Engel 2002, Engel et al. 2004, Riebesell et al. 2007). En effet, Riebesell et al. (2007) ont démontré que la pompe biologique peut s'intensifier sous des conditions d'élévation de CO_2 , et donc créer une rétroaction négative par rapport à l'augmentation du CO_2 atmosphérique (Engel et al. 2004a, Arrigo 2007, Engel et al. 2014). En réponse à cela, Arrigo (2007) a émis l'hypothèse soutenant que dans un océan saturé en CO_2 , la formation des TEP contribuera significativement au « pompage biologique » du CO_2 , en amplifiant l'exportation du COP. Cette hypothèse a été confirmée par Schulz et al. (2008) dans une autre expérience en mésocosme, suggérant que l'exportation de carbone organique vers la couche profonde est considérablement renforcée dans des conditions de CO_2 élevé par l'agrégation et la

formation de neige marine. Cela nous laisserait croire que la formation accrues des TEP pourrait contribuer significativement à l'accumulation du POC.

Cependant, nous avons des connaissances limitées sur la façon dont les effets combinés du réchauffement et de l'acidification (p. ex. synergiques, antagonistes ou additifs) peuvent affecter les processus physiologiques comme l'assimilation du carbone, le métabolisme et l'exsudation du carbone. En particulier, on manque d'information sur la façon dont ces facteurs de stress affecteront la matière organique particulaire, et en particulier la formation des TEP.

L'objectif central de cette thèse est de caractériser la dynamique des TEP dans le cycle du carbone et étudier les impacts des facteurs environnementaux (dans des scénarios présent et futur) influençant la production des TEP. L'un des buts à court terme était de combler cette lacune et de documenter la dynamique des TEP et leurs relations avec le réservoir de carbone particulaire dans l'EMSL, ainsi que d'explorer quelques facteurs environnementaux qui pourraient contrôler leur formation. Ensuite, l'accent a été mis en particulier sur la compréhension des effets futurs de l'acidification sur la production des TEP, la communauté planctonique et de la dynamique du carbone organique dans l'EMSL. Ces réponses ont été comparées à ceux des effets de l'acidification et du réchauffement dans l'écosystème de Méditerranée et sur les implications potentielles dans ces deux écosystèmes (mésotrophe et oligotrophe) à deux latitudes différentes (subarctique et subtropical). En effet, on dispose de peu sur la façon dont les effets du réchauffement et de l'acidification pourraient affecter des processus physiologiques tels que l'assimilation du carbone, l'exsudation du carbone et son devenir ainsi que sa rétroaction possible sur le climat futur.

Cette thèse est divisée en trois chapitres suivis d'une conclusion générale et d'une section sur les perspectives de recherche.

Le chapitre 1 est consacré à l'étude des TEP dans le système estuarien du Saint-Laurent. L'objectif du chapitre est d'étudier la distribution verticale et la variabilité

saisonnaire des TEP, identifier les facteurs influençant leur formation, ainsi que d'estimer leur contribution au réservoir de carbone organique dans la colonne d'eau de l'EMSL. Ce dernier, est l'un des grands systèmes estuariens sur terre et l'un des plus complexes d'un point de vue hydrologique. C'est également l'un des estuaires les plus étudiés. Cependant, malgré l'importance écologique et biogéochimique des TEP, aucune information n'est disponible sur leurs concentrations et variabilités temporelles. J'ai échantillonné sur base hebdomadaire à la station fixe (IML-4) afin d'examiner la distribution verticale et la variabilité saisonnière des TEP et leurs relations avec le réservoir de COP dans l'EMSL, ainsi que d'explorer quelques facteurs environnementaux qui pourraient contrôler leur formation. Cette étude m'a permis de tester l'hypothèse selon laquelle les TEP représentent une fraction significative du réservoir du COP dans l'EMSL.

Le chapitre 2 étudie les effets d'un gradient de pH sur les TEP et sur la communauté planctonique naturelle de l'EMSL à l'aide d'une expérience en microcosmes. L'objectif du chapitre est d'étudier l'effet de l'acidification sur la formation des TEP et l'ensemble de la communauté planctonique associée dans l'EMSL. Les estuaires et les milieux côtiers se caractérisent par la présence d'une grande variabilité des conditions physiques et chimiques. Le phytoplancton est ainsi exposé à une grande étendue de pH, aussi bien à l'échelle journalière que saisonnière à laquelle s'ajoute la tendance à long terme associée à l'augmentation du CO₂ atmosphérique. Ainsi, fort de nos résultats du premier chapitre concernant la caractérisation des TEP dans l'EMSL (source, accumulation et contribution au réservoir de POC), j'ai effectué une expérience cinétique en microcosme portant sur un gradient de pH afin d'examiner comment la production de TEP et la communauté planctonique et bactérienne sont affectées par l'acidification croissante dans le EMSL, et d'étudier ces effets sur la répartition du carbone particulaire dans cet écosystème subarctique. Cette étude m'a permis de tester l'hypothèse selon laquelle il y aurait une formation accrue des TEP qui contribuerait significativement à l'accumulation du carbone organique particulaire sous des conditions de CO₂ élevées dans l'EMSL.

Le chapitre 3 porte sur l'étude sur les effets séparés et combinés de l'acidification et du réchauffement sur la contribution du phytoplancton, bactéries et TEP au réservoir de carbone de la lagune de Thau, en Méditerranée. L'objectif du chapitre est d'étudier l'effet des changements globaux futurs (réchauffement et acidification) sur la formation des TEP et l'ensemble de la communauté planctonique en Méditerranée. Le réchauffement et l'acidification risquent d'affecter la dynamique du réseau trophique, et par conséquent le rôle de la pompe biologique, ce qui aura des implications sur le cycle du carbone dans l'océan. J'ai effectué une expérience en mésocosmes afin d'examiner comment la formation de TEP est affectée par l'augmentation de la température et/ou l'acidification dans un écosystème côtier méditerranéen peu profond. J'ai également examiné les effets distincts et combinés du réchauffement et de l'acidification sur l'allocation de carbone organique dans le système planctonique pélagique et discuté des effets possibles du changement climatique sur l'océan de demain. Cette étude m'a permis de tester les hypothèses selon lesquelles : (1) il y aurait une formation accrue des TEP qui contribuerait significativement à l'accumulation du COP sous des conditions de CO₂ élevées, et (2) la diminution des TEP réduirait l'accumulation du COP dans des conditions de réchauffement en Méditerranée.

CHAPITRE 1

CONTRIBUTION DES PARTICULES EXOPOLYMÉRIQUES TRANSPARENTES (TEP) AU RÉSERVOIR DE CARBONE ORGANIQUE PARTICULAIRE ESTUARIEN

Ce premier article, intitulé « *Contribution of transparent exopolymeric particles (TEP) to estuarine particulate organic carbon pool* », fut corédigé par moi-même ainsi que par le professeur Gustavo Ferreyra, ma collègue Liliane St-Amand et prof. Émilien Pelletier et Prof. Michel Starr. Il fut accepté pour publication dans sa version finale en 2015 par les éditeurs de la revue *Marine Ecology Progress Series*. En tant que premier auteur, ma contribution à ce travail fut l'essentiel de la recherche sur l'état de l'art, le travail de terrain et de laboratoire, les analyses statistiques et la rédaction de l'article. Le professeur Gustavo Ferreyra, chef de projet, le prof. Émilien Pelletier et le prof. Michel Starr ont fourni l'idée originale. Ils ont contribué à la révision de l'article. Liliane St-Amand a contribué au travail de terrain et laboratoire. Une version abrégée de cet article a été présentée à la conférence *Québec Océan* à Rivière du loup, QC, Canada à l'automne 2013.

1.1 RÉSUMÉ

Les particules exopolymériques transparentes (TEP) contribuent à l'exportation du carbone et peuvent représenter une fraction importante du réservoir de carbone, notamment dans les estuaires. Cette étude examine, pour la première fois, la variabilité saisonnière et la distribution verticale des TEP et leur contribution au réservoir de carbone dans l'estuaire maritime du Saint-Laurent (EMSL), un estuaire subarctique hautement productif. La variabilité des TEP a été étudiée sur une base hebdomadaire à la station fixe (IML-4) de mai à octobre 2011. Les TEP sont restées relativement faibles ($15 \mu\text{g GX eq l}^{-1}$) au printemps, mais ont augmentées de façon marquée en été et en automne, atteignant $1548 \mu\text{g GX eq l}^{-1}$. Les concentrations des TEP ont été corrélées positivement avec la biomasse du phytoplancton dans les eaux de surface. Aucune relation significative entre les TEP et d'autres facteurs biologiques et physico-chimiques n'a été trouvée. La teneur en TEP-C représentait la seconde fraction la plus importante dans le réservoir du carbone organique particulaire après le phytoplancton-C (41 et 54 %, respectivement) dans la couche de surface. La contribution de TEP-C a diminué dans les couches intermédiaires froides et de fond au cours de l'été et de l'automne (entre 24 et 35 %). Cependant, cette contribution a été particulièrement élevée au printemps (> 94 %) dans les couches intermédiaires froides et de fond, probablement en raison de la fraction du carbone organique colloïdal contribuant au TEP-C dans les eaux profondes. Nos résultats suggèrent que les TEP-C combinés au phytoplancton-C contribuent largement au réservoir de carbone et pourraient contribuer de manière significative à l'exportation ultérieure de macro-agrégats. Ceci pourrait en partie expliquer la diminution de la concentration d'oxygène et du pH dans la couche de fond de l'EMSL, en liaison avec les processus de respiration/reminéralisation.

1.2 CONTRIBUTION OF TRANSPARENT EXOPOLYMERIC PARTICLES (TEP) TO ESTUARINE PARTICULATE ORGANIC CARBON POOL

Authors:

Annane S.¹, St-Amand L.², Starr M.², Pelletier E.¹, Ferreyra G. A.¹

Institutions:

¹ Institut des sciences de la mer de Rimouski (ISMER), Université du Québec à Rimouski, Québec, 10 allée des Ursulines, Rimouski, Québec, Canada G5L 3A1

² Maurice Lamontagne Institute, Fisheries and Oceans Canada, 850 Route de la Mer, Mont-Joli, Québec, Canada G5H 3Z4

ABSTRACT

Transparent exopolymer particles (TEP) contribute to carbon export and can represent a significant fraction of the carbon pool, most notably in estuarine systems. This study investigates, for the first time, TEP seasonal variability, vertical distribution, and contribution to the carbon pool in the Lower St. Lawrence Estuary (LSLE), a highly productive subarctic estuary. TEP variability was investigated on a weekly basis at a fixed station (IML-4) from May to October 2011. TEP remained relatively low ($15 \mu\text{g GX eq l}^{-1}$) during spring, but increased markedly in summer and fall, with surface concentrations reaching up to $1548 \mu\text{g GX eq l}^{-1}$. TEP concentrations were positively correlated with the phytoplankton biomass in surface waters. No significant relationship between TEP and other biological and physico-chemical factors was found. TEP-C content represented the second most important contributor to the particulate organic carbon pool after phytoplankton-C (41 and 54 %, respectively) in the surface layer. The TEP-C contribution decreased in the cold intermediate and bottom layers over the summer and fall (ranging between 24 and 35 %). However, this contribution was particularly high during the spring (>94 %) in the cold intermediate and bottom layers, possibly due to the colloidal organic carbon fraction contributing to TEP-C in deep waters. Our results suggest that TEP-C combined with phytoplankton-C are major contributors to the carbon pool and could significantly contribute to the subsequent export of macro-aggregates, and probably explain the decrease in oxygen concentration and pH in the bottom layer of the LSOLE by respiration/ remineralisation processes.

Keywords: Transparent exopolymeric particles, TEP, Estuary, Phytoplankton, Particulate organic carbon, Bacteria, pH, Nutrients.

INTRODUCTION

Estuaries represent a narrow area of the total marine surface (0.3 %). However, these environments show high physical and biogeochemical complexity mainly related to organic particulate matter inputs from both terrestrial and marine sources. They are very important in terms of carbon fluxes, sequestration and export, and the study of their dynamics is essential for the estimation of global carbon budgets (Cai 2011). These ecosystems were traditionally considered as a net source of CO₂ to the atmosphere, due to their dominant heterotrophic activity (Borges et al. 2005, Hopkinson & Smith 2005). However, it has recently been suggested that estuaries can be mainly a sink for CO₂, if the total contribution of salt marshes and pelagic contributions are considered, in coincidence with the rapid advection of carbon in surface waters (Cai 2011). Despite that there exists a significant amount of information available, there is still a large uncertainty regarding the carbon budget of these environments due to their high variability and lack of understanding of significant aspects of their dynamics. In particular, the contribution of the transparent exopolymeric particles (TEP) fraction to the carbon pool is poorly understood and have been largely ignored in the build up of carbon budgets. TEP are ubiquitous gel particles present in the water column, playing a central role in sinking fluxes and food webs in aquatic ecosystems, formed abiotically by coagulation and aggregation from dissolved and colloidal precursors (Passow 2002b, Thornton 2002, Verdugo et al. 2004). These precursors are mainly composed of acid polysaccharides (Zhou et al. 1998a, Passow et al. 2001, Passow 2002b, Engel, Delille, et al. 2004, Wetz & Wheeler 2007) and are primarily produced by phytoplankton and bacterioplankton exudation (Grossart et al. 1997, Passow et al. 2001, Passow 2002b, a), constituting most of the colloidal organic carbon pool in the water column (Mari et al. 2009). Although classified as particles, TEP exhibit gel-like properties, including high flexibility, stickiness, and surface-active nature. These properties enable them to attach to each other and coagulate with other particles (i.e. bacteria, microzooplankton, phytoplankton and detritus) to promote the formation of larger organic aggregates (“marine snow”) (Passow et al. 2001, Simon et al. 2002b, Wetz et al. 2009,

Arnous et al. 2010). Marine snow represents a major contribution to the export of carbon from the surface to the deep ocean (Wurl & Holmes 2008).

While most research on TEP focused on their distribution in various marine and lake environments, few research studied their concentrations, distribution, and contribution to the particulate organic carbon pool in estuarine ecosystems. Estuaries are influenced not only by diurnal variability (i.e. tides) but also by seasonal river runoff and nutrients (Sun et al. 2012). They also present strong gradients in salinity, pH, metals, cations and turbulence, that alter the structure of exopolysaccharides (Mari & Burd 1998, Wetz et al. 2009). Therefore, these particles may exhibit wide temporal and spatial variations of their sticking properties within the estuarine domain, which in turn can affect the biogeochemical functioning of the system (Mari et al. 2012). The Estuary and Gulf of St. Lawrence is one of the largest estuarine systems on Earth ($> 230,000 \text{ km}^2$). However, despite their biogeochemical and ecological importance, no information is available about TEP concentrations and their contribution to the particulate organic carbon (POC) pool. Particularly, the Lower St-Lawrence estuary (LSLE) is the zone with the highest primary productivity and organic matter accumulation (Le Fouest et al. 2005). The hydrography of the LSLE is very complex and dynamic, with a surface estuarine circulation forced by mixing of seawater with high freshwater runoff discharging downstream through the St. Lawrence River (average flow: $12\,000 \text{ m}^3/\text{sec}$) and a deep inflow of oceanic water from the North Atlantic (Laurentian and Esquiman channels, depth 250-500 m) landward up the LSLE (Savenkoff et al. 2000, Thibodeau et al. 2006). This zone shows the maximum seaward advective surface (0-30 m) water transport (0.9 Sv; Savenkoff et al. 2001) compared with other zones of the system, and plays a significant role in the horizontal transport of particles (Zakardjian et al. 2000). The phytoplankton spring bloom is characterised by a high primary production, dominated by large cells mostly constituted by diatoms (Levasseur et al. 1984, Roy et al. 1997, Savenkoff et al. 2000, Vézina et al. 2000). Diatoms are especially well known for excreting copious quantities of polysaccharides during all phases of their growth (Passow & Alldredge 1995a, Mari & Kiørboe 1996, Passow 2002a) which can be partly advected seaward and also exported to bottom waters

as TEP integrating the marine snow. This process may further contribute to the hypoxia and increasing acidification observed in the bottom water (>250 m) since 1980's by fueling the benthic/pelagic respiration of organic carbon (Gilbert et al. 2005, Genovesi et al. 2011, Mucci et al. 2011).

The main goal of this work is to understand the status of TEP in highly dynamic estuaries, considering the LSLE as a case study. In this context, our specific research objectives were (1) to study the seasonal pattern and the vertical distribution of TEP and (2) to estimate their contribution to the organic particulate carbon pool.

MATERIALS AND METHODS

Study site and sampling strategy

Sampling was carried out at the Rimouski station (IML-4; 48°40' N, 68°35' W; ~340 m depth; Fig.1) in the Lower St. Lawrence Estuary (LSLE). This estuary is characterized by a semi-diurnal tidal regime, ranging between ~ 5.4 m and ~3.8 m for spring and neap tides, respectively (value above the minimum, Fisheries and Ocean Canada). The station was visited weekly from May to October 2011, as a part of the Atlantic Zone Monitoring Program (AZMP; Therriault et al. 1998), whenever climatic conditions were favourable. Seawater samples were collected using Niskin bottles (5 L) at 0.5, 5, 10, 15, 20, 25, 35, 50, 100, 200, 320 m depth and stored in isothermal containers in darkness until returned to the laboratory for processing (<2 h). The parameters measured were: TEP, chlorophyll *a* (Chl *a*) and particulate organic carbon (POC) concentrations, bacterial abundance (BA), phytoplankton composition and abundance, pH levels and nutrient concentrations. Vertical profiles of salinity, temperature, fluorescence, and oxygen content were measured at each sampling day using a Sea-Bird 19plus CTD, whereas a Secchi disk was used to determine the light attenuation in the water column.

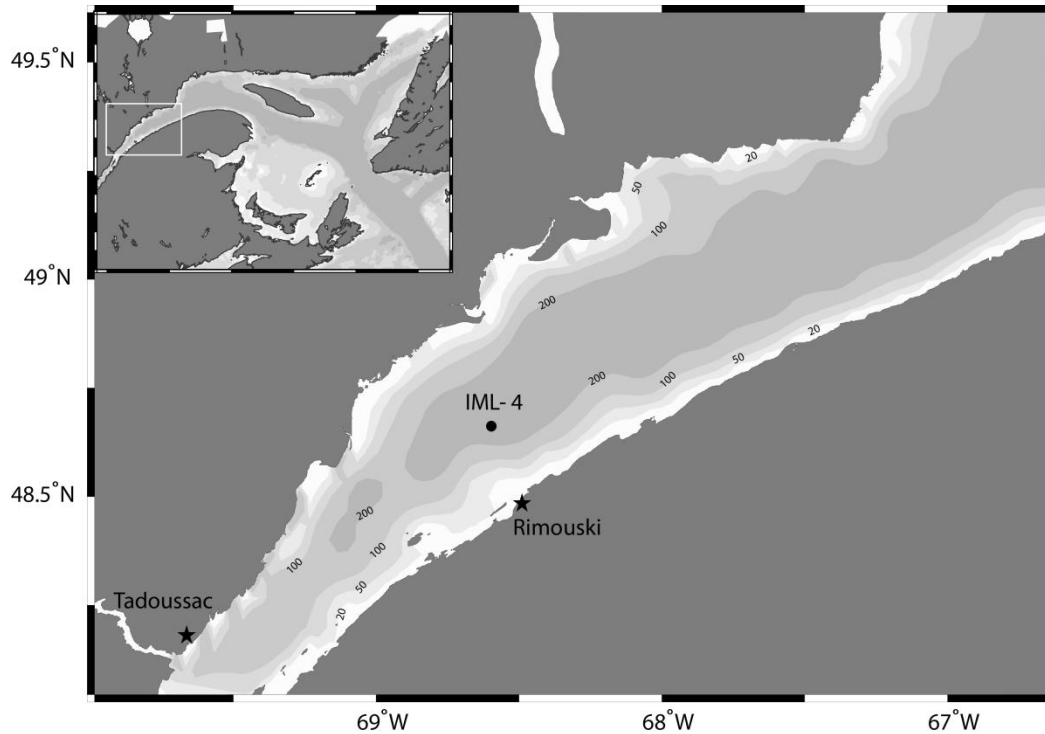


Figure 1 : Map showing the location of the Rimouski fixed sampling station (IML-4) in the Lower St. Lawrence Estuary

Chemical and biological analyses

TEP concentration was determined colorimetrically following the procedure described in Passow & Alldredge (1995). Briefly, 40-200 mL samples (depending on particle concentration) were filtered onto 0.2 μm polycarbonate Isopore membrane filters (Merck Millipore) under low vacuum (<10 mbar). Particles retained on the filters were stained for <5 s with 500 μl of 0.02 % aqueous solution of Alcian blue in 0.06 % acetic acid (pH 2.5) and subsequently rinsed with 1 mL of deionised water. Filters were then soaked in 80 % sulphuric acid (6 mL) for 2 h and measured spectrometrically at 787 nm, using stained filters without sample as blanks. Alcian Blue absorption was calibrated using a solution of the polysaccharide Gum Xanthan. TEP concentrations were expressed in μg

Gum Xanthan equivalents per liter ($\mu\text{g GX eq L}^{-1}$). These values were converted into carbon equivalent units using a natural diatom population conversion factor of $0.75 \mu\text{g C}/\mu\text{g GX eq L}^{-1}$, according to Engel & Passow (2001). It should be noted that the diatom species examined in their experiments presented a series of slopes, ranging from 0.51 to $0.88 \mu\text{g C}/\mu\text{g GX eq L}^{-1}$, due to differences in phytoplankton composition; thus TEP-C content estimated here may present some uncertainties.

Water samples for nutrient analyses were pre-filtered through Acrodisc® syringe filters with $0.8 \mu\text{m}$ Versapor® membranes. The filtrates were stored at -80°C in acid-cleaned polycarbonate cryogenic vials until subsequent analyses of nitrate plus nitrite ($\text{NO}_3^- + \text{NO}_2^-$), nitrite (NO_2^-), orthophosphate (PO_4^{3-}), and silicic acid (Si(OH)_4) using a Technicon II Autoanalyzer (Mitchell et al. 2002).

Samples for pH measurements were collected on board under bubble free and no head space conditions in 300 mL glass bottles and processed following "Guide to best practices for Ocean CO_2 Measurements" (Dickson et al. 2007). pH was determined in the laboratory at the Maurice Lamontagne Institute (MLI). The pH was measured with a Perkin Elmer (Lambda 2S) spectrometer and 10-cm quartz cell using the indicator dye *m*-cresol purple (Sigma-Aldrich) within 1-2 h after sampling. Absorbance was measured at 730, 578 and 434 nm before and after dye addition at 25°C (Clayton & Byrne 1993). A similar procedure was carried out before and after each set of sample measurements using a TRIS (tris(hydroxymethyl)-aminomethane) buffer prepared at a practical salinity(S) of approximately 30 (Millero 1986). Certified Reference Material (CRM) (supplied by Professor Andrew Dickson, Scripps Institution of Oceanography, San Diego, USA) was used for quality control of our pH TRIS buffer. All measurements were converted to the total proton scale (pH_T) using the measured salinity of each sample and the HSO_4 association constants given by Dickson (1990). Reproducibility and accuracy of our TRIS buffer measurements were in the order of 0.005 pH unit or better. The pH_T value was then corrected for *in situ* pressure and temperature using the CO2SYS program (Lewis &

Wallace 1998) with measured pH, total soluble reactive phosphate and silicate concentrations as input parameters.

Chl *a* was measured using the Parsons et al. (1984) acidification method. Briefly, duplicate samples were filtered onto 25 mm Whatman GF/F filters and extracted overnight in 10 mL of 90 % acetone at 4°C in the dark. The extracts were analyzed with a TD-700 Turner Designs fluorometer. Phytoplankton Chl *a* data were converted to carbon using a POC:Chl *a* ratio of 40 following Levasseur et al. (1992).

Duplicates (250 mL to 1 L) seawater samples were filtered through pre-combusted (450°C, 4 h) Whatman GF/F filters and frozen with silica gel until analysis. The POC filters were then oven dried 24 h at 50°C prior to analysis. POC concentrations were determined with a CHN elemental analyzer (EA) COSTECH ECS 4010 (Costech Analytical). Quantification was based on external Acetanilide standard with a calibration range from 0.025 to 0.080 mg and 0.170 to 0.550 mg for nitrogen and carbon, respectively, and included a blank capsule. Blank capsules and blank filters were also analyzed in every run to confirm the absence of contamination.

Samples for the identification and enumeration of phytoplankton >2 µm were collected at 10 m depth (usually representing the depth of chlorophyll maximum; DCM). They were preserved in acidic Lugol's solution (Parsons et al. 1984) and stored in the dark until analysis. Phytoplankton cells were identified to the lowest possible taxonomic level using an inverted microscope according to Lund et al. (1958). For each sample, at least 300 cells were counted. The main taxonomic references used to identify the phytoplankton were Bérard-Therriault et al. (1999).

Samples for heterotrophic bacterial abundance measurements were pre-filtered (200 µm Nitex mesh size) and fixed with glutaraldehyde (Grade I; Sigma) 0.5 % final concentration (Marie et al. 2005), placed in the dark at 4°C for 30 min and then frozen at -80°C until flow cytometric analysis. Samples were analyzed using an EPICS ALTRA

flow cytometer (Beckman Coulter) equipped with a 488 nm laser (15 mW output) at a flow rate of 60 $\mu\text{L min}^{-1}$.

Heterotrophic bacteria were analyzed after staining their nucleic acids with SYBR Green I (0.1 % final concentration; Invitrogen Inc.) following Belzile et al. (2008) modified from Lebaron et al. (1998). 600 μL of Tris-EDTA 10x buffer pH 8 (Laboratoire MAT) were added to 400 μL of sample in order to maintain an optimum pH of the staining with SYBR Green I. Dilution with the buffer also avoided coincidence of several particles in the laser beam, and minimized the error due to low-volume pipetting. Yellow Fluoresbrite beads of 1 μm (Polysciences) were added in all analyses as an internal standard and allowed to verify that there was no degradation of the side scatter signal despite the relatively high flow rate used. The green fluorescence of nucleic acid-bound SYBR Green I was measured at 525 ± 5 nm. BA was determined as the sum of LNA and HNA count. The results showed that this technique is accurate enough, showing a root mean squared difference of 4.5 % ($n=40$) between duplicates (Belzile et al. 2008). Bacterial counts were expressed in terms of carbon biomass by using a conversion factor of 14 fg C.cell⁻¹ (Zubkov et al. 2001).

Euphotic and mixed layer depth

The euphotic zone depth (Z_{eu} , considered as 1 % of incident light in the surface), was estimated from the diffuse attenuation coefficient (K_d). K_d was derived from Secchi disk observations, following the empiric relationship of Kirk (1983). The surface mixed layer depth (Z_{mix}) was estimated based on the Brunt-Väisälä frequency (N^2).

Statistical analysis

All statistical analyses were carried out using Statistica (version 7.0) and XLstat (AddinsoftTM) software. Interpolation of temporal distributions of the different parameters studied were represented by section scope using the software package Ocean Data View

(ODV) 4.5.1 (Schlitzer 2002). The carbon contribution to each water layer from the various particulate fractions (TEP-C, Phyto-C, Bac-C) was expressed as % POC. ANOVA was carried out to test seasonal variability and depth effects on the studied variables. In order to meet the ANOVA requirements (normality and homoscedascity), data were log transformed (Log_e) and then pooled by season (Spring =May-June; Summer=July-August; Fall= September-October). A Tukey HSD post hoc test was used to compare TEP in each of the three seasons to one another. The Akaike Information Criterion (AIC) (Burnham et al. 2011) was used to assess the contribution of different carbon sources (phytoplankton, bacteria and TEP, as independent variables) to the POC pool. The AIC allows for the selection of the best model from a collection of models based on its quality (i.e., minimal information loss), helping to avoid overfitting (use of excess predictor variables). We performed calculations using the log-transformed data for three independent variables, subsets of two and only one variable. AIC computations were performed with the Generalized Linear Models option of the Statistica 10 package, and models were fitted using the General Linear Models option of the same program. Given the small sample size, a correction to the AIC results (AICc), was applied (Burnham & Anderson 2002). Finally, the AICc values were ranked considering the AICc minimum value, in order to compare the n models studied (Schloss et al. 2014):

$$\Delta_i = \text{AICc}_i - \text{AICc}_{\min} \text{ (for } i = 1, 2, 3 \dots n\text{)}$$

Statistical analyses, including partial correlation analysis, were performed to assess the potential chemical and biological drivers of TEP distribution, and linear regression analysis were performed for the results of AIC for the best carbon source predictor for POC.

RESULTS

1. Hydrographic conditions

Surface water temperature in 2011 increased from 3.3°C in May to 11.5°C in late June and remained stable until early October (Fig. 2a). The water column was characterized by the presence of a three layered vertical distribution of the temperature, which is typical in the Lower St. Lawrence Estuary (LSLE) during summer period: surface layer (SL), cold intermediate layer (CIL) and the bottom layer (BL). Depth of these water layers is given in Table 1 according to the criteria proposed by Gilbert & Pettigrew (1997) and Smith (2005) (CIL $T \leq 3^\circ\text{C}$).

Table 1 : Seasonal depth intervals (m) for each of the water layers identified at the IML-4 station

| | Spring (May- June) | Summer (July - August) | Fall (September -October) |
|-----|-------------------------------------|---|--|
| SL | 0 - 16.33 | 0 - 37.4 | 0 - 46.66 |
| CIL | 16.33 - 168.5 | 37.4 - 147.4 | 46.66 - 132.3 |
| BL | 168.5 - 320 | 147.4 - 320 | 132.3 - 320 |

Surface water salinity shows the freshwater spring runoff characteristic of the LSLE associated with neap-tide stratified interval with salinity <25 PSU around 0 - 20 m depth until mid July (Fig. 2b). Salinity increased slightly in the surface (average 27 PSU) until the end of the study.

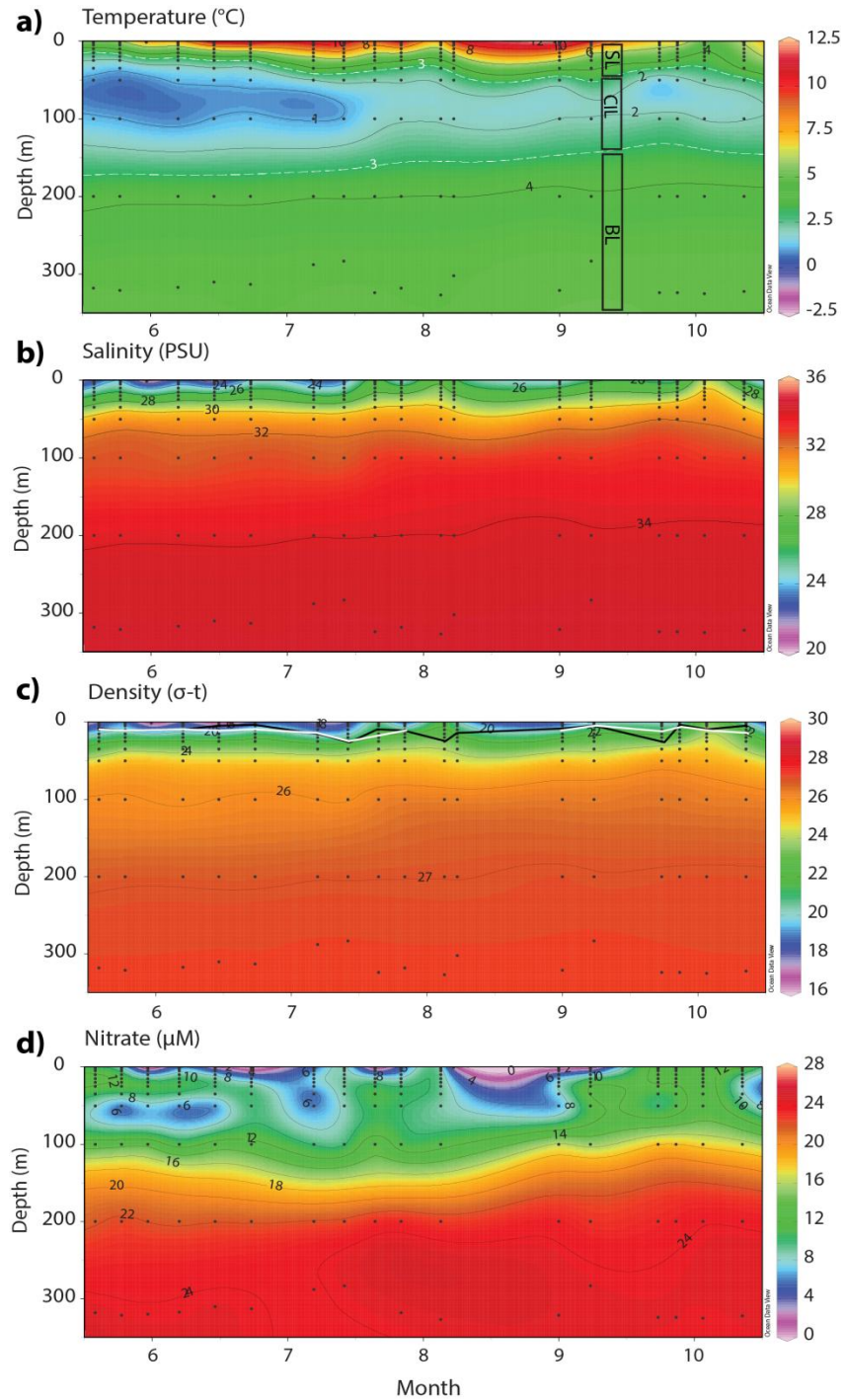


Figure 2 : Vertical and seasonal distributions of: (a) temperature ($^{\circ}\text{C}$), (b) salinity (PSU), (c) density ($\sigma\text{-t}$) and (d) nitrates (μM) in the water column at the IML-4 station from May to October 2011. Black line: pycnocline depth; white line: euphotic zone depth (Z_{eu}); White dashed line: CIL limit ($T \leq 3^{\circ}\text{C}$)

The water column was strongly stratified during the three seasons, presenting a well-developed pycnocline between 5 and 32 m (average depth ~13 m) (Fig. 2c). The Z_{eu} was very stable along the seasons (Fig. 2c), varying between 8 and 14 m. In turn, the Z_{eu}/Z_{mix} ratio was close or higher than 1 during almost the whole period of the study, suggesting the existence of favourable conditions for phytoplankton growth in surface waters.

Nitrate concentrations decreased from the beginning of the spring bloom in surface waters from ~12 μM to 0.05 μM in coincidence with the algal biomass accumulation episodes (Fig. 2d). Nitrate concentrations increased with depth to 15 μM over 100 m and reached up to 25 μM below 200 m depth. Both phosphate and silicate concentrations in surface waters showed the same seasonal pattern than nitrate (not shown here), decreasing from ~0.5 and ~20 μM , respectively, to below the detection limit of the method used. In the same way, the phosphate and silicate concentrations increased with depth, with 1.5 μM and 20 μM , respectively, around 100 m and reached up to 2.5 μM and 60 μM , respectively, below 200 m depth. Surface waters showed a strong nitrogen limitation (Redfield ratio: $0.4 < \text{N:P ratio} < 5.5$) in coincidence with the successive phytoplankton peaks observed during our study. Nutrients concentrations increased in the surface waters after the early autumn bloom up to ~13 μM for nitrate, ~1 μM for phosphate, and ~17 μM for silicate from middle September and remained high until the end of this study.

2. Vertical and seasonal distribution of the TEP, Chl *a*, BA and POC

The seasonal distribution of Chl *a* in the LSLE was characterized by four successive phytoplankton biomass accumulation events, with an important spring bloom in late June reaching an integrated value up to ~547 $\mu\text{g Chl } a \text{ m}^{-2}$ and a less pronounced early pulse around 31 May (~174 $\mu\text{g Chl } a \text{ m}^{-2}$), a summer pulse by 21 July (~122 $\mu\text{g Chl } a \text{ m}^{-2}$), and an early autumn bloom by 01 September (141 $\mu\text{g Chl } a \text{ m}^{-2}$) (Fig. 3a).

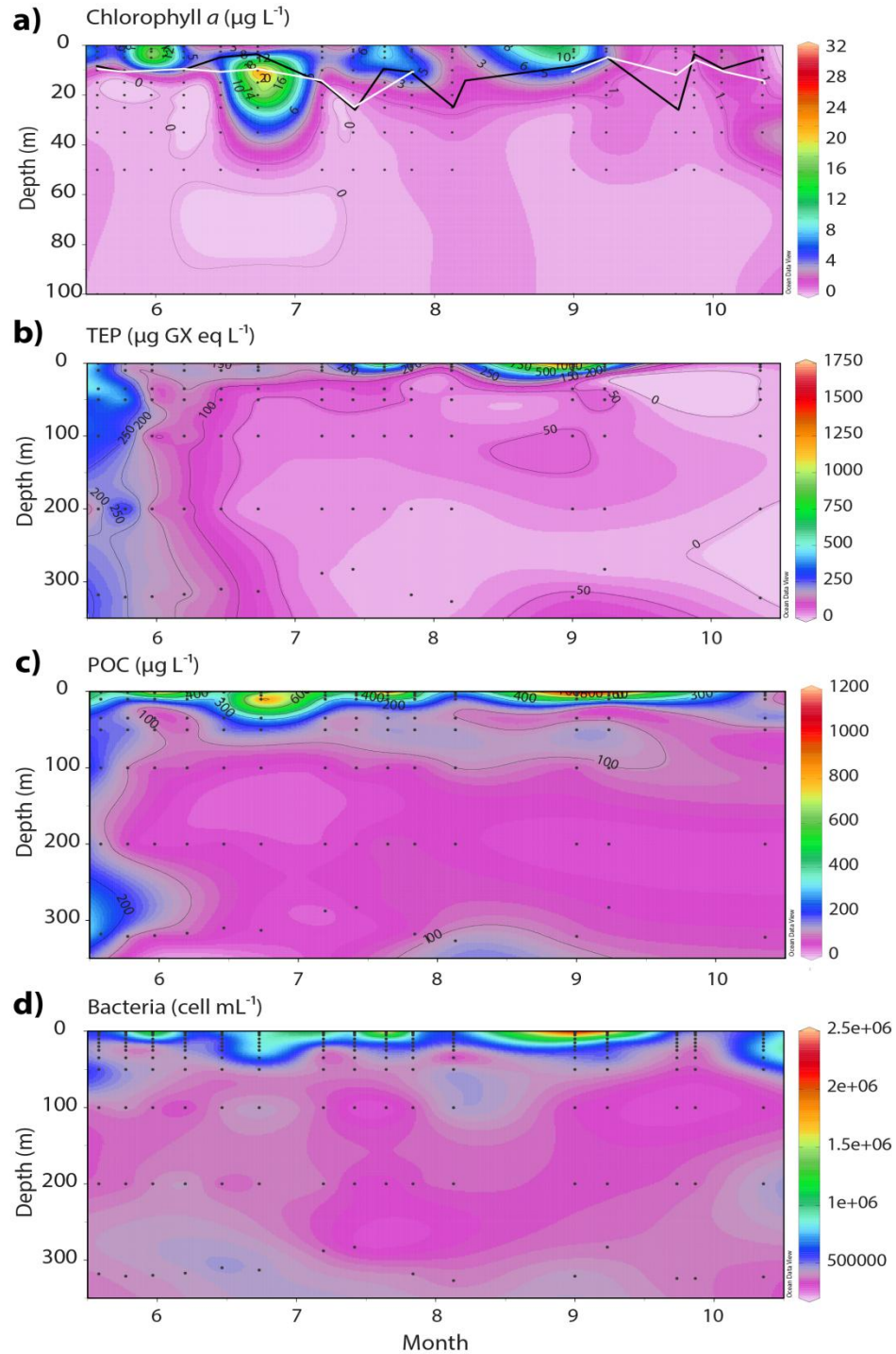


Figure 3 : Vertical and seasonal distributions of: (a) chlorophyll a ($\mu\text{g L}^{-1}$), (b) TEP ($\mu\text{g XG eq L}^{-1}$), (c) POC ($\mu\text{g L}^{-1}$) and (d) bacteria (Cell mL^{-1}) in the water column at the IML-4 station. Black line: pycnocline depth; white line: euphotic zone depth (Z_{eu})

Chl *a* concentrations did not differ among seasons ($F_{2, 70} = 0.483$, $p = 0.618$), but showed significant differences between the SL and the CIL ($F_{2, 70} = 48.96$, $p < 0.0001$) (Fig. 4a). Surface Chl *a* concentrations were consistent with the scientific buoy IML-4 *in-situ* fluorescence record for the same period (the St. Lawrence Global Observatory, data not shown), displaying a significant positive correlation between both data series ($r = 0.68$, $p = 0.007$). Phytoplankton assemblages were mainly constituted by diatoms (18-96 %) and autotrophic flagellates (3-63 %) during all seasons. Centric diatoms dominated numerically (17 to 96 % of the total cell number; data not shown), with *Thalassiosira nordenskiöldii* as the most important species in particular during the spring bloom, followed in abundance by *Skeletonema costatum*, *T. pacifica*, *T. spp* and *Chaetoceros sp.*. In contrast, dinoflagellates (~5 %) and cyanobacteria (~0.044 %) were minor contributors to the total cell abundance of surface waters.

Overall, TEP concentrations were significantly different among seasons and water layers ($F_{2, 94} = 16.99$, $p < 0.0001$ and $F_{2, 94} = 12.53$, $p < 0.0001$, respectively) (Fig. 4b). TEP concentrations were significantly higher in the SL, ranging between 15 and 1548 (average 291) $\mu\text{g GX eq L}^{-1}$, which correspond to 12 and 1161 (average 218) $\mu\text{g C L}^{-1}$, respectively. Maximum TEP values were in general observed above the pycnocline (between 0-10 m depth) after the spring bloom and throughout the summer and peaked in the early autumn by September 1st, simultaneously with the phytoplankton summer pulse and autumn blooms (Fig. 3b). Significant differences between the SL and the two other water layers (CIL and BL) were found during summer and fall, whereas no significant difference were observed in TEP concentration between the three layers during spring ($F_{4, 94} = 4.005$, $p = 0.004$) (Fig. 4b). In addition, a significant interaction existed between seasons and the three water column layers. These results can be explained by the high TEP concentrations measured in the whole water column during early spring, ranging from 140 to 501 (average 306) $\mu\text{g GX eq L}^{-1}$ which corresponded to 105 and 376 (average 230) $\mu\text{g C L}^{-1}$.

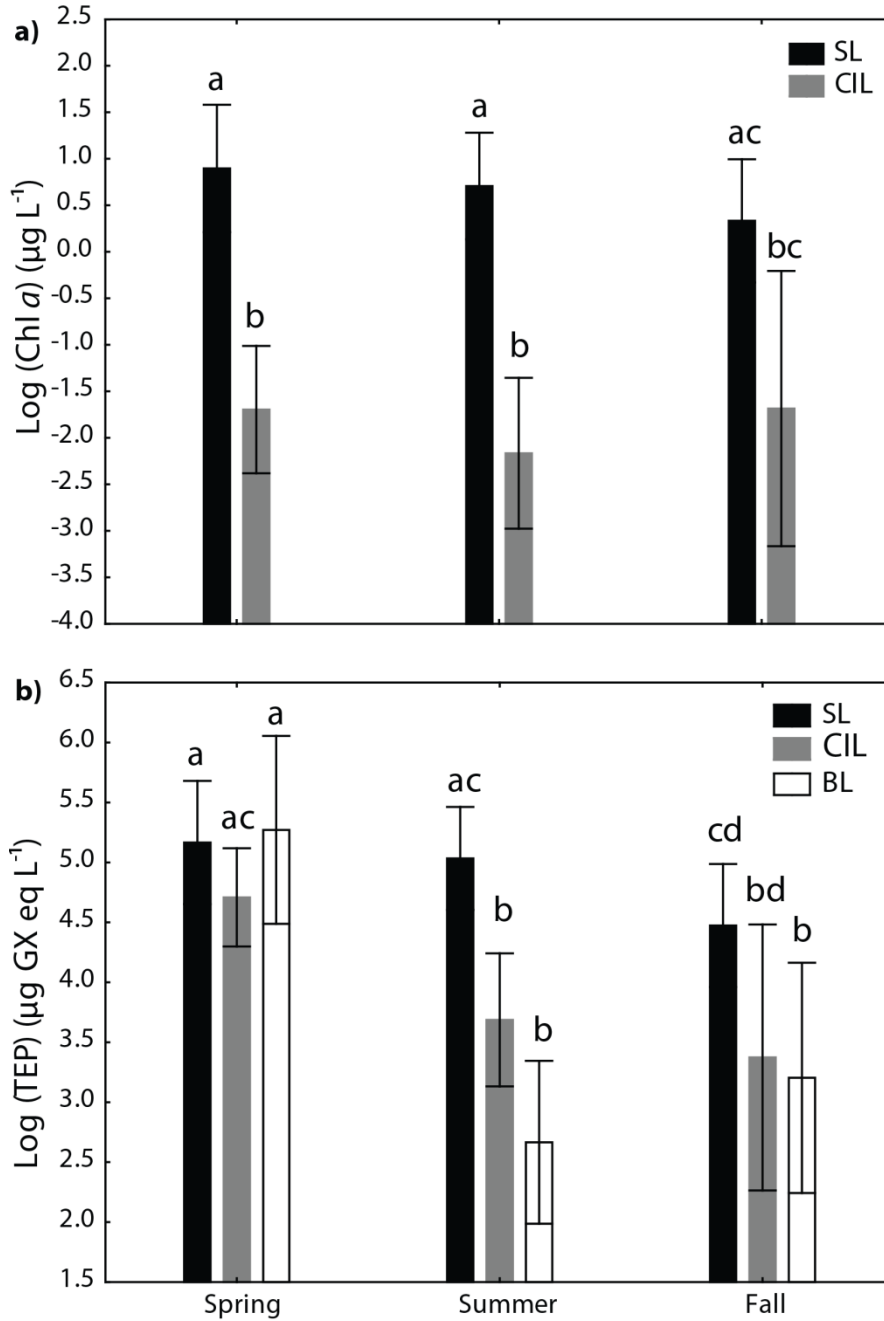


Figure 4 : Seasonal averages (\pm SE) of log transformed data: (a) Chl *a* concentration ($\mu\text{g L}^{-1}$) and (b) TEP concentrations ($\mu\text{g XG eq L}^{-1}$) corresponding to each water layer identified at the IML-4 station. Tukey HSD test results: Different letters above each bar indicate a significant difference between seasons and layers ($\alpha=0.05$)

For the whole studied period, POC concentrations (Fig. 3c) ranged from 44 to 1052 (average 228) $\mu\text{g C L}^{-1}$. Maximum POC concentrations were observed in the SL, in coincidence with the different phytoplankton pulses ($F_{2, 97} = 37.57$, $p < 0.0001$). No significant differences were detected among seasons ($F_{2, 97} = 1.23$, $p = 0.294$). Relatively high POC concentrations were measured in the whole water column during early spring, ranging from 48 to 409 (average 197) $\mu\text{g C L}^{-1}$. It should be noted that this distribution was consistent with the TEP vertical distribution in the water column during the same period.

BA ranged from 0.27×10^6 to 2×10^6 cell mL^{-1} (average 0.57×10^6 cell mL^{-1}) during this study (Fig. 3d). As observed for Chl *a* and POC, BA did not show significant differences among seasons ($F_{2, 170} = 1.52$, $p = 0.220$). However, BA in the SL was significantly higher than that in the deeper layers ($F_{2, 170} = 53.48$, $p < 0.0001$). Highest BA values were observed in this layer in coincidence with the successive phytoplankton peaks.

A marked decrease of pH was observed between the different layers. The ANOVA results show a significant difference between the three layers ($F_{2, 73} = 63.98$, $p < 0.0001$), with pH values in total proton scale of 7.96 ± 0.02 in the SL, 7.84 ± 0.026 in the CIL to 7.58 ± 0.004 in the BL. These observations corresponded to a reduction in pH of 0.12 between the SL and the CIL, 0.26 between the CIL and the BL, and a total reduction of 0.38 from the surface to the bottom layer. No significant differences were detected among seasons ($F_{2, 73} = 2.2$, $p = 0.123$).

The hypothesis that the main sources of TEP were phytoplankton and bacteria, and that the presence of exopolymeric particles was modulated by nutrient limitation, pH, salinity and temperature were examined by multiple regression analysis. Partial correlation coefficients were thus calculated for the three layers in the water column with Chl *a*, BA, nitrate, phosphate, pH, salinity and temperature as predictors and TEP as the dependent variable. The results indicate that during our study TEP concentrations were mainly related to phytoplankton biomass in the SL (partial correlation coefficient = 0.85, $p = 0.032$). No other significant correlations were detected for the CIL and BL (in the case of BL, Chl *a*

was not considered as an independent variable below the lower limit of the CIL, due to the absence of detectable phytoplankton biomass.

3. TEP contribution to the POC carbon pool

The relative contributions of TEP-C, Chl *a*-C and Bac-C to the POC integrated for each water layer studied are shown in Fig. 5. The residual part of POC was considered as residual-C. The main contribution to POC in the SL was represented by TEP-C and Chl *a*-C (41 % and 54 % in average of POC, respectively) for the whole sampling period (Fig. 5a). The standing stock of Chl *a*-C decreased slightly from 4.65 ± 4.43 in spring to 3.69 ± 1.40 mgC.m^{-2} in fall. In contrast, TEP-C increased from 1.95 ± 0.99 in spring to 5.68 ± 5.26 mgC.m^{-2} in fall (Table 2). TEP-C represented the most important fraction contributing to POC in the CIL (average 94 %; Fig. 5b) and BL (average 145 % ; Fig. 5c) during the spring period, although its contribution decreased over the summer and fall, reaching 35 % and 25 %, respectively, in the CIL and 25 % and 29 %, respectively, in the BL (Fig. 5b and c). The TEP-C pool reached 3.34 ± 1.77 and 2.19 ± 0.38 mgC.m^{-2} in CIL and BL, respectively, during the summer period and 1.31 ± 0.95 and 3.99 ± 3.80 mgC.m^{-2} in CIL and BL, respectively. Our estimates of TEP-C in spring were close to or slightly exceeded the POC pool in the CIL (18.34 ± 13.15 compared to 20.69 ± 8.87 mgC.m^{-2} respectively) as well as in the BL (17.10 ± 17.12 compared to 11.35 ± 6.67 mgC.m^{-2}) (Table 2)

Bac-C comprised the lowest fraction contributing to POC, relative to TEP-C and Chl *a*-C. On average the contribution of Bac-C to POC increased from 3 % in spring to 5 % in fall in the SL (Fig. 5a), representing a standing stock of 0.15 ± 0.06 to 0.51 ± 0.04 mgC.m^{-2} , respectively. Moreover, the contribution of Bac-C to POC increased with depth, reaching an average of 8 % of POC among all seasons in the BL (fig. 5c), which corresponded to 0.75 ± 0.20 to 1.11 ± 0.06 mgC.m^{-2} (Table 2).

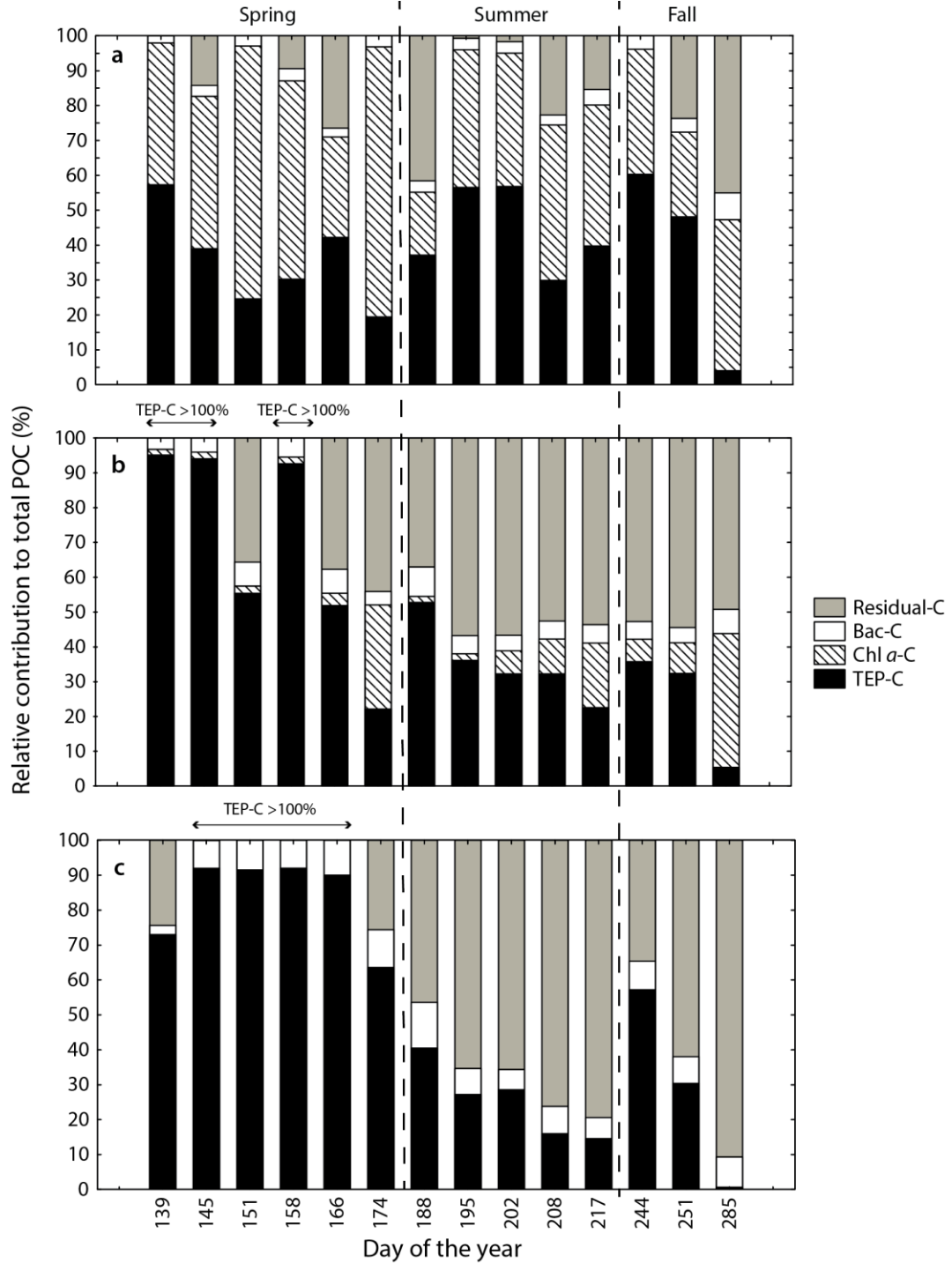


Figure 5 : Relative contributions of TEP (TEP-C), phytoplankton (Chl *a*-C), bacteria (Bac-C) and other organic matter (Residual-C) to POC in the three water layers identified: (a) Surface layer, (b) Cold intermediate layer, and (c) Bottom layer

Table 2 : Carbon standing stock (mgC m^{-2}) in the surface layer (SL), the cold intermediate layer (CIL) and the bottom layer (BL) for the three seasons studied (average \pm Std. Dev.). TEP (TEP-C), phytoplankton (Chl *a*-C), bacteria (Bac-C) and POC

| Water masses | Variable | Spring | Summer | Fall |
|--------------|-----------------|---------------------|------------------------|------------------------------|
| | | (May-june) (n=6) | (july-August) (n=5) | (September-October) (n=3) |
| SL | Chl <i>a</i> -C | 4.65 \pm 4.43 | 3.29 \pm 1.39 | 3.69 \pm 1.40 |
| | TEP-C | 1.95 \pm 0.99 | 4.04 \pm 1.75 | 5.68 \pm 5.26 |
| | Bac-C | 0.155 \pm 0.06 | 0.30 \pm 0.04 | 0.51 \pm 0.04 |
| | POC | 5.47 \pm 2.02 | 9.09 \pm 2.43 | 11.23 \pm 4.38 |
| CIL | Chl <i>a</i> -C | 1.82 \pm 3.51 | 0.60 \pm 0.50 | 0.79 \pm 0.65 |
| | TEP-C | 18.34 \pm 13.15 | 3.34 \pm 1.77 | 1.31 \pm 0.95 |
| | Bac-C | 0.96 \pm 0.21 | 0.53 \pm 0.24 | 0.26 \pm 0.01 |
| | POC | 20.69 \pm 8.87 | 9.18 \pm 3.08 | 4.99 \pm 0.92 |
| BL | TEP-C | 17.10 \pm 17.12 | 2.19 \pm 0.38 | 3.99 \pm 3.80 |
| | Bac-C | 0.75 \pm 0.20 | 0.769 \pm 0.34 | 1.11 \pm 0.06 |
| | POC | 11.35 \pm 6.67 | 10.51 \pm 6.11 | 13.66 \pm 0.20 |

We explored the relationships between POC and the other potential biological sources contributing to the particulate carbon pool in the study site (Chl a, TEP and BA converted to carbon). AIC was used to decide which variable or sum of variables could better predict POC concentrations, considering log-transformed average data for each of the independent variables for the different water column layers. The fitting of POC with these variables showed that the best model included Chl a-C and TEP-C as descriptors for both, the SL and the CIL (Table 3). Therefore, we performed a regression analysis of POC on the sum of TEP-C and Chla-C, which can explain 83 % and 35 % of the POC variance in the SL ($r = 0.91$, $p < 0.0001$) and the CIL ($r = 0.60$, $p < 0.05$), respectively. The unexplained fraction of the variance could be attributed to residual carbon (average ~17 % for the SL and ~49 % for the CIL). Consequently, the sum of TEP-C and Chla-C can be considered as a good predictor of POC concentration, particularly in the SL (Fig. 6). No significant correlations were found for the BL.

Table 3 : Models of POC fitted to the main potential sources of particulate carbon. AIC: Akaike Information Criterion; AICc: corrected AIC; p: probability; Δ : differences between models in relation to the minimum AIC value. Models are ranked from the minimum AIC (minimum loss of information) to maximum (maximum loss of information). POC: particulate organic carbon; TEP-C: transparent exopolymeric particle carbon; Chl *a*-C: phytoplankton carbon; Bac-C: bacterial carbon (data are log transformed averages for each water layer)

| Water layers | Dependent Variable | Independent variable | AIC | AICc | P | Δ |
|---------------------|---------------------------|-----------------------------|------------|-------------|----------|----------------------------|
| SL | POC | TEP+Chl <i>a</i> -C | -6.624 | -5.29 | <0.0001 | 0.00 |
| | | TEP-C | -4.828 | -4.43 | <0.0001 | 0.86 |
| | | TEP+Chl <i>a</i> +Bac-C | -4.722 | -1.72 | <0.0001 | 3.57 |
| | | TEP+Bac-C | -2.858 | -1.52 | <0.0001 | 3.77 |
| | | Chl <i>a</i> -C | 4.335 | 4.74 | <0.05 | 10.03 |
| | | Chl <i>a</i> +Bac-C | 5.708 | 7.04 | <0.05 | 12.33 |
| | | Bac-C | 12.383 | 12.78 | ns | 18.07 |
| CIL | POC | TEP+Chl <i>a</i> -C | -7.630 | -6.30 | <0.001 | 0.00 |
| | | TEP+Chl <i>a</i> +Bac-C | -5.652 | -2.65 | <0.001 | 3.64 |
| | | Chl <i>a</i> +Bac-C | -1.321 | 0.01 | <0.05 | 6.31 |
| | | Chl <i>a</i> -C | 0.009 | 0.41 | <0.05 | 6.71 |
| | | Bac-C | 0.973 | 1.37 | <0.05 | 7.67 |
| | | TEP-C | 1.798 | 2.20 | ns | 8.49 |
| | | TEP+Bac-C | 1.971 | 3.30 | ns | 9.60 |
| BL | POC | Bac-C | 22.181 | 22.58 | ns | 0.00 |
| | | TEP+ Bac-C | 22.335 | 22.67 | ns | 1.09 |
| | | TEP-C | 23.463 | 22.86 | ns | 1.28 |

ns : not significant

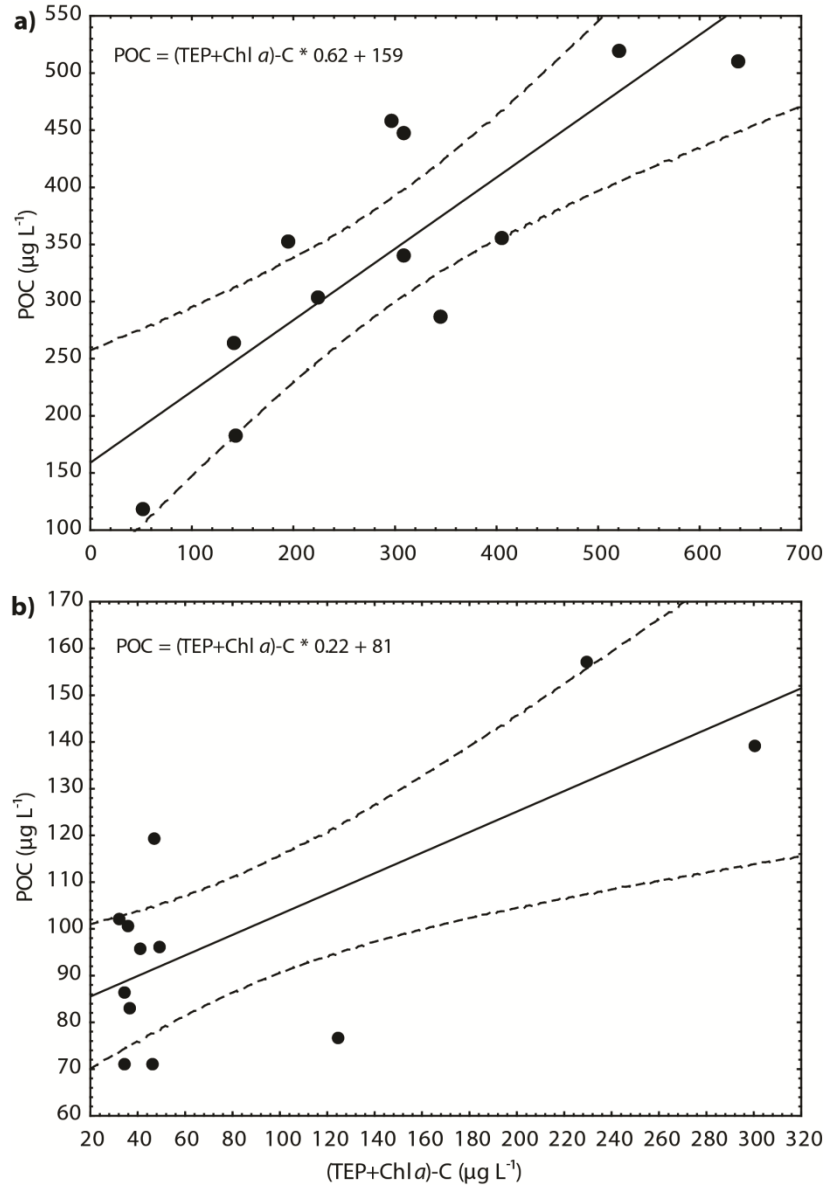


Figure 6 : Relationship between POC ($\mu\text{g L}^{-1}$) and the sum of TEP-C, Chl *a*-C ($\mu\text{g L}^{-1}$) (a) the surface layer (SL) and (b) the cold intermediate layer (CIL). Dashed lines represent the 0.95 confidence level.

DISCUSSION

1. Hydrological conditions and phytoplankton biomass

Our results show that the hydrological conditions were appropriate for phytoplankton development during almost the whole period of the study (from May to October), as suggested by the Z_{eu}/Z_{mix} ratio values. Successive blooms were observed during late spring, summer and early fall. The development of these blooms can be explained by periodic nutrient inputs during fortnightly spring-tides (Le Fouest et al. 2005) followed by neap-tide stratified intervals in the water column, which allowed a phytoplankton biomass accumulation typical to the LSLE (Levasseur et al. 1984, Savenkoff et al. 1997). During our study, the most intense bloom at the Rimouski station occurred around June 23rd, an observation consistent with previous reports for the LSLE (Levasseur et al. 1984, Starr et al. 1993, Plourde & Runge 1993, Starr et al. 2004, Plourde et al. 2014).

During these blooms, low nutrient concentrations were observed in surface waters that can be attributed to biological consumption by phytoplankton, along with N limitation as suggested by the observed Redfield ratios. This nutrient limitation may promote exopolymeric exudation by phytoplankton, as reported by several authors (Obernosterer & Herndl 1995, Mari et al. 2001, Beauvais et al. 2003, Underwood et al. 2004, Engel et al. 2004). Despite that Chl *a* concentrations were higher during the spring bloom than in the fall, no significant differences were found between seasons in the SL.

2. Temporal variability of TEP

Our results show an increase of TEP concentrations in SL at the end of the spring bloom, followed by a significant accumulation throughout the summer and a peak in coincidence with the early fall bloom. Measured TEP concentrations in SL during this

study were within the range of average values reported for estuaries and coastal waters (Table 4), but higher than those found in some other marine and freshwater environments (Wurl & Holmes 2008, Bar-Zeev et al. 2009, de Vicente et al. 2009, Harlay et al. 2009, Ortega-Retuerta et al. 2009, 2018).

The highest TEP concentrations coincided with the phytoplankton biomass peaks in the surface. This finding suggests that phytoplankton was the primary source of these compounds, as previously suggested (Alldredge et al. 1993, Passow & Alldredge 1995a, Mari & Burd 1998, Passow et al. 2001, Passow 2002a). Phytoplankton biomass was mainly dominated by diatoms ($r = 0.88$, $p = 0.00015$) during the three seasons, with nearly 17 to 96 % of centric diatoms as reported by other studies in the same zone (Levasseur et al. 1984, Roy et al. 1997, Savenkoff et al. 2000, Vézina et al. 2000, Romero et al. 2000, Lovejoy et al. 2000, Starr et al. 2004, Plourde et al. 2014). Diatoms are known to be a major source of TEP precursors (Williams 1990, Kiørboe & Hansen 1993, Passow & Alldredge 1994, Aluwihare & Repeta 1999, Mari 1999, Mari & Kiørboe 1996, Passow 2002b). However, their ability to produce these compounds depends on specific composition of the community (Passow & Alldredge 1994, Passow et al. 2001) and the physiological state of the cells (Passow & Alldredge 1995a, Passow 2002). The dominant species for most of the entire studied period (except during spring when it was sub-dominant), *S. costatum* has been described as a very important producer of TEP (Engel 2000, Beauvais et al. 2003b). The biomass accumulation of these species, together with other taxa of the Genus *Thalassiosira* and *Chaetoceros*, seems to be the main TEP source in our study.

Table 4 : Values reported on transparent exopolymer particles (TEP $\mu\text{g GX eq L}^{-1}$) and TEP contribution to the carbon pool for estuarine, marine and freshwater environments (minimum, maximum values are shown, with averages in parentheses)

| Location | Period | Depth (m) | TEP ($\mu\text{g GX eq L}^{-1}$) | Carbon (%) | Reference |
|--|---------------------------|------------------------|---------------------------------------|-------------------------|-----------------------------|
| Marine environments: | | | | | |
| Northern Adriatic Sea | April 1996 | nd | nd | 103% POC | Passow & Passow 2001 |
| Singapore Strait | January-May | Surface | 129 – 1073 (512) | nd | Wurl & Holmes 2008 |
| Gulf of Aqada | April | Profile (5-300 m) | 23- 228 | nd | Bar-Zeev et al. 2009 |
| Eastern Mediterranean Sea | Sept 2008, July 2009 | Profile (0-1000) | 48-420 | 63->100% POC | Bar-Zeev et al. 2011 |
| NW Mediterranean Sea | Summer | DCM | nd | 22% TOC 183% POC | Beauvais et al 2003 |
| NW Mediterranean Sea | 2012-2014 | 15 m | 33-147 | <10-100% POC | Ortega-Retuerta et al. 1981 |
| North Atlantic Ocean | May-June | Profile (3-120 m) | nd | 1.5-68% POC | Harlay et al. 2009 |
| Southern Ocean | Febuary | Profile (0-200 m) | 0-49 (15) | 18% POC | Ortega-Retuerta et al. 2009 |
| Freshwater: | | | | | |
| Quéntar reservoir (Spain) | Febuary 2004 - March 2006 | 5 and 30 m | 2-335 (48) | 40% POC | De Vicente et al. 2009 |
| Michigan lake | Summer | Surface | 36 - 1462 (256) | 33% POC | De Vicente et al. 2010 |
| Mediterranean Lake | Summer | Surface | 66 - 9038 (1572) | 36% POC | |
| Estuaries: | | | | | |
| Po River Delta – Rovinj (Italy- Croatia) | June 99-July 2002 | Profile (0-35 m) | 4 - 14800 (570) | nd | Radić et al. 2005 |
| Johor strait estuary (Singapore) | May 98- July 2000 | Surface | 281 - 8026 (2264) | 0.1-23% POC | Wurl & Holmes 2008 |
| Dona Paula Bay | May 98-July 2000 | Surface | 1.3 - 149 (57) | 0.12-22.8 (6.9)% POC | Bhaskar & Bhosle 2006 |
| North Carolina's Neuse River estuary | May-August | Surface | 805 - 3500 (2300) | 16% TOC | Wetz et al. 2009 |
| Pearl River estuary | January, August | Profile (2-30 m) | 89 – 1587 (828) , 522 – 1727 (989) | 2-26% TOC 5-15% TOC | Sun et al. 2012 |
| Rimouski station (IML-4) | May-October | Profile (0.5-320 m) | 15 -1548 (290) | 41-145% POC | This study |

nd: not determined

3. Vertical distribution of TEP

TEP concentrations followed the autotrophic biomass vertical distribution, with the highest values in surface followed by a sharp decrease at the depth of the pycnocline and more gradual towards the bottom. When data from late May are excluded from our statistical analysis, we found significant differences between the three water layers considered with persistent maximum values in the SL. In the particular case of late May, high TEP concentrations were present in the whole water column ranging from 105 to 376 (average 230) $\mu\text{g C L}^{-1}$. In turn, POC concentrations measured were in the range of 48 to 409 (average 197) $\mu\text{g C L}^{-1}$. Estuarine environments are strongly influenced by freshwater runoff, especially during spring in cold temperate latitudes. During such periods, high loads of particles are transferred from the main river basin to the Estuary, including allochthonous TEP (i.e. originated from microbial mats and macroalgal bed exudates; Bhaskar & Bhosle 2005). Under these conditions, TEP should contribute to the aggregation of organic and heavy inorganic particles allowing for a rapid export to deeper waters. Considering the fast sinking rates of particulate organic matter previously observed in the St. Lawrence Estuary (10-100 m d^{-1} ; Larouche & Boyer-Villemare 2010), we hypothesize that such dynamics can explain the relatively high POC and TEP concentrations measured in the whole water column at the beginning of this study. According to Passow et al. (2001) in a field study in California channel during 2 years, relative sedimentation rates of TEP at 500 m were comparable to those of POC suggesting that loss mechanisms were similar for both variables. Actually, few studies have reported results on TEP turnover time as a result of bacterial degradation, which appears to range from hours to months, depending on the chemical composition and age of TEP (Passow 2002b). First results on the degradation processes suggest that some fractions of TEP are rapidly recycled (Aluwihare & Repeta 1999), but evidence is accumulating that other fractions are semi-resistant to microbial degradation or transformed by bacteria into refractory compounds (Zhou et al. 1998,

Ogawa et al. 2001, Passow 2002a, Rochelle-Newall et al. 2010). Consequently, the turnover of TEP by grazing and microbial degradation needs to be explored further to evaluate the quantitative significance of these particles on carbon export to the bottom and especially those coming from rivers.

Considering the parameters affecting TEP aggregation and distribution in estuaries, Wetz et al. (2009) and Mari et al. (2012) highlighted the importance of salinity, pH and mixing in processes of aggregation and sedimentation of these particles. Similarly, Sun et al. (2012) indicated that formation and distribution of TEP were largely influenced by the interaction between physical and biogeochemical processes in the Pearl River Estuary. However, these processes vary largely from one estuary to another. As shown above TEP vertical variability in the SLE seems to be influenced by phytoplankton in the SL, especially by diatoms. In contrast, no significant relationships were found between TEP and the other biological and physico-chemical factors studied in the CIL and BL, which could influence TEP vertical distribution in this station.

We did not detect significant pH differences between seasons. However, a marked vertical pH decrease between water layers was measured. This observation is consistent with the results of Mucci et al. (2011) for the LSLE. They register a decrease of pH by 0.2 to 0.3 in the bottom waters over the last 75 years, which is four to six times greater than what can be attributed to the uptake of anthropogenic CO₂. These values were related to changes of water masses entering into the Gulf and, to some extent, an increase in benthic/pelagic respiration resulting from warming of the bottom waters (Genovesi et al. 2011, Mucci et al. 2011, Bourgault et al. 2012). pH changes have been shown to modify TEP stability by either swelling or shrinking of TEP particles, as revealed by their volume change (Li & Tanaka 1992, Chin et al. 1998b, de Vicente et al. 2010). According to Mari (2008), a decrease in pH by 0.2 units led to a reduction of TEP sticking properties. Wetz et al. (2009) explored the influence of pH changes on TEP formation, and found a positive correlation between pH and TEP. They suggested that this correlation may have been due in part to the covariance of pH with salinity. Similarly, de Vicente et al. (2010) also

revealed that pH control on TEP appears to be not significant or a secondary effect as a consequence to photosynthetic activity. Nevertheless, our results did not show a significant relationship between TEP concentrations and pH in the water column, despite the decrease of pH value with depth. More research is needed to further understand this relationship using TEP size frequency determined microscopically to explore the possible influence of pH on the size and structure of TEP, as well as chemical composition analyses to identify their origin.

It is well known that bacteria are also producing TEP or their colloidal precursors (Passow 2002a, Radić et al. 2006a, Ortega-Retuerta et al. 2010), and simultaneously can degrade and/or transform TEP (Radić et al. 2006a). In the context of the LSLE, it should also be noted that Piontek et al. (2010) showed that the degradation of polysaccharides by bacterial extracellular enzymes was significantly accelerated during experimental simulation of ocean acidification at the pH levels such as measured in bottom waters in our study area. However, our results from PCMA did not show a significant relationship between TEP and free-living bacteria at any water layer, which is consistent with some previous field studies (i.e. Passow & Alldredge 1994, Ramaiah et al. 2000, Bhaskar & Bhosle 2008, de Vicente et al. 2009b). The importance of bacteria in TEP production and notably its uptake as a suitable carbon source is a matter of debate, as both field and laboratory observations are inconsistent probably due to highly spatial and temporal variability in these processes (Bhaskar & Bhosle 2008) and the underestimated role of attached-bacteria (Bar-Zeev et al. 2011, Lapoussière et al. 2011). Therefore, we need to explore the bacteria activity and abundance for both free-living and attached bacteria to TEP particles in the water column for a better understanding of the formation and degradation of TEP in the SLE.

TEP dynamics in estuarine systems is complex since the physical, chemical, and biological mechanisms involved on its production/decomposition present a high spatio-temporal variability. According to the conceptual model of processes regulating TEP distribution proposed by Mari et al. (2012), there is a front of aggregation defined as an

"aggregation web", that seems to occur between salinities ranging from 10 to 15 PSU. Their study suggests that the physical and chemical reactivity of TEP along estuaries may result in a succession of recycling areas, corresponding to <10 PSU, and enhanced aggregation/sedimentation processes and export dominated areas for >10 PSU. This process could promote the formation of dense aggregates likely to be exported to the bottom. In contrast, particles may remain suspended in the water column leading to a system dominated by recycling in low salinity areas of the estuary. Without information of TEP and particle fluxes along the entire St. Lawrence system, this model cannot be tested. Nevertheless, our results suggesting the dominance of export in April-May mostly related with allochthonous particulate matter inputs in the portion of high salinity in the SLE is consistent with this conceptual model. Further investigations are crucially needed along the entire SLE system and especially in the context that these processes may contribute to the hypoxia and increasing acidification in the bottom water in the SLE (Gilbert et al. 2005, Genovesi et al. 2011, Mucci et al. 2011).

4. TEP contribution to the organic carbon pool

The present study suggests that the contribution of TEP accounts for an important portion of the carbon pool in the LSLE. Indeed, TEP-C represented the second most important fraction of carbon after the phytoplankton-C; accounting for 41 % and 54 % in average of POC, respectively, during the whole sampling period in the SL. As observed by Romero-Ibarra & Silverberg (2011) the main carbon contributor during the bloom period was phytoplankton, especially centric diatoms. The phytoplankton-C biomass in SL was nearly constant among the different seasons (4.65 ± 4.43 in spring to 3.69 ± 1.40 mg C m⁻² in fall). This result contrasts with TEP-C standing stock, which significantly increased in the same layer from 1.95 ± 0.99 in spring to 5.68 ± 5.26 mg C m⁻² in fall (Table 2).

The TEP-C pools measured in both the CIL and BL were high during the spring, representing ~94 % and 145 % of POC, respectively (Fig. 5b-c). However, TEP-C presented a more realistic contribution to POC in CIL and BL during summer and fall, representing between 25 % to 35 %. Similar results have been reported by Bar-Zeev et al. (2011), who registered a very high contribution of TEP-C as percentage of POC (>100 %) at 1000 m depth in the eastern Mediterranean Sea. Furthermore, Beauvais et al. (2003) calculated the TEP-C up to 183 % of the total standing stock of POC at DCM in the northwestern Mediterranean Sea. They suggested that either TEP carbon content calculated from freshly formed TEP produced in the laboratory from diatom batch cultures and natural communities can overestimate naturally occurring TEP-C, since the relationship between TEP and carbon content is species-specific (Engel & Passow 2001). On the other hand, POC was underestimated, since the pore-size used for filtration is larger than that used for TEP (0.2 μm for TEP vs 0.7 μm for POC). Indeed, several authors suggested that filters like those used in our work (0.2 μm) are the most efficient for collecting TEP (Passow & Alldredge 1995a, Passow 2002b, Bhaskar & Bhosle 2008, Wetz et al. 2009, Sun et al. 2012). Passow & Alldredge (1995) observed that >50 % of TEP were lost when 0.6 μm filters were used instead of 0.2 μm filters. Sun et al. (2012) in the Pearl River Estuary (China) found a difference of 42 % of TEP concentrations when using 0.2 μm instead of 0.4 μm filter. TEP are characterized as particulate material, ranging in length continuously from submicron (colloidal) scales (Wells & Goldberg 1992) to macroscopic particles (marine snow) that can reach a few cm in size (Alldredge & Silver 1988). Although, the colloidal fraction is very dynamic, involving high level of aggregation (Wells 1998). As reported by Bar-Zeev et al. (2011) by microscopical visualization of TEP in deep water, TEP presented newly formed aggregates with amorphous shapes, including different particle sizes. This point highlights the importance of the colloidal organic carbon fraction below 200 m depth that can contribute to TEP-C, as also observed by Kepkay (2000) and Bar-Zeev et al. (2011). Despite these methodological limitations in deeper waters, our AIC analysis results showed that the sum of TEP-C and Chl *a*-C presented a best fitting and is seen as a good predictor of POC, which suggests that overestimation of TEP-C during this

study was overall not significant (Table 3, Fig. 6). Then, our results suggest a direct relationship between TEP-C and phytoplankton-C as the main carbon contributors to the POC pool in SL.

Our findings concerning TEP-C are consistent with previous work conducted in the Gulf of St. Lawrence, where it has been reported that the contribution of marine snow to the total C flux was frequently >60 % in sediment traps deployed at 150 m (Romero et al. 2000, Romero-Ibarra & Silverberg 2011). However, these studies do not include the presence of TEP. The relative contribution of TEP-C to POC decreased over the summer and fall reaching 35 % and 25 %, respectively, in the CIL and 24 % and 29 % in the BL, respectively. Similar contributions to the carbon pool were already reported for other estuarine environments, with TEP contributing 6.9 % of POC (Bhaskar & Bhosle 2006), 16 % of total organic carbon (TOC) in the North Carolina's Neuse River Estuary (Wetz et al. 2009) and 15 % in the Pearl River Estuary in China (Sun et al. 2012). On the other hand, de Vicente et al. (2009, 2010) found a TEP-C contribution of 33 % to 40 % of POC in lake environments. Our estimations of residual-C (51 % in the CIL and 62 % in the BL) are consistent with previous results from the Gulf of St. Lawrence, where it has been found that detritus represent ~51 to 56 % of POC (Savenkoff et al. 2000, Vézina et al. 2000) mostly constituted by detrital organic matter (i.e., dead cells and zooplankton fecal pellets; Romero-Ibarra & Silverberg 2011). This constitutes a new evidence of the importance of TEP carbon linked to marine snow previously estimated in sediment traps, highlighting the importance of TEP in relation to the organic carbon pool not only in surface, but also in deep waters.

The bacteria-C standing stock did not change markedly among seasons and represented the lowest fraction of POC during our study. On average the contribution of bacteria-C to POC increased from ~3 % of POC in spring to ~5 % in fall in the SL. This contribution increased with depth, reaching ~8 % of POC among all seasons in the BL. These results agree with the observations of Savenkoff et al. (2000) in the Gulf of St. Lawrence, with bacteria-C constituting ~2 % of the POC in winter-spring to 4 % in

summer-fall. Our results suggest that TEP-C combined with phytoplankton-C biomass could contribute significantly to the subsequent export of macro-aggregates to the bottom, and probably contribute to the decrease in oxygen concentration and pH in the bottom layer of the LSLE by respiration/remineralisation processes.

This study provides the first semi-quantitative estimate of the contribution of TEP-C to the POC in the LSLE ecosystem. A characterization of TEP in terms of particle size distribution is nevertheless needed for a better knowledge of the aggregation processes in this ecosystem. Further research is also needed on TEP spatial and temporal variability as well as its contribution to POC export and advection, integrating both the St. Lawrence upper and lower portions of the Estuary as well as the Gulf. This is essential for the estimation of the carbon budget in this complex system as well as to understand the contribution of highly dynamic and productive marginal marine areas to the global carbon balance of the ocean.

ACKNOWLEDGEMENTS

This project was supported by grants from the Natural Sciences and Engineering Research Council (NSERC) of Canada to G.F. and the Fisheries and Oceans operating grants to M.S. The authors would like to thank Pierre Joly, Jean-Francois St-Pierre, Caroline Lafleur, Laure Devine and Marie-Lyne Dubé at the Maurice Lamontagne Institute and Mathieu Babin at Institut des sciences de la mer de Rimouski (ISMER) for their skilled help provided prior and during sampling period and for laboratory analyses. This research is part of fulfillment of the requirements for a Ph.D degree (S. Annane) at the Université du Québec à Rimouski. This is a contribution to the research and monitoring programs of AZMP of Fisheries and Oceans Canada, ISMER, and Québec-Océan.

CHAPITRE 2

IMPACT DE L'ACIDIFICATION DES OCÉANS SUR LES PARTICULES EXOPOLYMÉRIQUES TRANSPARENTES (TEP) ET L'ALLOCATION DU CARBONE ORGANIQUE DANS L'ESTUAIRE DU ST. LAURENT: UNE EXPERIENCE EN MICROSOCOSMES

Ce deuxième article, intitulé « *Impact of ocean acidification on transparent exopolymeric particles (TEP) and organic carbon allocation in the St. Lawrence Estuary: A microsocosm experiment* », fut corédigé par moi-même ainsi que par le professeur Gustavo Ferreyra, ma collègue Liliane St-Amand, le prof. Émilien Pelletier et le Prof. Michel Starr. L'article sera soumis à la revue *Estuarine, Coastal and Shelf Science* suite à la présentation de cette thèse. En tant que premier auteur, ma contribution à ce travail fut l'essentiel de la recherche sur l'état de l'art, le travail expérimental sur les microcosmes (préparation et fonctionnement), le travail d'échantillonnage et de laboratoire, les analyses statistiques et la rédaction de l'article. Le professeur Gustavo Ferreyra, chef de projet, le prof. Émilien Pelletier et le prof. Michel Starr ont fourni l'idée originale et ils ont contribué à la révision de l'article. Le professeur Michel Starr, le professeur Gustavo Ferreyra et Liliane St Amand ont contribué également au travail expérimental, d'échantillonnage et de laboratoire.

1.1 RÉSUMÉ

L'augmentation du CO₂ anthropique modifie la chimie de l'eau de mer vers une réduction du pH (« acidification des océans »), qui est soupçonnée d'avoir des effets importants sur les communautés marines ainsi que sur les cycles des nutriments et du carbone. Les écosystèmes estuariens connaissent une fluctuation naturelle du CO₂/pH et l'acidification des océans (AO) devrait baisser encore plus cet intervalle de pH. Une expérience cinétique a été réalisée en microcosmes pour étudier l'effet de l'acidification sur la communauté du plancton naturel, les particules exopolymériques transparentes (TEP) et l'allocation de la matière organique dans l'estuaire maritime du Saint-Laurent (EMSL). Six microcosmes d'intérieur avec des traitements de pH fixes (pH *in situ* de 7,86 à 6,90) et un microcosme de pH référence non modifié ont été suivis pendant 15 jours pour la communauté de plancton et les différents réservoirs de carbone (phytoplancton, TEP, POC, hétérotrophes, bactéries et virus). Aux faibles pH, la communauté phytoplanctonique a montré une réduction de la biomasse, des taux de croissance et de la prise de silice. Nos résultats suggèrent que le nanophytoplancton, et plus précisément les diatomées du genre *Thalassiosira spp.*, étaient moins affectés aux faibles pH que le pico- et le microphytoplancton. L'accumulation des TEP a été positivement corrélée à la biomasse du nanophytoplancton pendant les phases de floraison et de post-floraison. Les effets négatifs du pH sur le phytoplancton ont entraîné une diminution de la fixation du carbone et de l'accumulation de biomasse, ce qui a réduit l'accumulation des TEP et des concentrations de POC sous acidification (pH $\leq 7,55$). D'autre part, les flagellés hétérotrophes étaient favorisés par les faibles pH. La densité des bactéries a été réduite sous un pH faible probablement en raison d'une augmentation du broutage et/ou de la lyse virale. Au faible pH, le rapport POC: PON était plus faible, bien que nous ayons noté un changement de partition du carbone dissous vers le réservoir de POC via l'agrégation des TEP. Nous concluons que les changements anticipés de l'alcalinité et du pH pourraient affecter l'agrégation des TEP et leur structure, ce qui pourrait avoir un impact sur la sédimentation

de la matière organique avec des conséquences pour le pompage biologique du CO₂ et des rétroactions au changement global.

1.2 IMPACT OF OCEAN ACIDIFICATION ON TRANSPARENT EXOPOLYMERIC PARTICLES (TEP) AND ORGANIC CARBON ALLOCATION IN THE ST. LAWRENCE ESTUARY: A MICROCOSM EXPERIMENT

Authors:

Annane S.¹, St-Amand L.², Pelletier E.¹, Starr M.², Ferreyra G. A.¹

Institutions:

¹ Institut des sciences de la mer de Rimouski (ISMER), Université du Québec à Rimouski, Québec, 10 allée des Ursulines, Rimouski, Québec, Canada G5L 3A1

² Maurice Lamontagne Institute, Fisheries and Oceans Canada, 850 Route de la Mer, Mont-Joli, Québec, Canada G5H 3Z4

ABSTRACT

Increasing anthropogenic CO₂ is changing seawater chemistry by reducing pH (“ocean acidification”), which is suspected to have important effects on marine communities as well as on the nutrient and carbon cycles. Estuarine ecosystems are exposed to large fluctuations of CO₂/pH and ocean acidification (OA) is expected to lower further this pH range. A microcosm kinetic experiment was performed to investigate the effect of acidification on the natural plankton community, transparent exopolymeric particles (TEP) and organic carbon matter allocation in the lower St. Lawrence Estuary (LSLE). Six indoor microcosms with fixed pH treatments (pH_T from 7.86 to 6.90) and an unaltered pH reference microcosm were followed for the plankton community and different carbon pools (phytoplankton, TEP, POC, heterotrophs, bacteria, and viruses) over 15 days. Phytoplankton showed a reduced biomass, growth rates and silica uptake, under low pH. Our results suggest that nanophytoplankton, and more precisely diatoms from the *Thalassiosira spp.* group, were less affected to low pH than the pico- and microphytoplankton. TEP accumulation was positively correlated to nanophytoplankton biomass during the bloom and post-bloom phases. The negative effects of pH on phytoplankton resulted in a reduction of carbon fixation and biomass build-up, which reduced the accumulation of TEP and POC concentrations under acidification (pH ≤ 7.55). On the other hand, heterotroph flagellates were favored by low pH conditions. Bacteria decreased under low pH probably due to an increase of viral lysis and grazing. At low pH, POC:PON ratios were lower, though we noted a shift of carbon partition from dissolved into the POC pool via TEP aggregation. We conclude that anticipated changes in alkalinity and pH could affect TEP aggregation and TEP particle structure, which in turn could have an impact on the organic matter sedimentation with consequences for CO₂ biological pumping and feedback to global change.

Keywords: Transparent exopolymeric particles (TEP), CO₂, pH; nutrients, phytoplankton, particulate and dissolved organic carbon (POC, DOC), microcosm.

INTRODUCTION

Previous works on biological consequences of ocean acidification (OA) reported noteworthy changes in phytoplankton community structure and photosynthesis, showing significant increases in carbon assimilation (Engel 2002, Engel et al. 2003, Riebesell et al. 2007). This “carbon overconsumption” results in the release of large amounts of transparent exopolymer particles (TEP) that may enhance vertical export of particulate organic carbon (POC) (Engel 2002, Engel et al. 2004, Riebesell et al. 2007b). TEPs are acidic polysaccharide particles formed by aggregation of polymers exuded mainly by phytoplankton (especially diatoms) (Alldredge et al. 1993, Engel & Passow 2001) and, at a less degree, by bacteria (Simon et al. 2002). This process is viewed as a carbon ‘overflow’ for photosynthesis products under nutrient depletion (Jensen & Søndergaard 1982, Toggweiler 1993, Obernosterer & Herndl 1995, Engel 2002). These compounds form heavy aggregates (“marine snow”) by coagulation and aggregation processes of dissolved and colloidal organic carbon with other solid particles (e.g., phytoplankton cells, bacteria, detritus), accelerating the export of organic matter to deep waters (Logan et al. 1995, Passow & Alldredge 1995, Mari & Burd 1998, Simon et al. 2002, Nagata et al. 2021).

Over the last few years, an increasing number of studies investigated the effects of OA effects on TEPs production and organic carbon partitioning are a highly debated topic within the scientific community. Several studies showed enhanced TEP production and accumulation at higher $p\text{CO}_2$ in a natural phytoplankton assemblage (Engel 2002, Riebesell et al. 2007, Bellerby et al. 2008, Endres et al. 2014). Other experiments showed that high CO_2 supports the production and exudation of important DOC concentration, increasing TEP and the POC:PON ratio during mesocosms experiments (Engel et al. 2014a, Kim et al. 2014). These studies revealed a positive effect of high $p\text{CO}_2$ on TEP accumulation. But some have reported either no effect or a negative effect (Engel et al. 2014b, Bourdin et al. 2016). MacGilchrist et al. (2014) proposed a hypothesis to explain these contrasting results, attributing these variations to environmental setting experiments (community structure,

nutrient availability, and occurrence of phytoplankton growth) as a key factor determining the TEP response to OA. All these contrasting results highlight the fact that TEP and carbon partitioning response to OA depend on the interactions between environmental conditions (pH, CO₂, nutrients, estuary) and the planktonic community structure (phytoplankton, bacteria, viruses and microzooplankton) and its specific responses to OA.

Estuaries and coastal environments experience a great variability of physical and chemical factors. These ecosystems show a large diurnal and seasonal pH variability, due to multiple drivers such as photosynthesis, respiration, upwelling, tidal cycles, leaching water and anthropogenic nutrient inputs (Feely et al. 2008, Duarte et al. 2013, Capone & Hutchins 2013). Phytoplankton in estuarine and coastal waters is often highly productive and experience large fluctuations compared to oceanic species where the pH is relatively stable on a diurnal basis. Estuaries may promote coastal acidification even beyond the estimated pH projection for oceanic systems (Melzner et al. 2013, Wallace et al. 2014). Indeed, these ecosystems have been shown to vary as much as from 7.4 to 9.2 on a diurnal basis (Middelboe & Hansen 2007) and a 10 yrs. monitoring program in a Danish Fjord showed pH value to vary from 7.1 to 9.7 (Hansen 2002). Thus, the minimum pH in some coastal areas is lower than the 7.7 expected for the 21st century in the global ocean.

Previous records from our study site showed a surface *in situ* pH_(NBS) ranging between 7.7 and 8.1 (Pelletier & Lebel 1980, Lebel & Pelletier 1980). More recently, Annane et al. (2015) in the St. Lawrence Estuary (SLE), found surface *in situ* values pH_T in the range of 7.8 - 8.3 over spring to fall in 2011. However, upwelled deep water against the sill at the Head of the Laurentian Channel (8 km from our sampling site) over a distance of 20 km (Ingram 1975, Therriault & Lacroix 1976, Savenkoff et al. 1997), brings deep water with a pH of 7.54 - 7.60 which can further acidify the mixed surface waters (Mucci et al. 2011, Lefort et al. 2012, Annane et al. 2015). These conditions may lead to a pH much lower than the expected range of ~7.4 to 7.9 in the SLE for the end of the century. As emphasized by Thoisen et al. (2015), research on OA and more particularly in coastal and

estuarine areas should include *in situ* pH measurements before experimentally expose organisms to pH values beyond present-day naturally occurring levels.

In the study of Annane et al. (2015), it was evidenced that TEP was positively correlated with the phytoplankton biomass in surface waters, and TEP combined with phytoplankton carbon represented the major fraction of carbon pool in the SLE, suggesting that they could significantly contribute to macro-aggregate exports to the deep waters. In this context, it is crucial to investigate the natural plankton community as well as the responses of the organic carbon pool to future growing acidification scenarios. The present study aims to describe the results of a microcosm kinetic experiment considering a pH gradient to examine how TEP production and the planktonic community are affected by the growing acidification in the SLE, and to investigate these effects on particulate carbon allocation in this sub-arctic ecosystem.

MATERIALS AND METHODS

Experimental setup and sampling strategy

A microcosm experiment was performed between 4 and 22 May 2012 at the Maurice Lamontagne Institute (Fisheries and Oceans, Canada). Seven indoor microcosms (40L each) were filled with surface water (~1.5 m) from the head of the Laurentian channel zone (Lower St. Lawrence Estuary, LSLE; 48°07.185'N, 69° 40.503'W) just before the spring phytoplankton bloom start. Water was previously pre-filtered through a 200 µm Nitex mesh to remove mesozooplankton (*in situ* pH_T and salinity at the time of sampling were 7.86 and 20.7, respectively) and microcosms were immersed in a thermostated bath at 7 °C (representative of *in situ* spring temperature). Our experimental design considered the response of the natural plankton community to exposure to a gradient of six fixed pH levels (7.86 to 6.94). In addition, one microcosm was left unperturbed without pH manipulation and served as reference (Havenhand et al. 2010). Desired pH values were achieved by air bubbling the water column with an air/CO₂ mixing system placed near the bottom of the microcosms. Each microcosm was monitored continuously with a pH probe (InPro 3253, Mettler Toledo Ingold® for biotechnological and pharmaceutical application, 250 mm shaft length and temperature compensation Pt 100) and controlled by the gas bubbling addition to obtain stable pH targets (Fig. 1). The pH conditions were maintained using an automated valves system controlled by a software developed by the Engineering Department of University of Québec at Rimouski (UQAR, pH precision ±0.005). The microcosms are Plexiglas cylinders surrounded with four culture lamps each with a light: dark cycle of 15:9 h and photosynthetically active radiation (PAR) of 997 µmol m⁻² s⁻¹. The atmosphere at the surface of each microcosm was isolated from the outside with a clear Plexiglas cover.

Initial nutrient concentrations were 14.48 µM nitrate (NO₃⁻), 0.27 µM soluble reactive phosphate (SRP) and 31.62 µM silicic acid (Si(OH)₄). The SRP were rather low for the season in the SLE. To be in the normal range of SRP (0.29 to 1.31) and make the

experience more comparable to SLE nutrient concentrations, SRP concentration was adjusted from 0.27 to 0.84 μM . However, SRP increased in all microcosms on day 1 just before the nutrient adjustment which brings our adjustment of SRP to 1.28 μM .

Sampling was performed in each microcosm every two days during the morning (8h00 - 10h00), and the experiment lasted 15 days. Samples were gently reversed pumped using polycarbonate pump syringes and transferred to 2 L glass bottles cleaned with HCl 10 % for different analyses at the exception of pH, total alkalinity (TA) and dissolved organic carbon (DOC), which were sampled with glass graduated tubes and glass bottles.

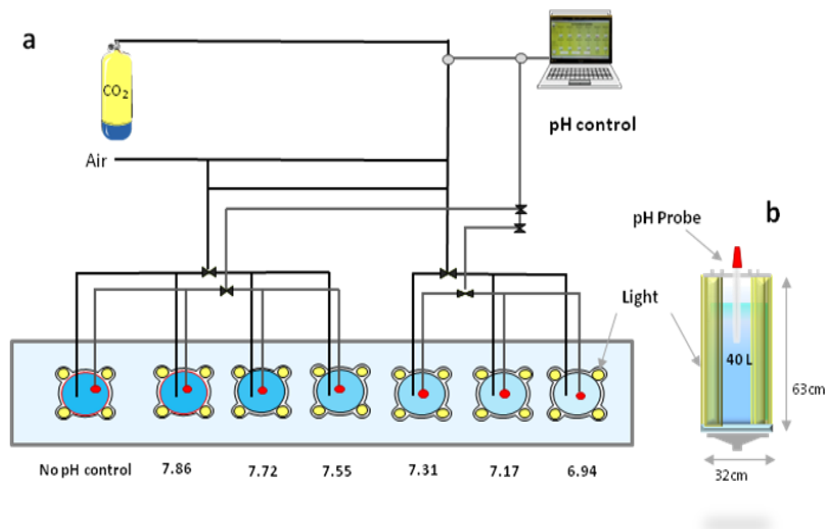


Figure 1: Experimental setup of CO₂ manipulation system and computer control of pH for each microcosm (a) and profile view of microcosm (b). A mixture of air and CO₂ was bubbled directly in the bottom of each microcosm thus achieving a gradient of 6 pH levels and a pH reference microcosm. The air/CO₂ mixing was adjusted for each microcosm by instant pH probe monitoring and adjustment.

Nutrient analyses

Water samples for nutrient analyses were filtered through Acrodisc® syringe filters with 0.8 µM Versapor® membranes. The filtrates were stored at -20 °C in acid-cleaned polycarbonate cryogenic vials for a month until analysis of nitrate plus nitrite ($\text{NO}_3^- + \text{NO}_2^-$), nitrite (NO_2^-), soluble reactive phosphate (SRP), and silicic acid ($\text{Si}(\text{OH})_4$) using a Technicon II Autoanalyzer (Mitchell et al. 2002).

Carbonate chemistry

The carbonate chemistry was monitored through pH and TA measurements. Samples for pH, expressed in the 'total hydrogen ion scale' (pH_T) and total alkalinity (TA) were drawn under a bubble free, and no head space conditions into 300 and 500 mL borosilicate glass flasks, respectively. 250 µL of saturated HgCl_2 solution was added to TA sample and processed following the "Guide to best practices for Ocean CO_2 Measurements" (Dickson et al. 2007). pH_T was determined immediately after sampling and TA determined a few months later in the laboratory at the Maurice Lamontagne Institute (MLI).

pH_T was determined spectrometrically using the indicator dye *m*-cresol purple (Sigma-Aldrich). Absorbance was measured at 730, 578 and 434 nm before and after dye addition in 10 cm quartz cells thermostated at 25 ± 0.05 °C (Clayton & Byrne 1993, Dickson et al. 2007). A similar procedure was carried out before each set of sample measurements using a TRIS (Tris (hydroxymethyl) -aminomethane) buffer prepared at a practical salinity (S) of approximately 30 (Millero 1986). Certified Reference Material (CRM) (supplied by Professor Andrew Dickson, Scripps Institution of Oceanography, San Diego, USA) was used for quality control of our pH TRIS buffer. All measurements were converted to the total proton scale (pH_T) using the measured salinity of each sample and the HSO_4 association constants given by Dickson (1990). Reproducibility and accuracy of our TRIS buffer measurements were in the order of 0.005 pH unit or better.

TA was determined by potentiometric titration in an open cell using an automated Radiometer potentiometric titrator (Titralab 865) and a pH combination electrode (pHC2001) in a continuous titrant addition mode, an algorithm specifically designed for shallow end-point detection (Dickson et al. 2003, 2007). The dilute HCl titrant 0.1 M in a solution of NaCl of 0.6 M was calibrated using certified reference materials provided by Professor Andrew G. Dickson of the Scripps Institute of Oceanography (La Jolla, USA).

The carbonate system parameters were corrected for *in situ* temperature based on the experimental data of $\text{pH}_{\text{T}25}$, TA, T, S, PO_4 , SiO_2 as input parameters with the CO2SYS program (Lewis & Wallace 1998). The constants of Mehrbach et al. (1973) as refitted by Dickson & Millero (1987) for the dissociation of carbonic acid and those of Dickson (1990) for KSO_4 equilibrium were used. The carbonate parameters for each treatment during the experiment are outlined in Table 1.

Table 1: Measured and calculated values (mean \pm SD, n=5) of carbonate system parameters for the microcosms pH treatments and the not controlled microcosm during the experiment.

| Microcosm | pH _T <i>in situ</i> (total scale) | Salinity | [H ⁺] (x 10 ⁻⁸ mol. L ⁻¹) | TA ($\mu\text{mol.kg}^{-1}$ sw) | pCO ₂ (μatm) | DIC ($\mu\text{mol.kg}^{-1}$ sw) | HCO ₃ ⁻ ($\mu\text{mol.kg}^{-1}$ sw) | CO ₃ ²⁻ ($\mu\text{mol.kg}^{-1}$ sw) | CO ₂ ($\mu\text{mol.kg}^{-1}$ sw) | Ω Ca | Ω Ar |
|------------|---|-------------------|---|--|---|---|---|---|---|------------------|------------------|
| No control | 7.95 \pm 0.04 | 20.82 \pm 0.02 | 1.14 \pm 0.09 | 1721 \pm 0.13 | 434 \pm 40 | 1667 \pm 8.80 | 1591 \pm 11.26 | 52 \pm 4.56 | 22.8 \pm 2.10 | 1.3 \pm 0.12 | 0.8 \pm 0.07 |
| M1 | 7.86 \pm 0.004 | 20.69 \pm 0.007 | 1.39 \pm 0.013 | 1708 \pm 2.6 | 534.7 \pm 5.8 | 1673 \pm 3.24 | 1602 \pm 3.2 | 43 \pm 0.35 | 28 \pm 0.30 | 1.1 \pm 0.009 | 0.7 \pm 0.005 |
| M2 | 7.72 \pm 0.01 | 20.69 \pm 0.005 | 1.92 \pm 0.06 | 1698 \pm 1.6 | 747 \pm 25.5 | 1691 \pm 3.19 | 1620 \pm 2.86 | 31 \pm 0.97 | 39.3 \pm 1.34 | 0.8 \pm 0.025 | 0.5 \pm 0.015 |
| M3 | 7.54 \pm 0.003 | 20.75 \pm 0.01 | 2.86 \pm 0.02 | 1720 \pm 4.5 | 1145 \pm 9.2 | 1748 \pm 4.71 | 1666 \pm 4.5 | 22 \pm 0.18 | 60.2 \pm 0.49 | 0.6 \pm 0.0047 | 0.3 \pm 0.003 |
| M4 | 7.31 \pm 0.02 | 20.72 \pm 0.007 | 4.90 \pm 0.24 | 1721 \pm 3.4 | 1989 \pm 97.5 | 1806 \pm 5.61 | 1689 \pm 3.11 | 13 \pm 0.67 | 104.6 \pm 5.13 | 0.3 \pm 0.0156 | 0.2 \pm 0.009 |
| M5 | 7.17 \pm 0.007 | 20.73 \pm 0.004 | 6.79 \pm 0.11 | 1729 \pm 0.02 | 2776 \pm 45.6 | 1861 \pm 2.37 | 1705 \pm 0.28 | 9.3 \pm 0.15 | 146 \pm 2.45 | 0.2 \pm 0.004 | 0.1 \pm 0.0023 |
| M6 | 6.93 \pm 0.04 | 20.73 \pm 0.016 | 11.69 \pm 1.18 | 1727 \pm 3.06 | 4805 \pm 484 | 1971 \pm 25 | 1713 \pm 2.86 | 5.5 \pm 0.56 | 252.7 \pm 25.4 | 0.1 \pm 0.014 | 0.1 \pm 0.0087 |

TEP analysis

TEP concentration was determined colorimetrically following the procedure described in Passow & Alldredge (1995). Briefly, 80-100 mL samples were filtered onto 0.2 μm polycarbonate Isopore membrane filters (Merck Millipore) under low vacuum (<10 mbar). Particles retained on the filters were stained during <5 s with 500 μL of 0.02 % aqueous solution of Alcian blue in 0.06 % acetic acid (pH 2.5) and subsequently rinsed with 1 mL of deionised water. Samples were stored at -80 $^{\circ}\text{C}$ for a month until analysis. Filters were then soaked in 80 % sulfuric acid (6 mL) for 2 h and measured spectrometrically at 787 nm, using stained filters without sample as blanks. Alcian Blue absorption was calibrated using a solution of the polysaccharide Gum Xanthan. TEP concentrations were expressed in μg Gum Xanthan equivalents per liter ($\mu\text{g GX eq L}^{-1}$). These values were converted into carbon equivalent units using a natural diatom population conversion factor of $0.75 \mu\text{g C}/\mu\text{g GX eq L}^{-1}$, according to Engel & Passow (2001). It should be noted that the diatom species examined in their experiments presented a series of slopes, ranging from 0.51 to 0.88 $\mu\text{g C}/\mu\text{g GX eq L}^{-1}$, due to differences in phytoplankton composition; thus TEP-C content estimated here may present some uncertainties.

Particulate organic carbon analysis (POC)

Duplicates of 250 mL seawater samples were filtered through pre-combusted (500 $^{\circ}\text{C}$, 4 h) Whatman GF/F filters and frozen with silica gel until analysis. The POC filters were then oven dried 24 h at 50 $^{\circ}\text{C}$ prior to analysis. POC concentrations were determined with a CHN elemental analyzer (EA) COSTECH ECS 4010 (Costech Analytical). Quantification was based on external Acetanilide standard with a calibration range from 0.025 to 0.080 mg and 0.170 to 0.550 mg for nitrogen and carbon, respectively, and included a blank capsule. Blank capsules and blank filters were also analyzed in every run to confirm the absence of contamination.

Dissolved organic carbon analysis (DOC)

Duplicates of 9 mL water samples were filtered through pre-combusted (500 °C, 5 h) Whatman GF/F filters in a glass tube and acidified with 100 µL of 2N HCl, then stored at 4 °C in the dark until analysis. DOC was measured immediately after the experience using the high temperature catalytic oxidation (HTCO) method with a TOC-Vcpn Shimadzu Analyser (Wurl & Min Sin 2009). This technique showed a CV 0.25 % (n = 84) between replicates.

Phytoplankton composition and abundance

Samples for the identification and enumeration of phytoplankton >2 µm were collected and preserved in acidic Lugol's solution (Parsons et al. 1984) and stored in the dark at 4 °C for three years until analysis. Phytoplankton cells were identified to the lowest possible taxonomic level (Bérard-Therriault et al. 1999) using an inverted microscope according to Lund et al. (1958). For each sample, at least 300 cells were counted.

Flow cytometry analysis

The pico and nanophytoplankton and the microphytoplankton were analyzed using two different types of flow cytometry instruments, in order to achieve accurate estimations of cell size and counts.

Duplicates of 12 mL seawater samples were fixed with glutaraldehyde (Grade I; Sigma) 1 % final concentration and frozen at -80 °C for a year until flow cytometric analysis. Nano- and microphytoplankton cells larger than ~6 µm were analyzed using a CytoSense flow cytometer (Cytobuoy b.v., The Netherlands) equipped with a 488 nm laser operated at 15 mW and a peristaltic pump speed of 6.15 µl s⁻¹ and a trigger level of 33 mV on FLR. Yellow fluorescent beads of 10 µm (Polysciences®) were systematically added to each sample as an internal standard. This procedure allowed to normalize the fluorescence

emission and light scatter signals obtained from CytoSense flow cytometer, as well as to ensure the quality control and calibrate the cell size. One mL of Tris-EDTA 10x buffer pH 8 (Laboratoire MAT) was added in order avoid coincidence of several particles in the laser beam. Each photosynthetic cell was characterized by an optical pulse shape, including their light scattering properties, forward light scatter (FWS) and sideward light scatter (SWS) and red (FLR, 668–734 nm), orange (FLO, 601–668 nm) and yellow (FLY, 536–601 nm) fluorescence emissions. Samples were then analyzed with the CytoClus software and cells sharing similar optical characteristics were manually grouped in clusters (Table 2) (Dubelaar et al. 2004).

Phytoplankton abundances were converted to carbon biomass by using a cellular carbon content conversion factor (Cell C, pg C cell⁻¹) derived from averaged cell biovolume (BV; μm^3) for each cluster (Table 2), using the equations proposed by Montagnes et al. (1994) for diatoms and flagellates dominated communities:

$$\text{Cell C} = 0.109 * \text{BV}^{0.991}$$

Table 2: Estimated FWS length (Avg. \pm Std) obtained from the Cytosense flow cytometer for the identified clusters.

| Clusters | FWS length (μm) | BV (μm^3) |
|---------------|------------------------------|------------------------|
| C1* | 22.9 \pm 3.1 | 1695 |
| C2 | 14.0 \pm 2.2 | 1039 |
| C3 | 9.7 \pm 1.1 | 491 |
| C4 | 18.4 \pm 2.8 | 1350 |
| Small chains* | 36.2 \pm 5.3 | 2668 |
| Long chains* | 81.5 \pm 13.2 | 6042 |

*Microphytoplankton clusters considered ($> 20 \mu\text{m}$)

The phytoplankton carbon biomass (Phyto-C, $\mu\text{g C L}^{-1}$) was obtained by multiplying cell abundance by cellular carbon content for each phytoplankton cluster. However, only the microphytoplankton size fraction was considered for this study, as to not have data overlap for nanophytoplankton size fraction.

For pico and nanophytoplankton ($<10 \mu\text{m}$) 4.5 ml samples were pre-filtered (200 μm Nitex mesh size) and fixed with glutaraldehyde (Grade I; Sigma) 0.5 % final concentration and frozen at $-80 \text{ }^\circ\text{C}$ for four years until flow cytometric analysis. Samples were analyzed using an FACSCalibur flow cytometer (Becton and Dickinson) equipped with a 488 nm laser (15 mW output) at a flow rate $50.84 \mu\text{L s}^{-1}$. Fluorescent beads 2 μm (Polysciences) were added to each sample as an internal standard. Pico- ($<2 \mu\text{m}$) and nanophytoplankton (2-20 μm) were discriminated based on forward scatter calibration with beads size and the optical parameters characteristic of each population, namely: forward and right angle light scatter, orange fluorescence from phycoerythrin ($575 \pm 20 \text{ nm}$) and red fluorescence from Chl *a* ($675 \pm 10 \text{ nm}$) following Tremblay et al. (2009).

Synechococcus and *Prochlorococcus* cell numbers were converted to carbon biomass by applying a conversion of $200 \text{ fg C cell}^{-1}$ (Mackey et al., 2002) and $49 \text{ fg C cell}^{-1}$ (Cailliau et al. 1996), respectively. Biomass for pico- and nanophytoplankton was calculated using the conversion factor of $0.22 \text{ pg C } \mu\text{m}^{-3}$ (Booth 1993). The resulting carbon biomasses per cell are 0.388 and $31.634 \text{ pg C cell}^{-1}$ for pico- and nanophytoplankton respectively.

Bacterial and virus abundance

Free-living bacteria and virus samples were pre-filtered (200 μm Nitex mesh size) and fixed with glutaraldehyde ($C_f = 0.5\%$, Grade I; Sigma) according to Lapoussière et al. (2011) and Marie et al. (1999) respectively, placed in the dark at $4 \text{ }^\circ\text{C}$ for 30 min and then frozen at $-80 \text{ }^\circ\text{C}$ for 18 months until flow cytometric analysis. Samples were analyzed

using an FACSCalibur flow cytometer (Becton and Dickinson) equipped with a 488 nm argon laser (15 mW output) at a low flow rate ($10.14 \mu\text{L s}^{-1}$ for 30 s) analysis.

Before analysis, samples were thawed at room temperature, and then diluted in a solution of TE buffer ($C_f = 0.1 \%$, 10 mM Tris, 1 mM EDTA, Sigma) and SYBR-Green I ($C_f = 0.01 \%$, Molecular Probes, Inc) in a final volume of 5 mL in order to maintain an optimum pH of the staining with SYBR Green I, according to Belzile et al. (2008). Dilution with the buffer also avoided coincidence of several particles in the laser beam and minimized the error due to low-volume pipetting. Samples were then placed 15 min in the dark in a 80°C water bath to optimize the staining (Marie et al., 1999). Bacteria and virus were analyzed using their green fluorescence (FL1) collected at 530 nm versus side scatter. Yellow Fluoresbrite beads of $0.5 \mu\text{m}$ (Polysciences) were added to the samples as internal standards for cell size and fluorescence emission. Bacteria and virus were enumerated and discriminated according to their size and nucleic acid content. Characterization and dissociation of bacteria with high (HNA) and low (LNA) nucleic acid contents were based on the SSC/FL1 ratio (Lapoussière et al., 2011; Lebaron et al., 2001). Final counts were corrected for a blank sample prepared and analyzed in an identical manner to the samples. Bacterial counts were expressed in terms of carbon biomass by using a conversion factor of $14 \text{ fg C.cell}^{-1}$ (Zubkov et al. 2001).

Statistical analysis

All statistical analyses were performed using Statistica (version 7.0) and SigmaPlot 10.0 software. The data from day 0 to 2 were not included in the analysis, as treatments had no time to affect the different variables. Analysis of covariance (ANCOVA) was used to test the effect of pH (in term of proton concentration $[\text{H}^+]$) on TEP-C and other variables. Concentrations and abundances as dependent variables, sampling times as factor and $[\text{H}^+]$ as a covariate. Separate slope model was applied to test the regression slope of proton concentration $[\text{H}^+]$ effect on TEP-C between each separate day using sampling days as the categorical variable; concentrations and abundances as dependent variables and $[\text{H}^+]$ as

continuous predictor. $P \leq 0.05$ were considered as statistically significant difference. All data were tested for normality and homogeneity of variances conditions with Kolmogorov-Smirnov and Cochran C tests, respectively. Regressions of the rate of change (accumulation or depletion) for each variable were calculated for the bloom and post-bloom period according to the following equation:

$$\mu = (\ln [N_2] - \ln [N_1]) / (t_2 - t_1)$$

Where N_1 and N_2 are the concentration of the studied variables at the given times t_1 and t_2 , respectively. Relationships between the variables rate of change and the proton concentration $[H^+]$ treatment were evaluated using the Pearson's linear regression square root (r). The $p \leq 0.05$ were considered as indicators of a significant relation between the predictor values and the response variable.

RESULTS

1. Carbonate chemistry

The CO_2 enrichment for each microcosm started on day 0 and reached the gradient pH target on day 2 (Fig. 2), from pH 7.86 to 6.94 representing an average decrease of 0.18 ± 0.04 between each pH treatment. The different levels of the pH treatment remained stable during the whole experiment. However, the reference microcosm showed a slight increase in day 4 to pH 8.01 due to photosynthetic activity, then remained stable (~ 7.93) during the rest of the experiment. Our pH probe monitoring data shows that the pH probe (NBS) fits almost perfectly with pH_T determined colorimetrically (total proton scale), presenting a highly significant correlation coefficient ($r = 0.998$, $p < 0.01$) (Fig. 3). These pH correspond to pCO_2 ranging from 434 to 1989 μatm (Table 1) according to the prediction of the IPCC (2014) applicable to this estuarine ecosystem. The other two pCO_2 (2776 and 4805 μatm) represent predictions up to 2200. TA was also stable during the

whole experiment and ranged between 1698 and 1729 $\mu\text{mol kg}_{\text{sw}}^{-1}$ compared to the pH reference microcosm 1721 $\mu\text{mol kg}_{\text{sw}}^{-1}$ (Table 1). However, these natural initial TA values were slightly lower compared to previous data from the same area in 2011 ($\sim 2100 \mu\text{mol kg}_{\text{sw}}^{-1}$, Annane et al. 2015.). DIC increased slightly from 1673 $\mu\text{mol kg}_{\text{sw}}^{-1}$ for M1 to 1971 $\mu\text{mol kg}_{\text{sw}}^{-1}$ for M6, though they stayed stable all along the experiment.

2. Inorganic nutrients

Nutrient concentrations were typical for the season at day 1 of the experiment, with 12.94, 1.28 and 30.73 μM for nitrate, SRP, and silicic acid, respectively (Fig. 4a-c). SRP increased in all microcosms on day 1 just before the nutrient adjustment from 0.27 to 0.84 μM which brings our adjustment of SRP to 1.28 μM (Fig. 4b). Nitrate and SRP dropped sharply until day 4, reaching the detection limit of the method used for nitrate

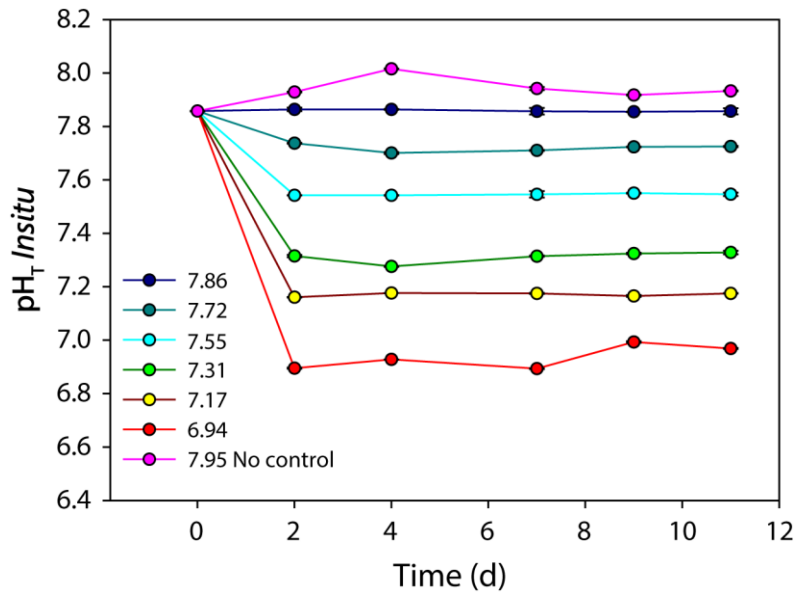


Figure 2: Temporal variation in $\text{pH}_T \text{ In situ}$ (total hydrogen ion scale) during the microcosm experiment.

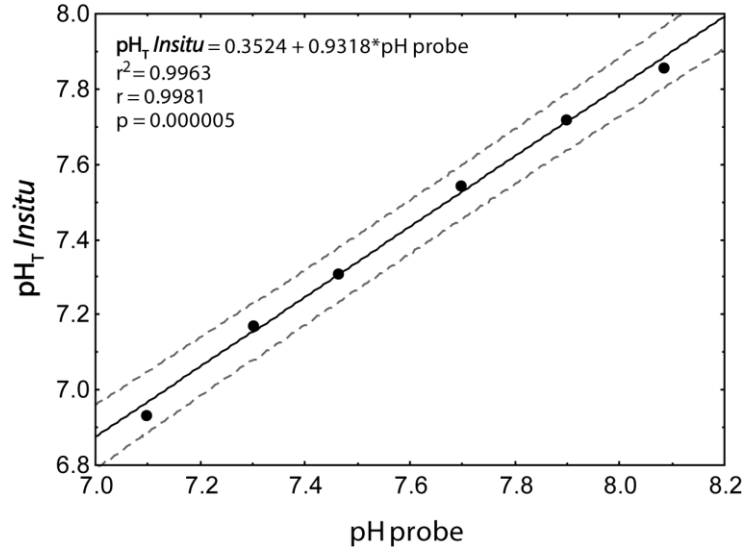


Figure 3: Regression between pH_T *in situ* values spectrometrically measured (total hydrogen ion scale) and those coming from continuous pH probes (NBS). Dashed lines represent the 0.95 confidence level.

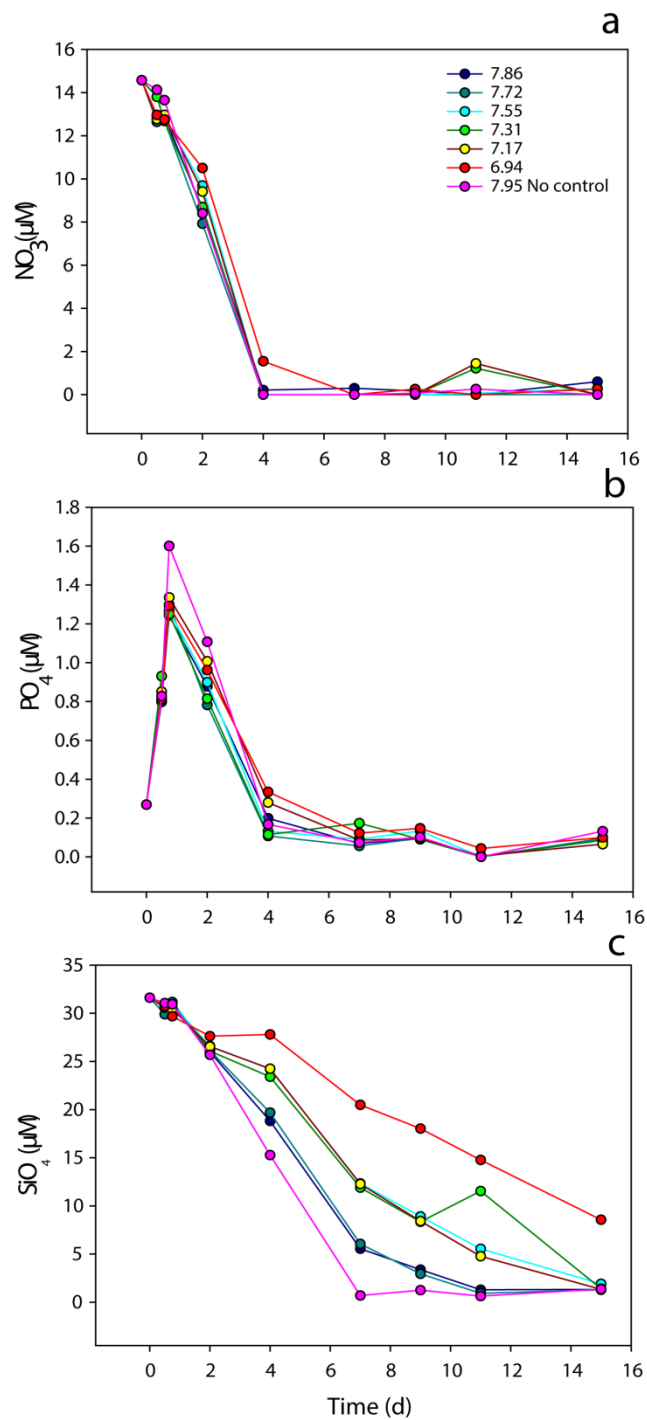


Figure 4: Nutrient time change for: (a) nitrate (b) SRP and (c) silicic acid in the pH perturbed and reference microcosms.

except for the lowest pH treatment (1.55 μM) and showing low concentrations for SRP (0.11 - 0.33 μM), which continued to decrease slowly until reaching the detection limit of the method on day 11 (Fig. 4a, b). The rates of nitrate depletion during the bloom was delayed in the lowest pH treatment ($r = -0.95$; $p < 0.01$; not shown), reaching below detection limit on day 7. However, no correlations were observed between the rate of SRP depletion and the pH gradient during this experiment ($r = -0.69$; $p > 0.05$; not shown). No statistical difference for the ratio $\Delta\text{NO}_3 : \Delta\text{SRP}$ uptake was found between pH treatments ($r = 0.44$; $p > 0.05$; not shown). On the other hand, silicic acid concentrations decreased gradually until the end of the experiment (Fig. 4c), reaching minimum concentrations between 1.28 to 8.56 μM . The rates of silicic acid change during the bloom showed a significant statistical difference between pH treatments ($r = -0.95$; $p < 0.01$), with minimum depletion rates corresponding to the most acidic conditions (Fig. 5a) and pH explaining 91 % of the variance of the regression. The ratio $\Delta\text{Si}(\text{OH})_4 : \Delta\text{NO}_3$ decreased linearly with increasing proton concentration $[\text{H}^+]$ ($r = -0.89$, $p < 0.01$; Fig. 5b). This change was mostly driven by a reduction in $\Delta\text{Si}(\text{OH})_4$ uptake, which exhibited a 6.46-fold difference between experimental pH extremes compared to a 1.13-fold difference for ΔNO_3 uptake (not shown). No statistical difference for the ratio $\Delta\text{Si}(\text{OH})_4 : \Delta\text{Diatoms}$ was found between pH treatments ($r = -0.08$, $p > 0.05$; Fig. 5c). Although $\Delta\text{Diatoms}$ exhibited a 7.61-fold difference between experimental pH extremes compared to $\Delta\text{Si}(\text{OH})_4$ uptake (not shown).

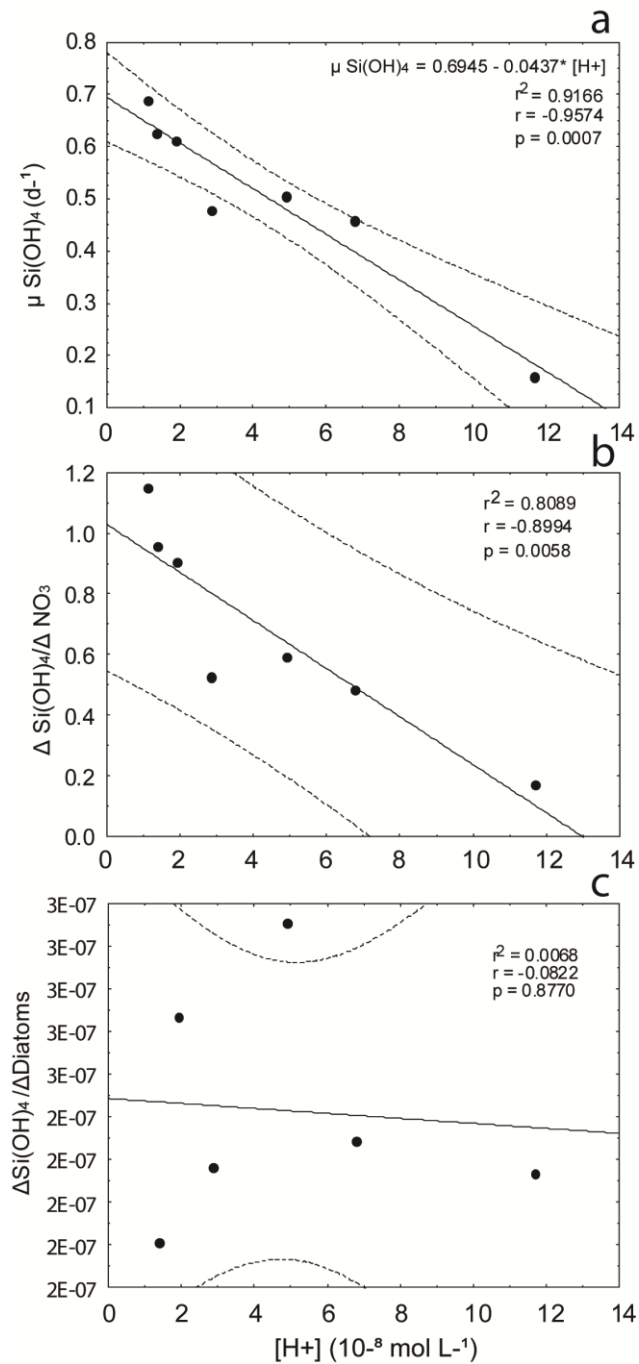


Figure 5: Relationship between the proton concentration values ($[H^+]$) and (a) the rate of silicic acid change, (b) the ratio $\Delta \text{Si(OH)}_4 : \Delta \text{NO}_3$ and (c) the ratio $\Delta \text{Si(OH)}_4 : \Delta \text{Diatoms}$ during the bloom development (day 1 to day 4). Significant regression (solid line) with (95%) confidence intervals (dashed lines) are shown.

3. Dynamics of organic material

Phytoplankton

Phytoplankton developed a bloom which was characterized by three phases: (1) Adaptation to treatment phase, from the beginning to day 2, (2) an exponential bloom phase, from day 2 to 7-9 and (3) a post-bloom phase, between days 7-9 to 15 (Fig. 6a, b).

Here we considered three phytoplankton carbon size fractions: picophytoplankton-C (<2 μm), nanophytoplankton-C (2-20 μm) and microphytoplankton-C (>20 μm), since the sum of pico-, nanophytoplankton-C, microphytoplankton-C and TEP-C presented the best linear fit with POC concentrations in all microcosms ($r = 0.90$, $p < 0.01$; Annex 1.1). It should be noted that these size categories match the category sizes defined by the literature. So to prevent any overlapping for nanophytoplankton size fraction due to the approximation to the instrument's resolution used during our study (FACSCalibur and CytoSense flow cytometer), we have chosen to use only nanophytoplankton analysed by FACSCalibur flow cytometer.

Picophytoplankton-C biomass was $2.16 \mu\text{g C L}^{-1}$ (Fig. 6a) in all microcosms at the start of the experiment, and then decreased during the adaptation phase to reach values between $0.4\text{-}0.62 \mu\text{g C L}^{-1}$ on day 1. Afterward, picophytoplankton-C increased during the exponential phase to reach a peak on day 4 with values between $1.12 - 2.45 \mu\text{g C L}^{-1}$, then decreasing in all treatments along the rest of the experiment. Picophytoplankton biomass presented the highest concentration at the high pH and the lowest at low pH with a significant negative pH effect during the bloom period (ANCOVA, $p < 0.01$). Separate Slope (Sslope) analysis showed a difference between days for the pH effect on picophytoplankton ($p < 0.01$), revealing a significant negative pH effect for all days ($p < 0.01$), with the lowest concentration observed in the acidified treatments especially during the bloom (phase 2).

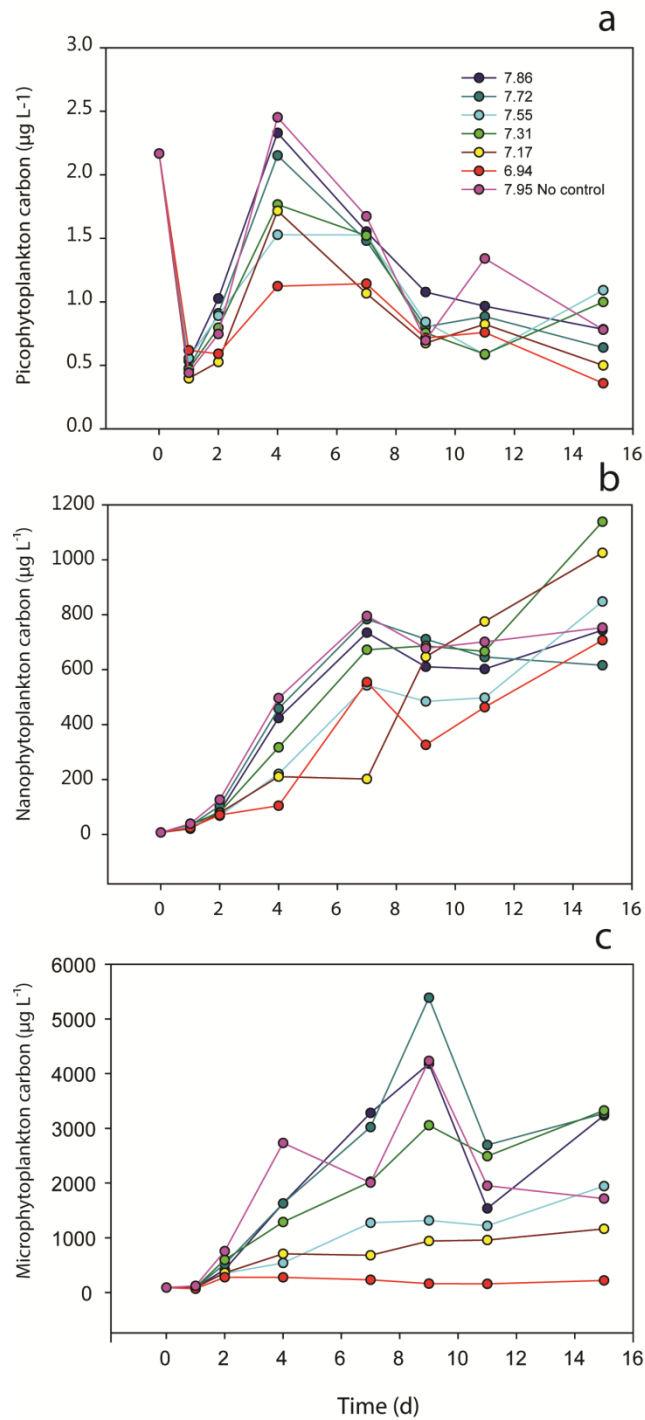


Figure 6: Temporal evolution of phytoplankton carbon ($\mu\text{gC L}^{-1}$) during the experiment: (a) Picoplanphytoplankton-C, (b) Nanophytoplankton-C and (c) Microphytoplankton-C. Each curve represents a microcosm with a specific pH treatment.

Nanophytoplankton-C at the start of the experiment was $9.15 \mu\text{g C L}^{-1}$ (Fig. 6b). The exponential phase reached a first biomass peak at day 7 and varied between $203\text{--}736 \mu\text{g C L}^{-1}$, with the highest concentration observed at the highest pH (ANCOVA, $p < 0.05$), with a decrease of ~ 26 to 72% at pH 7.55 and 7.17, respectively. A second peak developed during the third phase, reaching values between $616\text{--}1025 \mu\text{g C L}^{-1}$, with the highest concentrations observed at low pH values (pH = 7.17 - 7.31), reaching an increase of 38% at the end of the phase 3. However, Sslope analysis showed no difference between days for the pH effect on nanophytoplankton-C ($p > 0.05$), nor an interaction between days and pH effect on nanophytoplankton-C concentration ($p > 0.05$).

Microphytoplankton-C increased exponentially during phase 2 reaching values between ~ 165 and $\sim 5400 \mu\text{g C L}^{-1}$, with the highest concentration observed at pH 7.72 (ANCOVA, $p < 0.01$). Later, cell concentrations decreased slightly in the phase 3 reaching values around ~ 221 and $\sim 3327 \mu\text{g C L}^{-1}$, with the highest concentrations observed for high and intermediate pH values, between 7.86-7.31 (Fig. 6c). In contrast, the lower pH microcosm (6.94) presented a very low concentration during the whole experiment. Although the Sslope analysis showed no difference between days for the pH effect on microphytoplankton ($p > 0.05$), the maximum microphytoplankton-C concentrations showed a decrease with the reduction of pH conditions during the phase 2 ($r = -0.80$, $p < 0.05$), representing a decline from 20% to 89% of microphytoplankton-C at pH 7.55 and 6.94 values, respectively.

During phase 2 (d2-d7), nanophytoplankton growth rate (between 0.32 and 0.45 d^{-1}) was not affected by the pH decrease ($p > 0.05$; Fig. 7a). The same response was observed for the phase 3, showing a non significant positive trend to pH decrease ($r = 0.74$, $p > 0.05$). Growth rate values at high and low pH conditions (-0.02 and 0.12 d^{-1} , respectively) were lower during the second bloom period (phase 3, Fig. 7b). In contrast, microphytoplankton growth rates in phase 2 (d2-d9) presented a significant negative effect with pH decrease ($r = -0.95$, $p < 0.01$; Fig. 7c), with 0.32 d^{-1} at high pH and -0.08 d^{-1} at low pH. As for the case of nanophytoplankton during phase 3, a positive, but not significant correlation to pH

decrease, was observed for microphytoplankton ($r = 0.60$, $p > 0.05$), with -0.08 d^{-1} at high pH to 0.05 d^{-1} at low pH (Fig. 7d).

The phytoplankton assemblages were mainly constituted by diatoms (77 % of the total community) and autotrophic flagellates (13 %; Fig. 8a). Centric diatoms dominated numerically (95 to 99.85 % of the total diatom cell number), with *Skeletonema costatum* (73 %), followed in abundance by *Thalassiosira* spp. (5-10 μm ; 26 %) in the adaptation phase. During the exponential bloom phase 2 (d4), diatoms varied between 81 % and 45 %,

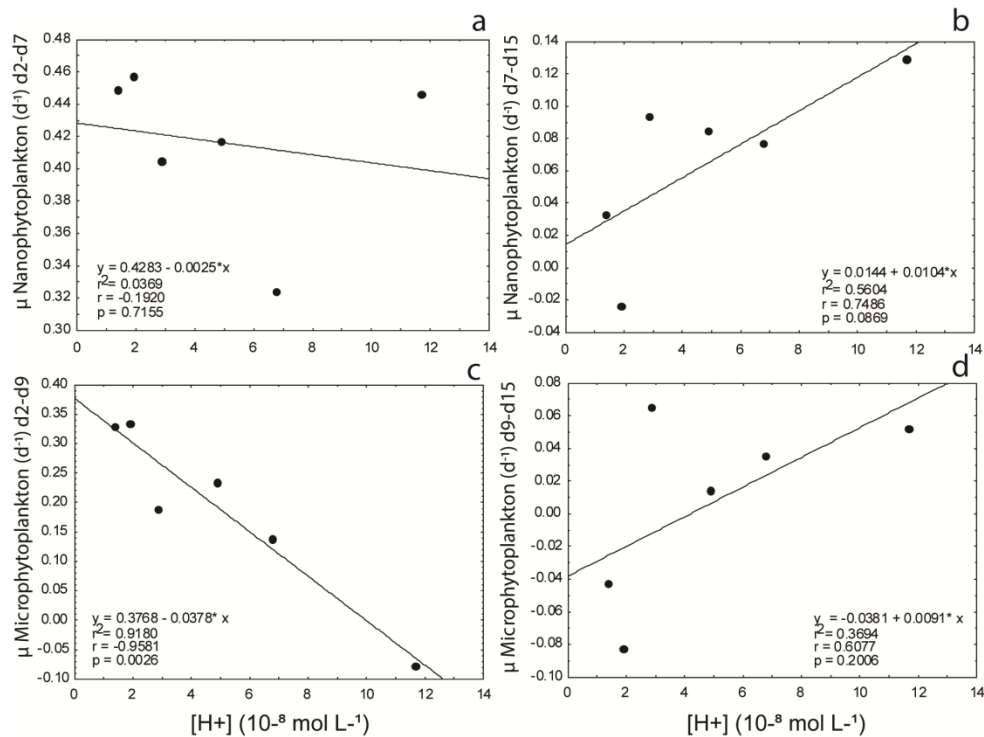


Figure 7: Relationship between the proton concentration values ($[H^+]$) and phytoplankton growth rate ($\mu \text{ d}^{-1}$) during the bloom development for (a) Nanophytoplankton-C (day 2 to day 7), (b) Nanophytoplankton-C (day 7 to day 15), (c) Microphytoplankton-C (day 2 to day 9) and (d) Microphytoplankton-C (day 9 to day 15). Linear regressions are shown with solid lines are shown. A negative growth rate indicates a cell loss.

with the highest percentage at pH 7.86 and the lowest at pH 6.94 (Fig. 8a). In turn, autotrophic flagellates increased from 13 % at pH 7.86 to 35 % at pH 6.94. At the end of

the phase 3, diatoms decreased, but were still dominant (50-77 %), and autotrophic flagellates increased (23 -50 %; Fig. 8a). Among centric diatoms, *S. costatum* varied between 79 % and 17 %, with the highest densities at pH 7.72 and lowest at pH 6.94 at the end of phase 3. In contrast, *Thalassiosira* spp. (5-10 μm) varied between 15 % and 74 %, with the lowest contribution to total biomass at pH 7.72 and the highest at pH 6.94 at the end of phase 3 (Fig. 8b). However, these last two negative and positive correlations with decreasing pH were not significant ($p = 0.119$ and $p = 0.113$, respectively). Dinoflagellates (9.71 %) were a minor contributor to the total cell abundance and decline to less than 1 % in all pH treatments at the end of phase 3. Heterotrophs varied from 20 % of the total protists abundance at the beginning to 15 - 43 % at day 4 and to ~9 - 27 % at the end of phase 3, both cases with the lowest density at pH 7.86 and the highest at pH 6.94 ($r = 0.96$, $p < 0.01$ and $r = 0.82$, $p < 0.05$ respectively; Fig. 8c, d). Flow cytometry showed that the percentage of nanophytoplankton cells (2-20 μm) group increased from 34 – 42 % during the adaptation phase to around 82 – 91 % at the end of the experiment in all microcosms, which corroborate our data from the microscopic identification for *Thalassiosira* spp. (5-10 μm).

TEP

The initial TEP-C concentration was 490 $\mu\text{g C L}^{-1}$ in all microcosms and decreased during the adaptation period to reach values between 155 to 233 $\mu\text{g C L}^{-1}$ (Fig. 9a). Afterwards, TEP-C concentrations increased presenting two accumulation phases, coinciding with the bloom and post-bloom periods. TEP-C followed the same pattern as nanophytoplankton-C, with which these particles showed a significant correlation ($r = 0.85$, $p < 0.01$; Annex 1.2). During phase 2, TEP-C concentration reached a first maximum (day 7), varying between 295 – 450 $\mu\text{g C L}^{-1}$, with the highest concentration observed in the pH reference treatment (ANCOVA, $p < 0.05$), which showed 10 to 30 % decrease at 7.55 and

6.94 pH treatments, respectively. During phase 3, a second maximum was observed (day 15) reaching 460 - 655 $\mu\text{g C L}^{-1}$, with the highest concentration observed for the lowest pH treatments and the lowest concentration for the higher pH (ANCOVA, $p < 0.05$). Sslope analysis showed a significant difference between days for the pH effect on TEP ($p < 0.01$), as well as a significant negative pH effect for all days ($p < 0.01$), except for day 15, where a higher concentration (+41 %) was reached in the more acidic treatments. TEP-C production rate (between 0.065 and 0.18 d^{-1}) showed no significant response to the pH treatments during the phase 2 ($p > 0.05$; Fig. 10a). However, during the phase 3, TEP-C accumulation rate presented a significant positive correlation with pH decrease ($r = 0.90$, $p < 0.05$), with 0.03 d^{-1} at high pH and 0.12 d^{-1} at low pH, which are similar to those of nanophytoplankton for the same period (Fig. 10b).

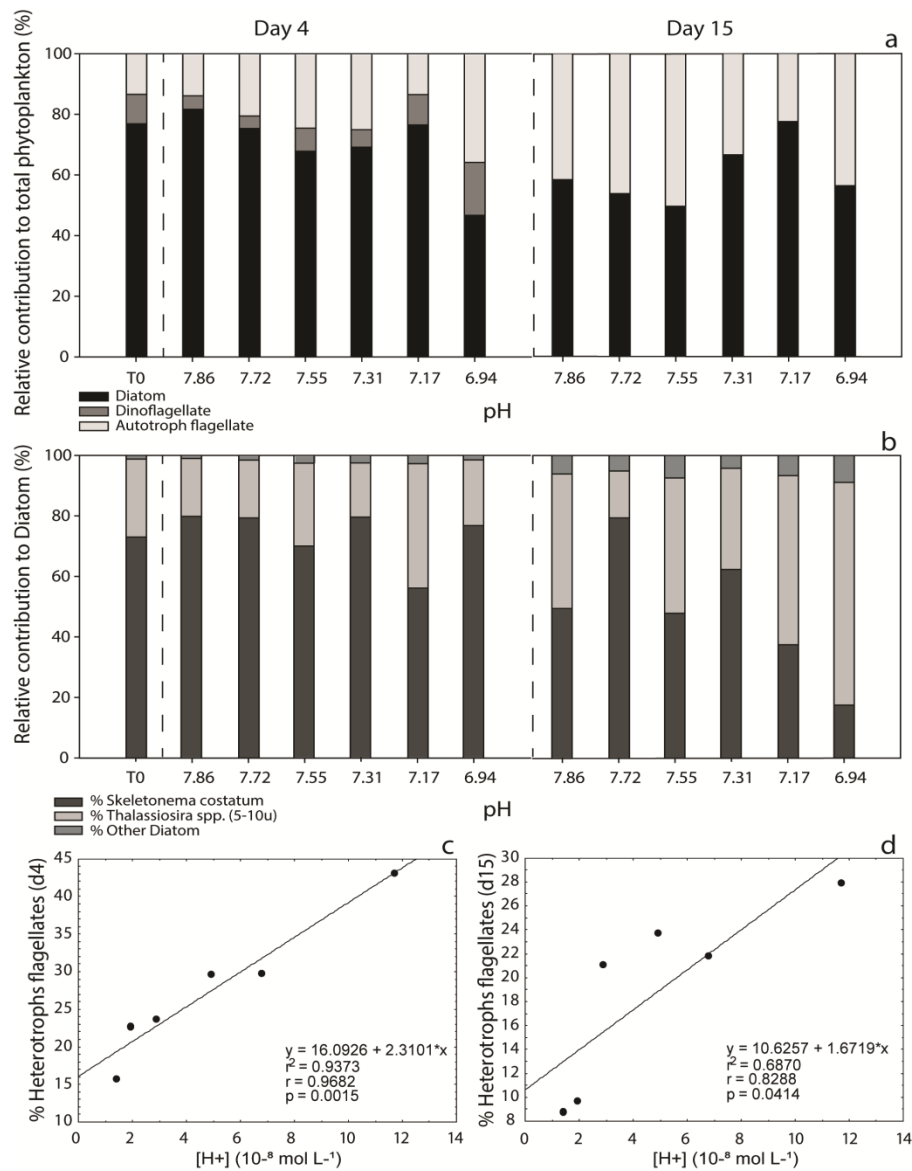


Figure 8: Microscopic relative contributions of (a) autotrophic group to total phytoplankton and (b) diatom species at the beginning (T0), around the bloom (day 4) and at the end of the experiment (day 15) in each pH treatment. Relationship between heterotrophs flagellates (% of the total protists abundance) and the proton concentration values ($[H^+]$) during (c) the bloom and (d) at the end of the experiment. Linear regressions are shown with solid lines.

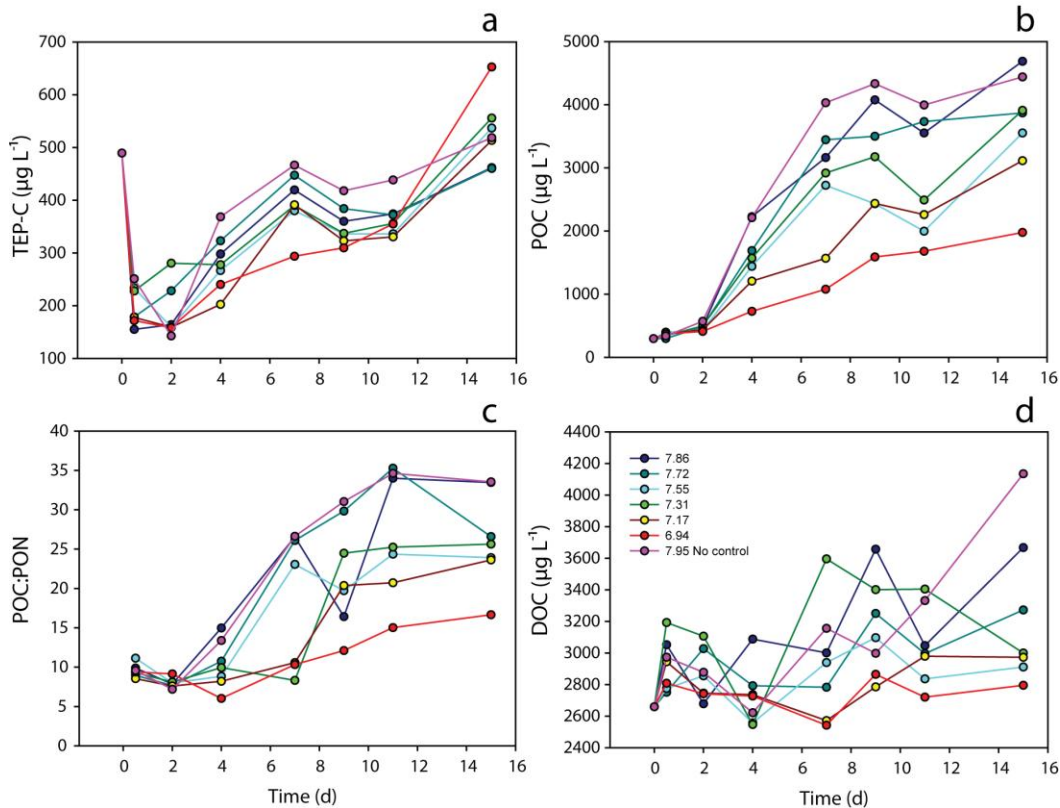


Figure 9: Temporal evolution during the experiment ($\mu\text{g C L}^{-1}$) of: (a) transparent exopolymeric particles carbon (TEP-C), (b) particulate organic carbon (POC), (c) particulate organic carbon to particulate organic nitrogen ratio (POC:PON) and (d) dissolved organic carbon (DOC). Each curve represents a microcosm with a specific pH treatment.

POC and C/N ratio

POC concentration was $293 \mu\text{g C L}^{-1}$ at the beginning and started to accumulate in parallel to the development of the microphytoplankton bloom (Fig. 9b). During this phase POC concentration reached at day 9 maximum values ($1589 - 4077 \mu\text{g C L}^{-1}$), with the highest concentration corresponding to pH reference (ANCOVA, $p < 0.01$). Under these conditions there was a decrease of 40 – 61 % at pH 7.55 and 6.94, respectively. At the end of phase 3, a second relatively small POC accumulation was observed, reaching 1978 -

4688 $\mu\text{g C L}^{-1}$, with the highest concentration observed in the high and intermediate pH treatments (7.86-7.31) (ANCOVA, $p < 0.01$), as shown in the case of microphytoplankton. In contrast, the lower pH microcosm presented a very low POC concentration during the whole experiment. Maximum concentrations showed a decline from 34 % to 58 % of POC at 7.17 and 6.94 pH treatments, respectively. Although Sslope analysis showed no difference between days for the pH effect on POC ($p > 0.05$), a significant negative pH effect for all days was nevertheless observed ($p < 0.01$), with the lowest concentration corresponding to the more acidic treatments during phases 2 and 3. During the bloom, POC accumulation rate showed a significant negative correlation with pH ($r = -0.92$, $p < 0.01$), with 0.30 d^{-1} at high pH and 0.19 d^{-1} at low pH (Fig. 10c). However, during post-bloom, POC accumulation rate showed no significant correlation with a pH decrease ($p > 0.05$; Fig. 10d).

The initial POC:PON ratio started around 8.05 ± 0.56 in all microcosms, close to the standard Redfield C:N ratio of 6.6 (Fig. 9c). This ratio increased exponentially during the bloom and post-bloom following the biomass accumulation process, presenting ratios between 31 for the higher pH value and 12 for the lowest pH value during the phase 2. At the end of phase 3, these ratios reached up to 34 and 17 for high and low pH, respectively, relative to the Redfield, C:N ratio ($r = 0.89$; ANCOVA, $p < 0.01$). Although Sslope analysis showed no difference between days for the pH effect on POC:PON ratio ($p > 0.05$), a significant negative pH effect for all days as for POC and microphytoplankton was observed ($p < 0.01$), with the lowest ratio observed in the acidic treatments during phase 2 and 3.

DOC and DOC:POC ratio

DOC concentration was $2660 \mu\text{g C L}^{-1}$ at the beginning of the experiment and showed a small accumulation during the adaptation period to reach values between 2751 - 3193 $\mu\text{g C L}^{-1}$. Afterwards, DOC increased slightly through the bloom and post-bloom periods to reach values between 2795 to 4135 $\mu\text{g C L}^{-1}$ at day 15 (Fig. 9d). The highest

concentration was observed in the pH reference treatment (ANCOVA, $p < 0.01$), which showed a decrease of 18 to 24 % under pH 7.55 and 6.94, respectively. Sslope showed a significant difference between days for the pH effect on DOC ($p < 0.05$), as well as a significant negative pH effect for all days ($p < 0.05$), with the lowest concentration observed in the most acidic treatments during bloom and post-bloom phases. During both phases, DOC accumulation rate (d4 to d15) showed a significant negative effect with pH treatments ($r = -0.92$, $p < 0.01$), with 0.015 d^{-1} at high pH and 0.002 d^{-1} at low pH (Fig. 10e).

The initial DOC:POC ratio was around 7 to 9 for low and high pH treatments, respectively. Afterwards, this ratio decreased sharply during the bloom (d4) in all microcosms to reach 1.38 for the higher pH value and 3.74 for the lowest pH value (Fig. 10f). This ratio continued to decrease during post-bloom to reach 0.78 to 1.41 for high and low pH value, respectively (ANCOVA, $p < 0.01$). Sslope did not show difference between days for the pH effect on DOC:POC ratio ($p > 0.05$). However, a significant interaction between days and pH treatments were evidenced for all days ($p < 0.01$), with the highest ratio observed in the acidified treatments during phase 2 and 3.

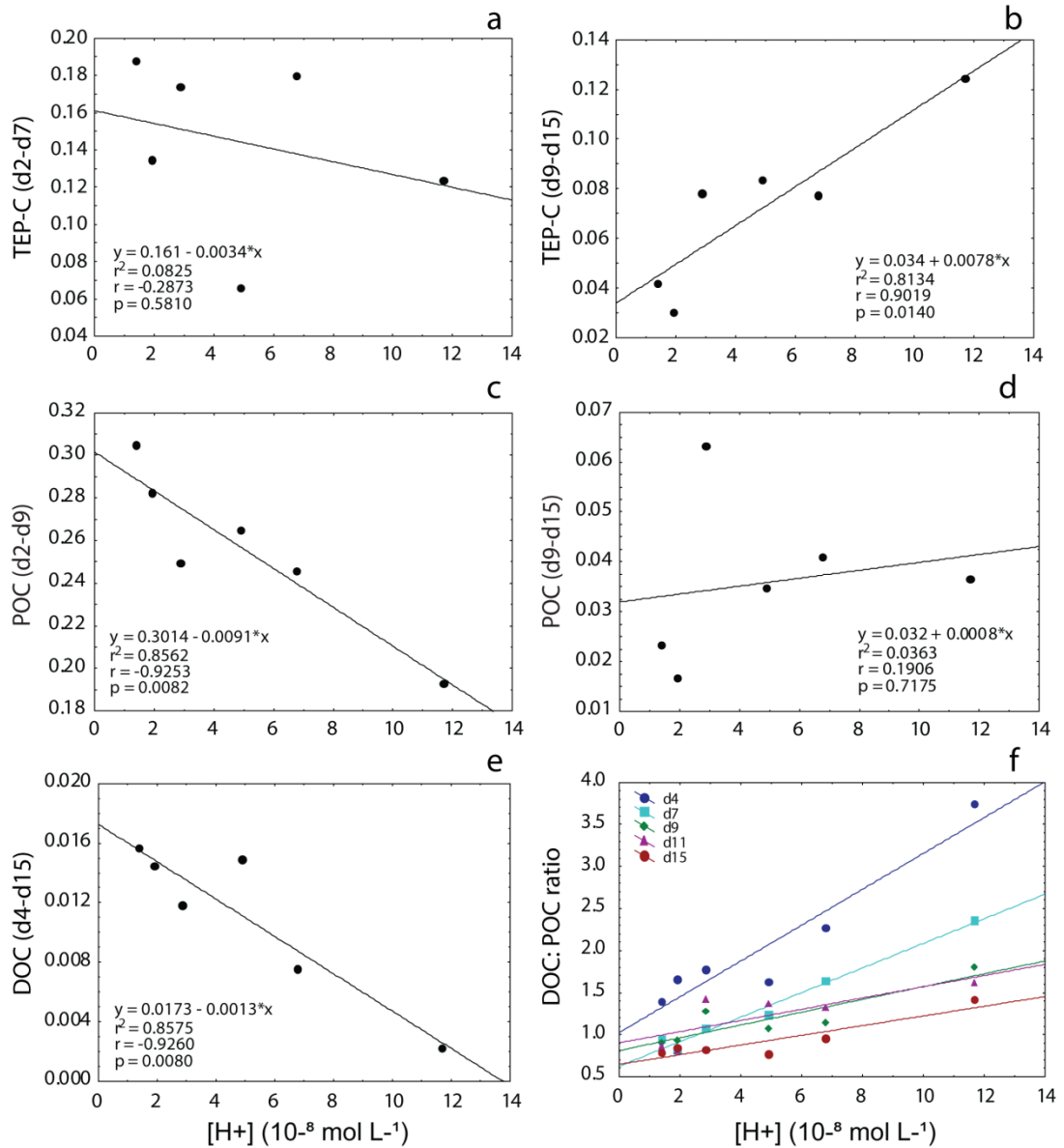


Figure 10: Relationship between the proton concentration values ($[H^+]$) and particulate and dissolved organic carbon accumulation rate during the experiment for TEP-C from day 2 to day 7 (a), from day 9 to day 15 (b); POC from day 2 to day 9 (c), from day 9 to day 15 (d); DOC from day 4 to day 15 (e) and DOC:POC ratio for each experimental day (f). Linear regression relationships are shown with solid lines are shown.

Bacteria and viruses

The initial abundance of heterotrophic bacteria was $2.98 \times 10^4 \text{ mL}^{-1}$ in all treatments and increased during the adaptation period to reach concentrations between 5.40×10^4 to $7.03 \times 10^4 \text{ mL}^{-1}$ (Fig. 11a). Afterwards, bacterial abundance dropped abruptly during the phase 2 reaching values less than the initial concentrations around 2.45×10^3 to $4.86 \times 10^3 \text{ mL}^{-1}$ at day 7 with no significant differences between pH treatments (ANCOVA, $p > 0.05$). Viruses' density increased from 6.09×10^5 to around $18 \times 10^5 - 13.4 \times 10^5 \text{ mL}^{-1}$ in the adaptation period (Fig. 11b). Afterwards, these values decreased steadily until the end of the experiment, throughout the phase 2 and 3 reaching values between 4.31×10^5 to $2.61 \times 10^5 \text{ mL}^{-1}$ with no significant differences between pH treatments (ANCOVA, $p > 0.05$). After day 7 bacterial abundance started to increase slightly by the end of the experiment reaching values between 1.02×10^4 and $0.80 \times 10^4 \text{ mL}^{-1}$ at pH 7.86 and 6.94, respectively. During the same period, %HNA also increased again up to 76 and 93 at pH 7.86 and 6.94 respectively (Fig.12a). Sslope analysis showed no interaction between days and pH effect on bacteria and viruses ($p > 0.05$), showing only a slight negative but not significant pH

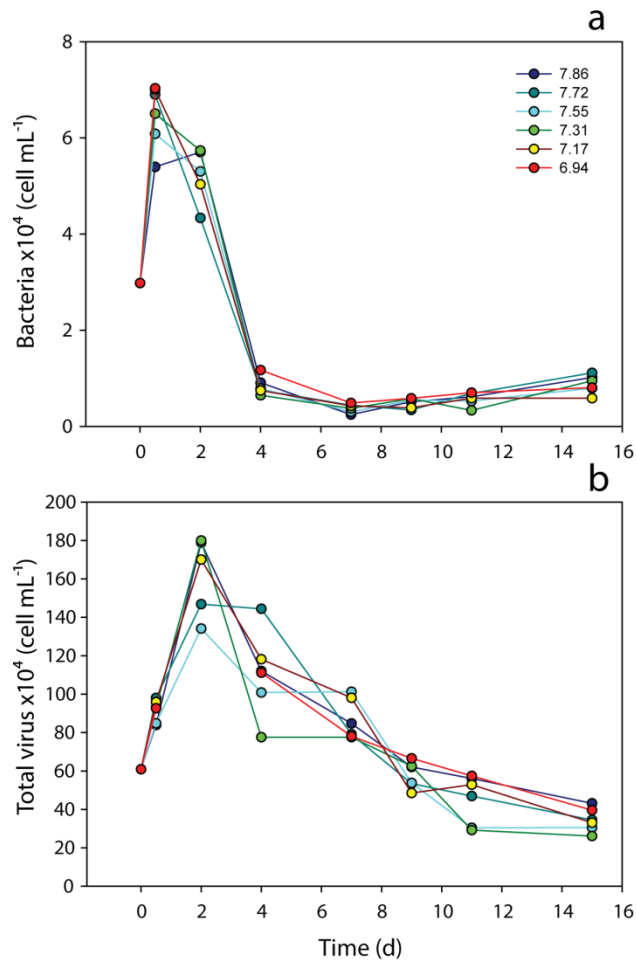


Figure 11: Temporal evolution of (a) bacteria abundance and (b) viruses. Each curve represents a microcosm with a specific pH treatment.

effect on day 15 for bacteria which decreased by 42 % in the acidic treatments (pH 7.17). On the other hand, no effects of pH on viruses were observed. The decrease of bacteria compared to viruses concentrations resulted in a sharp increase of viruses to bacteria ratio from 14 to up to 346 and 161 at pH 7.86 and 6.94 respectively, during phase 2 (day 7, Fig. 12b) and then decreased until the end of the experiment reaching a ratio of 41. The bacterial abundance decrease rate during phase 2 (d2-d7) did not present a significant correlation

with pH ($p > 0.05$; Fig. 13a). In contrast, the bacterial growth rate in phase 3 (d7-d15) presented a significant negative correlation with pH treatments ($r = -0.77$, $p < 0.05$; Fig. 13b). A similar trend was found in the viruses decrease rate during phases 2 and 3 (d2-d15). However, the correlation with pH treatments was not significant ($r = -0.67$, $p > 0.05$; Fig. 13c).

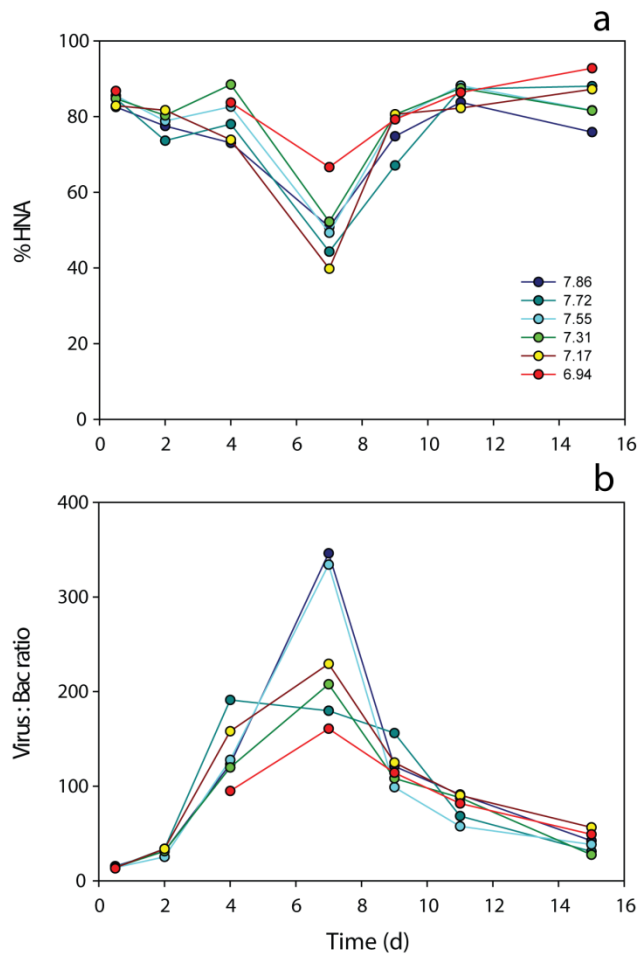


Figure 12: Temporal evolution of (a) percentage of bacteria with high nucleic acids (HNA) and (b) virus to bacteria ratio during the experiment. Each curve represents a microcosm with a specific pH treatment.

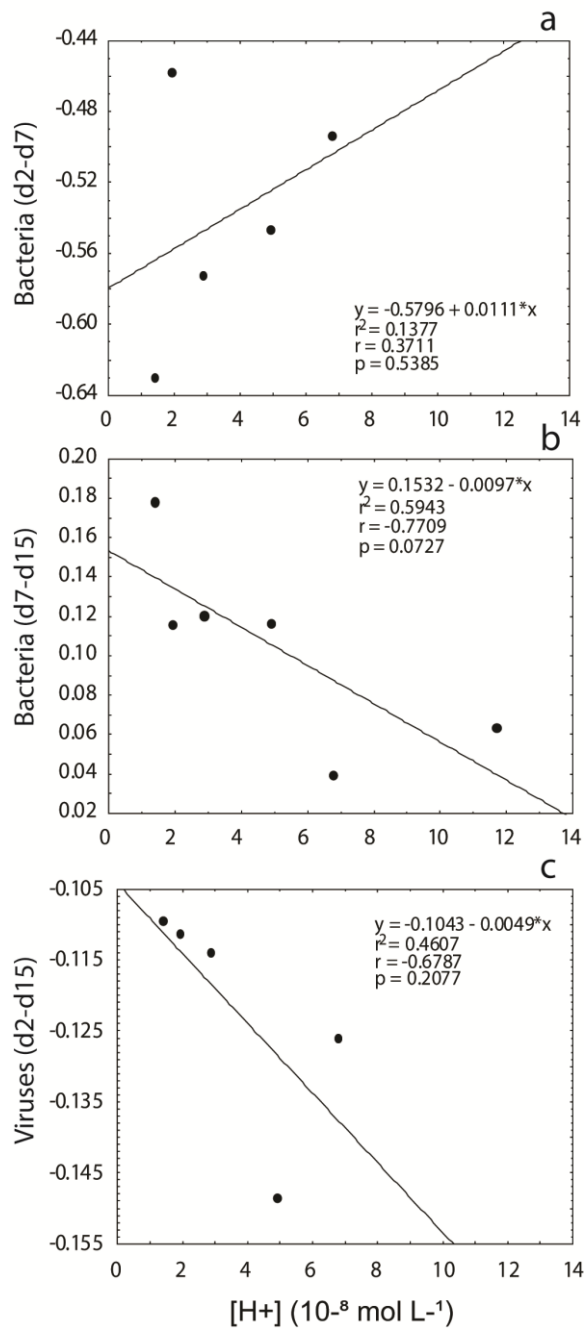


Figure 13: Relationship between the proton concentration values ($[H^+]$) and the rate of abundance change during the experiment (a) Bacteria (day 2 to day 7), (b) Bacteria (day 7 to day 15), and (c) viruses (day 2 to day 15). Linear regressions are shown with solid lines are shown.

DISCUSSION

Estuarine and coastal ecosystems experience a natural large range of pH variability, due to seasonal and even diurnal change basis. In these ecosystems, a much lower pH decrease related to ocean acidification is expected by the end of the century (Nielsen et al. 2012, Thoisen et al. 2015, Li et al. 2016). Little is known about the consequences of acidification on natural plankton communities and the organic carbon pool in estuarine environments, and no information is available for the particular case of the St. Lawrence Estuary (SLE). In our microcosms kinetic experiment, we exposed organisms to constant pH conditions, simulating predominant conditions under future scenarios in the SLE ecosystem to test the effects of acidification on TEP and the contribution of the plankton community to the carbon pool.

Phase 1

Water mass characteristics at the start of the experiment

The natural plankton community collected during the setup of our experiment was in pre-bloom stage, as evidenced by the initial cell density and nutrient concentrations. The initial pH was 7.86, which was in the range of previous pH values reported for this study site, between 7.7 and 8.3 (Pelletier & Lebel 1980, Annane et al. 2015). Initial total alkalinity (TA) was $\sim 1721 \mu\text{mol.kg}^{-1}\text{sw}$, slightly lower than the range recently reported by Dinuer & Mucci (2017) for the LSLE over 13 years during the spring-summer period, which was between 1752 to $2185 \mu\text{mol.kg}^{-1}\text{sw}$. This is probably due to fluctuations in the carbonate chemistry during the spring freshwater runoff and the dilution of salinity of the surface mixed water in this area (~ 20.7), which is in the range reported by Silverberg & Sundby (1979) and Saucier et al. (2009). According to Belzile & Lebel (1983) TA is usually conservative within the estuary with respect to chlorinity. However, the TA of the freshwater end member is related to the river flow, and this is attributed to dilution of the

water with bicarbonate-poor rain water especially, during the spring runoff (see Table1). Our initial dissolved inorganic carbon (DIC) and sea-water $p\text{CO}_2$ value ($1667 \mu\text{mol.kg}^{-1}\text{sw}$ and $434 \mu\text{atm}$, respectively) are consistent with data recently reported by Dinauer & Mucci (2017) for the LSLE (between $1634 -2083 \mu\text{mol.kg}^{-1}\text{sw}$ and $400-578 \mu\text{atm}$, respectively). Nevertheless, after our CO_2 enrichment and pH target was reached on day 2, all variable values of the carbonate chemistry manipulated stayed stable until the end of the experiment.

Initial SRP concentrations were very low ($\sim 0.27 \mu\text{M}$) for the season in the SLE. An adjustment was made on day 1 so the SRP concentration for this experiment be as close as possible to the normal natural range of RSP in the SLE. However, SRP concentrations increased in all microcosms on day 1 ($+0.17 \mu\text{M}$) just before our adjustment, which was not planned, though they were in the range of SRP concentrations ($\sim 1.28 \mu\text{M}$) for the spring in the LSLE (Levasseur & Therriault 1987, Annane et al. 2015). This phenomenon was observed in other mesocosms experiments (Neveux et al. 2010, Mostajir et al. 2013, Annane et al., to be submitted), probably due to the death/physiological lysis of cells and organisms acclimation to the microcosm confinement.

Initial phytoplankton biomass was $\sim 180 \mu\text{g C L}^{-1}$, mainly dominated by diatoms, with nearly 95 to ~ 100 % of centric species *Skeletonema costatum*, followed in abundance by *Thalassiosira* spp in the nanophytoplankton range ($5-10 \mu\text{m}$). This is consistent with previous studies from the same area (Levasseur et al. 1984, Levasseur & Therriault 1987, Savenkoff et al. 1997, 2000, Le Fouest et al. 2005, Starr et al. 2004, Annane et al. 2015). The initial phytoplankton biomass fraction ($<10 \mu\text{m}$) was also dominated by nanophytoplankton (~ 98 %) and picophytoplankton represented <2 %. The phytoplankton community included also a lower contribution of autotrophic flagellates and a minor percentage of dinoflagellates.

During this phase, picophytoplankton-C concentrations decreased in all microcosms in day 1 to values less than $1 \mu\text{g C L}^{-1}$. These were probably due to grazing by heterotrophs which represented around 20 % of total plankton cells at the beginning of the experiment or suffered a viral lysis. This is consistent with results of grazing and viral lysis on

picophytoplankton in the Arctic (Brussaard et al. 2013), also in coincidence with the SRP rise discussed above.

During the adaptation phase of the experiment, the TEP-C concentrations decreased in all microcosms in day 1 to values ranging between 155 to 233 $\mu\text{g C L}^{-1}$. These values are similar to the values reported by Annane et al. (2015) in the LSLE for the same period. This decrease was consistent with the increase of DOC accumulation during the same day. This could be explained by the simultaneous increase of bacterial density during the same day, which could enhance the heterotrophic degradation of the particulate TEP-C into dissolved organic matter (Aluwihare & Repeta 1999, Passow 2002b). After a maximum of bacterial abundance in day 1, they started to decrease afterward. This trend matched with the increase of viruses density to a maximum on day 2. This doubled the Virus:Bacteria ratio value suggesting that viral lysis probably limited the bacterial biomass accumulation during the adaptation phase.

Phase 2

During this phase, picophytoplankton biomass peaked before the other phytoplankton fractions around day 4. Picophytoplankton biomass was significantly and negatively affected by pH. Hopkins et al. (2010) and Brussaard et al. (2013) reported a similar finding in a mesocosm experiment in the Arctic, showing a lower abundance of picophytoplankton subpopulation under high $p\text{CO}_2$ (~750-1100 μatm) than at present day $p\text{CO}_2$ conditions. Although, it is unclear whether this fraction is affected by acidification directly or indirectly through increased loss by grazing in the more acidified treatments, as we found no difference of growth rate for picophytoplankton between treatments. Interestingly, heterotrophs were positively favored by low pH presenting a significant increase of 43 % at low pH (pH ~6.94) during the bloom. This is consistent with previous work of Brussaard et al. (2013) and Aberle et al. (2013) who indicated a high tolerance of heterotrophic flagellates to changes in $p\text{CO}_2/\text{pH}$ in the Arctic. Moreover, picophytoplankton has been reported to be stimulated by decreasing pH in contrast to nanophytoplankton in the Arctic

ecosystem (Hussherr et al. 2017), while in the LSLE picophytoplankton biomass seem to be either sensitive to pH decrease or to heterotrophs grazing and contributed to less than 1 % of the phytoplankton carbon fraction (<10 μm). Therefore, they probably contributed very little to TEP accumulation.

During this bloom phase, both nano- and microphytoplankton biomass fractions peaked around day 7 and 9, respectively, with a dominance of microphytoplankton carbon biomass. The two biomass fractions were negatively affected by low pH as their respective biomass decreased with decreasing pH, with microphytoplankton biomass being the most strongly impacted. This represents a decline of 26 to 72 % of nanophytoplankton (decrease of $\sim 533 \mu\text{g C L}^{-1}$ at pH 6.94) and 20 to 89 % of microphytoplankton (decrease of $\sim 5235 \mu\text{g C L}^{-1}$ at pH 6.94) within a pH range from 7.72 to 6.94. The phytoplankton bloom was dominated by diatoms, with *S. costatum* (10-40 μm) and *Thalassiosira* spp. (5-10 μm) representing most of the phytoplankton biomass. In low pH-high $p\text{CO}_2$, the Carbon Concentrating Mechanism (CCM, cellular process used by algae to overcome CO_2 limitation in water) could enhance phytoplankton growth rate by facilitating CO_2 uptake and reducing the energy cost in some phytoplankton species like diatoms (Gao & Campbell 2014). However, our results suggest that net carbon fixation and biomass build-up by diatoms was negatively affected by decreasing pH. This result is in agreement with previous studies showing that alteration of seawater carbonate chemistry due to ocean acidification could perturb the energy requirements of diatom cells, leading to changes in respiration, cell surface and intracellular pH stability, as well as their costs for photoprotection (Yang & Gao 2012, Flynn et al. 2012, Gao & Campbell 2014). This can induce phytoplankton cells to re-allocate their energy partitioning to repair physiological impacts such as modifications in membrane potential, ions transport against the acid-base perturbation, enzyme activity, protein function and nutrient uptake (Nimer et al. 1994, Riebesell 2004, Giordano et al. 2005). As a consequence, their productivity and growth rate may be affected through direct pH effects (Berge et al. 2010). Indeed, the observation that microphytoplankton growth rate was negatively affected by decreasing pH (0.32 d^{-1} vs. -0.08 d^{-1} at low pH), is consistent with the biomass decrease evidenced under these

conditions. Thaisen et al. (2015) and Schulz et al. (2013) showed that growth rate of diatoms and Chlorophyceae were reduced at elevated CO₂/low pH. In turn, the nanophytoplankton growth rate did not seem to be affected by pH including the lowest pH (6.94) even if they suffer a decrease in biomass. This suggests that microphytoplankton is more sensitive to low pH than nanophytoplankton.

Diatom contribution during the bloom varied from 81 % to 45 % at the pH 7.86 and 6.94, respectively showing here again a negative impact for low pH. This result was consistent with the significant linear decrease of the Si(OH)₄ : NO₃ uptake ratio with decreasing pH, which was mostly driven by a reduction by decrease of silicic acid uptake. As diatoms were still dominant even in the low pH, this suggests that diatom cells consumed less silicic acid in more acidified conditions. As evidenced previously, external pH influences cell growth of diatoms and modify the physiology of intracellular silicic acid and biogenic silica in the cells, but not nutrient uptake (Hervé et al. 2012). These results are also consistent with a recent microcosm experiment in the Arctic by Husserr et al. (2017), who found similar results at pH ≤ 7.6. These authors suggest that the negative impact of low pH on silicification does not prevent blooms development in nature. In addition, in a laboratory microcosm experiment with phytoplankton from the Derwent River Estuary (Tasmania) it was reported a silicate uptake reduction around pH 6.3, which translated in lowered diatom growth rate, cellular carbon and total POC accumulation (Nielsen et al. 2012). Contrasting with these results, Schulz et al. (2013), in a mesocosm experience in the Arctic Kongsfjorden (Norway), showed that autotrophic dinoflagellates, cryptophytes, haptophytes and chrysophytes were favored by high CO₂, while diatoms were negatively affected by high CO₂ conditions. These observations are consistent with those from this study regarding diatoms and heterotrophic flagellates, suggesting that non silicifying and non calcifying organisms would likely encounter a lack of competition for the ecological niche and thus would be stimulated in this ecosystem under more acidified conditions.

During the bloom phase, the TEP-C accumulation followed the same pattern as that of the nanophytoplankton-C, reaching maximum concentrations at day 7. TEP-C

accumulation showed a significant negative effect with respect to lower pH conditions. These results are consistent with the adverse effects of low pH on nano- and microphytoplankton observed in our experiment, with ~10 to 30 % of TEP decrease for pH between 7.55 to 6.94. This is also consistent with the decrease of DOC accumulation and bacteria biomass at lower pH, which suggests that there was less carbon release and thus less TEP production under acidic conditions. However, these TEP-C concentrations were still within the lower range of those reported recently in the LSLE during the spring bloom (Annane et al. 2015). TEP-C contribution to the POC pool was also affected by low pH, as TEP-C contribution increased from 20 to 33 % of POC at low pH.

Nonetheless, the negative effect of pH on TEP aggregation and on diatom silicification could probably affect the particle density and carbon export under low pH conditions. Indeed, it has been shown that a decrease of seawater pH between 0.2 to 0.8 could decrease TEP stickiness and modify the TEP structure (Mari 2008) due to the protonation of the carboxylic groups, which may reduce the amount of inter- and intrachain hydrogen bonds. This can help the disaggregation of TEP structure into smaller particles and colloids as evidenced by the work of Chin et al. (1998) and/or prevent the formation of ionic bridges between carboxylic groups ($R-COO^-$) and Ca^{2+} ions (Li et al. 2013, Meng & Liu 2016), leading to a decrease of TEP abundance and aggregation. However, other results from laboratory experiments did not show a clear trend in TEP stickiness and aggregation due to ocean acidification (Mari 2008, Passow 2012). Although, Mari (2008) suggested that when the acidification was caused by an alkalinity perturbation like in nearshore areas, this low pH may decrease TEP stickiness. However, no change in TEP stickiness has been reported when this low pH was due to an increase in DIC concentration, as expected for future OA (Passow 2012, Mari et al. 2017). As it is the case in the present study low TA and low pH could most likely alter the TEP structure and sticking properties, lowering the size and density of marine aggregates, or even slowing down the vertical carbon flux.

Diatom silicic frustules are known to efficiently ballast organic matter and facilitate their export (Klass & Archer 2002, Passow 2004, Iversen & Ploug 2010). A decrease in

diatom biomass and silicification could alter this process, reducing sinking velocity of organic matter. It should be noted, however, that ballasting alone does not guarantee the formation of sinking aggregates, given that the rate of aggregation is a function of particle number, size, collision rate and stickiness (Jackson 1990, Jackson & Burd 1998). Consequently, these results suggest that the alteration of diatom silicification together with TEP structure and stickiness under ocean acidification could impact the future organic matter vertical fluxes with consequences for the ecosystem productivity and atmospheric CO₂ sequestration.

During this phase, the TEP accumulation rate showed no clear response to low pH, presenting once again the same response as the nanophytoplankton growth rate. Moreover, nanophytoplankton biomass explained here 85 % of the variance of TEP-C. The unexplained fraction of the variance could probably be attributed to the microphytoplankton biomass. Indeed, *Thalassiosira* spp seem to be somewhat less sensitive to low pH than *S. costatum*, even if it is the dominant species during this phase, which translated by a less TEP precursor production and TEP-C formation in the more acidified treatment. This contrasts with previous mesocosm studies which showed an increase in carbon fixation and precursor release as well as TEP-C accumulation (Engel et al. 2004, Riebesell et al. 2007, Kim et al. 2011, Engel et al. 2014, Endres et al. 2014, Taucher et al. 2015). *S. costatum* and *Thalassiosira* spp. have been reported to produce important quantities of TEP under present $p\text{CO}_2$ (Engel 2000, Passow 2002b), which is consistent with results showing that phytoplankton is the main TEP source in the LSLE (Annane et al. 2015). However, the negative effect of pH on nano- and microphytoplankton biomass and the possible reallocation of energy to maintain the stability of internal cell pH likely lead to decrease in release of carbon rich compounds like DOC, TEP precursors and TEP accumulation.

POC accumulation followed the same pattern as that of microphytoplankton biomass, peaking on day 9. These POC concentrations were also negatively affected by low pH, decreasing ~40 to 61 % for pH in the range of 7.55 and 6.94. These results are consistent

with the decrease in microphytoplankton biomass and TEP-C during this phase. These results contrast with previous mesocosm studies which showed an increase in carbon fixation and build-up of sinking POC under high CO₂ conditions (Sambrotto et al. 1993, Engel 2002, Wetz & Wheeler 2007, Riebesell et al. 2007a, Engel et al. 2013, Engel, Piontek, et al. 2014). We speculate that our contrasting results may be due to the low pH impact on the phytoplankton physiology leading to a decrease in biomass accumulation during our experiments under acidic conditions. Indeed, Nielsen et al. (2012) in a laboratory microcosm experiment showed that a decrease down to pH 6.3 highly reduced the photosynthesis and biomass of phytoplankton and POC build-up. However, despite that POC in our experiment decreased with pH, concentrations were unexpectedly 2 to 4 times higher than those registered in the LSLE. This is probably because POC accumulated in the microcosms, while in the LSLE the POC material is subject to periodically lateral advection (tidal waterflush) and vertical (sinking) export, which keep these concentrations lower than those reported in this experiment. Nevertheless, the POC accumulation rate was reduced in the more acidic conditions during the bloom showing a rate of 0.30 d⁻¹ vs. 0.19 d⁻¹ at low pH, which follows the same trend as microphytoplankton, which contributed the most to the POC pool. Consequently, these results suggest that POC accumulation could be greatly reduced and thus limit the particle flux and carbon sequestration under future acidification scenarios.

Bacterial abundance dropped abruptly during the bloom phase reaching their minimum on day 7 (around 2.45 - 4.86 x10³ mL⁻¹). This bacterial loss was likely due to heterotrophs flagellates grazing and/or to viral lysis, as the virus to bacteria ratio increased sharply from 14 to up to 346 – 161 virus/bacteria at high and low pH in day 7. Moreover, bacterial as well as virus abundances presented no significant effect from low pH during this phase. These results are in contrast with previous studies which showed that the bacterial community benefited directly and indirectly from decreasing seawater pH (Piontek et al. 2010, 2013, Brussaard et al. 2013, Endres et al. 2014). Our results were also associated with a decline in bacterial high nucleic acid percentage (HNA), which dropped from 85 % to 40 – 67 % at day 7, following the inverse pattern of the virus to bacteria ratio.

These results suggest that viruses targeted more HNA than low nucleic acid (LNA) bacteria. Furthermore, the bacterial decrease rate during this phase did not show a significant effect with low pH. These result is consistent with those of Brussaard et al. (2013) in a mesocosm experiment on the influence of ocean acidification on Arctic microbial community, who showed similar responses of bacterial loss by viral lysis in the early bloom, as well as the HNA targeting by viruses. Indeed, it has been considered that HNA represents the most metabolically active members of the microbial community (Lebaron et al. 2001). However, it is still discussed among the scientific community about the metabolic activity of LNA, as some studies did show that LNA can also be an active part of the microbial population (Zubkov et al. 2001, Brussaard et al. 2005, Wang et al. 2009). This HNA selectivity by viruses remains to be elucidated.

In this case, the negative effect of viral lysis on bacteria most likely allowed the aggregation of polysaccharide precursors to generate TEP particles by limiting the degradation potential (reducing the enzymatic activity) of the microbial community. It should be noted that degradation of polysaccharides by bacterial extracellular enzymes can be significantly accelerated under acidification conditions, as experimentally shown by Piontek et al. (2010). These authors reported that a decrease in seawater pH of 0.5 unit almost doubled the production rates of both enzymes, β -glucosidase, and leucine-aminopeptidase. In contrast, SLE microbial community was more affected by viral activity and potential grazing than by pH.

Phase 3

During the decline phase microphytoplankton biomass declined at the end of the experiment, still showing the same negative responses to low pH. In contrast, nanophytoplankton biomass reached a second development peak at the end of this phase, presenting a positive response to low pH, with a 38 % biomass increase in the more acidic treatment. However, despite the microphytoplankton decline, it still represented the dominant carbon fraction in the community (~ 221 and $\sim 3327 \mu\text{g C L}^{-1}$). Both nano- and

microphytoplankton growth rates were positive, but not significantly affected by low pH. However, nanophytoplankton growth rate during the second biomass accumulation period was lower than in the first one (-0.02 and 0.12 d⁻¹, respectively). Indeed, microscopic results showed that diatoms remained dominant, even if they decreased up to 50 – 77 % of the total community. Interestingly, *S. costatum* and *Thalassiosira spp.* (5 - 10 µm) response to acidification were more pronounced in this phase, showing a negative response of *S. costatum* (decrease from 79 % to 17 %), and a positive response of *Thalassiosira spp.* (increase from 15 % to 74 %) under low pH conditions. This is in agreement with a previous study showing that *S. pseudocostatum* growth is optimal at pH 7.7, and that lower pH or a more prolonged period under low pH has adverse effects on the development and growth of this diatom species (Nielsen et al. 2012). The second bloom of nanophytoplankton is consistent with the increase of *Thalassiosira spp.* at the end of the experiment. Thoisen et al. (2015) showed that *Thalassiosira spp.* growth rate was part of the group gradually affected by acidification. Our results suggest that *S. costatum* is probably more sensitive to low pH than *Thalassiosira spp.* This supports the hypothesis that the responses of phytoplankton to acidification are species-specific.

During the postbloom period, it was observed a higher TEP-C accumulation under low pH (~41 %). This increase came along with the nanophytoplankton biomass variations under acidic conditions during this phase. These results corroborate other studies where the production of large amounts of TEP was also attributed to nanophytoplankton (Mari et al. 2001, Passow 2002a, b, Taucher et al. 2015, Bourdin et al. 2016). Indeed, the increase of nanophytoplankton abundance and more precisely that of *Thalassiosira spp.* (5 - 10 µm) most likely helped to produce an important quantity of carbon rich organic matter which might aggregate into TEP particles at the end of the experiment. In other hand, the decline of *S. costatum* could also contributed to the TEP accumulation by releasing fresh precursors. This hypothesis is supported by TEP significant positive accumulation rate under low pH treatment (0.03 d⁻¹ and 0.12 d⁻¹ at low pH) coincident with the DOC negative accumulation rate (0.015 d⁻¹ and 0.002 d⁻¹ at low pH), which showed a slight decrease

between the two phases. Such dynamics suggest transformation of organic carbon from dissolved into particulate through aggregation.

We observed an increase of POC:PON ratio throughout the bloom and stationary phases. However, this ratio presented a negative response to acidification, decreasing from 34 to 17 at the low pH at the end of the experiment. This was in contrast with previous studies which showed that elevated $p\text{CO}_2$ can enhance carbon fixation by phytoplankton resulting in an increase in accumulation of carbon-rich components (POC and TEP) (Riebesell et al. 1993, 2007, Wolf-Gladrow et al. 1999, Hutchins et al. 2007, Engel et al. 2014a). Kim et al. (2011b) though found no change in the total organic carbon to nitrogen (TOC:TON) ratio with increasing $p\text{CO}_2$ concentration. They suggested that this discrepancy may be explained by species-specific responses to increased CO_2 concentration. In contrast, the lower POC:PON ratio at low pH conditions in this study could be the result of other type of response to acidification. This is probably due to adverse effects of pH on carbon fixation by the phytoplankton community and the decrease of accumulation of organic carbon rich compounds like TEP to the autotrophic biomass.

The DOC:POC ratio decreased in all microcosms during the bloom and stationary phases, presenting a steeply decrease in more acidic conditions than at high pH. This ratio presented a significant positive response to acidification, especially during the bloom period, with values around 3.74 at low pH compared to 1.38 in high pH. This means that during the bloom the proportion of DOC to POC accumulation was higher at low pH conditions, which can in turn contributes to explain the lower accumulation of TEP and POC at low pH during the phase 2 of the experiment. In the stationary phase, the DOC:POC ratio decreased more in the acidic treatment reaching 1.41 compared to 0.78 at high pH. The DOC portion decreased relative to POC, explaining the increase of TEP concentrations at the end of the experiment in the acid treatment. This is probably due to aggregation of DOC into TEP particles. As indicated by previous studies, one of the possible fates of DOC is the compartment of TEP (Engel et al. 2004, Riebesell et al.

2007b). Consequently, these results suggest a shift of carbon partitioning from dissolved into the POC pool via TEP aggregation under low pH.

During this phase, bacterial abundance increased slightly in all microcosms (around 1.02×10^4 and 0.80×10^4 cells mL^{-1} at pH 6.94). However, their growth rate presented a significant negative response to pH. Bacteria abundance did not seem to be affected by viral lysis or very little during this period, as viruses abundance continued to decrease through phases 2 and 3 with no significant effect from low pH. This decrease was likely due to depletion of their bacterial target species. This was also associated with a decrease of virus to bacteria ratio to around 41 viruses per bacteria at the end. Moreover, heterotrophs were positively affected by low pH in this study during the whole experiment. As discussed above, this is in agreement with previous studies that showed a high resistance of heterotrophs and a bacterial regulation by grazing and viruses with decreasing pH in the Arctic (Piontek et al. 2013, Brussaard et al. 2013, Aberle et al. 2013, Endres et al. 2014). Here, grazing presumably regulated bacterial abundance, which explains the decrease of bacteria abundance in the low pH treatment. This suggests that bacteria were most likely indirectly affected by low pH.

Conclusions

The present study shows that the blooming plankton community was globally affected by low pH, especially with pH values lower than 7.55, which is within the range expected by the end of the century (7.9 – 7.3) for the LSLE. Phytoplankton community did not benefit from acidification, showing a reduced silicic uptake, biomass and growth rates under low pH, most likely due to adverse effects of pH on the internal cell pH and their physiological processes. Our results suggest that nanophytoplankton, and more precisely the diatom *Thalassiosira spp.*, were less sensitive to low pH than the pico- and microphytoplankton size fractions. On the other hand, heterotrophic flagellates were stimulated by low pH, thus, showing the presence of species-specific responses to acidification. TEP accumulation was clearly linked to the phytoplankton community

composition and the environmental conditions. However, we noted that TEP was mainly produced by nanophytoplankton during the bloom and stationary phases, and that the inverse response of TEP at the end of the experiment mimicked nanophytoplankton dynamics. These negative effects of pH on phytoplankton translated by a reduction of carbon fixation and biomass build-up by diatoms, which reduced the accumulation of particulate organic matter (like TEP and POC) under acidification ($\text{pH} \leq 7.55$), though we noted a shift of carbon partition from dissolved into the POC pool via TEP aggregation. Under these conditions, TEP aggregation and size particles could be affected by changes in alkalinity and pH (Mari 2008), which in turn could have an impact on the future organic matter vertical fluxes with consequences for ecosystem productivity and atmospheric CO_2 biological pumping. Further studies are needed to fully assess the consequences of future changes of not only acidification but warming, hypoxia and nutrient concentration on the SLE ecosystem.

ACKNOWLEDGEMENTS

This project was supported by grants from the Natural Sciences and Engineering Research Council (NSERC) of Canada and the Québec-Océan grant to G.F. and the Fisheries and Oceans operating grants to M.S. The success of our microcosm experiment was achieved with the help of Maurice Lamontagne Institute employees and facilities (Fisheries and Oceans Canada) and the CO_2/pH system control supported by a Québec-Océan/FQRNT grant, which was developed and setup by the Engineering Department of UQAR. The authors would like to thank Alexandre Boudreau at the Engineering Department of UQAR for set up, as well as Sylvie Lessard and Marie-Lyne Dubé at the Maurice Lamontagne Institute and Wahiba Ait Youcef, Mélanie Simard, Pascal Rioux and Mathieu Babin at Institut des sciences de la mer de Rimouski (ISMER) for their skilled help provided prior and during the microcosm experiment and for laboratory analyses. This research is part of fulfillment of the requirements for a Ph.D degree (S. Annane) at the Université du Québec à Rimouski. This is a contribution to the research from ISMER, Fisheries and Oceans Canada and Québec-Océan.

CHAPITRE 3

LES EFFETS DE L'ACIDIFICATION ET DU RÉCHAUFFEMENT SUR LES PARTICULES EXOPOLYMÉRIQUES TRANSPARENTE (TEP) DANS UN ENVIRONNEMENT CÔTIER DE LA MÉDITERRANÉE (LAGUNE DE THAU)

Ce troisième article, intitulé « *Effects of acidification and warming on transparent exopolymeric particles (TEP) in a Mediterranean coastal environment (Thau lagoon)* », fut corédigé par moi-même ainsi que par le professeur Gustavo Ferreyra, le prof. Michel Starr, le prof. Behzad Mostajir et la prof. Francesca Vidussi, et mes collègues Dre. Scalett Sett, Dr. Sébastien Mas, Dre Carolina Cantoni, Dre Anna Luchetta and prof. Ulf Riebesell. L'article sera soumis avec d'autres articles du même projet de mésocomes (MESOAQUA) à la revue *Biogeosciences* en juin 2017. En tant que premier auteur, ma contribution à ce travail fut l'essentiel de la recherche sur l'état de l'art, le travail expérimental et de laboratoire, les analyses statistiques et la rédaction de l'article. La professeure Francesca Vidussi chef de projet, le prof. Behzad Mostajir et le prof. Gustavo Ferreyra ont fourni l'idée originale. Ils ont contribué à la révision et l'amélioration de la qualité de l'article en association avec le prof. Michel Starr. Dre Scalett Sett, Dr Sébastien Mas, Dre Carolina Cantoni, Dre Anna Luchetta ont contribué au travail de terrain et laboratoire. Une version abrégée de cet article a été présentée à la conférence *Québec Océan* à Rivière du loup, QC, Canada à l'automne 2014.

1.1 RÉSUMÉ

Le changement global de l'océan devrait modifier le cycle du carbone et affecter les écosystèmes marins. Dans ce contexte, nous présentons ici les résultats d'une expérience en mésocosmes conçue pour étudier les effets séparés et combinés du réchauffement et de l'acidification sur la formation des particules exopolymériques transparentes (TEP) et sur l'allocation de matière du carbone organique dans les écosystèmes chauds de latitude moyenne. Au cours du printemps 2012, douze mésocosmes (2,3 m³ chacun) ont été déployés dans la lagune de Thau sous quatre conditions : contrôle (22 °C, ~ 445 µatm), CO₂ élevé (22 °C, ~ 900 µatm), température élevée (25 °C, ~ 445 µatm) et CO₂ et température combinée élevée (25 °C, ~ 900 µatm). Nous avons induit une floraison de phytoplancton par addition de nutriments et suivi les changements quotidiens dans les différents réservoirs de carbone (phytoplancton, bactéries, TEP, POC et DIC) pendant 12 jours. À *p*CO₂ élevée, l'accumulation de la teneur en carbone des TEP (TEP-C) était 47 % plus élevée, et le retrait biologique du carbone inorganique dissous (DIC) était également plus élevé (39 %). Cette consommation excessive de carbone a été associée à l'accumulation de carbone organique colloïdal (3 fois) par rapport aux niveaux actuels. Ces résultats suggèrent une stimulation de l'agrégation de particules et du partitionnement dans le réservoir de POC sous *p*CO₂ élevée. En revanche, le réchauffement a diminué la prise de DIC et l'accumulation du carbone particulaire (TEP-C et POC). Cela suggère une réduction de la formation de particules et des exportations de carbone en faveur de la dégradation microbienne. De façon inattendue, nos résultats montrent que l'effet combiné du réchauffement et de l'acidification n'a eu aucun effet sur les TEP-C, POC et le retrait du DIC, jouant ainsi un rôle antagoniste en particulier sur la production de TEP-C. Cependant, le traitement combiné réchauffement-acidification a présenté un effet positif sur le carbone phytoplanctonique (+32 %) et bactérien (+42 %). Dans l'ensemble, nos résultats suggèrent que les conditions océaniques futures pourraient avoir le potentiel de réduire la séquestration du carbone particulaire en faveur de l'accélération de la boucle microbienne et conduisant à des conséquences de rétroaction de l'océan sur le changement global.

1.2 EFFECTS OF ACIDIFICATION AND WARMING ON TRANSPARENT EXOPOLYMERIC PARTICLES (TEP) IN A MEDITERRANEAN COASTAL ENVIRONMENT (THAU LAGOON)

Authors:

Annane S.¹, Sett S.², Mas S.³, Cantoni C.⁴, Luchetta A.⁴, Starr M.⁵, Riebesell U.², Mostajir B.^{3,6}, Vidussi F.⁶, Ferreyra G. A.¹

Institutions:

¹ Institut des sciences de la mer de Rimouski, Université du Québec à Rimouski, 310 allée des Ursulines, (G5L 3A1) Rimouski, Qc, Canada

² Helmholtz Centre for Ocean Research, Kiel GEOMAR, Düsternbrooker Weg 20, 24105 Kiel, Germany

³ Centre d'écologie marine expérimentale MEDIMEER, Université Montpellier-CNRS (UMS 3301), 34200 Sète, France

⁴ ISMAR Trieste, ITALY

⁵ Fisheries and Oceans Canada, Maurice-Lamontagne Institute, 850 route de la Mer (G5H 3Z4), Mont-Joli, Qc, Canada

⁶ Laboratoire d'Écologie des systèmes marins côtiers (ECOSYM), Université Montpellier-CNRS-IFREMER-IRD-Université Montpellier 1 (UMR 5119), 34095 Montpellier, France. Present address: Center of Marine Biodiversity, Exploitation and Conservation (MARBEC), UMR 9190, University of Montpellier – CNRS – IFREMER – IRD, Montpellier, France.

ABSTRACT

Ocean global change is expected to modify the carbon cycle and affect marine ecosystems. In this context, we present here results of a mesocosms experiment designed to investigate the separate and combined effects of warming and acidification on TEP formation and on the organic carbon matter allocation in warm mid-latitude ecosystems. Twelve mesocosms (2.3 m³ each) were deployed in the Thau lagoon during spring 2012 under four conditions: control (22°C, ~445 µatm), high CO₂ (22°C, ~900 µatm), higher temperature (25°C, ~445 µatm) and high CO₂ and temperature combined (25°C, ~900 µatm). We induced a plankton bloom by nutrient addition and followed the daily changes in the different carbon pools (phytoplankton, bacteria, TEP, POC and DIC) over 12 days. At high pCO₂, TEP-C accumulation was 47 % higher, and the biological DIC drawdown was also higher (39 %). This excess carbon consumption was associated with colloidal organic carbon accumulation (3 fold) compared to present levels. These results suggest a stimulation under high pCO₂ of particle aggregation and partitioning into the POC pool. In contrast, warming decreased the DIC drawdown and particle carbon accumulation (TEP-C and POC). This suggests a reduction of particle formation and carbon export in favor of microbial degradation. Unexpectedly, our results showed that the combined effect of warming and acidification had no effect on TEP-C, POC and DIC drawdown, playing an antagonistic role especially on TEP-C production. However, the warming-acidification combined treatment presented a positive effect on phytoplanktonic (+32 %) and bacterial (+42 %) carbon. Altogether, our results suggest that future oceanic conditions would have the potential to reduce the particle carbon sequestration in favor of accelerating the microbial loop and driving consequences of ocean feedbacks to global change.

Keywords: Transparent exopolymeric particles (TEP), Ocean acidification, Warming, Global change, Phytoplankton, bacteria, Particulate and dissolved organic carbon.

INTRODUCTION

Since the beginning of the industrial era large-scale human greenhouse inputs, particularly atmospheric CO₂, have increased exponentially and are expected to impact marine organisms and ecosystems (Raven et al. 2005, Hare et al. 2007, Riebesell et al. 2009). Nearly one third of annual anthropogenic CO₂ emissions have been transferred into the ocean by physical, chemical and biological processes (Sabine et al. 2004, Raven et al. 2005). This absorption process is chemically changing the ocean and occurring at an unprecedented rate (Rost et al. 2008). In particular, biology has played a central role in modulating the climate in the past by assimilating the dissolved inorganic carbon (DIC) through the "biological carbon pump" process and thereby limiting the rise of atmospheric CO₂ (Schlesinger 2005, Rost et al. 2008). In this context, CO₂ emission models predict a rise of *p*CO₂ in the atmosphere from 400 to 750 μatm (IPCC Scenario IS92a) or even >1300 μatm (IPCC, 2014) by the end of this century. This rise, together with the input of other climatically active gases, contributes to global atmospheric mean temperature increases (Meehl et al. 2007). As a consequence, it is expected a global increase in ocean temperature ranging between ~ 2 and 6°C by the end of the century (IPCC, 2014). In addition, it has been estimated that temperature increases may favor the formation of a stronger and shallow pycnocline which, in turn, may indirectly affect phytoplankton production and community structure by limiting nutrient supply from deeper layers (Sarmiento et al. 2004, Doney 2006). In a more stratified ocean, a significant reduction of CO₂ fluxes between the atmosphere and the surface waters is expected due to the supersaturation of this gas in the upper mixed layer (Raven et al. 2005). These processes will lead to alterations in the ocean's carbonate system, resulting in a decrease of seawater pH (Zeebe & Wolf-Gladrow 2001, Rost et al. 2008). These changes in carbonate chemistry, often referred to as "ocean acidification", are already occurring and are projected to intensify in the future reaching a reduction of pH by about 0.4 units by the end of the 21st century. This value represents a large decline compared to the 0.1 units drop already observed since the beginning of the industrial revolution (Caldeira & Wickett 2005).

Ocean warming and acidification will inevitably affect marine organisms in numerous ways at the physiological (e.g. changing metabolic rates, growth rates and calcification) and ecological levels (shifts in the community composition, species succession and trophic interactions) (Falkowski et al. 1998, Boyd & Doney 2002). Global warming induced modifications of the carbon cycle represent one of the most important impacts on marine ecosystems (Schröter et al. 2005). These effects involve productivity, carbon flows, CO₂ sequestration and resources quality (Yvon-Durocher et al. 2010). Ocean warming is expected to cause major shifts in the flow of carbon and energy through the pelagic system due to the differences of temperature sensitivities of marine autotrophic and heterotrophic activation energy (López-Urrutia et al. 2006, Taucher et al. 2015). In addition, Wohlers et al. (2009) and Biermann et al. (2014) showed an increase in bacterial respiration and a concomitant increase in dissolved organic carbon (DOC) in response to warming. Therefore, they suggested that under warming carbon produced in excess will be stocked in the dissolved pool instead of being transferred through the food web to the upper trophic levels.

Mesocosms studies have shown an increased formation of transparent exopolymeric particles (TEP). TEP consist of acidic sugars exudated by phytoplankton (Alldredge et al. 1993b) and bacteria (Simon et al. 2002b), and their formation by phytoplankton has been related to a “carbon overflow” due to nutrient limitation (Engel 2002). In this sense, nutrient limitation prevents biomass accumulation, but not photosynthesis, so that carbon is excreted as dissolved organic carbon (DOC), passing through the colloidal state (colloidal organic carbon), and aggregating to form TEP, thereby achieving the transition from the DOC to POC pool (Chin et al. 1998, Passow 2000, Engel et al. 2004a). This process facilitates vertical carbon flux to the deep ocean. It should be noted that ~10 % of surface DOC of the actual ocean can be assembled to form TEP, yielding $\sim 70 \times 10^{15}$ g of organic carbon (Verdugo et al. 2004). Other experimental studies have suggested that a higher assimilation of carbon into organic matter at high CO₂ may increase extracellular organic matter release from phytoplankton cells (Engel 2002, Kim et al. 2011, Engel et al. 2014). In line with these results, several mesocosm experiments showed an increase of TEP

concentrations associated with a concomitant rise of organic sinking particles under elevated $p\text{CO}_2$ conditions, due to enhanced particle aggregation and export of carbon-rich components (Beauvais et al. 2003b, Riebesell et al. 2007). This process has been proposed as a negative feedback mechanism, counteracting the future expected increase in atmospheric CO_2 levels (e.g. Engel et al. 2004a, Arrigo 2007, Engel et al. 2014).

The extent to which enhanced TEP formation could affect particle sinking in a warming ocean critically depends on the timing of TEP formation and the interplay with other biological processes (such as microbial degradation and grazing). Wohlers et al. (2009) and Biermann et al. (2014) recently showed an increase of TEP concentrations during mesocosm experiments, while the particulate organic matter and carbon loss by sinking was reduced at elevated temperatures. However, little is known about how the combined effects of increased temperature and $p\text{CO}_2$ (e. g. synergistic, antagonistic or additive) can affect physiological processes such as carbon assimilation, metabolism and carbon exudation. In particular, there is a lack of information about how these stressors will affect the particulate organic matter, especially TEP formation in warm mid-latitude systems such as the Mediterranean Sea in a future ocean.

In this study, we describe the results of a mesocosms experiment to examine how TEP formation is affected by enhancing temperature and/or acidification in a Mediterranean shallow coastal ecosystem: the Thau lagoon. We also describe the separate and combined effects of warming and acidification on organic carbon matter allocation in the pelagic plankton system and discuss about possible effects of climate change in the future ocean.

MATERIALS AND METHODS

Experimental setup

The study was conducted at the mesocosm facility of the Mediterranean platform for Marine Ecosystem Experimental Research (MEDIMEER) between May 30 to June 11, 2012. The platform is located on the Thau Lagoon shore in Sète, France (43°24'49"N, 3°41'19"E). Twelve (12) mesocosms of 2 m depth and 1.2 m wide (~2300 L each), were immersed in the lagoon and filled with prefiltered (<1000 μm) natural surrounding subsurface waters (1 m) on May 30, 2012 (day 0). Mesocosm bags were made of two transparent, UV stabilized, 200 mm thick vinyl acetate mixed-polyethylene films separated by reinforcing nylon mesh which transmitted 77 % of the incident PAR (photosynthetic active radiation, incident light between 400 – 700 nm, Nougulier et al. 2007). Mesocosms were covered with transparent (crystal clear PVC film) dome during the whole experiment to prevent any atmospheric contamination and water exchange. In addition to the dome, the surface of the mesocosm water was covered with a transparent (crystal clear PVC) film to reduce gas exchanges. The water column in each mesocosm was constantly homogenized using a pump (Rule 500, Model 26D, 24 volt) with a turnover time set at 1 d^{-1} . Previous tests showed that the pump did not affect abundances of bacteria, phytoplankton, heterotrophic flagellates, and ciliates. However, negative effects of the pumping and the homogenization systems on more fragile species is not excluded (Vidussi et al. 2011).

The experimental design comprised four treatments: 1) high $p\text{CO}_2$ (A treatment), 2) high temperature (T treatment), 3) both high $p\text{CO}_2$ and high temperature (AT treatment), and 4) control (C treatment; natural water $p\text{CO}_2$ and natural *in situ* temperature). Three replicate mesocosms were set up for each treatment.

High temperature treatments were under the control of an automated temperature system and consisted of 3°C increase in water temperature with respect to the *in situ* natural temperature control treatments, that matched the temperature of the surrounding water and were submitted to the same variability (Nougulier et al. 2007).

The temperature increase in the T and AT treatments was gradually achieved in two steps: 1.5°C at day 1 and then 1.5°C at day 2 using submersible heating elements (Galvatec) immersed vertically at 1 m depth as detailed in Nougulier et al. (2007). In the

high $p\text{CO}_2$ treatments water $p\text{CO}_2$ was increased to approximately 900 μatm using CO_2 enriched seawater addition in three steps (addition of 4 - 7 L in acidified mesocosms on days 1, 2 and 3), reaching final corresponding $\text{pH}_{\text{total scale}}$ value between 7.73 and 7.80. Treatments began on 31 May (day 1) for both enhanced temperature and acidification in related mesocosms. Dissolved inorganic nutrients were added to all mesocosms (final concentrations: 4 μM NO_3^- , 0.25 μM PO_4^{3-} and 4 μM $\text{Si}(\text{OH})_4$) at mid-time of the experiment (day 5) to mimic a nutrient input in the water column, which frequently occurs in this system due to resuspension of matter upon wind events.

Sampling strategy

Water temperature was monitored every 2 minutes at 3 depths (0.5, 1.0, 1.5 m) using an array of automatic sensors installed in each mesocosm unit. Salinity, pH, dissolved oxygen concentrations and chlorophyll fluorescence were monitored every 2 minutes at one depth (1 m) using automatic sensors installed in one mesocosm per treatment. Water sampling for the chemical and biological laboratory analysis (see below) was performed daily every morning (8h00-10h00) at 1 m depth for 12 days. For sampling pH, total alkalinity (TA), dissolved organic carbon (DOC) and dissolved oxygen, a Niskin bottle (5 L) was used. For the other variables, water was collected into 20 L polycarbonate carboys by gently reversed pump system. Aliquots were then sampled from the 20 L polycarbonate carboys or Niskin bottles for chemical and biological analysis.

Nutrient and carbonate analysis

Water samples for nutrient analyses were pre-filtered through GF/F filters and stored at $-20\text{ }^\circ\text{C}$ in acid-cleaned polypropylene bottles until subsequent analyses. Nitrate (NO_3^-),

reactive phosphorus (PO_4^{3-}) and reactive silicate (SiO_3^{2-}) were determined using a Flow Solution III autoanalyser (Perstorp Analytical-Alpkem), following standard colorimetric methods in line with those reported by Grasshoff et al. (1999).

Daily monitoring concerned pH and TA in all mesocosms to confirm that our manipulation (acidification) changed the system as expected and that the changes reflected those anticipated in the future ocean.

Samples for pH, expressed in the 'total hydrogen ion scale' ($\text{pH}_{\text{T}25}$) at 25 °C and total alkalinity (TA) were drawn from the Niskin bottles directly into cylindrical optical glass 10 cm pathlength cells and into 300 ml borosilicate bottles, respectively, according to standard operation protocols (Dickson et al. 2007). Samples were analyzed immediately after sampling at the site laboratory: PHT with a spectrometric procedure (Clayton and Byrne 1993) and TA with potentiometric titration in an open cell with a difference derivative readout (Hernandez-Ayon et al. 1999).

The titrating HCl solution was calibrated against certified reference seawater for DIC and TA (batch no. 117, Scripps Institute of Oceanography; USA). Accuracy was checked by the titration of replicates ($n=6$) of reference seawater (batch no. 117), obtaining an experimental average TA value of $2565.5 \pm 10.7 \text{ mmol kg}^{-1}$ (certified value TA = $2214.06 \pm 0.24 \text{ mmol kg}^{-1}$). Long-term system performance was monitored by a daily analysis of reference seawater samples ($n = 56$, SD = 3.4 mmol kg^{-1}).

$\text{pH}_{\text{T}25}$ was determined spectrometrically using the indicator dye *m*-cresol purple (Sigma-Aldrich). Absorbance was measured at 730, 578 and 434 nm before and after dye addition in 10 cm cells regulated at $25 \pm 0.05 \text{ °C}$ (Clayton & Byrne 1993, Dickson et al. 2007). The $\text{pH}_{\text{T}25}$ analytical accuracy and precision resulted: $- 0.019 \pm 0.003 \text{ pH}_T$ units (tested against CRM's provided by Dickson), determined by the triplicate analysis of samples. Long-term performance was also monitored by analysing the same batch of reference seawater used to control TA measures.

The carbonate system parameters (pH_T , TA, DIC and pCO_2) for *in situ* temperature were computed with CO2SYS program (Lewis & Wallace 1998) using the measured experimental values of pH_{T25} , TA, temperature, salinity, PO_4^{3-} , SiO_3^{2-} as input parameters. We used the best set of CO_2 constants (k_1 , k_2) recommended by Alvarez (Alvarez et al 2014) for the Mediterranean Sea (Mehrbach et al. 1973 as refitted by Dickson & Millero (1987) for carbonic acid dissociation, and that of Dickson carbonic acid 1990 for KSO_4 equilibrium).

TEP analysis

TEP concentration was determined colorimetrically following the procedure described in Passow & Alldredge (1995). All mesocosm samples were prepared in triplicates of 60-100 mL (depending on particle concentration) and filtered onto 0.2 μm polycarbonate Isopore membrane filters (Merck Millipore) under low vacuum (<10 mbar). Particles retained on the filters were stained for <5 s with 500 μL of 0.02 % aqueous solution of Alcian blue in 0.06 % acetic acid (pH 2.5) and subsequently rinsed with 1 mL of deionised water. The filters were stored at -80 °C until processing. Filters were then soaked in 80 % sulphuric acid (6 mL) for 2 h and measured spectrometrically at 787 nm, using stained filters without sample as blanks. Alcian Blue absorption was calibrated using a solution of the polysaccharide Gum Xanthan. TEP concentrations were expressed in μg Gum Xanthan equivalents per liter ($\mu\text{g GX eq L}^{-1}$). TEP carbon content was determined according to Engel & Passow (2001), applying a conversion factor of 0.63 $\mu\text{g C}/\mu\text{g GX eq L}^{-1}$. It should be noted that this conversion factor was determined for diatom species. Consequently, TEP-C content, estimated in our study, could present some uncertainties due to differences in phytoplankton composition.

Particulate organic carbon analysis (POC)

Water samples (1 L) for particulate organic carbon (POC) analysis were filtered (200 mbar) onto pre-combusted Whatmann GF/F filters (500 °C for 6 hours) and frozen in glass petri-dishes at -20 °C until analyses. The POC filters were placed in a desiccator above fuming (37 %) HCl for 2 hours to remove all inorganic particulate carbon (PIC) and subsequently dried overnight at 60 °C. POC concentrations were then analyzed with an EuroVector Elemental analyzer (EuroEA-3000).

Phytoplankton and heterotrophic bacteria carbon biomasses

Samples (0.5-1 L) for phytoplankton pigment analysis using HPLC were filtered onto glass-fibre filters (Whatman GF/F) at a low vacuum (<200 mm Hg), stored in liquid nitrogen, and then frozen at -80 °C until analysis. For the chlorophyll and carotenoid analyses, pigments were first extracted in 3 mL of 95 % Methanol for 1 h at 220 °C, sonicated for a few seconds and finally clarified using glass-fibre filters (Whatman GF/F). Chlorophyll and carotenoids concentrations were analysed by high performance liquid chromatography (HPLC) with the method of Zapata et al. (2000) as detailed in Vidussi et al. (2001). Only Chl a concentrations are reported here and they were converted to carbon concentrations using the conversion factor $C/Chl\ a = 57$ (Latasa et al. 2005).

Samples for counting heterotrophic bacteria using flow cytometry were fixed with formaldehyde (2 % final concentration), and then frozen and stored at -80 °C until analysis. Heterotrophic bacteria samples were thawed at room temperature, and stained with nucleic acid-bound SYBR Green I (2 % final concentration; Invitrogen), and incubated at room temperature for 15 min in the dark. Mixed fluorescent beads (20 µl) of 0.96 and 2 µm diameters (PolySciences INC.) and Trucount beads (50 µL with known concentration, BD Biosciences) were added as an internal standard to 280 µL of diluted sample. Heterotrophic bacteria were then enumerated using a FACSCalibur flow cytometer (Becton–Dickinson) equipped with an air-cooled laser (488 nm, 15 mW), at a low flow rate (12-15 µl min⁻¹) and

with 2 min acquisition time. Bacteria were detected through the green fluorescence of SYBR Green I, collected by the FL1 detector ($\lambda = 530$ nm) of flow cytometer. To calculate the cell abundance, specific calibrated Becton–Dickinson Trucount™ beads were used. The flow cytometric data were analysed using the CellQuest Pro software (Becton–Dickinson). Bacterial abundance were expressed in terms of carbon biomass by using a conversion factor of 14 fg C cell⁻¹ (Zubkov et al. 2001c).

Statistical analysis

One of the replicates of the T treatment and one of the A treatment yielded abnormal data for several variables due to probable sac perforation during the experiment and therefore corresponding data were excluded. All statistical analyses were performed using Statistica (version 7.0) and SigmaPlot 10.0 software. All data were tested for normality and homogeneity of variance conditions with Kolmogorov-Smirnov and Cochran C tests, respectively. Repeated-measures analyses of variance (RM-ANOVA) was used to test the overall effects of main factors in this study (acidification and temperature). Newman-Keuls post hoc test was used to determine the significance of the differences between group means in the RM-ANOVA. If differences between treatments were found, univariate ANOVA tests for each dependent variable (day) were performed and p-values ≤ 0.05 were considered to indicate statistically significant differences. Effects of each treatment were calculated in % relative to the control. Changes in dissolved inorganic carbon (Δ DIC) were calculated as the difference between the beginning of the exponential phytoplankton growth subsequent to nutrient addition and the end of the bloom for each treatment (day 6 - 8) and expressed by $\mu\text{g C L}^{-1}$. We define here the DIC removal as the balance between phytoplankton DIC uptake, the DIC produced by respiration and atmosphere gas exchange. t-test was applied to test the difference of Δ DIC value between treatments compared to the control. A linear regression analysis was performed between POC and the sum of TEP-C, phytoplankton and Bac C-biomass.

RESULTS

Inorganic nutrient drawdown

Initial nutrient concentrations were low on average in all mesocosms ($0.45 \pm 0.31 \mu\text{M}$, $0.03 \pm 0.01 \mu\text{M}$ and $2.08 \pm 0.58 \mu\text{M}$ for nitrate, orthophosphate and silicate, respectively) at day 1 (Fig. 1a, b and c). A peak of orthophosphate ($0.14 - 0.23 \mu\text{M}$) was observed at day 3 in all treatments, probably due to the acclimation of the organisms to the confined experimental conditions as previously observed by Neveux et al. (2010) and Mostajir et al. (2013). This phenomenon may be due to physiological death and subsequent lysis of some planktonic cells and/or grazing. This is evidenced by the decrease of Chl *a* and an increase of DOC concentrations during the same period. As previously mentioned, nutrients were added to all mesocosms on day 5 in the afternoon, after the daily sampling. Half of the final nutrient concentrations reached after addition was consumed between that moment and the following sampling, attaining on day 6 in all mesocosms average values of $2.01 \pm 0.15 \mu\text{M}$, $0.10 \pm 0.02 \mu\text{M}$ and $6.10 \pm 0.85 \mu\text{M}$ for nitrate, orthophosphate and silicate, respectively. Furthermore, this sharp uptake continued during the following day (day 7), reaching nitrate and orthophosphate concentration values similar to those observed before nutrient addition in all treatments (Fig. 1a, b). In contrast, silicate concentration decreased to $\sim 3.50 \pm 0.45 \mu\text{M}$, with the exception of higher values in the T treatments. However, no significant concentration difference between treatments was observed for all nutrients during this experiment ($p > 0.05$).

Temperature, pH and DIC perturbation

The initial water temperature average within all mesocosms at day 1 was $22.08 \pm 0.015 \text{ }^\circ\text{C}$, and the target treatment temperatures were reached at day 3 ($25.94 \pm 0.20 \text{ }^\circ\text{C}$,

25.77 ± 0.36 °C, 23.16 ± 0.03 °C and 23.13 ± 0.02 °C in the T, AT, A and C treatments, respectively; Fig. 2a). The water temperature in all treatments reproduced the natural daily changes of the *in situ* surrounding water. However, the differences between the increased water temperature treatments (T and AT) with those of C and A treatments was maintained nearly constant (2.96 ± 0.14 °C) from day 3 to the end of the experiment on day 12.

The target pH_T values of 7.778 ± 0.016 and 7.802 ± 0.019 units for the A and AT treatments (Fig. 2b) were reached on day 4, (corresponding to 899 and 848 $\mu\text{atm } p\text{CO}_2$ scenarios, respectively). On the other hand, the C and T treatments were maintained at 8.064 ± 0.001 and 8.010 ± 0.003 pH_T units, respectively (415 and 475 $\mu\text{atm } p\text{CO}_2$ scenarios, respectively). A sharp increase in the pH values was observed from day 4 to 8 in the A and AT treatments, which was consistent with the decrease of DIC value calculated from carbonate chemistry from 2388 ± 1.8 and 2358 ± 13 $\mu\text{mol kg}_{\text{sw}}^{-1}$, respectively (corresponding to 28658.7 ± 22 and 28297.8 ± 160 $\mu\text{g C L}^{-1}$). pH_T values reached 7.987 ± 0.012 and 7.964 ± 0.013 in the A and AT treatments, respectively, at the end of the experiment, which was accompanied by DIC values of 2300 ± 14 and 2290 ± 15 $\mu\text{mol kg}_{\text{sw}}^{-1}$, respectively for the same treatments (corresponding to 27605 ± 174 and 27476 ± 184 $\mu\text{g C L}^{-1}$, Fig. 2c). In contrast, lower pH and DIC variability were observed in the T and C treatments, with pH increasing to 8.033 and 8.126 from days 6 to 8 for T and C treatments, respectively, which coincided with the decrease of DIC for both treatments reaching 2234 and 2222 $\mu\text{mol kg}_{\text{sw}}^{-1}$, respectively (corresponding to 26807 and 26666 $\mu\text{g C L}^{-1}$). Thereafter, DIC concentrations increased again up to final concentrations of 2242 and 2243 $\mu\text{mol kg}_{\text{sw}}^{-1}$ (corresponding to 26906 and 26916 $\mu\text{g C L}^{-1}$) at the end of the experiment for T and C treatments, respectively.

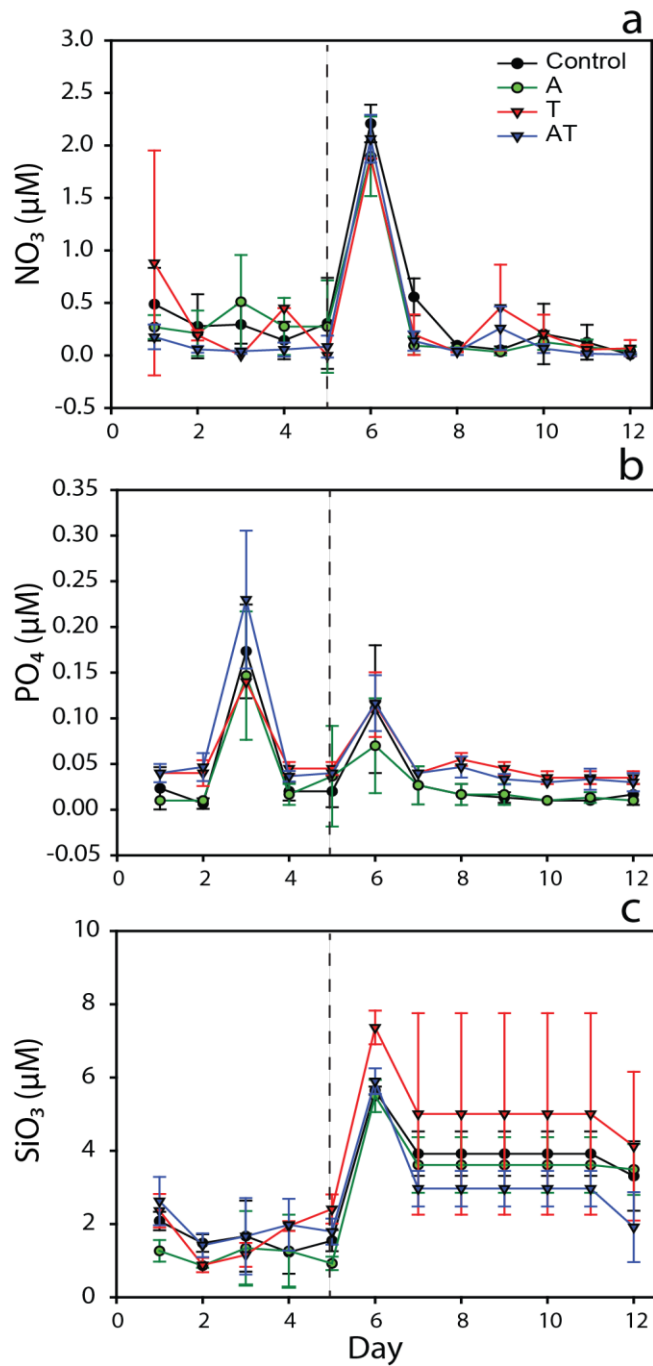


Figure 1 : Temporal variation of inorganic nutrients (a) nitrate (μM), (b) orthophosphate (μM) and (c) silicates (μM) (averages $\pm\text{SD}$) of the mesocosms experiment with the following treatments: Control, actual temperature and $p\text{CO}_2$ (black); high $p\text{CO}_2$, A (green); high temperature, T (red) and high $p\text{CO}_2$ and high temperature, AT (blue).

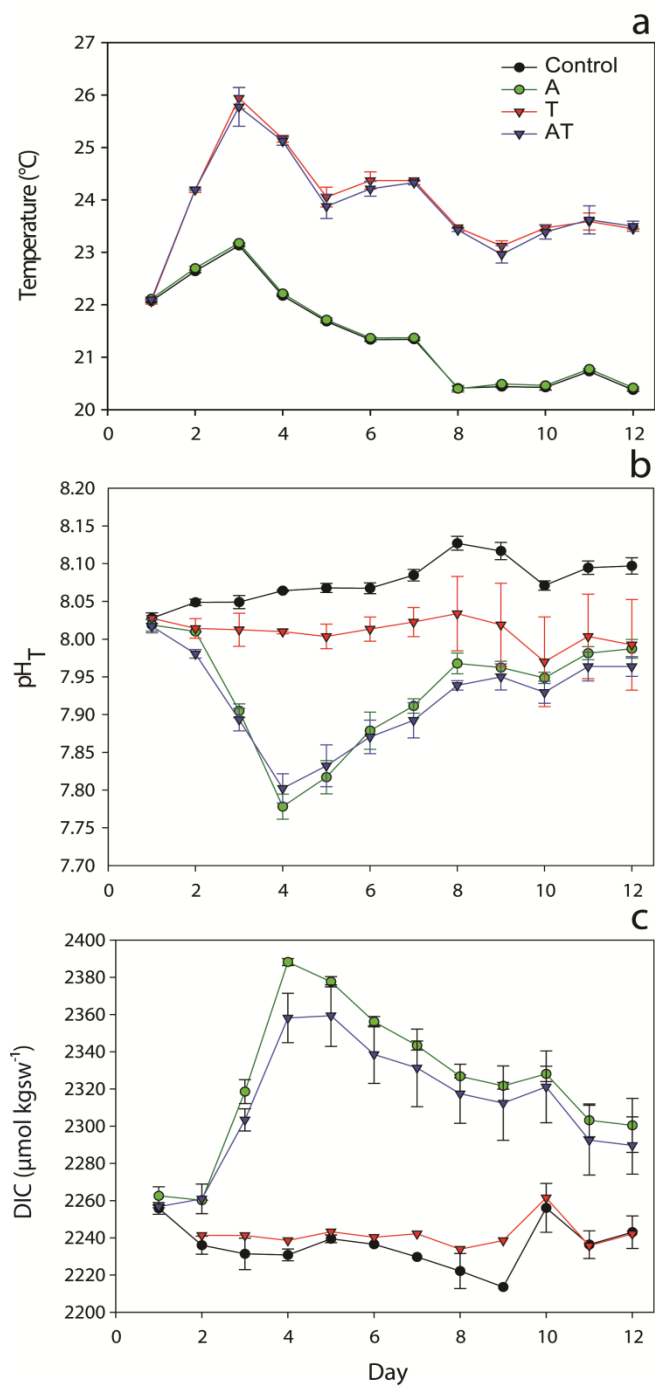


Figure 2 : Temporal variation of (a) temperature (°C), (b) pH_T *in situ* and (c) DIC (μmol kg_{sw}⁻¹) (averages ± SD) during the mesocosms experiment with the following treatments: Control, actual temperature and pCO₂ (black); high pCO₂, A (green); high temperature, T (red) and high pCO₂ and temperature, AT (blue)

Dynamics of organic material build-up

During the experiment, the phytoplankton dynamics expressed in terms of carbon concentration (Figure 3a) exhibited three phases in the phytoplankton bloom: i) a pre-bloom from day 1 to 5, where the plankton community acclimated to the experimental conditions; ii) bloom (exponential phytoplankton growth) from day 5-6 to 7, and iii) a post-bloom after day 8, when nutrients were exhausted and phytoplankton abundance dropped in all mesocosms.

Phytoplankton carbon biomass (phyto-C) was low at the start of the experiment and did not show significant differences between treatments ($116.71 \pm 15.67 \mu\text{g C L}^{-1}$; $p > 0.05$). During the pre-bloom, Phyto-C decreased slightly until day 3 in the T and AT treatments, and until day 4 in the C and A treatments, most probably due to the acclimation to the mesocosm confined. Phyto-C significantly increased in the T and AT treatments from day 4 to 6 relative to the C and A treatments ($p < 0.05$). Following the nutrient addition in day 5, Phyto-C increased until day 7 reaching $178.65 - 236.43 \mu\text{g C L}^{-1}$, representing an increase of 28 %, 32 % and 18 % for A, AT and T treatments, respectively, compared to the Control. Thereafter, Phyto-C decreased continuously in all treatments until the end of the experiment, attaining similar concentrations than at day 1. Phyto-C showed no significant difference between treatments during the whole experiment except at day 7 in the acidified treatments (A and AT; $p < 0.05$). Phytoplankton species composition derived from specific marker pigments was dominated by diatoms (42-57 % of the total community), followed by prymnesiophyceae (16-34 %) and dinoflagellates (19-25 %), both during bloom and no-bloom conditions (F. Vidussi pers. comm. HPLC). Nanophytoplankton cells in the range 3-6 μm represented 49-78 % of the total carbon biomass during the whole experiment, followed by $>6 \mu\text{m}$ nanophytoplankton (19- 47 %) (flow cytometry, data not shown). Thus, no change was evidenced in phytoplankton succession and community composition.

At the beginning of the experiment, TEP-C concentrations were $435 \pm 42.66 \mu\text{g C L}^{-1}$, without significant difference between treatments (Fig. 3b). In the post bloom phase,

TEP-C concentrations in A and T treatments were respectively higher and lower than the Control ($p < 0.05$), showing thus throughout the experiment an opposite effect of $p\text{CO}_2$ or temperature increase. In contrast, over the whole experiment, the AT treatment did not induce a significant difference in TEP concentration with respect to the Control. We observed a significant increase of TEP-C concentration in the A treatment during the post-bloom ($p < 0.05$) with a maximum value ($1381 \pm 262.77 \mu\text{g C L}^{-1}$) on day 11, representing a 47 % increase with respect to the Control. In contrast, TEP-C concentrations in the T treatment decreased significantly ($p < 0.05$) during the post-bloom reaching on day 12 the lower value ($293 \pm 28.60 \mu\text{g C L}^{-1}$) in all treatments (33 % less than in the Control; Annex 2.1).

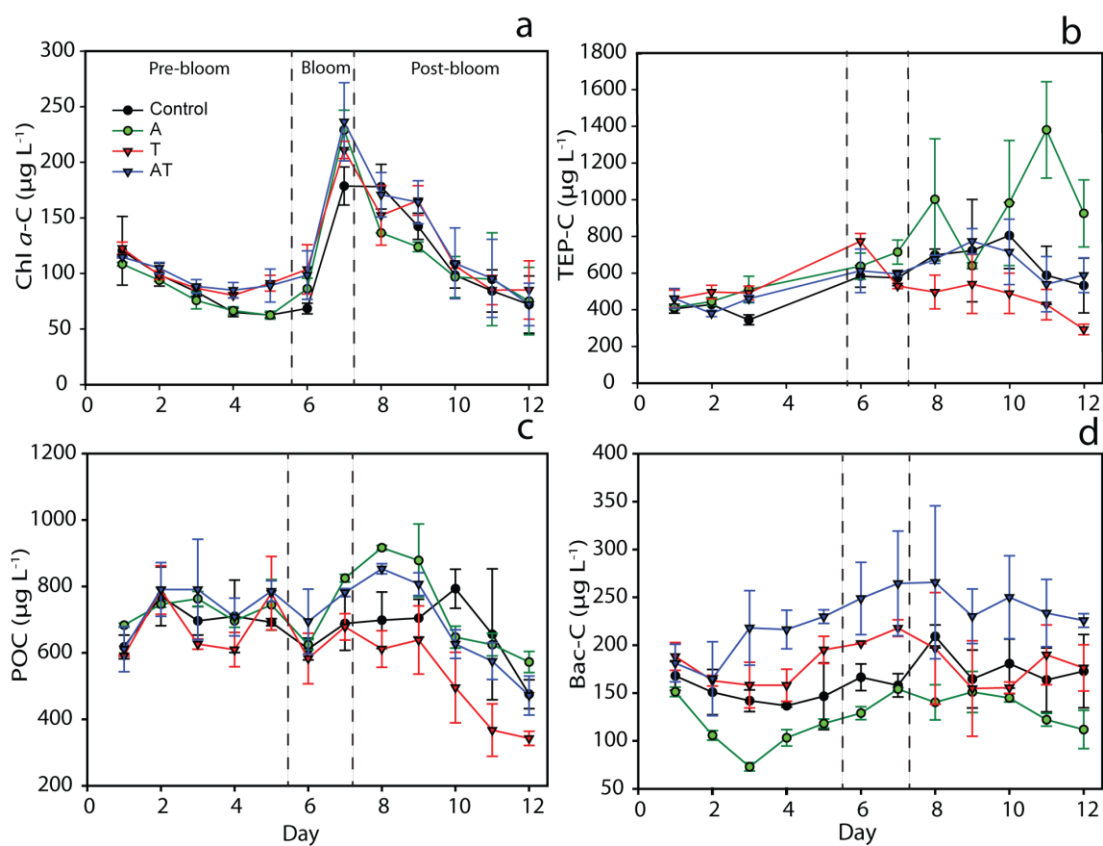


Figure 3 : Temporal variation of (a) Chl a -C, (b) TEP-C, (c) POC and (d) Bac-C (averages \pm SD) during the mesocosms experiment with the following treatments: Control, actual temperature and $p\text{CO}_2$ (black); high $p\text{CO}_2$, A (green); high temperature, T (red) and high $p\text{CO}_2$ and temperature, AT (blue)

Average POC concentrations were $626 \pm 39.82 \mu\text{g C L}^{-1}$ at the beginning of the experiment and did not increase until the end of the phytoplankton bloom period on day 7 (Fig. 3c). POC concentrations were significantly higher in the acidified treatments (A and AT; $P < 0.01$) and a global negative effect of temperature was evidenced ($P < 0.05$). We observed a significant POC increase in the acidified treatments relative to the Control on days 7 to 9 ($p < 0.05$), which coincided with the maximum TEP-C concentration observed in the A treatment. In contrast, POC concentration was lower in the T treatment than in the control during the post-bloom period and especially on days 10 to 12 ($p < 0.05$; univariate ANOVA test). During the post-bloom period, POC concentration was 12 % higher in the A treatment and 22 % lower in the T treatment compared to the Control. After day 9, POC concentration declined in all treatments, reaching values lower than at the initial ones ($342.69 \pm 21.43 \mu\text{g C L}^{-1}$ and $572.45 \pm 31.99 \mu\text{g C L}^{-1}$ in the T and A treatments, respectively).

The initial heterotrophic bacterial-carbon biomass (Bac-C) was on average $172.23 \pm 16.29 \mu\text{g C L}^{-1}$. Thereafter, Bac-C biomass was significantly highest and lowest in the AT and A treatments, respectively, relative to the Control, until the end of the experiment ($p < 0.05$; Fig. 3d). During the pre-bloom and bloom periods, a significant increase of Bac-C values was observed in the high temperature treatments (T and AT), compared to the other treatments ($p < 0.05$). It should be noted that Bac-C was significantly higher in the AT treatment than in the control during the whole experiment ($p < 0.05$). During the phytoplankton bloom, the maximum Bac-C values observed for the A and AT treatments, were $154 \pm 1.65 \mu\text{g C L}^{-1}$ and $265 \pm 54.59 \mu\text{g C L}^{-1}$ respectively, which represented 22 % lower and 42 % higher respectively, than heterotrophic bacterial-carbon biomass in the Control (Annex 2.2).

Net changes in DIC concentration (ΔDIC) were calculated during the bloom phase (Fig. 4). In the A treatment, significant high DIC removal (average $352 \pm 23 \mu\text{g C L}^{-1}$) was observed compared to the control (t-test: $p < 0.01$). However, no significant difference was observed between the other treatments (average 78 ± 00 and $253 \pm 156 \mu\text{g C L}^{-1}$ in T and

AT, respectively) compared to the control ($253 \pm 00 \mu\text{g C L}^{-1}$; t-test: $p > 0.05$). During the exponential growth period, the carbon-to-nitrate ($\text{DIC}:\text{NO}_3^-$) ratio increased to 18.25 for the A treatment and decreased to 3.52 for the T treatment relative to the Redfield C:N ratio of 6.6. Similarly, no difference was observed for C:N ratio for AT treatment 10.43 compared to the Control 9.97. However, AT and C treatment C:N ratios were higher than the standard Redfield C:N ratio. Thus, for the same inorganic uptake, the DIC removal represented an increase of 39 % for the A treatment and a decrease of 69 % for the T treatment, compared to the C treatment. In contrast, no difference between AT (0.33 %) and C treatments was observed (Annex 2.2).

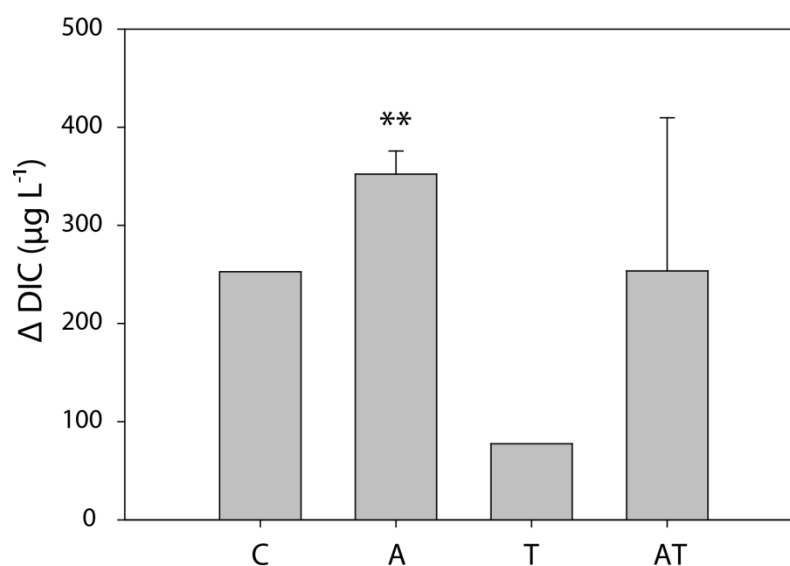


Figure 4 : Dissolved inorganic carbon changes (ΔDIC) during the bloom phase in the Control (C), Acidified (A), high Temperature (T) and Acidified and high Temperature (AT) treatments during the exponential phytoplankton growth. t-test significant difference (** $P < 0.01$)

Biological and TEP particulate carbon contribution to the particulate organic carbon pool

The contribution of TEP-C, Phyto-C and Bac-C concentrations (TPB-C: sum of the three concentrations) to the particulate carbon pool in the different treatments is shown in Fig. 5. As displayed in the figure, Bac-C concentration was consistently higher than that of Phyto-C in all treatments. However, the most important contribution to the TPB-C came from the TEP-C during the whole experiment. TEP-C concentrations were twice the sum of Phyto-C and Bac-C concentrations, with $605 \pm 209 \mu\text{g C L}^{-1}$ for TEP-C against 111 ± 43 and $174 \pm 44 \mu\text{g C L}^{-1}$ for Phyto-C and Bac-C, respectively. The highest TPB-C concentration was observed in the A treatment (Fig. 5b), whereas the lowest value belonged to the T treatment (Fig. 5c). The results of the RMANOVA analyses showed overall both significant positive and negative effects on the TPB-C concentration in the acidified and warmer treatments, respectively ($p < 0.05$), which was consistent with the main effects observed for the POC. It is notable that TPB-C concentrations largely exceeded POC levels in the phytoplankton bloom and post-bloom periods in all treatments. Nevertheless, we observed a significant correlation between TPB-C and POC for T and AT treatments, explaining 67 % and 70 % respectively of the variance of POC ($r = 0.81$, $p < 0.05$; $r = 0.83$, $p < 0.05$ respectively; Table 1) as well as for the control ($r = 0.83$, $p < 0.05$). In contrast, no significant correlation was found for A treatment.

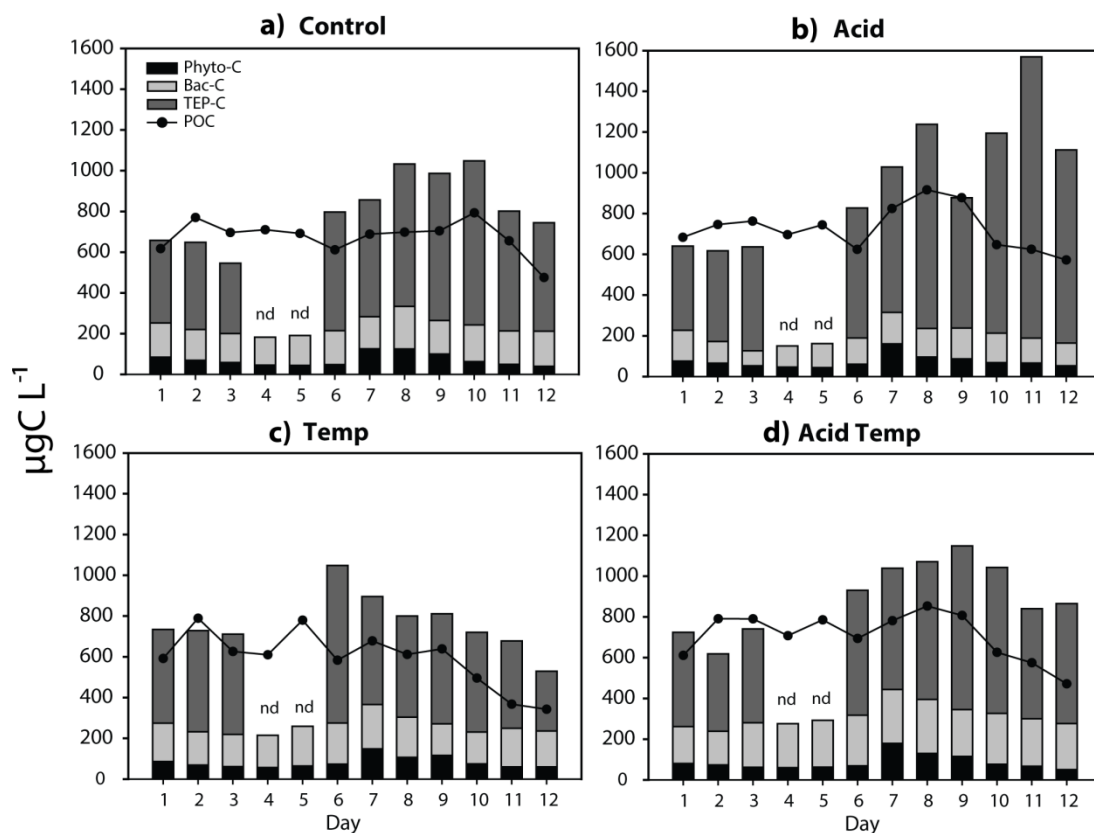


Figure 5 : Temporal contribution of the sum of TEP-C, Phyto-C and Bac-C (TPB-C sum) and POC compartments studied for the a) Control and b) Acid, c) Temperature and d) Acid Temperature treatments. Bars represent phytoplankton-C (black); HBacteria-C (light grey); TEP-C (dark grey) and the black line with points is POC. Units for all variables are $\mu\text{g C L}^{-1}$

Table 1 : Results of the linear correlation analyses between POC ($\mu\text{g C L}^{-1}$) as the dependent variable and the sum of TEP-C, Phyto-C and Bac-C (TPB-C sum, $\mu\text{g C L}^{-1}$) for each treatment (independent variable)

| Treatments | R | <i>p</i> |
|------------|-------|----------|
| C | 0.83 | 0.02 |
| A | -0.16 | ns |
| T | 0.81 | 0.02 |
| AT | 0.83 | 0.02 |

DISCUSSION

1. Acidification effects

Aggregation and coagulation of dissolved and colloidal carbon compounds (mainly polysaccharides) specially produced by phytoplankton can lead to a rapid formation of transparent exopolymeric particles (TEP) and contribute to the particle sinking and carbon sequestration. In spite of no difference between treatments regarding nitrate uptake, our results show high TEP-C accumulation in the post-bloom period under high $p\text{CO}_2$ conditions. This accumulation can be mainly explained by "carbon overconsumption" and nutrient stress (Toggweiler 1993, Riebesell et al. 2007b). In the post-bloom period of the A treatment, TEP-C increase up to 47 % with respect to the control which was consistent with the observed intensification (+12 %) in POC accumulation in the same treatment. This result is in agreement with previous studies showing increased extracellular release of organic rich carbon compounds by phytoplankton under CO_2 excess and nutrient limitation (Obernosterer & Herndl 1995, Engel 2002, Engel et al. 2004a, Kim et al. 2011). It has also been shown that phytoplankton production of TEP is stimulated by higher $p\text{CO}_2$ conditions at both, species and community levels (Engel 2002, Engel et al. 2004a, Mari 2008, Pedrotti et al. 2012), through coagulation and aggregation of individual colloidal polymers to larger particles (Endres et al. 2014). In this sense, TEP can enhance the total particle abundance as well as bulk particle stickiness and could play a significant role in the formation of aggregates, stimulating carbon export under high $p\text{CO}_2$ conditions, a potential export mechanism substantiated by Engel et al. (2004b).

The high TEP formation was consistent with the highest inorganic carbon drawdown in the A treatment (ΔDIC , $352 \mu\text{g C L}^{-1}$; Fig 4). For the same uptake of nitrate, net community inorganic carbon consumption in the A treatment was 39 % larger than in the control. These results are in the same range as the DIC drawdown in a natural diatom-dominated community reported by Riebesell et al. (2007) (39 %) under acidified conditions

(3xCO₂) in the Raune fjorden, Norway. Our DIC results are consistent with the build up of Phyto-C during the bloom period under high *p*CO₂, showing a positive effect of CO₂ on phytoplankton biomass (+28 %) relative to the control in a community dominated by diatoms (42 - 57 % in all treatments), as in the study of Riebesell et al. (2007). Moreover, our results showed a high carbon-to-nitrate ratio (~ 18.25) under increased CO₂ conditions, more than the Redfield C:N ratio (~6.625), demonstrating a carbon overconsumption under high *p*CO₂. This is in line with previous studies which demonstrated that elevated *p*CO₂ can enhance both growth rate and carbon fixation by phytoplankton (Riebesell et al. 1993, 2007, Wolf-Gladrow et al. 1999, Hutchins et al. 2007). In addition, a significant loss of POC by enhanced TEP aggregation and sinking was reported (Wolf-Gladrow et al. 1999, Riebesell et al. 2000, Engel et al. 2005). Our study demonstrates that the observed overconsumption of DIC by phytoplankton resulted in an increase of POC and TEP, which leads to enhanced particulate organic matter accumulation under high *p*CO₂ conditions.

The high uptake of DIC over inorganic nitrogen is the result of the phytoplankton “carbon overflow” mechanism that helps to preserve the metabolic functionality of the cell when there is an imbalance between light and nutrients (Fogg 1983, Taucher et al. 2015), releasing it as DOC exudates. However, the absence of acidification effects on DOC accumulation (data not shown here, Sett pers. comm.) was unexpected since previous studies showed a stimulation of extracellular release from phytoplankton and to some extent bacteria (Riebesell et al. 2007, Kim et al. 2011, Engel et al. 2014, Bar-Zeev et al. 2011). We believe that freshly produced DOC (including TEP precursors) was rapidly partitioned from dissolved into the colloidal and TEP particle phases by coagulation and aggregation, preventing the accumulation of excess exudates in the dissolved fraction. Previous studies have shown that abiotic chemical processes (pH, ion density, type and concentration of precursors and their adhesive properties), and physical processes (turbulence, particle density, and sedimentation) can transform a substantial fraction of DOC exudates into TEP on very short timescales (Passow 2000, Engel et al. 2004a). Due to high surface active nature of TEP-precursors, their turn-over time ranges from hours to days (Mopper et al. 1995), reducing the ambient precursor concentration but not their

release rate. Moreover, previous findings showed that waters with high algal activity produced the highest concentrations of surface-active carbohydrates and new TEP (Kepkay et al. 1990, Zhou et al. 1998). Consequently, our results suggest that, in high $p\text{CO}_2$, TEP production contributes to enhance the particle aggregation and carbon partitioning into the POC pool.

Another argument which could contribute to explain the high TEP-C accumulation is that the unexpected low bacterial biomass observed here probably resulted in a limited enzymatic activity and hence degradation of these particles. Indeed, the surprising result of this experiment was the negative effect of high $p\text{CO}_2$ on bacterial biomass in spite of an increase of aggregated polysaccharides in form of TEP (and the availability of energy-rich dissolved substrates) which should stimulate bacterial growth and production. This result contrasts with findings from previous studies which showed that marine bacteria benefit directly and indirectly from decreasing seawater pH (Grossart et al. 2006, Piontek et al. 2010, 2013, Brussaard et al. 2013, Endres et al. 2014). In particular, Endres et al. (2014) in an off-shore mesocosm experiment showed an increase in bacterial abundance of 28 % under high $p\text{CO}_2$ (3000 μatm). The authors suggested that high $p\text{CO}_2$ /low pH stimulates both, availability of gel particles as a food source and substrate to grow upon, as well as enhanced enzymatic hydrolysis of organic matter. Piontek et al. (2010) showed that the degradation of polysaccharides by bacterial extracellular enzymes was significantly accelerated during experimental simulation of ocean acidification. These authors have shown that enzymes β -glucosidase and leucine-aminopeptidase almost doubled their production rates under a decrease of 0.5 units in seawater pH. Grossart et al. (2006) also reported increased particle-attached bacteria at high $p\text{CO}_2$ during the decline of the bloom when the release of algal-derived organic matter was high. In contrast with these studies, our results show that acidification have an adverse effect on bacterial biomass, which was 22 % lower under high $p\text{CO}_2$. While we do not have information about bacterial respiration or bacterial carbon demand, the low bacterial biomass seem to present less impact on TEP degradation. We hypothesize that bacterial biomass at low pH can be controlled by viral lysis or by flagellates heterotrophic grazing. Brussaard et al. (2013) found a stronger

regulation of bacterial abundances due to viral lysis at higher $p\text{CO}_2$ during a mesocosm experiment in the Arctic. We conclude that the decrease of bacterial biomass and probably of the bacterial activity in addition to the accumulation of TEP carbon could favor TEP-mediated particle export and hence provides a negative feedback to rising atmospheric CO_2 .

2. Temperature effects

Our results demonstrate that temperature had an overall negative effect on TEP carbon accumulation during the post-bloom, representing a decrease of 33 % of carbon relative to the control. Although, we observed a small increase of TEP concentration on day 6 presumably as a result of the early onset of the phytoplankton bloom, still TEP-C decreased after that (Fig 3b). The observed TEP-C reduction was consistent with reduction of POC accumulation during the same period, representing 22 % less than the control. These results contrast with the experimental mesocosm studies of Wohlers et al. (2009), Biermann et al. (2014) and Seebah et al. (2014) who found a stimulation of TEP production and aggregation of organic matter at elevated temperatures, while the particulate organic matter and carbon loss by sinking was reduced. Those results were also associated with a faster and more intense partitioning of polysaccharides within the DOC compartment (Wohlers et al. 2009, Engel et al. 2011, Taucher et al. 2012). We speculate that our contrasting results may be due to the taxonomic composition of the phytoplankton assemblage during our experiments under warming conditions. Indeed, Claquin et al. (2008) in a batch culture with eight species of microalgae showed that warming increased TEP production in 3 diatoms and 2 prymnesiophytes up to an optimal species-specific temperature (~22 to 25 °C). Furthermore, Taucher et al. (2015) recently highlighted the importance of diatom species-specific physiological optima and temperature range in response to warming, where temperature act as a stressor beyond the optimal range. These authors have shown that a warming from 15 to 20 °C translated in a decrease of 30 % of TEP accumulation for the diatom *Dactyliosolen fragilissimus* and not for *Thalassiosira*

weissflogii. In agreement with these studies, our phytoplankton community was dominated by diatoms and prymnesiophytes. Their TEP precursor production was probably sensitive to high temperature. However, this low TEP-C accumulation does not seem to be due to a community composition change or phytoplankton succession since no effect on phytoplankton species composition was observed between treatments. Our results suggest that reduced TEP and POC accumulation under warming conditions could greatly reduce the sinking aggregates in this phytoplankton community and thereby limit the particle flux and carbon sequestration.

During the bloom in the high temperature treatment, the low TEP-C concentration was consistent with the observed lower net DIC drawdown, $78 \mu\text{g C L}^{-1}$ compared to $252 \mu\text{g C L}^{-1}$ for the control (i.e., 69 % less under warming). These diminutions of DIC drawdown at high temperature are consistent with the work of Wohlers et al. (2009). These authors showed that increasing temperature by 2 - 6 °C resulted in a lessening in the biological drawdown of DIC by up to 31 % during an indoor mesocosm experiment. More recently, Taucher et al. (2015) showed a decrease of carbon uptake by 33 % for the diatom *D. fragilissimus* in a batch culture under warming conditions. Although the low DIC drawdown at high temperature could have resulted from a reduction in photosynthetic carbon fixation such as suggested by Wohlers et al. (2009), this hypothesis cannot be supported by the phytoplankton biomass results in the present study, which represented +18 % relative to control during the bloom. This latter is consistent with previous mesocosm (e.g.: Wohlers et al. 2009, Vidussi et al. 2011, Biermann et al. 2014) and microcosm (Wohlers-Zöllner et al. 2011) studies showing an acceleration of exponential phytoplankton growth by 1-2 days earlier under warming conditions. In our case, the early onset of the bloom translated in a small increase of TEP concentration until day 6 and decreased afterwards. Indeed, temperature controls basic metabolic processes like enzymatic activity and growth (Feng et al. 2009, Torstensson et al. 2013) for both autotrophic and heterotrophic organisms until a species optimum. Further increases in temperature would have unfavorable physiological responses, leading to reduced growth rates and cellular damage (Boyd et al. 2010), which could probably alter the quantity and quality of TEP

precursors. However, the negative effects of temperature on TEP production in our study did not appear to be caused by a change in phytoplankton community as mentioned earlier.

The low TEP-C accumulation can be also explained by the high bacterial biomass observed here in response to the elevated temperature during almost the whole experiment. Indeed, bacterial biomass increased by 7 % under warming conditions. This high bacterial biomass could have enhanced respiration and hence heterotrophic recycling of the organic matter as evidenced by the negative correlation between bacterial abundance and the reduction of POC and TEP ($r = -0,94$ and $r = -0,87$, respectively) under warming conditions at the end of our experiment. These results are consistent with previous research on the effects of temperature on bacterial production and respiration rates (Vazquez-Dominguez et al. 2007, Hoppe et al. 2008, Piontek et al. 2009, Biermann et al. 2014). According to Verdugo (2012), experiments using size fractionation emphasize that colloidal rather than dissolved organic matter are probably the principal source of nutrients for heterotrophic microbial production in seawater (Simon et al. 2002b). They suggested that gels may comprise a rich source of microbial nutrients. In agreement with this study, the DOC pool here, in contrast to TEP pool, remained constant during the bloom and post-bloom periods, and DOC release did not differ between treatments (not shown). Thus, we hypothesize that, as a result of the increase of bacterial biomass under warming conditions, the bacterial enzymatic activity could have prevented the accumulation of colloids and TEP particles by degradation/respiration. These results may also be due to the potential sensitivity to temperature on the amount and quality of polysaccharides produced including TEP precursor by this phytoplankton community and their subsequent conversion to TEP. It has been previously suggested that warming drives the ecosystem balance in favor of respiration, consequently increasing CO_2 production by the microbial community (Vazquez-Dominguez et al. 2007, Wohlers et al. 2009, Yvon-Durocher et al. 2010). This could explain the high difference in the net DIC concentration between high temperature and control treatments as discussed above. This suggests that TEP-C was probably used as an adequate substrate by heterotrophic bacteria limiting the accumulation of these particles. This response would accelerate the carbon recycling by the microbial loop against the

biological C uptake under high temperature conditions; thus, providing a positive feedback to rising atmospheric CO₂.

3. Temperature and Acidification combined effects

Combined elevated temperature and high $p\text{CO}_2$ (AT), showed no effect on TEP-C production during the post-bloom period (-2 %) compared to the control (Fig 3b). This result was also consistent with the lack of change of POC and DOC accumulation in the same treatment relative to the control. These results contrast with the roller tanks experiment of Seebah et al. (2014) who showed an increased of TEP production under high temperature (20 °C vs 15 °C) and $p\text{CO}_2$ for the diatom *T. weissflogii*, but with a decrease in aggregation and sinking velocity of aggregates. However, Taucher et al. (2015) results suggest a substantial sensitivity of TEP formation in the diatom *D. fragilissimus* to temperature and $p\text{CO}_2$. Although the lack of a clear trend and the contrasting results concerning the effect of warming and acidification on TEP accumulation and its fate was suggested to be highly variable among the dominant phytoplankton species and the acceleration of the microbial respiration making uncertain the net effect on TEP of warming and acidification (Taucher et al. 2015). Nevertheless, our results suggest that these two factors may play an antagonistic role on TEP-C production in a future ocean scenario.

During the bloom, our data showed that Phyto-C increased up to 32 % over the control value in the AT treatment whereas the increase was only 28 % and 18 % in A and T treatments, respectively. This result agrees with previous studies showing an increase in maximum biomass values under elevated temperature and $p\text{CO}_2$ conditions (Hare et al. 2007, Torstensson et al. 2013). According to Torstensson et al. (2013) in a batch culture experiment, phytoplankton growth rate in their warmer treatment (+2.4 to 5 °C) was stimulated by elevated $p\text{CO}_2$. The authors suggested that the interaction between warming and rising $p\text{CO}_2$ facilitated the use of available extra carbon to potentially increase

phytoplankton growth rate. In our case, the availability of excess CO₂ had probably protected the cellular metabolic functionality from damage. However, no change in the net DIC concentrations was observed in the AT treatment relative to the control. It should be also noted that in our study bacterial biomass was twice higher under combined warming and acidification (AT) scenario during the bloom, showing an increase of 42 % of bacterial biomass compared to the control. These conditions had the potential to stimulate bacterial production and enhance the microbial respiration and recycling, with potential consequences on energy transfer toward higher trophic levels and sequestration of carbon in the ocean. In this case, the extent to which TEP-C could form and accumulate most likely depends on the rate of TEP production by phytoplankton and the interplay with bacterial remineralisation in a future ocean. All together, this would have the potential to reduce the particle carbon sequestration with a potent acceleration of the microbial loop.

4. Temperature and CO₂ effects on biological and TEP carbon contribution to the particulate carbon pool

The sum of TEP-C, Phyto-C and Bac-C (TPB-C) was compared to POC for the different treatments. The treatments showed the same general effect on the TPB-C as on POC and TEP response. This TPB-C concentration largely exceeded POC concentration in the bloom and post-bloom period in all treatments (Fig. 5). However, significant correlations between TPB-C and POC concentrations were found in the high temperature treatments (T and AT) and the control, which contrasted with the A treatment (Table 1). This carbon excess in the TPB-C could be due to an increase in the TEP colloidal fraction especially under acidified conditions, where the TPB-C seemed extremely high. This dissimilarity can be explained by the difference of carbon concentration between POC and TEP-C particularly during the post-bloom. TEP-C represented on average 96 % of POC for warmer (T and AT) and control treatments, whereas it represented 134 % of POC for high pCO₂ treatments. This agrees with previous results of Beauvais et al. (2003) in a field

experiment in the NW Mediterranean sea, who also reported a TEP-C contribution of 183 % of POC using the same pore size filter (0.2 μm) and more recently by Annane et al. (2015) for the St. Lawrence Estuary. These authors suggested that either TEP carbon content overestimates naturally occurring TEP-C, or POC was underestimated. This can be explained by: (1) TEP-C content calculated from freshly formed TEP produced in the laboratory from diatom batch cultures and natural communities naturally overestimates the occurring TEP-C, since the relationship between TEP and carbon content is species-specific (Engel & Passow 2001); (2) POC was probably underestimated, since the pore-size used for the filtrations is larger than that used for TEP (0.2 μm for TEP vs. 0.7 μm for POC). Several authors suggested that filters like those used in our work (0.2 μm) are the most efficient for collecting TEP (Passow & Alldredge 1995, Passow 2002a, Bhaskar & Bhosle 2008, Wetz et al. 2009, Sun et al. 2012). TEP are characterized as particulate material, ranging in length continuously from submicron (colloidal) scales (Wells & Goldberg 1992) to macroscopic particles (marine snow) that can reach a few cm in size (Alldredge & Silver 1988). It should be noted that the colloidal fraction is very dynamic, involving high levels of aggregation (Wells 1998). Indeed, Passow & Alldredge (1995) observed that >50 % of TEP were lost when 0.6 μm filters were used instead of 0.2 μm filters. All these observations highlight the importance of the colloidal carbon fraction of TEP-C as also shown by Kepkay (2000) and Bar-Zeev et al. (2011). Consequently, we estimated an operational colloidal carbon concentration for the fraction between 0.2 to 0.7 μm (as the difference between TPBC sum and POC). This colloidal fraction represented 1 and 1.5 fold for T and AT treatment, respectively, relative to the control and 3 folds under high $p\text{CO}_2$. This suggests that acidification enhance not only the TEP fraction, but also the colloidal carbon compounds. This may explain why the aggregation rates are usually high under the acidified conditions (Engel et al. 2004a).

5. Implications for a future ocean

Global change is warming and acidifying the ocean. This study was performed to explore the possible responses of TEP-C and the impact of these changes on the carbon budget under future separate and combined effects of warming and acidification (Fig. 6).

This study showed that acidification may enhance POC accumulation and especially stimulate the formation of high concentrations of aggregate organic particles like TEP and colloids. These high particle accumulations resulted from enhanced DIC assimilation by biological over-consumption of CO₂. These increases of organic aggregates would lead to an increase of sinking and export of organic matter in a more acidified ocean. In addition, the decrease of bacterial biomass under high *p*CO₂ may probably induce lessened microbial recycling and indirectly contribute to POM accumulation. In this case this would favor export and sequestration of carbon and hence have a negative feedback on the CO₂ rising in the atmosphere (Fig. 6a).

On the other hand, a reduction of accumulation of particulate organic matter (like TEP and POC) was found under high temperature in our study. Conversely, bacterial carbon increased, enhancing most likely heterotrophic recycling and respiration of the organic matter, thereby, replenishing the DIC pool. Hence, probably preventing the accumulation of TEP-C by reducing the carbon flow to the particulate organic matter or by degradation of the freshly formed colloids and TEP under high temperature conditions. This suggests a faster carbon cycling within the microbial loop which would drive the metabolic balance towards a more heterotrophic community under elevated temperatures. These processes may weaken the biological carbon pump, ultimately representing a positive feedback to rising atmospheric CO₂ (Fig. 6b).

However, even if the combined effect of warming and acidification could favor phytoplankton biomass accumulation (increase ~58 µg C L⁻¹), the synergistic effect of these factors enhancing bacterial biomass (increase ~106.5 µg C L⁻¹) and thus probably heterotrophic respiration, could counteract the global effect of the phytoplankton biomass accumulation. This is consistent with the lack of changes observed on TEP and POC accumulation and net DIC drawdown. In the context of a future ocean, warming and ocean

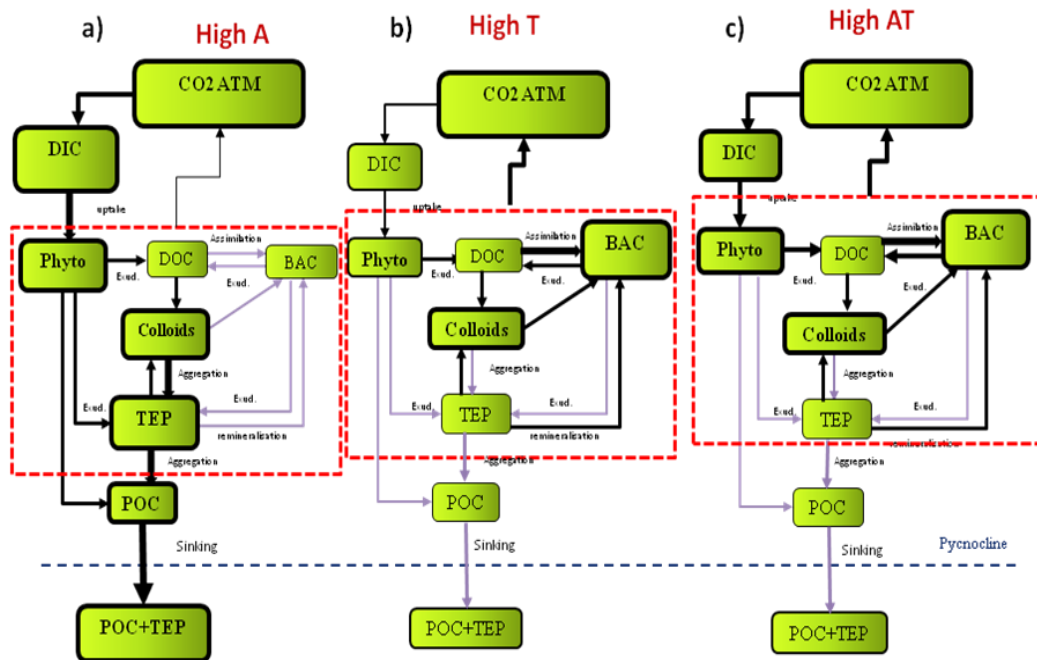


Figure 6: Conceptual model of the carbon pathway implicated for each scenario a) High acidification, b) High temperature and c) High acidification and temperature. Boxes represent the different carbon compartments (DIC, phytoplankton, Bacteria, TEP, colloids, POC and DOC) for each partition. Arrows represent processes of uptake, exudation, assimilation, aggregation, remineralization and sinking. The positive effect in each treatment is in bold black and those negative or presenting no effect to change in CO_2 and/or temperature are grey. The uptake of DIC by phytoplankton is modulated by CO_2 and temperature change. The excess of fixed carbon is exudate as DOC, with a portion of the DOC rapidly transformed into colloids and TEP by abiotic aggregation process, which contributes to a large fraction of the POC. This partitioning into particulate fraction is elevated under the acidification scenario. On the other hand, the warming scenario results in an increase of bacterial carbon leading to an enhanced respiration of the organic carbon, thereby, replenishing the DIC compartment, and reducing the accumulation of particulate organic matter (like TEP and POC) for export. The combined effect of warming and acidification scenario results in enhanced bacterial carbon, which could counteract the phytoplankton carbon increase by enhancing the microbial respiration of the organic carbon, associated with the lack of change in TEP, POC and DIC compartments. Together, these responses to the combined effect may present a positive feedback to rising atmospheric CO_2 . The dotted red square represents the surface layer ecosystem.

acidification could play antagonistically and most likely favor the microbial loop by fast recycling organic carbon, causing a simultaneous reduction of carbon export. Consequently, this may represent a positive feedback on the future atmosphere with release of CO₂ in shallow ecosystems like the Thau Lagoon (Fig. 6c).

It should be noted that future scenarios of climate change will include other stressors, in addition to warming and acidification, which may increase the complexity of plankton community responses (i.e. increased stratification and nutrient limitation). Thereby, the extent to which our results can be extrapolated to the real world must be taken with caution.

ACKNOWLEDGEMENTS

This project was supported by grants from the Natural Sciences and Engineering Research Council (NSERC) of Canada and the Québec-Océan grant to G.F. This study is part of the project " Global WARMing and ACIDification effect on the functioning of the Mediterranean plankton food WEB (WARMACIDWEB)" supported by the European Union Seventh Framework Program (FP7/2007-2013) under grant agreement n° 228224, MESOAQUA. The authors would like to thank Emilie Le Floc'h and David Parin at MEDIMEER (Sète) and Romain Pete at ECOSYM (Montpellier-Sète) for their skilled help provided prior and during the experiment and Stefano Cozzi at ISMAR (Italy) for laboratory analyses. This research is part of fulfillment of the requirements for a Ph.D degree (S. Annane) at the Université du Québec à Rimouski. This is a contribution to the research to MESOAQUA, ISMER and Québec-Océan.

CONCLUSION GÉNÉRALE

Nos travaux de recherche de cette thèse représentent une première contribution à la caractérisation des Particules Exopolymériques Transparentes (TEP) dans l'EMSL. L'étude de la variabilité saisonnière et de la distribution verticale des TEP dans l'EMSL nous a permis d'obtenir une vision globale de la formation et du devenir de ce type de particule dans cet écosystème, ainsi que de leur contribution au réservoir du carbone organique marin. Cette étude nous a également permis d'explorer certains facteurs environnementaux qui pourraient affecter la production et la distribution des TEPs (Annane et al. 2015). Ensuite, l'approche expérimentale en milieu contrôlé nous a permis de comprendre les réponses des TEP et de l'ensemble de la communauté planctonique quant aux modifications futures des changements globaux dans deux écosystèmes marins : les effets de l'acidification dans l'EMSL et ceux de l'acidification et du réchauffement en Méditerranée. L'ensemble des résultats nous a permis d'affiner notre compréhension de la dynamique du carbone organique dans chaque système et de mieux prévoir les conséquences de ces changements sur l'impact des TEP dans l'exportation du carbone organique en milieux sub-arctique et Méditerranéen.

Les TEP dans l'EMSL

Le monitoring de la station IML-4 du printemps à l'automne 2011 nous a permis de mettre en évidence que les TEP sont positivement corrélées à la biomasse phytoplanctonique dans les eaux de surface. En effet, l'accumulation des TEP a montré la même tendance que la succession des floraisons de phytoplancton. Ceci suggère que le phytoplancton était la principale source de ces particules (chapters 1, 2 et 3). Les diatomées centriques ont été le groupe dominant de ces floraisons phytoplanctoniques.

C'est notamment le cas de *Skeletonema costatum*, qui était l'espèce dominante pendant pratiquement toute la période échantillonnée, suivie de près par des espèces correspondant aux genres *Thalassiosira* sp. et *Chaetoceros* sp.

La distribution verticale a montré que la concentration des TEP était maximale en surface (0 à 10 m de profondeur), en diminuant fortement jusqu'à la profondeur de la pycnocline et ensuite plus progressivement jusqu'au fond, suivant ainsi la même distribution verticale que la biomasse autotrophique durant l'été et l'automne. Cependant, durant le printemps, de fortes valeurs de TEP ont été observées dans toute la colonne d'eau, en coïncidence avec la distribution verticale du POC. Durant cette période, l'EMSL est le principal collecteur d'apports continentaux du vaste bassin du Saint-Laurent. La majeure partie (~75 %) de la matière organique particulaire (POM) terrigène transportée par le fleuve Saint-Laurent est déposée sur le fond de l'EMSL (Lucotte et al. 1991), avec son lot de TEP d'origine allochtone telles que des exsudats microbiens et de macroalgues et facilitant ainsi l'agrégation et la formation de particules organiques réparties dans la colonne d'eau durant le printemps. Notre étude suggère que les TEP devraient contribuer à l'agrégation et l'exportation de particules organiques et inorganiques lourdes (d'avril à mai) principalement liées aux apports de particules allochtones dans l'EMSL.

Dans les conditions naturelles de l'EMSL, nous avons considéré certains facteurs biologiques et physico-chimiques du milieu qui ont été identifiés dans d'autres milieux estuariens comme pouvant influencer l'agrégation et la distribution des TEP. Par exemple, on note que le phytoplancton et les bactéries peuvent agir comme sources possibles des TEP, tandis que la salinité, le pH, les nutriments et la température pourraient contrôler l'agrégation ou la dissolution de ce type de particule. Cependant, mise à part l'influence du phytoplancton sur la variabilité des TEP en surface, aucune relation significative entre les TEP et les autres facteurs biologiques et physico-chimiques n'a été trouvée dans les autres couches d'eau.

Notre étude a également montré l'importance de la contribution des TEP au réservoir de carbone particulaire dans l'EMSL. Ces particules présentent la seconde fraction la plus

importante de carbone organique après celle du phytoplancton, soit 41 % contre 54 % en moyenne du réservoir du POC en surface. Ces TEP représentent donc une importante fraction du carbone organique dans cet écosystème, à ne pas négliger. Durant l'été et l'automne, nos données indiquent que la contribution des TEP au réservoir du POC a diminué avec la profondeur, représentant respectivement de 25 à 35 % du POC. On remarque que la contribution des TEP au réservoir de POC était particulièrement élevée au cours du printemps dans la couche intermédiaire froide et de fond (>94 %) probablement due à la fraction du carbone organique colloïdal qui contribue aux TEP en profondeur.

Effets de l'acidification

Nos travaux des chapitres 2 et 3 présentent les résultats de manipulation expérimentale pour tester les effets de l'acidification sur l'accumulation des TEP et la communauté planctonique dans deux écosystèmes : l'EMSL et la Méditerranée. Ces deux expériences ont montré des réponses contraires pour l'ensemble de chaque communauté face à l'effet d'acidification alors que les deux communautés étaient dominées par les diatomées. Néanmoins, il semble que la réponse globale de chaque écosystème à l'acidification soit une conséquence due à la réponse du phytoplancton aux changements de CO_2/pH . La communauté phytoplanctonique semble être le compartiment clé dans ces deux écosystèmes qui exercent un contrôle sur l'efficacité du pompage biologique et le devenir de la matière organique dans le cycle du carbone (Fig. 1). L'accumulation des TEP était clairement dépendante de la réponse de la communauté phytoplanctonique aux changements de CO_2/pH dans les deux écosystèmes. En effet, nous avons montré au chapitre 2 que le phytoplancton a été affecté négativement, particulièrement à faible $\text{pH} \leq 7,55$ qui est inclus dans la gamme de pH prévue pour la fin du siècle (7,9 - 7,3) dans l'EMSL. Cette communauté phytoplanctonique a montré tout particulièrement une baisse dans la dépletion de silice dans l'eau, d'accumulation de biomasse et des taux de croissance réduits à faible pH . Cela était probablement dû à l'effet indésirable de l'acidification sur le

pH interne des cellules et de leurs processus physiologiques. Dans cette étude, seules les cellules nanophytoplanctoniques et plus précisément la diatomée *Thalassiosira spp.*, semblent être moins sensibles au pH que les fractions du pico et microphytoplancton, ce qui suggère une réponse espèce-spécifique à l'acidification. On note que l'accumulation des TEP était principalement produite par cellules nanophytoplanctoniques pendant les phases de floraison et stationnaire mimant la dynamique de cette classe de taille. Ces effets négatifs du pH sur la fixation du carbone par le phytoplancton se sont traduits par une réduction de l'accumulation de biomasse et de DOC exsudé, ce qui a réduit la formation des TEP et du POC de 10 à 30 % et de 40 à 61 %, respectivement, pour les valeurs de pH $\leq 7,55$. Cela a eu pour conséquence de réduire l'accumulation de matière organique particulaire dans cette étude sous acidification (pH $\leq 7,55$). Par conséquent, nos résultats suggèrent que l'accumulation des TEP et POC pourrait être considérablement réduite à faible pH et ainsi limiter le flux de particules et la séquestration de carbone sous conditions d'acidification future dans l'EMSL.

Nos résultats du chapitre 3 ont montré un effet positif de l'augmentation du CO₂ sur la biomasse phytoplanctonique (+28 %) ainsi qu'une assimilation stimulée du DIC (+39 %) par le phytoplancton sous des conditions d'acidification (pH $\sim 7.73 - 7.8$) prévue à la fin du siècle en Méditerranée. L'excès de carbone fixé par le phytoplancton s'est traduit par une transformation rapide du DOC exsudé en colloïdes et TEP par un processus d'agrégation sous excès de CO₂. Dans notre étude, l'agrégation de ces composés carbonés a induit une augmentation des TEP de 47 % ainsi qu'une augmentation de POC de 12 % sous acidification. Affectant ainsi l'abondance totale des particules et l'adhérence de l'ensemble des particules, ce type de processus pourrait jouer un rôle important dans la stimulation de l'exportation de carbone dans des conditions de $p\text{CO}_2$ élevée. Nos résultats ont également démontré la surconsommation de carbone sous $p\text{CO}_2$ élevée avec un ratio C/N élevé ($\sim 18,25$) par rapport au ratio de Redfield (C/N $\sim 6,625$). Par conséquent, nos résultats suggèrent que la surconsommation observée de DIC par le phytoplancton a entraîné une augmentation des TEP et du POC, ce qui conduit à une augmentation de l'accumulation de

matière organique particulaire facilitant potentiellement la sédimentation et les flux de particules carbonées dans des conditions de $p\text{CO}_2$ élevées en Méditerranée.

Nos résultats des chapitres 2 et 3 ont montré une diminution des proportions de DOC par rapport au POC surtout dans la phase de post-floraison dans les conditions d'acidification. Ceci explique l'augmentation des concentrations des TEP à la fin des deux expériences et est probablement dû à l'agrégation de DOC fraîchement produit et rapidement partitionné de la portion du carbone dissous dans le réservoir de POC par l'agrégation colloïdale et de TEP, empêchant l'accumulation des exsudats en excès dans la fraction dissoute. Par conséquent, nos résultats suggèrent un déplacement de la portion du carbone dissous dans le réservoir de POC par l'agrégation des TEP sous acidification.

De plus, nos travaux ont montré que l'acidification avait un effet négatif sur la biomasse bactérienne. Il semble que la biomasse bactérienne était régulée par l'activité virale et le broutage des flagellés hétérotrophes, ce qui explique la diminution des bactéries dans le traitement à faible pH. Cela suggère que les bactéries étaient plus probablement indirectement affectées par les faibles pH. En effet, les hétérotrophes ont été stimulés par les faibles pH présentant une augmentation de 43 %. Dans ce cas, cet effet négatif sur les bactéries a très probablement permis l'agrégation des précurseurs polysaccharidiques présents en TEP particuliers en limitant le potentiel de dégradation (réduisant l'activité enzymatique) de la communauté microbienne. Par conséquent, les faibles biomasses bactériennes semblent présenter moins d'impacts sur la dégradation des TEP dans les deux écosystèmes.

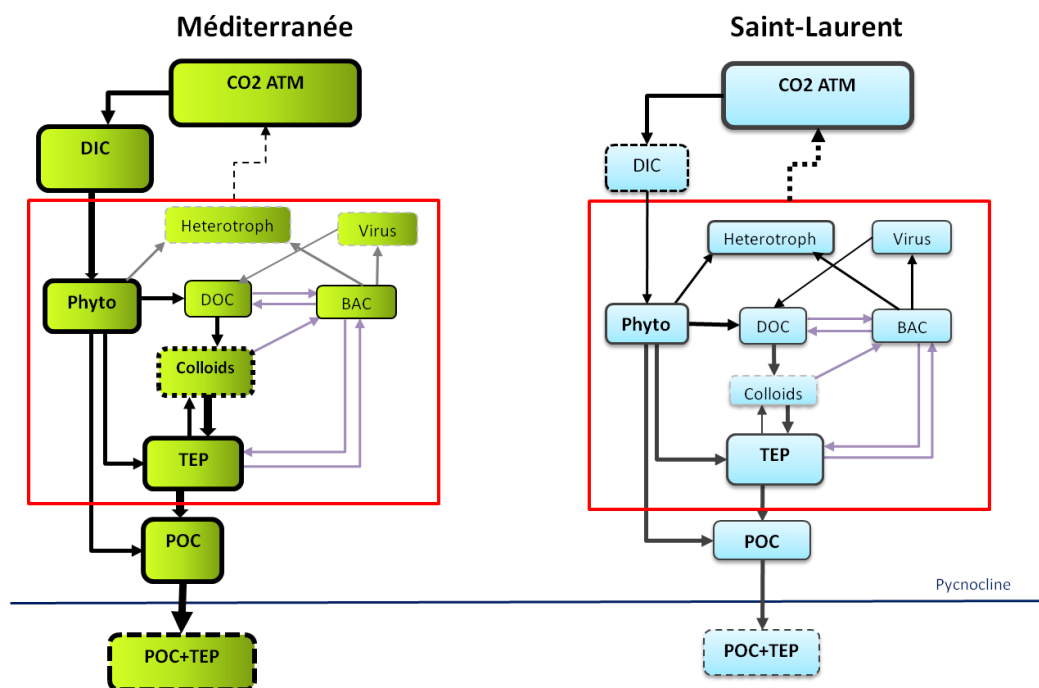


Figure 1: Diagramme conceptuel illustrant la réponse de l'écosystème de la Méditerranée (à gauche) et du Saint-Laurent (à droite) et la voie du carbone sous des conditions d'acidification. Les flèches représentent des processus d'absorption, exsudation, assimilation, agrégation, reminéralisation et sédimentation. L'effet positif dans chaque traitement est en noir gras et ceux négatifs où ne présentant aucun effet au changement de CO_2 sont en gris. Les compartiments non échantillonnés sont en ligne pointillée. Le carré rouge représente l'écosystème de la couche de surface. CO_2 atmosphérique (CO_2 ATM), carbone inorganique dissous (DIC), phytoplancton (Phyto), hétérotrophes (Heterotroph), carbone organique dissous (DOC), bactéries (BAC), carbone organique colloïdal (Colloids), particules exopolymériques transparentes (TEP) et carbone organique particulaire (POC).

Ainsi les résultats des chapitres 2 et 3 montrant la présence d'une réponse espèce-spécifique à l'acidification suggèrent : (a) qu'il existe une gamme de CO_2/pH pour laquelle la croissance de la communauté phytoplanctonique dominée par les diatomées est optimale et positive (jusqu'à $\text{pH} \sim 7,7$), comme pour le cas de la communauté phytoplanctonique de Méditerranée, et (b) qu'une diminution supplémentaire du pH (ex. $\text{pH} \leq 7,55$) pourrait entraîner des effets adverses sur la croissance et la physiologie des cellules. Dinauer &

Mucci (2017) ont montré tout récemment que l'EMSL présente un flux de CO₂ air-mer négatif ou positif entre -21,9 et 15,1 mmol m⁻² d⁻¹, selon la période de floraison, car le bilan est contrôlé par le processus de photosynthèse et que dans l'ensemble l'estuaire du Saint-Laurent est une source faible de CO₂ vers l'atmosphère. Par conséquent, l'altération de la pompe biologique par acidification pourrait avoir des conséquences sur le bilan du flux CO₂ air-mer de cet estuaire. Ceci pourrait avoir un impact sur les flux verticaux futurs de la matière organique avec des conséquences pour la productivité de l'écosystème et le pompage biologique du CO₂ atmosphérique.

Effets de l'acidification et de la température

Nos données sur les effets combinés du réchauffement et de l'acidification ont montré une stimulation de la biomasse phytoplanctonique avec une augmentation de 32 % suite à la hausse de la température et de la réduction du pH, par rapport au contrôle (Fig. 2). Dans notre cas, ces deux facteurs ont joué de façon synergique sur la communauté phytoplanctonique pour l'utilisation de l'excès de carbone en accumulant la biomasse phytoplanctonique. Cependant, aucun changement n'a été observé dans l'utilisation nette du DIC. De même, aucun changement n'a été enregistré pour l'accumulation des TEP et de POC ainsi qu'aucune variation de DOC n'a été remarquée entre les traitements. Par conséquent, nos résultats suggèrent que ces deux facteurs jouent un rôle antagoniste sur la production des TEP et l'accumulation de matière organique dans un futur scénario de changement climatique en Méditerranée.

D'un autre côté, nos travaux présentés dans le chapitre 3 ont montré une stimulation de la biomasse bactérienne beaucoup plus élevée dans le scénario combiné de réchauffement et d'acidification que sous des conditions de réchauffement seul (42 % contre 7 %, respectivement). Cet effet du réchauffement sur l'augmentation de la biomasse bactérienne et stimule la respiration microbienne du carbone organique pourrait expliquer le

réapprovisionnement du DIC, ce qui pourrait ainsi contrecarrer l'effet de l'acidification sur l'augmentation de la biomasse phytoplanctonique par surconsommation de DIC. Cela suggère également que les TEP étaient probablement utilisées comme un substrat adéquat par les bactéries hétérotrophes limitant l'accumulation de ces particules. Dans ce scénario, la mesure dans laquelle les TEP pourraient se former et s'accumuler dépendrait probablement du taux de production des TEP par le phytoplancton et de l'interaction avec la reminéralisation bactérienne dans un futur océan. De telles conditions ont le potentiel de stimuler la production bactérienne et d'améliorer la respiration microbienne et le recyclage, avec des conséquences potentielles sur le devenir de la matière organique dans l'océan.

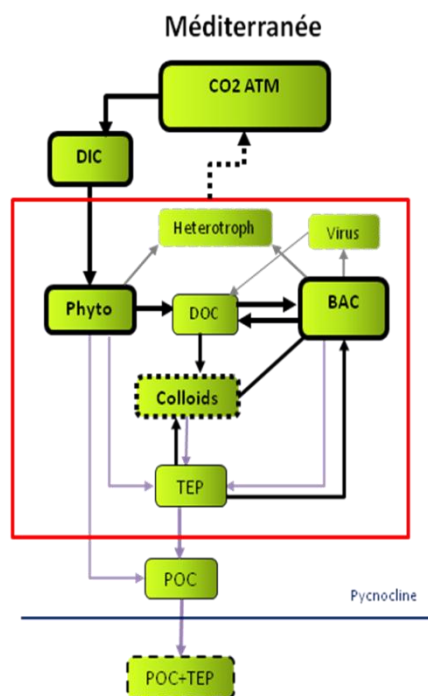


Figure 2: Diagramme conceptuel illustrant la réponse de l'écosystème de Méditerranée et la voie du carbone sous des conditions de réchauffement et d'acidification. Le réchauffement a pour effet d'augmenter la biomasse bactérienne et stimule la respiration microbienne du carbone organique réapprovisionnant ainsi le compartiment du DIC, ce qui pourrait contrecarrer l'effet de l'acidification sur l'augmentation de la biomasse phytoplanctonique par surconsommation de DIC, associé à l'absence de changements dans les compartiments de TEP, POC et DIC. Ensemble, ces réponses à l'effet combiné de réchauffement et d'acidification peuvent présenter une rétroaction positive à la hausse du CO₂ atmosphérique. Les flèches représentent des processus d'absorption, d'exsudation,

d'assimilation, d'agrégation, de reminéralisation et de sédimentation. L'effet positif dans chaque traitement est en noir gras et ceux négatifs où ne présentant aucun effet de changement combiné de CO₂ et température sont en gris. Le carré rouge représente l'écosystème de la couche de surface. CO₂ atmosphérique (CO₂ ATM), carbone inorganique dissous (DIC), phytoplancton (Phyto), hétérotrophes (Heterotroph), carbone organique dissous (COD), bactéries (BAC), carbone organique colloïdal (Colloids), particules exopolymériques transparentes (TEP) et carbone organique particulaire (POC).

Dans le contexte de changements globaux, le réchauffement et l'acidification des océans pourraient jouer de manière antagoniste et favoriseront probablement la boucle microbienne (augmentation ~ 106,5 µg C L⁻¹) par rapport à la production de biomasse (augmentation ~ 58 µg C L⁻¹) par le recyclage rapide du carbone organique, potentiellement entraînant une réduction des exportations de carbone. Par conséquent, cela peut représenter une rétroaction positive sur l'atmosphère future avec la libération de CO₂ dans les écosystèmes peu profonds. Cependant, les scénarios potentiels incluront d'autres facteurs de stress, en plus du réchauffement et de l'acidification, qui pourraient accroître la complexité des réponses de la communauté planctonique (c'est-à-dire une stratification accrue et une limitation des nutriments).

Avantages et limitation des systèmes expérimentaux utilisés

L'un des objectifs de cette thèse était d'utiliser des systèmes expérimentaux le plus proches possible de chaque écosystème. Afin de comprendre et prévoir les conséquences de l'acidification et du réchauffement au niveau de la communauté et de l'écosystème, il fallait tout d'abord prendre en considération les caractéristiques de chaque écosystème (conditions du milieu, variabilité naturelle du pH, accessibilité au milieu), les facteurs de stress à étudier (acidification et/ou réchauffement), ainsi que de considérer les difficultés techniques et budgétaires (dimensions, nombre d'unités expérimentales, réplicats par traitement et logistique impliquée). Dans le chapitre 2, nous avons utilisé des microcosmes

de grand volume en suivant avec un modèle expérimental cinétique. Il consistait en un gradient des niveaux de perturbation de pH par rapport à un microcosme de référence, sachant que les communautés phytoplanctoniques des écosystèmes côtiers et estuariens tels que l'EMSL sont soumises à une large variation de pH entre 7,4 à 9,2 (Hansen 2002, Middelboe & Hansen 2007). Le choix d'un système expérimental en gradient de pH nous a permis non seulement de suivre la communauté planctonique lors de la diminution des valeurs de l'intervalle de pH actuel (pH ~7,8 à 8,3) à celui prévu pour 2100 (pH ~7,4 à 7,9), mais aussi d'étudier la tendance de chaque compartiment à la diminution de pH. Cela nous a également permis de déterminer (pH ~7,55) le niveau à partir duquel le pH devient un facteur de stress défavorable pour la communauté phytoplanctonique et par conséquent pour le fonctionnement de l'écosystème planctonique.

Dans le chapitre 3, le système expérimental utilisé est un système de mésocosmes pélagiques *in situ* qui fait partie du réseau MESOAQUA, financé par le Septième Programme-Cadre de l'Union Européenne. Ce système de mésocosmes a été choisi pour son utilisation dans des écosystèmes côtiers et pélagiques avec de faibles variations de pH contrairement aux écosystèmes estuariens. Ces mésocosmes avaient l'avantage de comprendre 3 réplicats pour chaque traitement, ce qui permet une analyse statistique robuste (ANOVA à mesures répétées). Ceci nous a permis d'utiliser deux facteurs de stress (acidification et réchauffement) combinés et séparés afin de bien comprendre l'effet de chaque facteur et leur interaction sur la biologie et l'écosystème. De plus, le grand volume de chaque mésocosme (2300 L) a permis également le prélèvement d'un grand nombre d'échantillons journaliers et ainsi de réunir une grande quantité d'information à l'aide d'une équipe scientifique multidisciplinaire, allant de la biologie cellulaire, à la physiologie, l'écologie marine et la biogéochimie marine, et composée de chercheurs provenant de plusieurs pays et institutions. La combinaison d'un large éventail de disciplines dans une seule étude offre l'occasion unique d'étudier les interactions de la dynamique des écosystèmes et de la biogéochimie et suivre les conséquences des sensibilités à l'acidification et au réchauffement des océans à travers ce système fermé (Riebesell et al. 2010).

Une des limites dans ces deux systèmes est la durée de l'expérience. En effet, la durée moyenne pour ce genre d'expérience est entre 10 jours à 1 mois considérant les phases de développement et sénescence du phytoplancton et des brouteurs. De plus, en raison de l'influence grandissante de l'effet parois (de l'anglais «wall effect») et de la dérive graduelle des communautés isolées du système naturel après quelques jours, les réponses des organismes et la chaîne trophique associée dans les études de mésocosmes peuvent ne pas être adéquatement représentatives du milieu naturel (voir Belzile et al. 2006). D'autre part, ce qui n'est pas encore pris en compte dans ces expériences dues aux difficultés techniques et financières, c'est la possible adaptation à long terme ou non aux facteurs de stress. De plus, l'augmentation des phosphates qui a été observée au début des deux expériences est probablement le résultat de mortalité ou lyse cellulaire et d'acclimatation au confinement des mésocosmes quel que soit le volume du mésocosme, ceci est un facteur à considérer dans le futur surtout dans le cas d'expériences étudiant les nutriments comme facteur de stress. Cependant, ces systèmes expérimentaux mimant l'évolution du milieu naturel restent pour le moment le meilleur outil expérimental de perturbation pour explorer les conséquences à long terme des changements climatiques.

Perspectives de recherche

En se basant sur ces premiers résultats de mésocosmes en Méditerranée, il serait intéressant et important d'explorer des futurs changements sur l'écosystème du Saint-Laurent à l'aide de mésocosmes afin d'évaluer pleinement leurs conséquences. En effet, il se pourrait que la réponse de la communauté et l'allocation du carbone soient quelque peu différentes du résultat de l'effet de l'acidification seule. Ces deux facteurs de stress pourraient agir de façon additive ou antagoniste. Jusqu'à présent, le compartiment des bactéries dans les chapitres 1 et 2 ne semble pas influencer grandement la dégradation des TEP et la contribution au réservoir de carbone par leur faible densité ou les effets indirects de l'acidification. Cependant, un réchauffement des eaux de fond a déjà causé une

augmentation des taux de respiration entre 10 et 32 % dans tout le système du Saint-Laurent et a contribué à l'établissement des conditions hypoxiques sévères dans les fonds de l'EMSL (Genovesi et al. 2011). Par contre, l'augmentation de la température pourrait prolonger la période libre de glace et ainsi permettre des floraisons phytoplanctoniques plus tôt au printemps et plus tard à l'automne (Galbraith et al. 2012). Cela nous suggère qu'une association de ces deux facteurs de stress (réchauffement et acidification) pourrait mener à un tout autre bilan de carbone dans cet écosystème estuarien et sa rétroaction sur le flux de CO₂ atmosphérique.

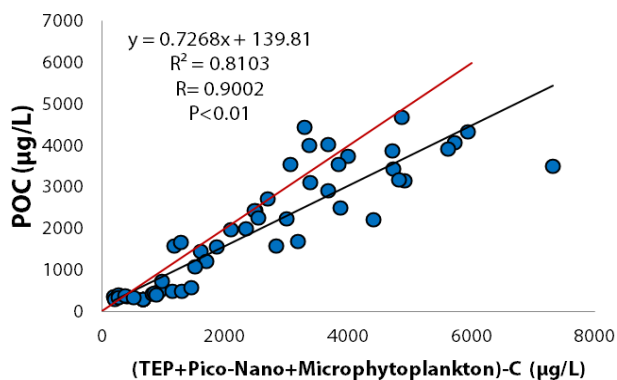
De plus, l'une des difficultés dans notre travail de recherche était d'avoir accès à des références concernant la variabilité du pH dans l'EMSL. En effet, il existe très peu de données historiques sur le pH et le CO₂ de l'eau de mer dans l'estuaire et le golfe du Saint-Laurent. Il serait donc souhaitable de mettre en place un programme de monitoring du pH, CO₂ et température de surface au niveau de la région côtière. En effet, le suivi à long terme du pH des eaux de surface et principalement celui de l'EMSL est indispensable dans la problématique actuelle et future de l'effet de l'acidification et du réchauffement climatique sur la structure et la composition des communautés planctoniques, ainsi que sur la production et le devenir du carbone organique de surface. On estime que ces effets seront de plus en plus notables dans les écosystèmes côtiers et estuariens. L'EMSL est plus vulnérable aux effets de l'acidification, car il reçoit au printemps des eaux de ruissellement d'eau douce et des lessivages acides, ainsi qu'une remontée d'eau profonde hypoxique et acide au niveau du seuil en amont de l'EMSL. De surcroît, c'est une région où la production primaire et de zooplancton est élevée et c'est également une zone d'intérêt pour les mammifères marins. Ceci rend le suivi à long terme de cette zone nécessaire à plus d'un titre.

Dans l'optique de mieux comprendre la contribution des TEP à l'hypoxie et l'acidification des eaux de fonds de l'EMSL, il serait nécessaire d'examiner la reminéralisation de cette matière et les taux de respiration sous les conditions actuel et futur des changements climatiques.

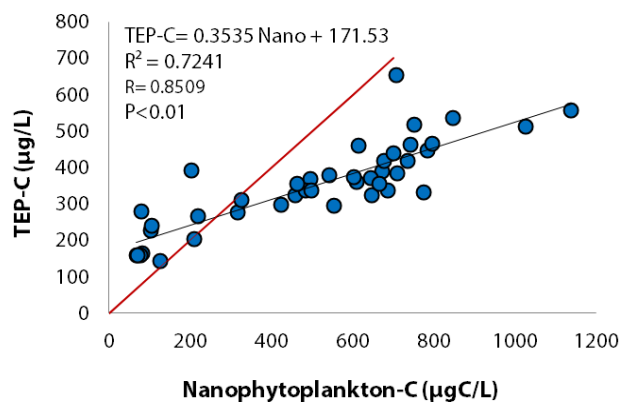
De plus, afin de mieux caractériser les TEP dans le Saint-Laurent, il serait nécessaire de les étudier en termes de structure de taille de particules (en utilisant la méthode microscopique), leur composition chimique, ainsi que leur distribution spatiale et temporelle et leur contribution à l'exportation et/ou à l'advection du POC dans l'estuaire et le golfe du Saint-Laurent.

D'autre part, l'une de nos perspectives de recherche est de documenter assez la formation et la distribution des TEP dans le Saint-Laurent afin de les inclure avec le processus d'agrégation dans les futures paramétrisations des études de modélisation biogéochimiques des écosystèmes.

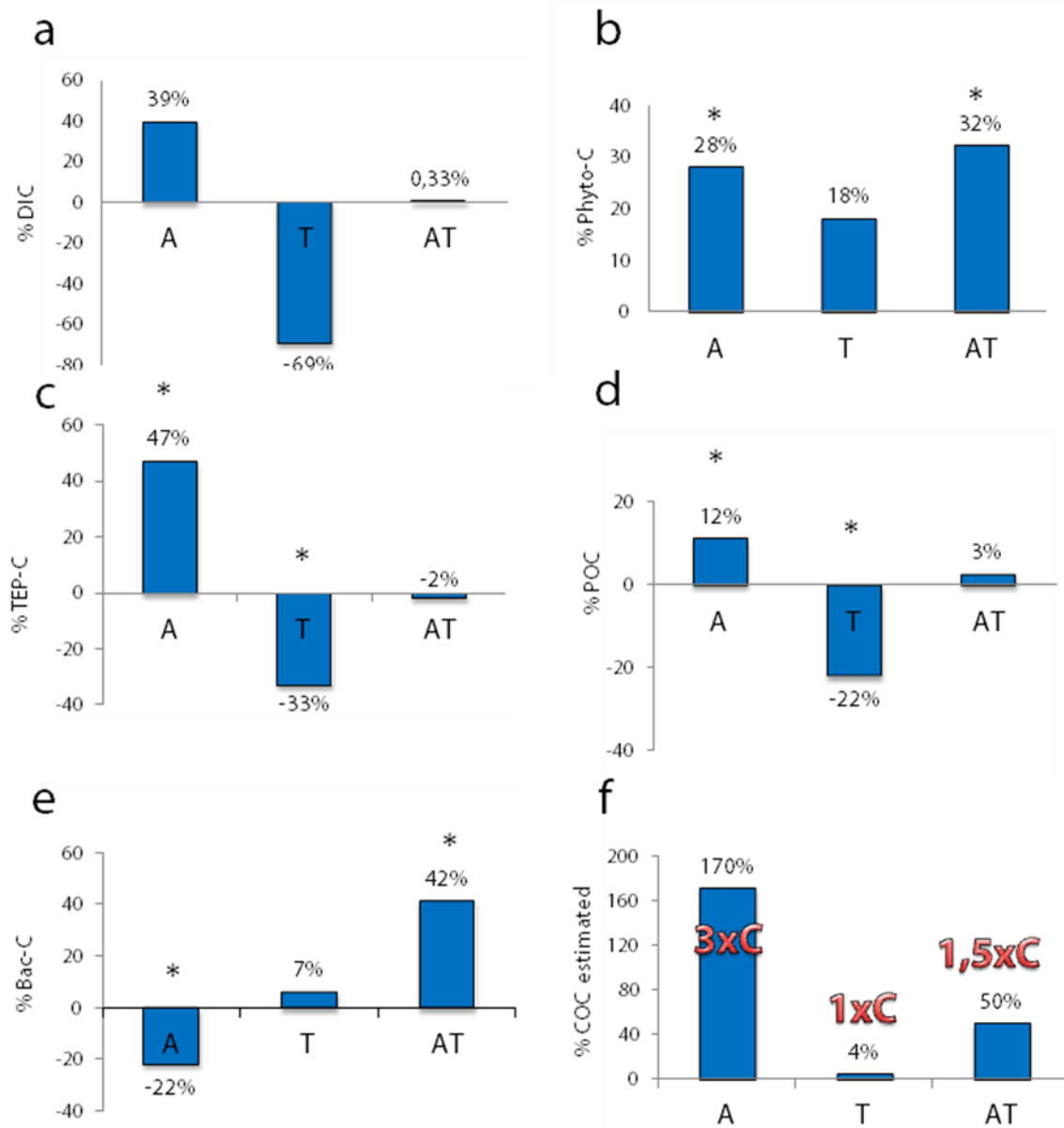
ANNEXES



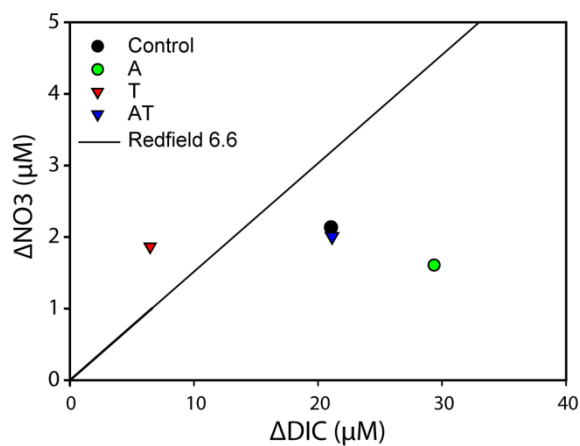
ANNEX 1.1: Summary of the Relationship between particulate organic carbon (POC) and the sum of transparent exopolimeric particles carbon (TEP-C) and pico-, nano- and microphytoplankton carbon in all microcosms. The black line represents the regression line and the red line represents 1:1 relation line



ANNEX 1.2: Relationship between Nanophytoplankton carbon and transparent exopolimeric particles carbon (TEP-C) in all microcosms. The black line represents the regression line and the red line represents 1:1 relation line



ANNEX 2.1: Summary of the treatment effect for each carbon compartment relative to the control treatment. a) % of DIC uptake, b) % of phytoplankton carbon, c) % of TEP carbon, d) % of POC, e) % of bacterial carbon, f) % of estimated Colloidal organic carbon. This latter represents 3 folds relative to the control for Acidified treatment (A) and represent 1 and 1.5 fold for high Temperature (T) and Acidified and high Temperature (AT) treatment. (* P ≤ 0.05).



ANNEX 2.2: Carbon overconsumption. Ratio ΔDIC to ΔNO_3 drawdown for Control, actual temperature and $p\text{CO}_2$ (black); high $p\text{CO}_2$, A (green); high temperature, T (red) and high $p\text{CO}_2$ and temperature, AT (blue). The black line represents Redfield, C: N ratio of 6.6.

RÉFÉRENCES BIBLIOGRAPHIQUES

- ABERLE, N, SCHULZ KG, STUHR A, MALZAHN AM, LUDWIG A, RIEBESELL U. 2013. High tolerance of microzooplankton to ocean acidification in an Arctic coastal plankton community. *Biogeosciences* 10:1471–1481
- ALDERKAMP, A-C, VAN RIJSSEL M, , BOLHUIS H. 2007. Characterization of marine bacteria and the activity of their enzyme systems involved in degradation of the algal storage glucan laminarin. *FEMS Microbiol Ecology* 59:108–117
- ALLDREDGE, AL, CROCKER KM. 1995. Why do sinking mucilage aggregates accumulate in the water column? *Science of The Total Environment* 165:15–22
- ALLDREDGE, AL, GOTSCHALK CC. 1990. The relative contribution of marine snow of different origins to biological processes in coastal waters. *Continental Shelf Research* 10:41–58
- ALLDREDGE, AL, PASSOW U, LOGAN BE. 1993. The abundance and significance of a class of large transparent organic particles in the ocean. *Deep Sea Research Part I: Oceanographic Research Papers* 40:1131–1140
- ALLDREDGE, AL, SILVER MW. 1988. Characteristics, dynamics and significance of marine snow. *Progress in Oceanography* 20:41–82
- ALUWIHARE, LI, REPETA DJ. 1999. A comparison of the chemical characteristics of oceanic DOM and extracellular DOM produced by marine algae. *Marine Ecology Progress Series* 186:105–117
- ANNANE, S, ST-AMAND L, STARR M, PELLETIER E, FERREYRA G. 2015. Contribution of transparent exopolymeric particles (TEP) to estuarine particulate organic carbon pool. *Marine Ecology Progress Series* 529:17–34
- ARNOUS, M-B, COURCOL N, CARRIAS J-F. 2010. The significance of transparent exopolymeric particles in the vertical distribution of bacteria and heterotrophic nanoflagellates in Lake Pavin. *Aquatic Sciences* 72:245–253
- ARRIGO, KR. 2007. Carbon cycle: Marine manipulations. *Nature Reports Climate Change*:100–101
- AZAM, F. 1998. Microbial Control of Oceanic Carbon Flux: The Plot Thickens. *Science* 280 (5364):694-696

- AZAM, F, FENCHEL T, FIELD JG, GRAY JS, MEYER-REIL LA, THINGSTAD F. 1983. The ecological role of water-column microbes in the sea. *Marine Ecology Progress Series* 10:257–263
- AZAM, F, MALFATTI F. 2007. Microbial structuring of marine ecosystems. *Nature Reviews Microbiology* 5:782–791
- AZAM, F, SMITH DC, STEWARD GF, HAGSTRÖM Å. 1994. Bacteria-organic matter coupling and its significance for oceanic carbon cycling. *Microbiol Ecology* 28:167–179
- BAR-ZEEV, E, BERMAN T, RAHAV E, DISHON G, HERUT B, BERMAN-FRANK I. 2011. Transparent exopolymer particle (TEP) dynamics in the eastern Mediterranean Sea. *Marine Ecology Progress Series* 431:107–118
- BAR-ZEEV, E, BERMAN-FRANK I, STAMBLER N, VÁZQUEZ DOMÍNGUEZ E, ZOHARY T, CAPUZZO E, MEEDER E, SUGGETT D, ILUZ D, DISHON G, BERMAN T. 2009a. Transparent exopolymer particles (TEP) link phytoplankton and bacterial production in the Gulf of Aqaba. *Aquatic Microbiol Ecology* 56:217–225
- BEARDALL, J, RAVEN JA. 2004. The potential effects of global climate change on microalgal photosynthesis, growth and ecology. *Phycologia* 43(1):26–40
- BEAUVAIS, S, PEDROTTI ML, EGGE J, IVERSEN K, MARRASÉ C. 2006. Effects of turbulence on TEP dynamics under contrasting nutrient conditions: implications for aggregation and sedimentation processes. *Marine Ecology Progress Series* 323:47–57
- BEAUVAIS, S, PEDROTTI ML, VILLA E, LEMÉE R. 2003. Transparent exopolymer particle (TEP) dynamics in relation to trophic and hydrological conditions in the NW Mediterranean Sea. *Marine Ecology Progress Series* 262:97–109
- BELLERBY, RGJ, SCHULZ K, RIEBESELL U, NEILL C, NONDAL G, JOHANNESSEN T, BROWN KR. 2008. Marine ecosystem community carbon and nutrient uptake stoichiometry under varying ocean acidification during the PeECE III experiment. *Biogeosciences (BG)* 5:1517–1527
- BELZILE, N, LEBEL J. 1983. Hydrochemistry of the rimouski river, a tributary to the St. Lawrence estuary. *Marine Chemistry* 12 (2-3):231

- BELZILE, C, BRUGEL S, NOZAIS C, GRATTON Y, DEMERS S. 2008. Variations of the abundance and nucleic acid content of heterotrophic bacteria in Beaufort Shelf waters during winter and spring. *Journal of Marine Systems* 74:946–956
- BELZILE, C, DEMERS S, FERREYRA GA, SCHLOSS I, NOZAIS C, LACOSTE K, MOSTAJIR B, ROY S, GOSSELIN M, PELLETIER E, GIANESELLA SMF, VERNET M. 2006. UV Effects on Marine Planktonic Food Webs: A Synthesis of Results from Mesocosm Studies. *Photochemistry and Photobiology* 82:850–856
- BÉRARD-TERRIAULT, L, POULIN M, BOSSÉ L. 1999. Guide d'identification du phytoplancton marin de l'estuaire et du golfe du Saint-Laurent: incluant également certains protozoaires. Publication spéciale canadienne des sciences halieutiques et aquatiques 128. 387 p.
- BERGE, T, DAUGBJERG N, BALLING ANDERSEN B, HANSEN P. 2010. Effect of lowered pH on marine phytoplankton growth rates. *Marine Ecology Progress Series* 416:79–91
- BHASKAR, PV, BHOSLE NB. 2005. Microbial extracellular polymeric substances in marine biogeochemical processes. *Current Science* 88:45–53
- BHASKAR, PV, BHOSLE NB. 2006. Dynamics of transparent exopolymeric particles (TEP) and particle-associated carbohydrates in the Dona Paula bay, west coast of India. *Journal of Earth System Science* 115:403–413
- BHASKAR, PV, BHOSLE NB. 2008. Bacterial production, glucosidase activity and particle-associated carbohydrates in Dona Paula bay, west coast of India. *Estuarine, Coastal and Shelf Science* 80:413–424
- BIERMANN, A, ENGEL A, RIEBESELL U. 2014. Changes in organic matter cycling in of plankton community exposed to warming under different light intensities. *Journal of Plankton Research* 36:658–671
- BORGES, AV, DELILLE B, FRANKIGNOULLE M. 2005. Budgeting sinks and sources of CO₂ in the coastal ocean: Diversity of ecosystems counts. *Geophysical Research Letters* 32:L14601
- BORNE DE GRANDPRÉ, C, EL-SABH M. 1980. Etude de la circulation verticale dans l'estuaire du St-Laurent au moyen de la modélisation mathématique. *Atmosphere Ocean*, 18:304–321.
- BOURDIN, G, GAZEAU F, KERROS M-E, MARRO S, PEDROTTI ML. 2016. Dynamics of transparent exopolymeric particles and their precursors during a

- mesocosm experiment: Impact of ocean acidification. *Estuarine, Coastal and Shelf Science* 186:112-124
- BOURGAULT, D, CYR F, GALBRAITH PS, PELLETIER E. 2012. Relative importance of pelagic and sediment respiration in causing hypoxia in a deep estuary. *Journal of Geophysical Research* 117:C08033
- BOYD, PW, DONEY SC. 2002. Modelling regional responses by marine pelagic ecosystems to global climate change. *Geophysical Research Letters* 29:53-1
- BOYD, PW, STRZEPEK R, FU F, HUTCHINS DA. 2010. Environmental control of open-ocean phytoplankton groups: Now and in the future. *Limnology and Oceanography* 55(3):1353-1376
- BRATBAK, G, THINGSTAD TF. 1985. Phytoplankton-bacteria interactions: an apparent paradox? Analysis of a model system with both competition and commensalism. *Marine ecology progress series* 25:23-30
- BRUSSAARD, CPD. 2004. Optimization of Procedures for Counting Viruses by Flow Cytometry. *Applied and Environmental Microbiology* 70:1506-1513
- BRUSSAARD, CPD, MARI X, BLEIJSWIJK JDLV, VELDHUIS MJW. 2005. A mesocosm study of *Phaeocystis globosa* (Prymnesiophyceae) population dynamics. *Harmful Algae* 4:875-893
- BRUSSAARD, CPD, NOORDELOOS AAM, WITTE H, COLLENTEUR MCJ, SCHULZ K, LUDWIG A, RIEBESELL U. 2013. Arctic microbial community dynamics influenced by elevated CO₂ levels. *Biogeosciences* 10:719-731
- BURKHARDT, S, RIEBESELL U. 1997. CO₂ availability affects elemental composition (C: N: P) of the marine diatom *Skeletonema costatum*. *Marine Ecology Progress Series* 155:67-76
- BURNHAM, K, ANDERSON D. 2002. Model selection and multimodel inference: A practical information-theoretic approach, 2 nd ed. ISBN 0-387-95364-7
- BURNHAM, KP, ANDERSON DR, HUYVAERT KP. 2011. AIC model selection and multimodel inference in behavioral ecology: some background, observations, and comparisons. *Behavioral Ecology and Sociobiology* 65:23-35
- CAI, W-J. 2011 Estuarine and Coastal Ocean Carbon Paradox: CO₂ Sinks or Sites of Terrestrial Carbon Incineration? *Annual Review of Marine Science* 3:123-145

- CALDEIRA, K, WICKETT ME. 2003. Oceanography: Anthropogenic carbon and ocean pH. *Nature* 425:365–365
- CALDEIRA, K, WICKETT ME. 2005. Ocean model predictions of chemistry changes from carbon dioxide emissions to the atmosphere and ocean. *Journal of Geophysical Research*
- CAPONE, DG, HUTCHINS DA. 2013. Microbial biogeochemistry of coastal upwelling regimes in a changing ocean. *Nature Geoscience* 6:711–717
- CLAYTON, TD, BYRNE RH. 1993. Spectrophotometric seawater pH measurements: total hydrogen ion concentration scale calibration of m-cresol purple and at-sea results. *Deep Sea Research Part I: Oceanographic Research Papers* 40:2115–2129
- CHEN, CY, DURBIN G. 1994. Effects of pH on the growth and carbon uptake of marine phytoplankton. *Marine Ecology Progress Series* 109:83-94
- CHIN, WC, ORELLANA MV, QUESADA I, VERDUGO P. 2004. Secretion in unicellular marine phytoplankton: demonstration of regulated exocytosis in *Phaeocystis globosa*. *Plant and cell physiology* 45:535
- CHIN, WC, ORELLANA MV, VERDUGO P. 1998. Spontaneous assembly of marine dissolved organic matter into polymer gels. *Nature* 391:568–571
- CLAQUIN, P, PROBERT I, LEFEBVRE S, VERON B. 2008. Effects of temperature on photosynthetic parameters and TEP production in eight species of marine microalgae. *Aquatic Microbial Ecology* 51:1–11
- CLAYTON, TD, BYRNE RH. 1993. Spectrophotometric seawater pH measurements: total hydrogen ion concentration scale calibration of m-cresol purple and at-sea results. *Deep Sea Research Part I: Oceanographic Research Papers* 40:2115–2129
- DECHO, AW. 1990. Microbial exopolymer secretions in ocean environments: their role in food webs and marine processes. *Oceanography and Marine Biology* 28:73-154
- DELILLE, B, HARLAY J, ZONDERVAN I, JACQUET S, CHOU L, WOLLAST R, BELLERBY RGJ, FRANKIGNOULLE M, BORGES AV, RIEBESELL U, GATTUSO J-P. 2005. Response of primary production and calcification to changes of $p\text{CO}_2$ during experimental blooms of the coccolithophorid *Emiliania huxleyi*. *Global Biogeochemical Cycles* 19, GB2023
- DE VICENTE, I, ORTEGA-RETUERTA E, MAZUECOS IP, PACE ML, COLE JJ, RECHE I. 2010. Variation in transparent exopolymer particles in relation to

biological and chemical factors in two contrasting lake districts. *Aquatic Sciences* 72:443–453

- DE VICENTE, I, ORTEGA-RETUERTA E, ROMERA O, MORALES-BAQUERO R, RECHE I. 2009. Contribution of transparent exopolymer particles to carbon sinking flux in an oligotrophic reservoir. *Biogeochemistry* 96:13–23
- DICKSON, AG. 1990. Standard potential of the reaction: $\text{AgCl(s)} + 1/2\text{H}_2(\text{g}) = \text{Ag(s)} + \text{HCl(aq)}$, and the standard acidity constant of the ion HSO_4^- in synthetic sea water from 273.15 to 318.15 K. *The Journal of Chemical Thermodynamics* 22 (2): 113-127
- DICKSON, AG, MILLERO FJ. 1987. A comparison of the equilibrium constants for the dissociation of carbonic acid in seawater media. *Deep Sea Research Part I* 34 (10): 1733-1743
- DICKSON, AG, SABINE CL, CHRISTIAN JR. 2007. Guide to Best Practices for Ocean CO_2 Measurements, PICES Special Publication 3: 191 pp.
- DINAUER, A, MUCCI A. 2017. Spatial variability of surface-water $p\text{CO}_2$ gas exchange in the world's largest semi-enclosed estuarine system: St. Lawrence Estuary (Canada). *Biogeosciences* 14, 3221–3237,
- DUARTE, CM, HENDRIKS IE, MOORE TS, OLSEN YS, STECKBAUER A, RAMAJO L, CARSTENSEN J, TROTTER JA, MCCULLOCH M. 2013. Is Ocean Acidification an Open-Ocean Syndrome? Understanding Anthropogenic Impacts on Seawater pH.. *Estuaries and Coasts* 36:221–236
- DONEY, SC. 2006. Oceanography: Plankton in a warmer world. *Nature* 444:695–696
- DONEY, SC, FABRY VJ, FEELY RA, KLEYPAS JA. 2009. Ocean Acidification: The Other CO_2 Problem. *Annual Review of Marine Science* 1:169–192
- DUFOUR, R, OUELLET P. 2007. Estuary and Gulf of St. Lawrence marine ecosystem overview and assessment report. Canadian Technical Report Fishery and Aquatic Sciences. 2744E: vii + 112 p.
- DUBELAAR, GBJ, GEERDERS PJF, JONKER RR. 2004. High frequency monitoring reveals phytoplankton dynamics. *Journal of Environmental Monitoring* 6(12):946-952
- EL-SABH, M. 1988. Physical oceanography of the St. Lawrence Estuary. In KJERFVE, B., editor, *Hydrodynamics of estuaries*, volume Vol. II, pages 61–78. CRC Press.

- ENDRES, S, GALGANI L, RIEBESELL U, SCHULZ K-G, ENGEL A. 2014. Stimulated Bacterial Growth under Elevated $p\text{CO}_2$: Results from an Off-Shore Mesocosm Study. PLOS ONE 9(6): e99228
- ENGEL, A. 2000. The role of transparent exopolymer particles (TEP) in the increase in apparent particle stickiness (α) during the decline of a diatom bloom. Journal of Plankton Research 22:485–497
- ENGEL, A. 2002. Direct relationship between CO_2 uptake and transparent exopolymer particles production in natural phytoplankton. Journal of Plankton Research 24:49–53
- ENGEL, A, DELILLE B, JACQUET S, RIEBESELL U, ROCHELLE-NEWALL E, TERBRUGGEN A, ZONDERVAN I. 2004. Transparent exopolymer particles and dissolved organic carbon production by *Emiliana huxleyi* exposed to different CO_2 concentrations: a mesocosm experiment. Aquatic Microbial Ecology 34:93–104
- ENGEL, A, HÄNDEL N, WOHLERS J, LUNAU M, GROSSART H-P, SOMMER U, RIEBESELL U. 2011. Effects of sea surface warming on the production and composition of dissolved organic matter during phytoplankton blooms: results from a mesocosm study. Journal of Plankton Research 33:357–372
- ENGEL, A, PASSOW U. 2001. Carbon and nitrogen content of transparent exopolymer particles (TEP) in relation to their Alcian Blue adsorption. Marine Ecology Progress Series 219:1–10
- ENGEL, A, PIONTEK J, GROSSART H-P, RIEBESELL U, SCHULZ KG, SPERLING M. 2014. Impact of CO_2 enrichment on organic matter dynamics during nutrient induced coastal phytoplankton blooms. Journal of Plankton Research 36:641–657
- ENGEL, A, SCHULZ KG, RIEBESELL U, BELLERBY R, DELILLE B, SCHARTAU M. 2008. Effects of CO_2 on particle size distribution and phytoplankton abundance during a mesocosm bloom experiment (PeECE II). Biogeosciences 5:509–521
- ENGEL, A, THOMS S, RIEBESELL U, ROCHELLE-NEWALL E, ZONDERVAN I. 2004. Polysaccharide aggregation as a potential sink of marine dissolved organic carbon. Nature 428:929–932
- ENGEL, A, ZONDERVAN I, AERTS K, BEAUFORT L, BENTHIEN A, CHOU L, DELILLE B, GATTUSO JP, HARLAY J, HEEMANN C, others 2005. Testing the direct effect of CO_2 concentration on a bloom of the coccolithophorid *Emiliana huxleyi* in mesocosm experiments. Limnology and Oceanography 50:493–507

- FALKOWSKI, PG, BARBER RT, SMETACEK V. 1998. Biogeochemical Controls and Feedbacks on Ocean Primary Production. *Science* 281:200–206
- FATIBELLO, SHS, VIEIRA AAH, FATIBELLO-FILHO O. 2004. A rapid spectrophotometric method for the determination of transparent exopolymer particles (TEP) in freshwater. *Talanta* 62:81–85
- FENG, Y, HARE CE, LEBLANC K, ROSE JM, ZAHNG Y, DITULLIO GR, LEE PA, WILHELM SW, ROWE JM, SUN J, NEMCEK N, GUENGUEN C, PASSOW U, BENNER I, HUTCHINS DA. 2009. The Effects of Increased $p\text{CO}_2$ and Temperature on the North Atlantic Spring Bloom: I. Phytoplankton Community and Biogeochemical Response. *Marine Ecology Progress Series* 388:13–25
- FIELD, BEHRENFELD, RANDERSONL, FALKOWSKI. 1998. Primary production of the biosphere: integrating terrestrial and oceanic components. *Science* 281:237–240
- FOGG, GE. 1983. The Ecological Significance of Extracellular Products of Phytoplankton Photosynthesis. *Botanica Marina* 26: 3-14
- FUKAO, T, KIMOTO K, KOTANI Y. 2010. Production of transparent exopolymer particles by four diatom species. *Fisheries Science* 76(5):755–760
- GALBRAITH, PS, CHASSÉ J, GILBERT D, LAROUCHE P, BRICKMAN D, PETTIGREW B, DEVINE L, GOSSELIN A, PETTIPAS RG, LAFLEUR C. 2012. Physical Oceanographic Conditions in the Gulf of St. Lawrence in 2011. DFO Canadian Science Advisory Secretariat. Research. Document. 2012/023. iii + 85 p.
- GATTUSO, JP, BIJMA J, GEHLEN, M, RIEBESELL U, TURLEY C. 2011. Ocean acidification: knowns, unknowns, and perspectives. In: GATTUSO J.-P, HANSSON L. (Eds.), *Ocean Acidification*. Oxford University Press, Oxford, pp. 291e311.
- GATTUSO, JP, HANSSON L. 2011. *Ocean acidification*. Oxford University Press, New York, 408 pp
- GENIN, F, LALANDE, C, GALBRAITH, PS, LAROUCHE, P, FERREYRA, GA, GOSSELIN, M. 2021. Annual cycle of biogenic carbon export in the Gulf of St. Lawrence. *Continental Shelf Res.* 221:104418
- GENOVESI, L, DE VERNAL A, THIBODEAU B, HILLAIRE-MARCEL C, MUCCI A, GILBERT D. 2011. Recent changes in bottom water oxygenation and temperature in the Gulf of St. Lawrence: Micropaleontological and geochemical evidence. *Limnology and Oceanography* 56:1319–1329

- GILBERT, D, CHABOT D, ARCHAMBAULT P, RONDEAU B, HEBERT S. 2007. Appauvrissement en oxygène dans les eaux profondes du Saint-Laurent marin: causes possibles et impacts écologiques. *Le naturaliste Canadien*, 31(1): 67-75.
- GILBERT, D, PETTIGREW B. 1997. Interannual variability (1948–1994) of the CIL core temperature in the Gulf of St. Lawrence. *Canadian Journal of Fisheries and Aquatic Sciences* 54(Suppl. 1):57–67
- GILBERT, D, SUNDBY B, GOBEIL C, MUCCI A, TREMBLAY GH. 2005. A seventy-two-year record of diminishing deep-water oxygen in the St. Lawrence estuary: The northwest Atlantic connection. *Limnology and Oceanography* 50(5):1654–1666
- GAO, K, CAMPBELL DA. 2014. Photophysiological responses of marine diatoms to elevated CO₂ and decreased pH: a review. *Functional Plant Biology* 41:449–459
- GIORDANO, M, BEARDALL J, RAVEN JA. 2005. CO₂ concentrating mechanisms in algae: Mechanisms, Environmental Modulation, and Evolution. *Annual Review of Plant Biology* 56:99-131
- GOVINDJEE, BRAUN, BZ. 1974. Light Absorption, Emission and Photosynthesis. In: *Algal Physiology and Biochemistry*. ed. W.D.P. Stewart. Blackwell Scientific Publication Ltd, Oxford, pp. 346-390
- GROSSART, H, ALLGAIER M, PASSOW U, RIEBESELL U. 2006. Testing the effect of CO₂ concentration on the dynamics of marine heterotrophic bacterioplankton. *Limnology and Oceanography* 51(1):1-11
- GROSSART, H-P, SIMON M, LOGAN BE. 1997. Formation of macroscopic organic aggregates (lake snow) in a large lake: The significance of transparent exopolymer particles, phytoplankton, and zooplankton. *Limnology and Oceanography* 42:1651–1659
- HANSELL, DA, CARLSON CA, REPETA DJ, SCHLITZER R. 2009. Dissolved organic matter in the ocean: a controversy stimulates new insights. *Oceanography* 22(4):202-211
- HANSEN, PJ. 2002. Effect of high pH on the growth and survival of marine phytoplankton: implications for species succession. *Aquatic Microbial Ecology* 28:279–288
- HARE, CE, LEBLANC K, DITULLIO GR, KUDELA RM, ZHANG Y, LEE PA, RISEMAN S, HUTCHINS DA. 2007. Consequences of increased temperature and

CO₂ for phytoplankton community structure in the Bering Sea. *Marine Ecology Progress Series* 352:9–16

- HARLAY, J, DE BODT C, ENGEL A, JANSEN S, D'HOOP Q, PIONTEK J, VAN OOSTENDE N, GROOM S, SABBE K, CHOU L. 2009. Abundance and size distribution of transparent exopolymer particles (TEP) in a coccolithophorid bloom in the northern Bay of Biscay. *Deep Sea Research Part I: Oceanographic Research Papers* 56:1251–1265
- HARRIS, GP. 1980. Temporal and spatial scales in phytoplankton ecology. Mechanisms, methods, models and management. *Canadian Journal of Fisheries and Aquatic Sciences* 37:877-900
- HAVENHAND, JN, DUPONT S, QUINN GP. 2010. Designing ocean acidification experiments to maximise inference. *in Guide to best practices for ocean acidification research and data reporting*, p260 Edited by Riebesell U, Fabry V J, Hansson L, Gattuso J-P. Publications Office of the European Union, Luxembourg
- HEINONEN, KB, WARD JE, HOLOHAN BA. 2007. Production of transparent exopolymer particles (TEP) by benthic suspension feeders in coastal systems. *Journal of Experimental Marine Biology and Ecology* 341:184–195
- HERNANDEZ-AYON, JM, BELLI SL, ZIRINO A. 1999. pH, alkalinity and total CO₂ in coastal seawater by potentiometric titration with a difference derivative readout. *Analytica Chimica Acta* 394(1):101-108
- HERVÉ, V, DERR J, DOUADY S, QUINET M, MOISAN L, LOPEZ PJ. 2012. Multiparametric Analyses Reveal the pH-Dependence of Silicon Biomineralization in Diatoms. *PLOS ONE* 7(10):e46722
- HOPKINS, FE, TURNER SM, NIGHTINGALE PD, STEINKE M, BAKKER D, LISS PS. 2010. Ocean acidification and marine trace gas emissions. *PNAS* 107:760–765
- HOPPE, H, BREITHAUPT P, WALTHER K, KOPPE R, BLECK S, SOMMER U, JRGENS K. 2008. Climate warming in winter affects the coupling between phytoplankton and bacteria during the spring bloom: a mesocosm study. *Aquatic Microbial Ecology* 51:105–115
- HUSSHERR, R, LEVASSEUR M, LIZOTTE M, TREMBLAY J-É, MOL J, THOMAS H, GOSSELIN M, STARR M, MILLER LA, JARNIKOVÁ T, SCHUBACK N, MUCCI A. 2017. Impact of ocean acidification on Arctic phytoplankton blooms and dimethylsulfide production under simulated ice-free and under-ice conditions. *Biogeosciences* 14: 2407-2427

- HUTCHINS, DA, FU F-X, ZHANG Y, WARNER ME, FENG Y, PORTUNE K, BERNHARDT PW, MULHOLLAND MR. 2007. CO₂ control of Trichodesmium N₂ fixation, photosynthesis, growth rates, and elemental ratios: Implications for past, present, and future ocean biogeochemistry. *Limnology and Oceanography* 52:1293–1304
- INGRAM, RG. 1975. Influence of tidal-induced vertical mixing on primary productivity in the St. Lawrence estuary. In: *Memoires de la Societe Royale des Sciences de Liege* 7:59-74
- IVERSEN, MH, PLOUG H. 2010. Ballast minerals and the sinking carbon flux in the ocean: carbon-specific respiration rates and sinking velocity of marine snow aggregates. *Biogeosciences* 7:2613–2624
- IPCC, 2014. Summary for Policymakers. In: *Climate Change 2014: Mitigation of Climate Change. Contribution of Working Group III to the Fifth Assessment Report of the Intergovernmental Panel on Climate Change* [EDENHOFER O, PICHSMADRUGA R, SOKONA Y, FARAHANI E, KADNER S, SEYBOTH K, ADLER A, BAUM I, BRUNNER S, EICKEMEIER P, KRIEMANN B, SAVOLAINEN J, SCHLÖMER S, VON STECHOW C, ZWICKEL T and MINX JC (eds.)]. Cambridge University Press, Cambridge, United Kingdom and New York, NY, USA.
- JACKSON, GA. 1995. TEP and coagulation during a mesocosm experiment. *Deep-Sea Research Part II Topical Studies in Oceanography* 42:215–222
- JANSE, I, VAN RIJSSEL M, OTTEMA A, GOTTSCHAL JC. 1999. Microbial breakdown of Phaeocystis mucopolysaccharides. *Limnology and Oceanography* 44:1447–1457
- JENSEN, LM, SØNDERGAARD M. 1982. Abiotic formation of particles from extracellular organic carbon released by phytoplankton. *Microbial Ecology* 8:47–54
- JOHNSON, BD, ZHOU X, WANGERSKY PJ. 1986. Surface coagulation in sea water. *Netherlands Journal of Sea Research* 20:201–210
- KEPKAY, PE. 1994. Particle aggregation and the biological reactivity of colloids. *Marine Ecology Progress Series* 109:293–293
- KEPKAY, PE. 2000. Colloids and the ocean carbon cycle. In: Wangersky P.J. (eds) *Marine Chemistry. The Handbook of Environmental Chemistry* (Vol. 5 Series: Water Pollution), vol 5D. Springer, Berlin, Heidelberg

- KEPKAY, PE, HARRISON WG, IRWIN B. 1990. Surface coagulation, microbial respiration and primary production in the Sargasso Sea. *Deep Sea Research Part A Oceanographic Research Papers* 37:145–155
- KEPKAY, PE, JOHNSON BD. 1988. Microbial response to organic particle generation by surface coagulation in seawater. *Marine Ecology Progress Series* 48:193–198
- KEPKAY, PE, NIVEN SEH, JELLETT JF. 1997. Colloidal organic carbon and phytoplankton speciation during a coastal bloom. *Journal of Plankton Research* 19:369–389
- KIM, J-M, LEE K, SHIN K, YANG EJ, ENGEL A, KARL DM, KIM H-C. 2011. Shifts in biogenic carbon flow from particulate to dissolved forms under high carbon dioxide and warm ocean conditions. *Geophysical Research Letters* 38:L08612
- KIØRBOE, T, HANSEN JLS. 1993. Phytoplankton aggregate formation: Observations of patterns and mechanisms of cell sticking and the significance of exopolymeric material, *Journal of Plankton Research* 15(9):993–1018
- KIRK, JTO. 1983. *Light and Photosynthesis in Aquatic Ecosystems*. Cambridge–London–New York: Cambridge University Press 1983. ISBN 0 521 24450 1. 401 pp
- KLAAS, C, and ARCHER D.E. 2002. Association of sinking organic matter with various types of mineral ballast in the deep sea: Implications for the rain ratio. *Global Biogeochemical Cycles*, 16(4), 1116
- KREMBS, C, ENGEL A. 2001. Abundance and variability of microorganisms and transparent exopolymer particles across the ice–water interface of melting first-year sea ice in the Laptev Sea (Arctic). *Marine Biology* 138:173–185
- KUMAR, MD, SARMA VVSS, RAMAIAH N, GAUNS M, DE SOUSA SN. 1998. Biogeochemical significance of transport exopolymer particles in the Indian Ocean. *Geophysical Research Letters* 25:81–84
- LAPOUSSIÈRE, A, MICHEL C, STARR M, GOSELIN M, POULIN M. 2011. Role of free-living and particle-attached bacteria in the recycling and export of organic material in the Hudson Bay system. *Journal of Marine Systems* 88:434–445
- LAROUCHE, P, BOYER-VILLEMAIRE U. 2010. Suspended particulate matter in the St. Lawrence estuary and Gulf surface layer and development of a remote sensing algorithm. *Estuarine, Coastal and Shelf Science* 90:241–249

- LATASA, M, ANXELU X, MORAN G, SCHAREK R, ESTRADA M. 2005. Estimating the carbon flux through main phytoplankton groups in the northwestern Mediterranean. *Limnology and Oceanography* 50:1447–1458
- LEBARON, P, PARTHUISOT N, CATALA P. 1998. Comparison of Blue Nucleic Acid Dyes for Flow Cytometric Enumeration of Bacteria in Aquatic Systems. *Applied and Environmental Microbiology* 64(5):1725–1730
- LEBARON, P, SERVAIS P, AGOGUÉ H, COURTIES C, JOUX F. 2001. Does the High Nucleic Acid Content of Individual Bacterial Cells Allow Us To Discriminate between Active Cells and Inactive Cells in Aquatic Systems? *Applied and Environmental Microbiology* 67(4):1775–1782
- LEBEL, J, PELLETIER E. 1980. Contribution à l'étude du pH et de la saturation en calcite dans l'estuaire du St-Laurent (Canada). *Atmosphere-Ocean* 18(2):154–167
- LEFORT, S, GRATTON Y, MUCCI A, DADOU I, GILBERT D. 2012. Hypoxia in the Lower St. Lawrence Estuary: How physics controls spatial patterns. *Journal of Geophysical Research* 117:C07018
- LE FOUEST, V, ZAKARDJIAN B, SAUCIER FJ, STARR M. 2005. Seasonal versus synoptic variability in planktonic production in a high-latitude marginal sea: The Gulf of St. Lawrence (Canada). *Journal of Geophysical Research* 110:C09012
- LEGENDRE, L, RASSOULZADEGAN F. 1995. Plankton and nutrient dynamics in marine waters. *Ophelia* 41:153–172
- LEVASSEUR, M, THERRIAULT J-C, LEGENDRE L. 1984. Hierarchical control of phytoplankton succession by physical factors. *Marine Ecology Progress Series* 19:211–222
- LEVASSEUR, ME, THERRIAULT J-C. 1987. Phytoplankton biomass and nutrient dynamics in a tidally induced upwelling: the role of the NO₃: SiO₄ ratio. *Marine Ecology Progress Series* 39:87–97
- LEWIS, E, Wallace DWR. 1998. Program developed for CO₂ systems calculations, ORNL/CDIAC-105, Carbon Dioxide Information Analysis Center, Oak Ridge National Laboratory, U.S. Department of Energy, Oak Ridge, Tennessee
- LI F, WUY, HUTCHINS DA, FU F, GAO K. 2016. Physiological responses of coastal and oceanic diatoms to diurnal fluctuations in seawater carbonate chemistry under two CO₂ concentrations. *Biogeosciences* 13:6247–6259

- LI, X, LECK C, SUN L, HEDE T, TU Y, ÅGREN H. 2013. Cross-Linked Polysaccharide Assemblies in Marine Gels: An Atomistic Simulation. *Journal of Physical Chemistry Letters* 4(16):2637–2642
- LI, Y, TANAKA T. 1992. Phase Transitions of Gels. *Annual Review of Materials Science* 22:243–277
- LOGAN, BE, PASSOW U, ALLDREDGE AL, GROSSARTT H-P, SIMONT M. 1995. Rapid formation and sedimentation of large aggregates is predictable from coagulation rates (half-lives) of transparent exopolymer particles (TEP). *Deep Sea Research Part II: Topical Studies in Oceanography* 42:203–214
- LÓPEZ-URRUTIA, Á, MARTIN ES, HARRIS RP, IRIGOIEN X. 2006. Scaling the metabolic balance of the oceans. *Proceedings of the National Academy of Sciences* 103(23):8739–8744
- LOVEJOY, C, LEGENDRE L, THERRIAULT J-C, TREMBLAY J-E, KLEIN B, GRANT INGRAM R. 2000. Growth and distribution of marine bacteria in relation to nanoplankton community structure. *Deep Sea Research Part II: Topical Studies in Oceanography* 47:461–487
- LUCOTTE, M, HILLAIRES-MARCEL C, LOUCHOUARN P. 1991. First-order organic carbon budget in the St Lawrence Lower estuary from ^{13}C data. *Estuarine, Coastal and Shelf Science* 32:297–312
- LUND, JWG, KIPLING C, LE CREN ED. 1958. The inverted microscope method of estimating algal number and the statistical basis of estimations by counting. *Hydrobiologia* 11:143–170
- MACGILCHRIST, GA, SHI T, TYRRELL T, RICHIER S, MOORE CM, DUMOUSSEAUD C, ACHTERBERG EP. 2014. Effect of enhanced $p\text{CO}_2$ levels on the production of dissolved organic carbon and transparent exopolymer particles in short-term bioassay experiments. *Biogeosciences* 11:3695–3706
- MARI, X. 1999. Carbon content and C:N ratio of transparent exopolymeric particles (TEP) produced by bubbling exudates of diatoms. *Marine Ecology Progress Series* 183:59–71
- MARI, X. 2008. Does ocean acidification induce an upward flux of marine aggregates? *Biogeosciences* 5:1023–1031

- MARI, X, BEAUVAIS S, LEMÉE R, PEDROTTI ML. 2001. Non-Redfield C: N ratio of transparent exopolymeric particles in the northwestern Mediterranean Sea. *Limnology and Oceanography* 46:1831–1836
- MARI, X, BURD A. 1998. Seasonal size spectra of transparent exopolymeric particles (TEP) in a coastal sea and comparison with those predicted using coagulation theory. *Marine Ecology Progress Series* 163:63–76
- MARI, X, KIØRBOE T. 1996. Abundance, size distribution and bacterial colonization of transparent exopolymeric particles (TEP) during spring in the Kattegat. *Journal of Plankton Research* 18:969–986
- MARI, X, MIGON C, NICOLAS E. 2009. Reactivity of transparent exopolymeric particles: A key parameter of trace metal cycling in the lagoon of Nouméa, New Caledonia. *Marine Pollution Bulletin* 58:1874–1879
- MARI, X, PASSOW U, MIGON C, BURD AB, LEGENDRE L. 2017. Transparent exopolymer particles: Effects on carbon cycling in the ocean. *Progress in Oceanography* 151:13–37
- MARI, X, RASSOULZADEGAN F, BRUSSAARD CPD, WASSMANN P. 2005. Dynamics of transparent exopolymeric particles (TEP) production by *Phaeocystis globosa* under N- or P-limitation: a controlling factor of the retention/export balance. *Harmful Algae* 4:895–914
- MARI, X, TORRÉTON J-P, BICH-THUY TRINH C, BOUVIER T, VAN THUOC C, LEFEBVRE J-P, OUILLOIN S. 2012. Aggregation dynamics along a salinity gradient in the Bach Dang estuary, North Vietnam. *Estuarine, Coastal and Shelf Science* 96:151–158
- MARIE, D, BRUSSAARD CPD, THYRHAUG R, BRATBAK G, VAULOT D. 1999. Enumeration of marine viruses in culture and natural samples by flow cytometry. *Applied and Environmental Microbiology* 65:45–52
- MARIE, D, SIMON N, VAULOT D. 2005. Phytoplankton cell counting by flow cytometry. *Algal Culturing Techniques Academic Press* 596
- MEEHL, GA, STOCKER TF, COLLINS WD, FRIEDLINGSTEIN P, GAYE AT, GREGORY JM, KITOH A, KNUTTI R, MURPHY JM, NODA A, RAPER SCB, WATTERSON IG, WEAVER AJ, ZHAO Z-C. 2007. Global Climate Projections. In: Solomon S, Qin D, Manning M, Chen Z, Marquis M, Averyt KB, Tignor M, Miller HL (eds.), *Climate Change 2007: The physical Science Basis. Contribution of Working Group I to the Fourth Assessment Report of the Intergovernmental*

Panel on Climate Change. Cambridge University Press, Cambridge, United Kingdom and New York, NY, USA.

- MEHRBACH, C, CULBERSON CH, HAWLEY JE, PYTKOWICZ RM. 1973. Measurement of the apparent dissociation constants of carbonic acid in seawater at atmospheric pressure. *Limnology and Oceanography* 18:897-907
- MELZNER, F, THOMSEN J, KOEVE W, OSCHLIES A, GUTOWSKA MA, BANGE HW, HANSEN HP, KÖRTZINGER A. 2013. Future ocean acidification will be amplified by hypoxia in coastal habitats. *Marine Biology* 160:1875–1888
- MENG, S, LIU Y. 2016. New insights into transparent exopolymer particles (TEP) formation from precursor materials at various $\text{Na}^+/\text{Ca}^{2+}$ ratios. *Scientific Reports* 6:19747
- MIDDELBOE, AL, HANSEN PJ. 2007. High pH in shallow-water macroalgal habitats. *Marine Ecology Progress Series* 338:107–117
- MILLERO, FJ. 1986. The pH of estuarine waters. *Limnology and Oceanography* 34:839–847
- MITCHELL, MR, HARRISON G, PAULEY K, GAGNÉ A, MAILLET G, STRAIN P. 2002. Atlantic zonal monitoring program sampling protocol. *Canadian Technical Report Hydrography and Ocean Sciences* 223: iv+23 pp.
- MONTAGNES, DJ., BERGES JA, HARRISON PJ, TAYLOR FJR. 1994. Estimating carbon, nitrogen, protein, and chlorophyll a from volume in marine phytoplankton. *Limnology and Oceanography* 39:1044–1060
- MOPPER, K, ZHOU J, SRI RAMANA K, PASSOW U, DAM HG, DRAPEAU DT. 1995. The role of surface-active carbohydrates in the flocculation of a diatom bloom in a mesocosm. *Deep Sea Research Part II: Topical Studies in Oceanography* 42:47–73
- MOSTAJIR, B, LE FLOC'H E, MAS S, PETE R, PARIN D, NOUGUIER J, FOUILLAND E, VIDUSSI F. 2013. A new transportable floating mesocosm platform with autonomous sensors for real-time data acquisition and transmission for studying the pelagic food web functioning. *Limnology and Oceanography Methods* 11:394–409
- MUCCI, A, STARR M, GILBERT D, SUNDBY B. 2011. Acidification of Lower St. Lawrence Estuary Bottom Waters. *Atmosphere-Ocean* 49:206–218
- MYKLESTAD, SM. 1995. Release of extracellular products by phytoplankton with special emphasis on polysaccharides. *Science of the Total Environment* 165:155–164

- NAGATA, T. 2000. Production mechanisms of dissolved organic matter. Wiley Series in Ecological and Applied Microbiology
- NAGATA, T., YAMADA, Y, FUKUDA, H. 2021. Transparent exopolymer particles in deep oceans: Synthesis and future challenges. *Gels* 7:1-12
- NEU, H.J.A. 1970. A study on mixing and circulation in the St Lawrence Estuary up to 1964. Bedford Inst. Oceanogr. AOL Report 1970-9. Unpublished manuscript, 31 p.
- NEU, H.J.A. 1975. Run-off regulation for hydro-power and its effects on the ocean environment. *Canadian Journal of Civil Engineering* 2:583-591.
- NIELSEN, LT, HALLEGRAEFF GM, WRIGHT SW, HANSEN PJ. 2012. Effects of experimental seawater acidification on an estuarine plankton community. *Aquatic Microbial Ecology* 65:271-286
- NEVEUX, J, LEFEBVRE J-P, LE GENDRE R, DUPOUY C, GALLOIS F, COURTIES C, GÉRARD P, FERNANDEZ J-M, OUILLON S. 2010. Phytoplankton dynamics in the southern New Caledonian lagoon during a southeast trade winds event. *Journal of Marine Systems* 82:230-244
- NIMER, NA, BROWNLEE C, MERRET MJ. 1994. Carbon dioxide availability, intracellular pH and growth rate of the coccolithophore *Emiliana huxleyi*. *Marine Ecology Progress Series* 109:257-262
- NIXON, SW. 1995. Coastal marine eutrophication: a definition, social causes and future concerns. *Ophelia* 41:199-219.
- OBERNOSTERER, I, HERNDL GJ. 1995. Phytoplankton extracellular release and bacterial growth: dependence on the inorganic N: P ratio. *Marine Ecology Progress Series* 116:247-257
- OGAWA, H, AMAGAI Y, KOIKE I, KAISER K, BENNER R. 2001. Production of refractory dissolved organic matter by bacteria. *Science* 292:917-920
- ORR, J.C. 2011. Recent and future changes in ocean carbon chemistry, in *Ocean acidification*, edited by: GATTUSO, J.-P. and HANSSON, L, Oxford University Press, Oxford, UK, 41-66.
- ORR, JC, FABRY VJ, AUMONT O, BOPP L, DONEY SC, FEELY RA, GNANADESIKAN A, GRUBER N, ISHIDA A, JOOS F, KEY RM, LINDSAY K, MAIER-REIMER E, MATEAR R, MONFRAY P, MOUCHET A, NAJJAR RG,

- PLATTNER G-K, RODGERS KB, SABINE CL, SARMIENTO JL, SCHLITZER R, SLATER RD, TOTTERDELL IJ, WEIRIG M-F, YAMANAKA Y, YOOL A. 2005. Anthropogenic ocean acidification over the twenty-first century and its impact on calcifying organisms. *Nature* 437:681–686
- ORTEGA-RETUERTA, E, DUARTE CM, RECHE I. 2010. Significance of Bacterial Activity for the Distribution and Dynamics of Transparent Exopolymer Particles in the Mediterranean Sea. *Microbial Ecology* 59(4):808-818
- ORTEGA-RETUERTA, E, PASSOW U, DUARTE CM, RECHE I. 2009. Effects of ultraviolet B radiation on (not so) transparent exopolymer particles. *Biogeosciences* 6:3071–3080
- ORTEGA-RETUERTA, E, MARRASÈ, C, MUÑOZ-FERNÁNDEZ, A, MONTSERRAT SALA, M, SIMÓ, R, GASOL, JM. 2018. Seasonal dynamics of transparent exopolymer particles (TEP) and their drivers in the coastal NW Mediterranean Sea. *Sci. of the Total Environ.* 631-632:180-190
- PARSONS, TR, MAITA Y, LALLI CM. 1984. A manual of chemical and biological methods for seawater analysis. Oxford and New York : Pergamon Press 184 pp
- PASSOW, U. 2000. Formation of Transparent Exopolymer Particles, TEP, from dissolved precursor material. *Marine Ecology Progress Series* 192:1–11
- PASSOW, U. 2001. Origin of transparent exopolymer particles (TEP) and their role in the sedimentation of particulate matter. *Continental Shelf Research* 21:327–346
- PASSOW, U. 2002a. Production of transparent exopolymer particles (TEP) by phyto- and bacterioplankton. *Marine Ecology Progress Series* 236:1–12
- PASSOW, U. 2002b. Transparent exopolymer particles (TEP) in aquatic environments. *Progress in Oceanography* 55:287–333
- PASSOW, U, ALLDREDGE A. 1994. Distribution, size and bacterial colonization of transparent exopolymer particles (TEP) in the ocean. *Marine Ecology Progress Series* 113(1-2):185-198
- PASSOW, U, ALLDREDGE AL. 1995a. A dye-binding assay for the spectrophotometric measurement of transparent exopolymer particles (TEP). *Limnology and Oceanography* 40:1326–1335

- PASSOW, U, ALLDREDGE AL. 1995b. Aggregation of a diatom bloom in a mesocosm: The role of transparent exopolymer particles (TEP). *Deep Sea Research Part II* 42:99–109
- PASSOW, U, SHIPE R, MURRAY A, PAK D, BRZEZINSKI M, ALLDREDGE A. 2001. The origin of transparent exopolymer particles (TEP) and their role in the sedimentation of particulate matter. *Continental Shelf Research* 21:327–346
- PELLETIER, E, LEBEL J. 1980. La mesure du pH en milieu estuarien sur l'échelle NBS. *Canadian Journal of Fisheries and Aquatic Sciences* 37:703–706
- PEDROTTI, ML, FIORINI S, KERROS M-E, MIDDELBURG JJ, GATTUSO J-P. 2012. Variable production of transparent exopolymeric particles by haploid and diploid life stages of coccolithophores grown under different CO₂ concentrations. *Journal of Plankton Research* 34:388–398
- PIONTEK, J, BORCHARD C, SPERLING M, SCHULZ KG, RIEBESELL U, ENGEL A. 2013. Response of bacterioplankton activity in an Arctic fjord system to elevated pCO₂: results from a mesocosm perturbation study. *Biogeosciences* 10:297–314
- PIONTEK, J, HÄNDEL N, LANGER G, WOHLERS J, RIEBESELL U, ENGEL A. 2009. Effects of rising temperature on the formation and microbial degradation of marine diatom aggregates. *Aquatic Microbial Ecology* 54:305–318
- PIONTEK, J, LUNAU M, HÄNDEL N, BORCHARD C, WURST M, ENGEL A. 2010. Acidification increases microbial polysaccharide degradation in the ocean. *Biogeosciences* 7:1615–1624
- QIAN, J, MOPPER K. 1996. An automated, high performance, high temperature combustion dissolved organic carbon analyzer. *Analytical Chemistry* 68(18):3090–3097
- RADIĆ, T, IVANCIĆ I, FUKS D, RADIĆ J. 2006a. Marine bacterioplankton production of polysaccharidic and proteinaceous particles under different nutrient regimes. *FEMS Microbiological Ecology* 58:333–342
- RAMAIAH, N, SARMA VVSS, GAUNS M, KUMAR MD, MADHUPRATAP M. 2000. Abundance and relationship of bacteria with transparent exopolymer particles during the 1996 summer monsoon in the Arabian Sea. *Journal of Earth System Science* 109(4):443–451

- RAMAIAH, N, YOSHIKAWA T, FURUYA K. 2001. Temporal variations in transparent exopolymer particles (TEP) associated with a diatom spring bloom in a subarctic ria in Japan. *Marine Ecology Progress Series* 212:79–88
- RAVEN, JA, CALDEIRA K, ELDERFIELD H. 2005. Ocean acidification due to increasing atmospheric carbon dioxide. The Royal Society of London, Policy document 12/05, 60 pp.
- RAVEN, JA, BEARDALL J, GIORDANO M. 2014. Energy costs of carbon dioxide concentrating mechanisms in aquatic organisms. *Photosynthesis Research* 121:111–124
- REID, SJ. 1977. Circulation and mixing in the St. Lawrence Estuary near Ile Rouge. Bedford Institut Oceanography Data Report Series BI-R-77-1. Dartmouth, Nova Scotia, 36 p
- RICHARDSON, AJ, GIBBONS MJ. 2008. Are jellyfish increasing in response to ocean acidification? *Limnology and Oceanography* 53:2040–2045
- RIEBESELL, U. 2004. Effects of CO₂ enrichment on marine phytoplankton. *Journal of Oceanography* 60:719–729
- RIEBESELL, U, FABRY VJ, HANSSON L, GATTUSO J-P. 2010. Guide to best practices for ocean acidification research and data reporting. Luxembourg, Publications Office of the European Union, 258pp.
- RIEBESELL, U, KORTZINGER A, OSCHLIES A. 2009. Sensitivities of marine carbon fluxes to ocean change. *Proceedings of the National Academy of Sciences* 106(49):20602–20609
- RIEBESELL, U, SCHULZ KG, BELLERBY RGJ, BOTROS M, FRITSCHÉ P, MEYERHÖFER M, NEILL C, NONDAL G, OSCHLIES A, WOHLERS J, ZÖLLNER E. 2007. Enhanced biological carbon consumption in a high CO₂ ocean. *Nature* 450:545–548
- RIEBESELL, U, WOLF-GLADROW DA, SMETACEK V. 1993. Carbon dioxide limitation of marine phytoplankton growth rates. *Nature* 361:249–251
- RIEBESELL, U, ZONDERVAN I, ROST B, TORTELL PD, ZEEBE RE, MOREL FMM. 2000. Reduced calcification of marine plankton in response to increased atmospheric CO₂. *Nature* 407:364–367

- RIEMANN, L, STEWARD GF, AZAM F. 2000. Dynamics of bacterial community composition and activity during a mesocosm diatom bloom. *Applied and Environmental Microbiology* 66:578–587
- RIVKIN, RB, LEGENDRE L, DEIBEL D, TREMBLAY J-É, KLEIN B, CROCKER K, ROY S, SILVERBERG N, LOVEJOY C, MESPLÉ F, ROMERO N, ANDERSON MR, MATTHEWS P, SAVENKOFF C, VÉZINA A, THERRIault J-C, WESSON J, BÉRUBÉ C, INGRAM RG. 1996. Vertical Flux of Biogenic Carbon in the Ocean: Is There Food Web Control? *Science* 272:1163–1166
- ROCHELLE-NEWALL, EJ, MARI X, PRINGAULT O. 2010. Sticking properties of transparent exopolymeric particles (TEP) during aging and biodegradation. *Journal of Plankton Research* 32:1433–1442
- ROMERO, N, SILVERBERG N, ROY S, LOVEJOY C. 2000. Sediment trap observations from the Gulf of St. Lawrence and the continental margin of eastern Canada. *Deep Sea Research Part II: Topical Studies in Oceanography* 47:545–583
- ROMERO-IBARRA, N, SILVERBERG N. 2011. The contribution of various types of settling particles to the flux of organic carbon in the Gulf of St. Lawrence. *Continental Shelf Research* 31:1761–1776
- ROST, B, ZONDERVAN I, WOLF-GLADROW D. 2008. Sensitivity of phytoplankton to future changes in ocean carbonate chemistry: current knowledge, contradictions and research directions. *Marine Ecology Progress Series* 373:227–237
- ROY, S, CHANUT J-P, GOSSELIN M, SIME-NGANDO T. 1997. Characterization of phytoplankton communities in the lower St. Lawrence Estuary using HPLC-detected pigments and cell microscopy. *Marine Ecology Progress Series* 142:55-73
- SABINE, CL, FEELY RA, GRUBER N, KEY RM, LEE K, BULLISTER JL, WANNINKHOF R, WONG CS, WALLACE DWR, TILBROOK B, MILLERO FJ, PENG T-H, KOZYR A, ONO T, RIOS AF. 2004. The Oceanic Sink for Anthropogenic CO₂. *Science* 305:367–371
- SARMIENTO, JL, SLATER R, BARBER R, BOPP L, DONEY SC, HIRST AC, KLEYPAS J, MATEAR R, MIKOLAJEWICZ U, MONFRAY P, SOLDATOV V, SPALL SA, STOUFFER R. 2004. Response of ocean ecosystems to climate warming. *Global Biogeochem Cycles* 18:GB3003
- SAUCIER, FJ, CHASSÉ J. 2000. Tidal circulation and buoyancy effects in the St. Lawrence Estuary. *Atmosphere-Ocean* 38:505–556

- SAVENKOFF, C, VÉZINA AF, GRATTON Y. 1997a. Effect of a freshwater pulse on mesoscale circulation and phytoplankton distribution in the lower St. Lawrence Estuary. *Journal of Marine Research* 55:353–381
- SAVENKOFF, C, VÉZINA A., ROY S, KLEIN B, LOVEJOY C, THERRIAULT J-C, LEGENDRE L, RIVKIN R, BÉRUBÉ C, TREMBLAY J-E, SILVERBERG N. 2000. Export of biogenic carbon and structure and dynamics of the pelagic food web in the Gulf of St. Lawrence Part 1. Seasonal variations. *Deep Sea Research Part II: Topical Studies in Oceanography* 47:585–607
- SAVENKOFF, C, VÉZINA AF, SMITH PC, HAN G. 2001. Summer Transports of Nutrients in the Gulf of St. Lawrence Estimated by Inverse Modelling. *Estuarine, Coastal and Shelf Science* 52:565–587
- SCHLOSS, IR, WASILOWSKA A, DUMONT D, ALMANDOZ GO, HERNANDO MP, MICHAUD-TREMBLAY C-A, SARAVIA L, RZEPECKI M, MONIEN P, MONIEN D, KOPCZYNSKA EE, BERS AV, FERREYRA GA. 2014. On the phytoplankton bloom in coastal waters of southern King George Island (Antarctica) in January 2010: An exceptional feature? *Limnology and Oceanography* 59:195–210
- SCHRÖTER, D, CRAMER W, LEEMANS R, PRENTICE IC, ARAÚJO MB, ARNELL NW, BONDEAU A, BUGMANN H, CARTER TR, GRACIA CA, VEGALEINERT AC DE LA, ERHARD M, EWERT F, GLENDINING M, HOUSE JI, KANKAANPÄÄ S, KLEIN RJT, LAVOREL S, LINDNER M, METZGER MJ, MEYER J, MITCHELL TD, REGINSTER I, ROUNSEVELL M, SABATÉ S, SITCH S, SMITH B, SMITH J, SMITH P, SYKES MT, THONICKE K, THUILLER W, TUCK G, ZAEHLE S, ZIERL B. 2005. Ecosystem service supply and vulnerability to global change in Europe. *Science* 310:1333–1337
- SCHULZ, KG, RIEBESELL U, BELLERBY RGJ, BISWAS H, MEYERHÖFER M, MÜLLER MN, EGGE JK, NEJSTGAARD JC, NEILL C, WOHLERS J, ZÖLLNER E. 2008. Build-up and decline of organic matter during PeECE III. *Biogeosciences* 5:707–718
- SCHUSTER, S, HERNDL GJ. 1995. Formation and significance of transparent exopolymeric particles in the northern Adriatic Sea. *Marine Ecology Progress Series* 124:227–236
- SEEBAH, S, FAIRFIELD C, ULLRICH MS, PASSOW U. 2014. Aggregation and Sedimentation of *Thalassiosira weissflogii* (diatom) in a Warmer and More Acidified Future Ocean. *PLOS ONE* 9:e112379

- SIMON, M, GROSSART H, SCHWEITZER B, PLOUG H. 2002. Microbial ecology of organic aggregates in aquatic ecosystems. *Aquatic Microbial Ecology* 28:175–211
- STARR, M, ST-AMAND L, DEVINE L, BÉRARD-TERRIAULT L, GALBRAITH PS. 2004. State of Phytoplankton in the Estuary and Gulf of St. Lawrence During 2003. Canadian Science Advisory Secretariat 2004/123
- STARR, M, HIMMELMAN JH, TERRIAULT JC. 1993. Environmental control of green sea urchin, *Strongylocentrotus droebachiensis*, spawning in the St. Lawrence Estuary. *Canadian Journal of Fisheries and Aquatic Sciences* 50:894-901
- STEVEN, D.M. 1974. Primary and secondary production in the Gulf of St. Lawrence. Report Manuscript report No. 26, McGill University, Montréal, Québec.
- STODEREGGER, KE, HERNDL GJ. 1999. Production of exopolymer particles by marine bacterioplankton under contrasting turbulence conditions. *Marine Ecology Progress Series* 189:9–16
- SUN, C-C, WANG Y-S, LI QP, YUE W-Z, WANG Y-T, SUN F-L, PENG Y-L. 2012. Distribution characteristics of transparent exopolymer particles in the Pearl River estuary, China. *Journal of Geophysical Research Biogeosciences* 117, G00N17
- TAUCHER, J, JONES J, JAMES A, BRZEZINSKI MA, CARLSON CA, RIEBESELL U, PASSOW U. 2015. Combined effects of CO₂ and temperature on carbon uptake and partitioning by the marine diatoms *Thalassiosira weissflogii* and *Dactyliosolen fragilissimus*. *Limnology and Oceanography* 60:901–919
- TAUCHER, J, SCHULZ KG, DITTMAR T, SOMMER U, OSCHLIES A, RIEBESELL U. 2012. Enhanced carbon overconsumption in response to increasing temperatures during a mesocosm experiment. *Biogeosciences* 9:3531–3545
- TERRIAULT, J-C, LACROIX G. 1976. Nutrients, Chlorophyll, and Internal Tides in the St. Lawrence Estuary. *Journal of the Fisheries Research Board of Canada* 33(12):2747–2757
- THINGSTAD, F, BILLEN G. 1994. Microbial degradation of Phaeocystis material in the water column. *Journal of Marine Systems* 5:55–65
- THIBODEAU, B, VERNAL A DE, MUCCI A. 2006. Recent eutrophication and consequent hypoxia in the bottom waters of the Lower St. Lawrence Estuary: Micropaleontological and geochemical evidence. *Marine Geology* 231:37–50

- THOISEN, C, RIISGAARD K, LUNDHOLM N, NIELSEN TG, HANSEN PJ. 2015. Effect of acidification on an Arctic phytoplankton community from Disko Bay, West Greenland. *Marine Ecology Progress Series* 520:21–34
- THORNTON, DCO. 2002. Diatom aggregation in the sea: mechanisms and ecological implications. *European Journal of Phycology* 37:149–161
- THORNTON, DC, THAKE B. 1998. Effect of temperature on the aggregation of *Skeletonema costatum* (Bacillariophyceae) and the implication for carbon flux in coastal waters. *Marine Ecology Progress Series* 174:223–231
- TOGGWEILER, JR. 1993. Carbon overconsumption. *Nature* 363:210–211
- TORSTENSSON A, HEDBLOM M, ANDERSSON J, ANDERSSON MX, WULFF A. 2013. Synergism between elevated $p\text{CO}_2$ and temperature on the Antarctic sea ice diatom *Nitzschia lecointei*. *Biogeosciences* 10:6391–6401
- TORTELL, PD, DITULLIO GR, SIGMAN DM, MOREL FMM. 2002. CO_2 effects on taxonomic composition and nutrient utilization in an Equatorial Pacific phytoplankton assemblage. *Marine Ecology Progress Series* 236:37–43
- UNDERWOOD, GJC. 2006. Dynamics of extracellular polymeric substance (EPS) production and loss in an estuarine, diatom-dominated, microalgal biofilm over a tidal emersion-immersion period. *Limnology and Oceanography* 51(1):79–93
- UNDERWOOD, GJC, BOULCOTT M, RAINES CA, WALDRON K. 2004. Environmental Effects on Exopolymer Production by Marine Benthic Diatoms: Dynamics, Changes in Composition, and Pathways of Production1. *Journal of Phycology* 40:293–304
- VAZQUEZ-DOMINGUEZ, E, VAQUÉ D, GASOL JM. 2007. Ocean warming enhances respiration and carbon demand of coastal microbial plankton. *Global Change Biology* 13:1327–1334
- VERDUGO, P. 2012. Marine microgels. *Annual Review of Marine Science* 4:375–400
- VERDUGO, P, ALLDREDGE A, AZAM F, KIRCHMAN D, PASSOW U, SANTSCHI P. 2004. The oceanic gel phase: a bridge in the DOM–POM continuum. *Marine Chemistry* 92:67–85
- VÉZINA, A., SAVENKOFF C, ROY S, KLEIN B, RIVKIN R, THERRIAULT J-C, LEGENDRE L 2000. Export of biogenic carbon and structure and dynamics of the

- pelagic food web in the Gulf of St. Lawrence Part 2. Inverse analysis. *Deep Sea Research Part II: Topical Studies in Oceanography* 47:609–635
- VIDUSSI, F, CLAUSTRE H, MANCA BB, LUCHETTA A, MARTY J-C. 2001. Phytoplankton pigment distribution in relation to upper thermocline circulation in the eastern Mediterranean Sea during winter. *Journal of Geophysical Research* 106:19939–19956
- VIDUSSI, F, MOSTAJIR B, FOUILLAND E, LE FLOC'H E, NOUGUIER J, ROQUES C, GOT P, THIBAUT-BOTHA D, BOUVIER T, TROUSSELLIER M. 2011. Effects of experimental warming and increased ultraviolet B radiation on the Mediterranean plankton food web. *Limnology and Oceanography* 56:206–218
- WALLACE, RB, BAUMANN H, GREAR JS, ALLER RC, GOBLER CJ. 2014. Coastal ocean acidification: The other eutrophication problem. *Estuarine, Coastal and Shelf Science* 148:1–13
- WANG, Y, HAMMES F, BOON N, CHAMI M, EGLI T. 2009. Isolation and characterization of low nucleic acid (LNA)-content bacteria. *The ISME Journal* 3(8):889–902
- WEIBE, WJ, POMEROY, LR. 1972. Microorganisms and their association with aggregates and detritus in the sea: a microscopic study. *Memorial Institut Italian Idiobiology* 29 Supplement:325-352
- WELLS, ML. 1998. Marine colloids: A neglected dimension. *Nature* 391:530–531
- WELLS, ML, GOLDBERG ED. 1992. Marine submicron particles. *Marine Chemistry* 40:5–18
- WETZ, M, ROBBINS M, PAERL H. 2009. Transparent Exopolymer Particles (TEP) in a River-Dominated Estuary: Spatial–Temporal Distributions and an Assessment of Controls upon TEP Formation. *Estuaries and Coasts* 32:447–455
- WETZ, MS, WHEELER PA. 2007. Release of dissolved organic matter by coastal diatoms. *Limnology and Oceanography* 52:798–807
- WILLIAMS, PJL. 1981. Microbial contribution to overall marine plankton metabolism—direct measurements of respiration. *Oceanologica Acta* 4:359–364
- WOHLERS, J, ENGEL A, ZÖLLNER E, BREITHAUPT P, JÜRGENS K, HOPPE H-G, SOMMER U, RIEBESELL U. 2009. Changes in biogenic carbon flow in response

- to sea surface warming. *Proceedings of the National Academy of Sciences* 106(17):7067–7072
- WOHLERS-ZÖLLNER, J, BREITHAUPT P, WALTHER K, JÜRGENS K, RIEBESELL U. 2011. Temperature and nutrient stoichiometry interactively modulate organic matter cycling in a pelagic algal-bacterial community. *Limnology and Oceanography* 56:599–610
- WOLF-GLADROW, DA, RIEBESELL U, BURKHARDT S, BIJMA J. 1999. Direct effects of CO₂ concentration on growth and isotopic composition of marine plankton. *Tellus series b-chemical and physical meteorology* 51:461–476
- WOOD, AM, VAN VALEN LM. 1990. Paradox lost? On the release of energy-rich compounds by phytoplankton. *Marine Microbial Food Webs* 4: 103–116
- WURL, O, Holmes M. 2008. The gelatinous nature of the sea-surface microlayer. *Marine Chemistry* 110:89–97
- YVON-DUROCHER, G, JONES JI, TRIMMER M, WOODWARD G, MONTOYA JM. 2010. Warming alters the metabolic balance of ecosystems. *Philosophical Transactions of the Royal Society of London B: Biological Sciences* 365:2117–2126
- ZAKARDJIAN, BA, GRATTON Y, VZINA AF. 2000. Late spring phytoplankton bloom in the Lower St. Lawrence Estuary: the flushing hypothesis revisited. *Marine Ecology Progress Series* 192:31–48
- ZAPATA, M, RODRIGUEZ F, GARRIDO JL. 2000. Separation of chlorophylls and carotenoids from marine phytoplankton: a new HPLC method using a reversed phase C8 column and pyridine-containing mobile phases. *Marine Ecology Progress Series* 195:29–45
- ZEEBE, RE, WOLF-GLADROW DA. 2001. CO₂ in Seawater : Equilibrium, kinetics, isotopes 65:1-346 Elsevier Oceanography Series 65, Amsterdam, 2001, (Paperback) ISBN: 0444509461
- ZHOU, J, MOPPER K, PASSOW U. 1998a. The role of surface-active carbohydrates in the formation of transparent exopolymer particles by bubble adsorption of seawater. *Limnology and Oceanography*:1860–1871
- ZUBKOV, M., SLEIGH M., BURKILL P. 2001. Heterotrophic bacterial turnover along the 20°W meridian between 59°N and 37°N in July 1996. *Deep Sea Research Part II: Topical Studies in Oceanography* 48:987–1001

